Universe Scientific Publishing Pte. Ltd.
73 Upper Paya Lebar Road #07–02B–03 Centro Bianco Singapore 534818
Website: www.usp–pl.com
E–mail: contact@usp–pl.com

ISSN 2315-456X

2023 VOLUME 12 ISSUE 2
Advanced Emergency Medicine

Universe Scientific Publishing

2

2023 Volume 12 Issue 2
ISSN：2315–456X

Advanced Emergency Medicine

Universe Scientific Publishing

Editorial Board

Honorary Editor-in-Chief

Associate Editors

Editorial Board Members

Volume 12 Issue 2·2023
ISSN:2315-456X

Advanced Emergency Medicine

Universe
Scientific Publishing

Universe Scientific Publishing

2023 | Volume 12 | Issue 2

Advanced Emergency Medicine

http://aem.usp-pl.com/index.php/aem

Contents

Original Articles

Analysis of the Effectiveness of Globe Incision Mammaplasty in the Treatment of Early Breast Cancer

Zhu Wu, Zhuo Wang, Qingqing Ye, Rong Fan*
Jingzhou First People's Hospital, Jingzhou 434000, China.

Abstract: Objective: To observe the efficacy of different methods in the treatment of early stage breast cancer disease. Methods: 84 patients admitted from 2020.12 to 2022.8 were divided into groups I and II, 42 patients each, who received treatment after conventional breast-conserving and racket-shaped incision mammoplasty, respectively, and compared the surgical treatment of patients between groups. Results: The rates of cosmetic excellence and complications in group II were 95.2% and 7.1% respectively, compared with 73.8% and 35.7% in group I. The differences reached a significant level (X^2 5.825,8.556 respectively, P equals 0.016,0.003 both <0.05). Conclusion: The treatment of early breast cancer patients with racket-shaped incisions for mammaplasty is cosmetically effective and safe, and is worth promoting.

Keywords: Breast Cancer; Racket Incision Mammaplasty; Efficacy Observation

Introduction

Breast cancer has long been the most prevalent malignant tumour among women in China, and the number of patients with the disease has been increasing in recent years, with a trend of lower age. Surgery is the preferred treatment option for breast cancer, and the preservation of the physiological function of the breast and aesthetic enhancement is the goal of surgical treatment[1]. Although traditional breast-conserving surgery can preserve more breast tissue, many patients suffer from localised breast deformation, pain and skin folds after surgery, resulting in unsatisfactory cosmetic breast outcomes. In this paper, 84 patients were selected as data and compared in groups to confirm the efficacy of this procedure, which is reported as follows.

1. Data and methods

1.1 General information

Eighty-four patients diagnosed with early breast cancer from 2020.12 to 2022.8 were selected as the study sample and divided into 2 groups of 42 patients each, with each group as follows.

Group I age range 23-59 years old, TNM stage: 16, 10 and 16 cases of stage I, II and III respectively.

Group II ranged from 22 to 58 years of age, with TNM stages: 14, 13 and 15 cases in stages I, II and III, respectively.

The above information (P > 0.05) was comparable between the two groups of patients.

1.2 Methods

In group I, traditional breast-conserving surgery was performed by removing the tumour and the surrounding normal tissues above the range of 1cm and pectoral fascia through tumour enlargement, without intraoperative suture operation on the residual cavity. The incision plan was as follows: for the tumour in the nipple plane, a curved incision was made along

the Langer

A curved incision is made along the Langer line for tumours in the nipple plane; a radial incision is made when the tumour is at or below the nipple plane.

Group II: A racket incision mammaplasty with a choice of medial and lateral excision, vertical or "J" shaped incision in relation to the location of the tumour. The two areolar incisions are used as the basis for complete excision of the skin between the corresponding rings and complete excision of the tumour, with the non-cancerous glands being re-arranged and the deviated nipple areola being transferred to the central site in time. The axillary lymph was routinely cleared at an angle of 180° from the axillary fold and a drainage tube was placed in a stable manner.

1.3 Observation indicators

(1) Cosmetic breast effect: The assessment was made in terms of breast texture, compliance and skin touch on both sides, etc. The score was 35 out of 35, with excellent, good, fair and poor corresponding to a range of 31-35, 26-30, 21-25 and ≤20 points respectively. Excellent rate = (number of excellent + number of good)/total number of cases in the group x 100%.

(2) Postoperative complications

1.4 Statistical processing

SPSS33.0 software was used to process the data, and the measured and counted data were used, rate (%), X^2 test respectively. Difference detection performance: $P < 0.05$.

2. Results

2.1 Cosmetic effect

There were 33 cases and 7 cases in Group II who met the judgment criteria of excellent and good respectively, with an excellent rate of 95.2%; there were 20 cases and 11 cases in Group I who met the criteria of excellent and good respectively, with an excellent rate of 73.8%. The overall cosmetic effect of Group II was better than that of Group I ($P<0.05$). Table 1.

Table 1 Comparison of cosmetic breast outcomes between the two groups of patients

Group（n）	Excellent	Good	Fair	difference	Excellent（%）
Group II（42）	33	7	2	0	40（95.2）
Group I（42）	20	11	6	3	31（73.8）
X^2	/	/	/	/	5.825
P	/	/	/	/	0.016

2.2 Complications

In terms of postoperative complication rates, Group II was even lower than Group I ($p < 0.05$). Table 2.

Table 2 Comparison of the incidence of complications in patients between groups

Group（n）	Infection of the incision	Poor healing of the incision	Haematoma	Total occurrence（%）
Group II（42）	1	0	2	3（7.1）
Group I（42）	6	5	4	15（35.7）
X^2	/	/	/	8.556
P	/	/	/	0.003

3. Discussion

Breast-conserving surgery is the preferred option for early-stage breast cancer patients. Although conventional surgery can achieve results comparable to total mastectomy and can better preserve the shape of the lower breast, its promotion is limited because the location and size of the tumour can negatively affect the recovery of breast shape and patient satisfaction is poor. In recent years, clinical medical technology has made great progress in the development of minimally invasive plastic surgery and breast conservation combined with treatment techniques in the field of breast cancer disease treatment has been expanding the scope of application, while effectively treating the disease while better meeting the requirements of patients in terms of aesthetics [2].

In this procedure, the tumour is removed and the defect is repaired using plastic surgery and the breast's own glandular tissue, thus ensuring a good appearance of the breast. The incision is made in both areolas, allowing for smooth and complete excision of the peri-areolar tumour and peri-areolar skin, thus demonstrating a high degree of adaptability. It has been reported in the literature that this procedure can assist in improving the symmetry of the left and right breast, reducing the transverse and longitudinal deviation of the nipple and reducing postoperative scarring [3]. In the current study, the rate of excellent cosmetic breast appearance was higher in Group II patients than in Group I, while the rate of postoperative complications was below that of Group I, suggesting that the racket-shaped incisional mammaplasty procedure is more likely to increase the cosmetic appearance of the breast. In addition, traditional breast-conserving surgery allows fibrin and serum to gradually seep into the residual cavity in order to achieve a better cosmetic breast outcome, which controversially causes an increase in residual cavity pressure, which is not conducive to normal postoperative incision healing and increases the risk of associated complications. In conclusion, clinicians faced with early stage breast cancer are advised to undergo early treatment with rachid incision mammaplasty for good cosmetic results and a safe procedure, which is worthy of popular application.

References.

[1] Tao ZZ, Cao G, Li Y, et al. Analysis of the effect of breast lumpectomy with preserved nipple mastectomy for early breast cancer [J]. Chinese medicine,2020,15(10):1563-1566.

[2]Xu Q, Zheng L, Xu Danying, Liu Yue, Shen Jing. The application of ball-and-shoot incision mammaplasty in breast-conserving surgery for early-stage breast cancer[J]. Chinese general medicine, 2022,20(12):2041-2044.5.

[3] Jin LL. Clinical effects of globe shaped incision mammaplasty in the treatment of breast cancer patients[J]. Clinical Medicine Research and Practice,2020,5(11):71-72.

Author Bio:

First author

Name: Wu zhut (1982.5.14-), Male, Han Nationality, Place of Origin: Xiangtan, Hunan, Master, Title: Attending Physician, Unit: Jingzhou First People's Hospital, Department: Breast Surgery, Main Research Interests: Comprehensive treatment of breast cancer, diagnosis and treatment of non-lactating mastitis, postoperative reconstruction of breast tumor.

Corresponding author

Fan Rong (1980.1.10-), F, Han, Place of origin: Hubei. Jingzhou, Master, Title: Attending, Unit: Jingzhou First People's Hospital, Department: Department of Respiratory and Critical Care, Major research interests: chronic obstructive pulmonary disease, interstitial lung disease, pulmonary embolism, pulmonary hypertension, ECMO life support, etc.

Second author

Wang Zhuo (1968.10.10-), Male, Ethnicity: Han, Origin: Xiangyang City, Hubei Province, Highest Education: B.S., Title: Deputy Chief Physician, Unit: Jingzhou First People's Hospital, Department: Breast Surgery, Main Research Interests:

Comprehensive diagnosis and treatment of breast diseases and breast tumors, post-operative breast reconstruction, minimally invasive treatment of breast diseases, etc.

Third author

Ye Qingqing (1979.2.23-), Female, Ethnicity: Han, Place of origin: Nanning, Guangxi, Highest education: Master, Title: Deputy Chief Physician, Unit: Jingzhou First People's Hospital, Department: Breast Surgery, Main research interests: standard treatment of breast tumours, surgical management of breast cancer

Experience of Comprehensive Nursing Intervention in Perioperative Period of total Endoscopic Radical Thyroidectomy

Jing Wu, Zhiwen Xiao Corresponding author

The Sixth Affiliated Hospital of Sun Yat-sen University, Guangzhou 510000, China.

Abstract: Objective To summarize the perioperative nursing experience of comprehensive nursing intervention in 53 patients who underwent radical thyroidectomy under complete endoscopy in our department. Methods A retrospective analysis was made of the perioperative nursing points of 53 patients with total endoscopic radical thyroidectomy. Including preoperative psychological care, neck back position training, postoperative observation of changes in the condition, neck and shoulder function exercise, local cold compress, keep drainage tube unobstructed, complications prevention, observation and nursing. Results All the 53 patients were cured and discharged without hyperthyroidism crisis and parathyroid injury. Conclusion Perioperative implementation of comprehensive nursing intervention measures, close observation of the condition changes, patient guidance, seriously answer the doubts of patients so that patients actively cooperate with nursing treatment, can effectively reduce complications, reduce patient pain, improve patient satisfaction.

Keywords: Radical Operation of Thyroid Carcinoma; Perioperative Nursing; Comprehensive Nursing Intervention; Nursing Effect

Introduction

Thyroid cancer is one of the most common clinical tumor diseases. According to the statistics of relevant data, the number of patients with thyroid cancer in China is increasing year by year, and the incidence of thyroid cancer in women is higher than that in men.Surgical treatment is usually used in the treatment of thyroid cancer.Endoscopic thyroid surgery in our department includes three approaches through the oral vestibule, behind the ear and armpit.Compared with open surgery, the perioperative nursing of laparoscopic radical thyroidectomy requires medical staff to observe the changes in the appearance of the skin in the surgical area more closely, and timely treatment should be done when relevant symptoms are found, which can effectively improve the effectiveness of disease treatment. The perioperative nursing experience of 53 cases of radical laparoscopic thyroidectomy carried out in our hospital from March 2020 to March 2023 is reported as follows.

1. General Information

Among the 53 patients, 12 were males and 41 were females, aged 16-55 years old, including 5 through the mouth, 45 through the armpit, and 3 behind the ear. The patient was generally in good condition, could tolerate general anesthesia, and had no history of thyroiditis, neck surgery or radiotherapy. No cervical lymph node metastasis was found in preoperative physical examination, color ultrasound examination and intensive CT examination. Preoperative fibrolaryngoscopy showed that vocal cord function was normal. Thyroid function tests were in the normal range. The enrolled patients voluntarily chose to undergo complete endoscopic radical surgery and signed informed consent. All patients had no serious complications and were discharged from hospital on 4 ~ 7 days after surgery.

2. Perioperative nursing

2.1 Preoperative nursing

Nursing staff shall take care of the environment of the ward, strictly control the temperature, ventilation and humidity of the ward, and regularly disinfect the ward as a whole to provide a comfortable environment for the recovery of patients' conditions.

Preoperative assessment the patient's health, physical condition and psychosocial support were assessed. Cooperate with doctors to improve various preoperative examinations, such as heart, lung, liver, kidney, biochemical examination and coagulation mechanism, and carry out some important imaging examinations, such as thyroid B-ultrasound and neck CT.

Psychological nursing nursing staff need to carry out timely psychological intervention on patients, patients do not know enough about the disease, worry about postoperative recovery, manifested as anxiety, the department set up multimedia TV education and paper education sheet, responsible nurses to patients preoperative education, explain preoperative and postoperative preparation and precautions, and play neck function exercise education video, so that patients have full psychological preparation, eliminate concerns,Boost your confidence.For mental overstress, according to the doctor's advice to give sedatives or sleeping drugs, so that patients in the best state of surgery.

Postural training 2days before the operation, the neck backward position training must be implemented and strengthened, and the patient should be instructed to do the surgical position training with pillow under the shoulder and overextension of the head for 3-5 times, 10 to 20 minutes each time, in order to adapt to and cooperate with the intraoperative position, reduce and avoid postoperative discomfort, and improve the quality and efficiency of surgical treatment.

Dietary guidance fasting and water prohibition 8 h after general anesthesia operation. For patients undergoing surgery under general anesthesia in the morning, dinner should be given semi-liquid one day before the operation, and fasting and drinking water should be forbidden after 0:00. For afternoon operation, 250-500ml glucose water should be given orally on the morning of the operation day according to the doctor's advice.

Skin preparation the skin is prepared to remove hair and dirt from the operative area before surgery to avoid damage. Range of skin preparation: upper to lower lip, lower to umbilical level, left and right to posterior axillary line, including armpit hair, male patients shave beard, chest hair.

2.2 Postoperative Care

General Nursing at the end of the operation, the nursing staff should inform the patient about the precautions after the operation.Avoid talking for six hours after surgery. Before postoperative anesthesia, patients should be placed in the supine position with the head tilted to one side, temporarily given fasting water to prevent postoperative vomit aspiration leading to asphyxia.After anesthesia and consciousness, patients should be changed to the semi-decubitus position in time to facilitate breathing and drainage.For patients who are already awake, the news of successful operation should be informed so that they can rest at ease and cooperate with treatment;Continuous oxygen inhalation of 1-2L/min and electrocardiogram monitoring were given, all drainage tubes were properly fixed and continuous negative pressure drainage was maintained.Regular bedside tracheotomy kit.

Condition monitoring after the operation, the nursing staff strictly and comprehensively monitored the patient's heart rate, blood pressure, breathing and other indicators, such as hoarseness or reduced tone when communicating with the patient, closely observed breathing, wound blood leakage and edema, and observed whether the neck and chest area swelling and congestion, such as subcutaneous hematoma due to poor endoscopic wound drainage.Therefore, it is necessary to

actively understand the situation of neck incision and drainage fluid after surgery. If various complications such as dyspnea are found in patients, immediate measures should be taken for treatment.

Drainage tube nursing after surgery, a drainage tube was placed at the endoscopic wound, and a drainage bag containing 50mL negative pressure drainage ball or a 500ml negative pressure drainage bottle was connected.Nursing staff in the drainage tube care must closely observe the nature of the color and flow of the patient's drainage fluid, and guide the patients and their families to observe the main points of self-observation, accurate fixation of the drainage tube, prevent obstruction and pressure, such as neck hematoma, fluid drainage is not smooth, can directly compress the trachea caused by breathing difficulties and even asphyxia death.The normal drainage rate is less than 15mL/h, and not more than 100mL within 24h.Postoperative bleeding should be considered in case of sudden discharge of bright red fluid.Endoscopic thyroidectomy has smaller wounds and less postoperative bleeding complications than traditional surgery [1]. When the drainage rate is less than 20ml, the drainage tube should be removed.

Shoulder and neck functional training early post-operative neck and shoulder exercises, specifically as follows: ① Sitting or standing position, neck and shoulder filling. When lowering the head, the lower jaw should be close to the chest wall as far as possible. When raising the head, the head should be slightly backward. The backward amplitude is small in the early stage and gradually increases in the late stage. (2) Rotate the neck, the left and right rotation is not obvious pain limit, late can be close to 90°. (3) Bend the neck around and gradually increase the amplitude to the ear as close to the shoulder as possible. (4) Hands naturally hang down, shrug and turn the shoulders. (5) One side of the elbow joint flexion at a right Angle, rotate the shoulder and arm, forward and then back, gradually increase the rotation amplitude, and raise to the height as comfortable as possible. Switch to the opposite side. Exercise for at least 10min each time, 3 times a day, starting from the first day after surgery. Inform the patient that exercise will not affect wound healing and will not cause bleeding. During the exercise, ask the patient if there is any discomfort such as obvious pain.If the patient has neck discomfort during the exercise, the nurse and doctor should carefully examine the neck wound together to reassure the patient.[2]

Observation and treatment of complications compared with other operations, radical resection of thyroid cancer has higher risk. Therefore, patients are very likely to have complications after surgical treatment, which will cause serious impact on their life and health.If the patient coughs while drinking water within a day of surgery, the nursing staff should inject the patient with the appropriate medicine.If the patient has suffocation two days after the surgery, the nursing staff need to treat the patient with oxygen, so as to avoid these problems from adversely affecting the recovery effect of the patient.

Discharge guidance the nursing staff need to carry out health publicity and education before the patient is discharged, inform the patient of various matters requiring attention after discharge in detail, such as diet and so on, and inform the patient of the correct method and time of medication to ensure the effectiveness of medication and help the patient recover quickly. At the same time, the nursing staff also need to inform the patient of regular return visit[3] .

3. Discussion

Perioperative nursing is a commonly used nursing mode at present. Through the application of this nursing mode in the nursing of patients undergoing endoscopic radical resection of thyroid cancer, the adverse mood of patients can be relieved, the effect of surgical treatment can be improved, and the probability of various complications can be reduced at the same time, so that the quality of life of patients after surgery can be significantly improved and the recovery of patients can be helped at an early date.

In conclusion, the application of comprehensive nursing intervention in perioperative nursing of total endoscopic radical thyroidectomy has a very good nursing effect.

References

[1] Cui DJ, Wang F, Lin Q. Observation and nursing care of 129 cases of complications after thyroidectomy under endoscope [J]. Chinese Medical Innovation, 2013, 10(35): 140-142.

[2] Yan J, Li G. Effect of early neck and shoulder exercise on postoperative pain and discomfort after thyroid surgery [J]. Journal of Nursing, 2015, 30(6): 18-19.

[3] Li YZ, Wang LL, Gao NN, et al. Effect of rapid rehabilitation surgical nursing model on perioperative thyroid cancer [J]. Medical Higher Vocational Education and Modern Nursing, 2019, 2 (3): 217-220.

Correlation Between CT Body Fat Distribution and Carotid Plaque Characteristics

Mingqing Kou Huitong Liu
Department of Radiology, Shaanxi Provincial People'sHospital, Xi'an 710068, China.

Abstract: Objective: To analyze the relationship between CT body fat distribution and the characteristics of carotid artery plaques. Method: A retrospective analysis was conducted on the clinical and imaging data of 50 patients who underwent CT examination in our hospital. Within 2 weeks, 50 patients were required to undergo abdominal CT and head CTA examinations. Transfer various data to the workstation and conduct research and analysis on the type of carotid artery plaque and degree of stenosis evaluated by CT angiography of the patient's head and neck. Determine the type of carotid artery plaque in patients and divide them into stable plaque group and unstable plaque group. According to the degree of carotid artery stenosis, patients are divided into no/mild stenosis group and moderate/severe stenosis group. Compare clinical laboratory indicators separately. Use SPSS21.0 statistical software for data processing. The measurement data in line with normal distribution were compared between the two groups by t test; The measurement data of non normal distribution were compared between the two groups by Mann Whitney U test. The difference was statistically significant with $P<0.05$. The VFA/SFA ratio was higher in the unstable plaque group than in the stable plaque group, and the difference between the two groups was statistically significant (P=0.028); There was no statistically significant difference in VFA and SFA between the two groups (P=0.106, 0.695); The total cholesterol in the unstable plaque group was lower than that in the stable plaque group, and the difference was statistically significant (P=0.052). The incidence rate of coronary heart disease in patients with moderate/severe stenosis was higher than that in patients with no/mild stenosis, and the difference between the two groups was statistically significant (P=0.037); The quantitative parameters of CT body fat distribution (VFA, SFA, VFA/SFA ratio) showed no statistically significant differences between the no/mild stenosis group and the moderate/severe stenosis group (P values>0.05). Conclusion: The quantitative parameter VFA/SFA ratio of abdominal fat is closely related to the stability of carotid artery plaques. The higher the VFA/SFA ratio, the poorer the stability of plaques.

Keywords: Plaque Stability; Narrow Degree; Visceral Fat Area; Subcutaneous Fat Area

1. Materials and Methods

1.1 Clinical data

We selected 50 patients who came to our hospital for treatment as experimental subjects and analyzed the clinical and imaging data of the patients' head and neck CTA examination. The selection criteria for the experimental subjects are: firstly, patients need to undergo both abdominal CT examination and head and neck CTA examination, and the examination interval should not exceed two weeks. Secondly, the quality of scanned images can meet the requirements of clinical analysis. Thirdly, there is arterial stenosis, ranging from 10% to 99%.

Exclusion criteria for research subjects: Firstly, the patient does not suffer from other major diseases, such as abdominal tumors or a history of tumor treatment, and has undergone pelvic and abdominal surgery. Secondly, the patient has

congenital metabolic diseases and a history of chronic diseases that affect their weight. If suffering from hyperthyroidism, liver and kidney dysfunction, long-term chronic infectious diseases, or systemic blood diseases; The patient has received treatment for cardiovascular and cerebrovascular diseases, and has been taking medication such as statins and stent placement, resulting in carotid artery stenosis and other reasons. BMI is calculated according to the formula: BMI=weight (kg)/height (m).

1.2 Head and neck CTA examination method

Adopting a Canon 640 layer volumetric CT scanner (Aquilion ONE, Toshiba Medical Systems) or Siemens (SOMATOM Definition Flash) second-generation dual source CT 128 row CT. Scanning parameters: detector width is 0.625mm × 64, layer thickness 0.625mm, pitch 0.9, reconstruction interval 0.300mm, ball tube rotation time 0.5s/r, tube voltage 120kVp, effective tube current 200mAs. Using a non ionic contrast agent, iodofol (concentration 350mgl/mL, Jiangsu Hengrui Pharmaceutical Co., Ltd., specification 350mgl/ml), 40 to 60ml was administered through the elbow vein using a high-pressure intravenous syringe at a flow rate of 4-5ml/s. The scanning range is from the aortic arch to the skull top. Transfer the scanned images to the Philips post-processing workstation (IntelliSpace PortalRelease v6.0.6.20039) for image subtraction and vascular reconstruction. Observe the blood vessels from multiple angles and switch to Maximum Density Projection (MIP) to observe the condition of the vessel wall. Use multiplanar reconstruction (MPR) and surface reconstruction (CPR) to reconstruct the vessel structure.

1.3 Abdominal CT examination and measurement of abdominal fat area

The subject is placed in a supine position and subjected to a full abdominal CT plain scan or dual phase enhanced scan. Adopting a Canon 640 layer volumetric CT scanner (Aquilion ONE, Toshiba Medical Systems) or Siemens (SOMATOM Definition Flash) second-generation dual source CT 128 row CT. Scanning parameters: tube voltage 120kVp, effective tube current 200mAs, pitch 0.9, 0.5s per revolution, field of view (F0V): 512mm × 512mm, collimated width 128 × 0.6mm, scanning layer thickness 5mm, layer spacing 5mm, recombination layer thickness 0.625mm, layer spacing 0.300mm. The scanning range is from the diaphragm top to the level of pubic symphysis.

1.4 Evaluation criteria

1.4.1 Types of carotid artery plaques

Referring to Saba et al.'s methods, plaques are classified into soft plaques, calcified plaques, and mixed plaques based on their composition. Soft plaques: There are obvious lipid necrotic cores in the plaques, and CT shows obvious low-density areas within the plaques. The CT value of the core area is<50HU. Calcified plaques: The CT value of the core part of the plaque is>120HU. Mixed plaque: Contains two components: fat and calcium, with a core CT value of 50-120HU. Mixed plaques can be further divided into two subtypes: calcification or fatty composition. In this study, calcified plaques and mixed plaques mainly composed of calcified components were classified as stable plaques. Soft plaques and mixed plaques mainly composed of fat are classified as unstable plaques.

1.4.2 Measurement of degree of carotid artery stenosis

Refer to the North American Symptomatic Carotid endarterectomy Test (NASCET) standard for assessing the degree of carotid stenosis. Measure the degree of stenosis at the most severe location of each segment of the blood vessel using the following method: Stenosis degree=(diameter of the proximal stenosis artery - diameter of the most obvious stenosis artery)/diameter of the proximal stenosis artery × 100%. According to the degree of stenosis, it can be divided into mild

stenosis (10% -29%), moderate stenosis (30% -69%), severe stenosis (70% -99%), and complete occlusion (100%).

1.5 Statistical Analysis

Use SPSS21.0 for data processing. After the normality test of the measurement data, the measurement data conforming to the normal distribution is represented by ($x \pm s$), the comparison between the two groups is represented by t test, the measurement data of non normal distribution is represented by M (1/4,3/4), the comparison between the two groups is represented by Mann Whitney U test, and the counting data is represented by $\times^2$ Inspection. $P<0.05$ indicates a statistically significant difference.

2. Results

2.1 General Information

This study included a total of 50 patients, 31 males (62%) and 19 females (38%), with a male to female ratio of approximately 2.12:1, aged 42-87 years, and a median age of 63 years. The average SFA value is 177.24cm², Median 167.21cm². The average VFA value is 145.23cm², Median 164.44cm². The average value of VFA/SFA is 0.89, with a median of 0.87.

2.2 Clinical laboratory and abdominal fat quantification parameters for different types of carotid artery plaques

The VFA/SFA of patients with unstable plaques was higher than that of patients with stable plaques, and the difference was statistically significant (P=0.027). There was no statistically significant difference in SFA and VFA parameters between the two groups (P>0.05). The total cholesterol in the unstable plaque group was lower than that in the stable plaque group, with a statistically significant difference of P=0.033.

2.3 Clinical laboratory indicators and abdominal fat quantification for different degrees of carotid artery stenosis

There was no statistically significant difference in SFA, VFA, and VFA/SFA between the no/mild stenosis group and the moderate/severe stenosis group (P>0.05). The history of coronary heart disease showed statistical differences among groups with different degrees of stenosis, with a higher incidence of coronary heart disease in patients with moderate/severe stenosis compared to those without/mild stenosis (P=0.026).

3. Discussion

Through the content of this study, we understand the relationship between body fat distribution and the stability of carotid artery plaques. The results indicate that there is a stable relationship between quantitative parameters of abdominal fat and carotid artery plaques. Due to the presence of abdominal fat, patients are very prone to developing carotid artery plaque disease, making abdominal fat a potential disease risk factor for the human body. The above research indicates that the distribution of body fat, especially the reduction of visceral fat in the body, is directly related to the stability of carotid artery plaques. By reducing the visceral fat rate, it can alleviate the stability of the carotid artery and has certain significance in preventing cardiovascular and cerebrovascular events. By improving the distribution of body fat, patients can reduce their body fat, greatly reducing the risk of carotid artery plaque rupture and reducing the occurrence of cardiovascular and

cerebrovascular events.

There are still the following shortcomings in this study: (1) This study is a retrospective analysis, and the sample size included is relatively small; (2) The measurement of the area of abdominal visceral fat and subcutaneous fat requires manual delineation, and there may be some errors in the measurement results; (3) Although CT is the gold standard for quantifying abdominal fat, it also carries certain radiation risks. Therefore, this study found that the quantitative parameter VFA/SFA of abdominal fat is related to the stability of carotid artery plaques, with higher VFA/SFA leading to poorer plaque stability.

Summary

This study shows that coronary heart disease is directly related to carotid artery stenosis. Atherosclerosis is the main factor leading to coronary heart disease. In the current pathogenic analysis, carotid artery and coronary artery have the same pathological basis. Carotid atherosclerosis is positively correlated with coronary atherosclerosis. Carotid artery can be used as a window to reflect the degree of atherosclerosis in the body, thus indirectly suggesting the degree of coronary atherosclerosis, The carotid plaque occurred earlier than coronary atherosclerosis. Therefore, imaging monitoring of carotid atherosclerotic plaque load may predict coronary plaque, which has important clinical application value in the clinical evaluation of coronary heart disease.

References

[1] Cai LL, Wang C, Yu K, Li JJ Xu K. The predictive value of~(18) F-FDG uptake in PET/CT incidental carotid plaque for recurrence of ischemic stroke [J]. Journal of Clinical Radiology, 2021 (03).

[2] Zhao MM, Gan YG, Li JJ Xu K. Study on the correlation between visceral fat area and cerebrovascular diseases based on imaging [J]. Chinese Journal of Medical Computer Imaging, 2021 (02).

Human Papillomavirus Infection in Relation to Vaginal Microflora and Immune Factors

Xiaoge Li, Yutong Wu, Sijing Li, Xiaoling Huang, Ying Jia*
The First Affiliated Hospital of Chongqing Medical University, Chongqing 400016, China.

Abstract: **Objective:** Clarify the vaginal microflora and immune factors in women with human papilloma virus (HPV) infection, and explore its association with HPV infection. **Methods:** This study collected vaginal secretions and blood from 160 women initially diagnosed as HPV positive in our hospital from June 2020 to December 2020 and 80 healthy women with HPV negative physical examination in the same period. The vaginal microflora of the patients were detected by 16S rDNA sequencing and the expression of immune factors was measured by a high-performance liquid phase chip. **Results:** The different types of HPV were HPV mix (64,40%), HPV52 (39,24.375%), HPV16 (30,18.750%), HPV58 (18,11.250%), HPV18 (6,3.750%), HPV53 (1,0.625%), HPV55 (1,0.625%), and HPV68 (1,0.625%).α diversity analysis showed that there was no significant difference in vaginal microflora between different HPV types (P=0.733). The genus level abundance of vaginal microflora in each group was mainly *Lactobacillus*, followed by *Gardnerella* and *Prevotella*. LEfSe Analysis showed that the mix group was *Gardnerella* and the type HPV16 group was *Streptococcus*. The immune comparison showed that MIP-1β was significantly upregulated in the HPV-positive group, but EGF in the HPV-negative group. **Conclusion:** This study revealed that HPV infection can change the proportion of vaginal microbial bacteria and the expression of immune factors, which provides a basis for local vaginal treatment and prevention of HPV infection after HPV infection.

Keywords: HPV; Vaginal Microflora; Immune Factors; Cervical Cancer

1. Introduction

High-risk human papilloma virus (HR-HPV) infection is the leading cause of cervical cancer, the most common reproductive tract malignancy in women[1]. The most common type of HPV infection in cervical cancer was HPV16, followed by HPV18[2]. The vast majority of HPV infected women can turn negative through autoimmune response, and only a few of those with persistent high-risk HPV can progress to cervical cancer. The vaginal environment consists of local immunity, vaginal microflora and human endocrine regulation[3], which is in a dynamic and balanced state. When the balance is disrupted, it will increase the chance of HPV infection, promoting the development of HPV infection to cervical cancer with possible[4]. The main component of the vaginal microecology of healthy women of reproductive age period is *Lactobacillus*, which is involved in maintaining the weak acidic environment and maintaining the stability of the vaginal microecology, and is considered to be the first line of defense against pathogens[5]. When the balance is broken, the number of lactic acid bacteria is reduced or the function is inhibited, vaginal *Gardnerella* or mixed anaerobic bacteria multiply, produce many harmful metabolites, and then accelerate the occurrence and development of cervical lesions and cervical cancer[6-7]. Studies have shown that immune factors participate in the immune response of the body after HPV infecting the body[8]. When the body is infected by HR-HPV, it can induce the body to produce immune regulatory cells, jointly complete the immune regulation function of the body, and affect the occurrence and development of lesions and tumors. The purpose

of this study is the need to explore the relationship between vaginal microflora and immune factors and HPV infection, so as to provide a basis for the prevention of HPV infection and local vaginal treatment after infection.

2. Materials and Methods

2.1 Study subjects

Women who received or physical examination in our hospital from June 2020 to December 2020 were collected as the study subjects. The inclusion criteria were: Women aged 20 to 60 years with sexual history, No sex life and no vaginal treatment within 72h, informed consent, reviewed and approved by the hospital ethics committee. Exclusion criteria: ongoing vaginal or cervical disease, combined immune disease or other medical disease.

2.2 Detection methods

2.2.1 Vaginal microbiological test:

Secretions were collected with a sterile cotton swab on 1/3 of the patient's vagina and stored in a -80℃ refrigerator. Samples were collected and subjected to 16S rDNA sequencing.

2.2.2 Immune factor detection:

5 mL of peripheral blood was extracted from 5mL blood vessels without anticoagulant, and the serum was isolated, and the immune factors were detected by high-performance liquid phase chip.

2.3 Statistical methods

Microbiological analysis was performed using Kruskal-Wallis H test. The expression of immune factors in patients with different groups was analyzed by using independent samples t-test. $P<0.05$ was considered as a statistically significant difference.

3. Results

Depending on the HPV classification, 160 HPV positive patients were divided into 8 groups, types 16,18,52,53,55,58,68 and mix, respectively. The infection rates of different types of HPV were HPV mix (64,40%), HPV52 (39,24.375%), HPV16 (30,18.750%), HPV58 (18,11.250%), HPV18 (6,3.750%), HPV53 (1,0.625%), HPV55 (1,0.625%), and HPV68 (1,0.625%, Table 1). α Diversity is used to measure the diversity of the microflora in the sample, and we found that there was no significant difference in the vaginal microflora in each group (Figure 1, $P=0.733$).

Table 1: Distribution of the different HPV types

	HPV type(n=160)							
	16	18	52	53	55	58	68	mix
positive	30	6	39	1	1	18	1	64
	18.750%	3.750%	24.375%	0.625%	0.625%	11.250%	0.625%	40%

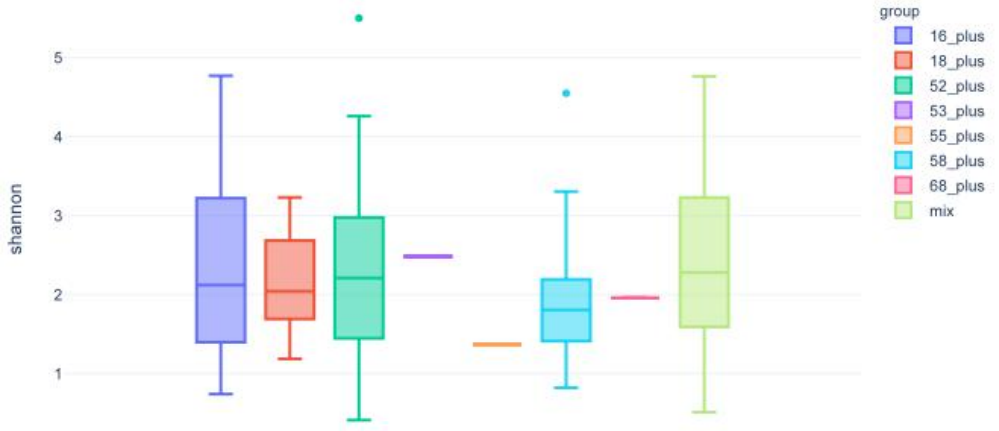

Figure1 The α-diversity of vaginal microbiota

To further analyze the similarities and differences of each group, we analyzed species relative abundance in each group. It can be clearly seen from the relative abundance bar chart that the genus level abundance of the vaginal microflora was dominated by lactobacillus, followed by *Gardnerella* and *Prevotella* (Figure 2).

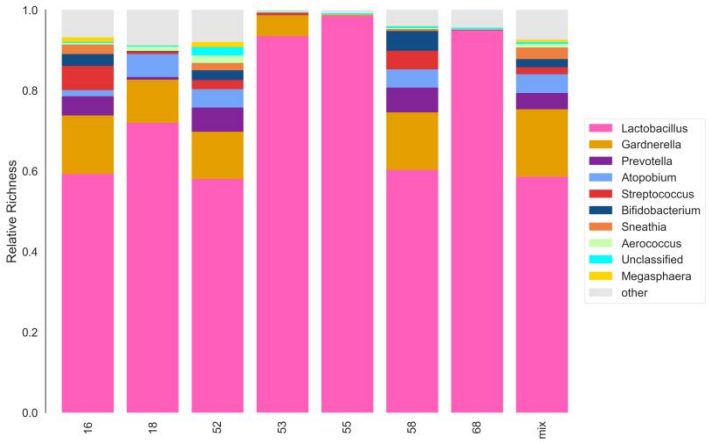

Figure2 Bar chart of the relative abundance of genus-horizontal species

In order to identify the significantly different microflora in each group, the effect size based on linear discriminant analysis (LEfSe analysis), and the microflora with LDA> 4 were used. Among them, the mix group was *Gardnerella* (Figure3, P <0.05), and the type HPV16 group was *Streptococcus* (Figure4, P <0.05). The remaining groups found no differential bacteria at the level of LDA> 4.

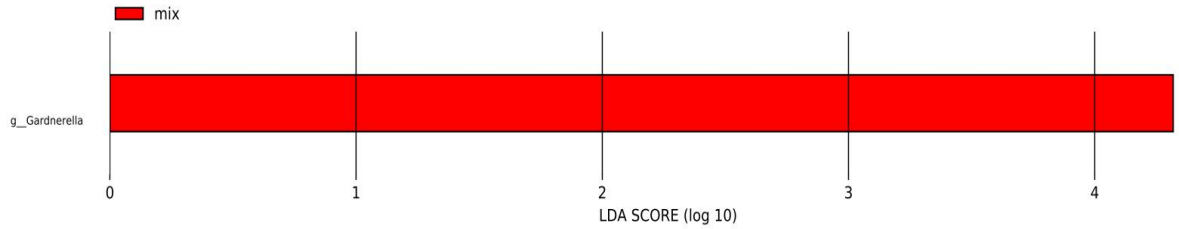

Figure3：LEfSe histogram of mix group (LDA> 4)

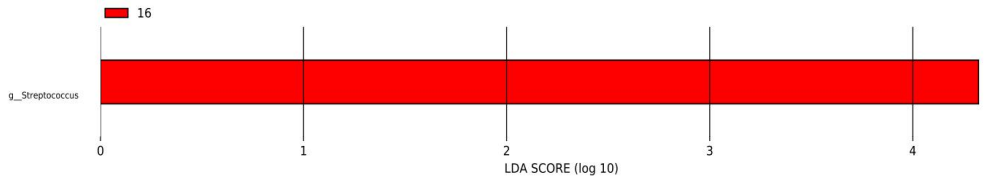

Figure 4 LEfSe histogramof HPV 16 group (LDA> 4)

To explore the relationship between HPV infection and immune factors, we compared and analyzed the differences in the expression of immune factors between HPV-positive and HPV-negative patients. Serserum of 80 HPV-positive patients were mixed into a new sample and divided into 4 groups (named C1, C2, C3 and C4), and 80 HPV-negative healthy women per 20 mixed samples (named D1, D2, D3 and D4) were analyzed for comprehensive analysis. The results showed that MIP-1β was significantly increased in the HPV positive group (C group), while EGF was significantly increased in the HPV-negative group (D group)(Figure5, $P<0.05$).

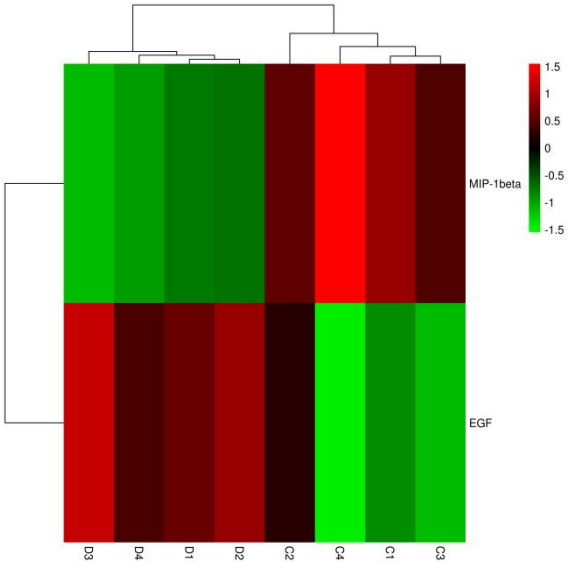

Figure 5 Heat map of the immune factors

4. Discussion

Under normal circumstances, the vaginal environment of women is acidic, and the dominant microflora and other bacteria are in a dynamic balance state, which can effectively prevent HPV infection. When this acidic environment is destroyed, the structure of the microflora will change [9-10]. Continuous HR-HPV infection is a key factor in the progression of cervical epithelial cells to cervical lesions and even to undergo malignant transformation [11]. Among them, HPV16/18 are the two most common high-risk types of HPV leading to cervical lesions[12]. Different types of HPV infection can lead to cervical cancer,with types 16,18, 31, 33, 39, 45, 51, 52, 56, 58, 59, 66 and 68 considered high-risk [13]. In our study, the top 5 most common HPV genotypes were HPV mix, HPV52, HPV16, HPV58 and HPV18. According to this study, the differential bacteria in mix group were *Gardnerella*, and the differential bacteria in type HPV16 group were *Streptococcus*. Therefore, it is speculated that *Gardnerella* and *Streptococcus* may be synergistic factors for HPV infection. In future clinical work, patients with types HPV mix and HPV16 should focus on the detection of microflora *Gardnerella* and *Streptococcus*.

Comparison of immune factors between the HPV-positive and HPV-negative groups revealed that MIP-1β was significantly upregulated in the HPV-positive group, whereas EGF was significantly upregulated in the HPV-negative

group.The results of this study showed that the expression of EGF in the HPV positive group was significantly reduced compared with the HPV negative group, so the reason for the decrease in EGF may be due to the massive replication of the virus, which led to the increased EGF consumption. It is speculated that EGF may play an important immune defense function. However, MIP-1β expression was significantly upregulated when HPV was positive, and it was speculated that the expression of MIP-1β might be increased by HPV infection.

5. Conclusion

In conclusion, this study showed that HPV infection could cause changes in vaginal microflora and body immune factors. When HPV infection, immune control is weakened and the expression of immune factor EGF is reduced. MIP-1β was increased after HPV infection. It is speculated that EGF may play an important immune defense function, and the microflora *Gardnerella* and *Streptococcus* may be the synergistic factors of HPV infection.

References

[1] Chen XJ, et al. “Telomere length in cervical exfoliated cells, interaction with HPV genotype, and cervical cancer occurrence among high-risk HPV-positive women.” Cancer medicine vol. 8,10 (2019): 4845-4851.

[2] Bhattacharjee, Rahul et al. “Mechanistic role of HPV-associated early proteins in cervical cancer: Molecular pathways and targeted therapeutic strategies.” Critical reviews in oncology/hematology vol. 174 (2022): 103675.

[3] Martin DH. “The microbiota of the vagina and its influence on women's health and disease.” The American journal of the medical sciences vol. 343,1 (2012): 2-9.

[4] Mitra, Anita et al. “The vaginal microbiota, human papillomavirus infection and cervical intraepithelial neoplasia: what do we know and where are we going next?.” Microbiome vol. 4,1 58. 1 Nov. 2016.

[5] O'Hanlon, Deirdre Elizabeth et al. “Vaginal pH measured in vivo: lactobacilli determine pH and lactic acid concentration.” BMC microbiology vol. 19,1 13. 14 Jan. 2019.

[6] Ilhan, Zehra Esra et al. “Deciphering the complex interplay between microbiota, HPV, inflammation and cancer through cervicovaginal metabolic profiling.” EBioMedicine vol. 44 (2019): 675-690.

[7] Chorna, Nataliya et al. “Cervicovaginal Microbiome and Urine Metabolome Paired Analysis Reveals Niche Partitioning of the Microbiota in Patients with Human Papilloma Virus Infections.” Metabolites vol. 10,1 36. 15 Jan. 2020.

[8] Torres-Poveda, K et al. “A prospective cohort study to evaluate immunosuppressive cytokines as predictors of viral persistence and progression to pre-malignant lesion in the cervix in women infected with HR-HPV: study protocol.” BMC infectious diseases vol. 18,1 582. 19 Nov. 2018.

[9] Dunlop AL, et al. “Maternal Microbiome and Pregnancy Outcomes That Impact Infant Health: A Review.” Advances in neonatal care : official journal of the National Association of Neonatal Nurses vol. 15,6 (2015): 377-85.

[10] Cao B et al. “Placental Microbiome and Its Role in Preterm Birth.” NeoReviews vol. 15,12 (2014): e537-e545.

[12] Zhang S, Zhao F. Comment on "Will HPV vaccination prevent cervical cancer"[J]. BMC Medicine, 2020, 18(1):38-41.

[13] Song F, Du H, Wang C, et al. The effectiveness of HPV16 and HPV18 genotyping and cytology with different thresholds for the triage of human papillomavirus-based screening on self-collected samples[J]. PLoS ONE, 2020, 15(6):518-522.

[14] Huh WK, Ault KA, Chelmow D, Davey DD, Goulart R A, Garcia F A R, et al. Use of Primary High-Risk Human Papillomavirus Testing for Cervical Cancer Screening: Interim Clinical Guidance. *Gynecol. Oncol.* 2015, *136* (2), 178–182.

Author Bio:

First author

Xiaoge Li, Female, Han Nationality,The First Affiliated Hospital of Chongqing Medical University, Main Research Interests: Comprehensive treatment of cervical cancer, HPV infection, and the vaginal microflora.

Corresponding author

Ying Jia, Female, Han Nationality, The First Affiliated Hospital of Chongqing Medical University, Main Research Interests: Diseases of the lower reproductive tract, cervical cancer, HPV infection, the vaginal microflora etc.

Acknowledgement

The study was sponsored by the Chongqing Medical Scientific Research Project (2021MSXM332) and the Municipal Graduate Student Research Innovation Project of Chongqing (CYS21219).

Progress of Clinical Research on the Treatment of Hyperplasia of Mammary Glands by Auricular Plaster Therapy

Ranran Liang, Xinyu Ma, Long Zhang, Haifa Qiao*
Shaanxi University of Traditional Chinese Medicine, Xianyang 712046, China.

Abstract: Hyperplasia of mammary glands (HMG), the most common benign breast disease in women of childbearing age, often has a long and recurrent course. Because of its mild pain, long-lasting efficacy, ease of operation, non-toxic side effects, ease of acceptance, and remarkable efficacy especially for pain, auricular plaster therapy has created a new way for the treatment of HMG. This article analyzes the efficacy of the current treatment of HMG by auricular plaster therapy, in order to pave the way for finding an ideal solution for the treatment of HMG by auricular plaster therapy in the future.

Keywords: Auricular Plaster Therapy; Hyperplasia of Mammary Glands; Research Progress

1. Introduction

HMG is a non-inflammatory, benign and comprehensive disease, which is essentially a disorder of the normal structure of the breast caused by varying degrees of hyperplasia and incomplete replenishment of the main and interstitial mammary glands. The main clinical manifestations are: lumps in the breast area, accompanied by breast pain and menstrual irregularities, and the severity of the disease varies with the menstrual cycle and mood[1]. HMG is a risk factor for breast cancer, it has an incidence of 78%. Therefore, the study of HMG can lay the foundation for the prevention of breast cancer. Currently, ultrasound imaging is usually used to confirm the diagnosis of HMG. However, ultrasound imaging can usually only detect organic disease, but some patients with HMG do not feel the symptoms at the beginning of the disease and the condition is easily overlooked, thus delaying the disease. Research has shown that auricular points can be positive not only in the presence of organic disease, but also in the early stages of the disease, providing a method and basis for early detection of the disease. Once HMG is detected and cured early, it can not only relieve the patient's pain and financial burden, but also effectively alleviate the disease or avoid its deterioration, which is of great significance to protect women's health.

2. Overview of HMG

HMG is in the category of Ru Pi of Traditional Chinese Medicine (TCM). Currently, no clear understanding of the specific pathogenesis of HMG has been achieved. However, many scholars have proposed that HMG is caused by endocrine hormone imbalance in the body[2].According to today's medical technology, the conventional treatment of HMG is based on hormonal drugs, such as the use of progesterone to regulate the body's endocrine disorders. The short-term efficacy of the treatment is definite, but in the long run, this method only treats the symptoms and does not cure the disease, therefore, the efficacy is not very stable, the disease is prone to recurrence, and there are obvious side effects. Doctors usually use surgery to treat patients who have a long history of the disease and whose treatment with hormones is less effective. However, surgical treatment can be traumatic and painful, and is also prone to recurrence, so patients are less likely to accept[3].

3. Overview of auricular plaster therapy

Auricular plaster therapy is a special Chinese medicine treatment method that stimulates ear acupuncture points by applying pressure to them to treat diseases. In recent years, ear points have been widely used in diagnosing diseases, treating diseases, preventing diseases and health care, and have made new research progress, and have gradually formed an ear point treatment system, becoming a unique new medical science. The study of ear points can not only improve the clinical diagnosis and treatment effect, but also have certain theoretical value for further understanding of meridian points and revealing the mysteries of the human body.

Domestic and foreign scholars have found that auricular plaster therapy is used to treat diseases by adjusting multiple aspects in multiple ways. It has been found that auricular pressure can lower estradiol levels and raise progesterone levels in patients, restoring the metabolic pattern of endocrine hormones[4].

4. Clinical Research Advances

4.1 HMG treated by auricular plaster therapy alone

Wang applied pressure to ear points on the breast, chest, endocrine, liver, and kidney. Conclusion: A total of 76 patients with HMG were selected, and 47 patients were cured after treatment, accounting for 61.8% of all cases; 16 cases showed a curative effect, accounting for 21.1% of all cases; 6 cases had some curative effect, accounting for 7.9% of all cases; and 7 cases were not effective, accounting for 9.2% of all cases[4]. Shen selected ear points for the breast, Shen Men, liver, gallbladder, Triple-Jiao, gastrointestinal, endocrine, subcortical, and occipital. Conclusion: A total of 112 patients with HMG were selected, 68 patients were cured after treatment, 41 cases improved after treatment, and 3 cases did not see any effect after treatment. The total effective rate was as high as 97.32%[5]. Zhu treated 89 patients with HMG by applying pressure to the ear points of the chest, endocrine, thoracic spine, and liver. Conclusion: 35 patients were cured, 45 patients showed efficacy, 5 patients were effective, 4 patients were ineffective, and the total effective rate was 95.5%[6].

4.2 Chinese medicine with auricular plaster therapy for HMG

Feng selected 101 patients with HMG and applied pressure to the ear points of the breast, liver, endocrine, sympathetic and subcortical. They also took Rupi Decoction with reduction. Composition of the formula: Radix Bupleuri, Ligusticum Wallichii, Epimedium, etc. Conclusion: 35 patients were cured after treatment, accounting for 35% of all cases; 41 patients showed efficacy, accounting for 41% of all cases; 21 patients were effective, accounting for 35% of all cases; 4 patients were ineffective, accounting for 4% of all cases. The total effective rate was as high as 96%[7]. Xing treated 82 patients with HMG, randomly grouped, the observation group selected ear points: Shen Men, breast, liver, sympathetic, spleen and endocrine. At the same time, the Rupi Sanjie Capsules was taken and stopped during menstruation; the control group was treated with Rupi Sanjie Capsules only. Results: The total effective rate of the observation group was 92.68%, which was significantly higher than that of the control group (75.61%)[8].

4.3 Acupuncture combined with auricular plaster therapy for HMG

Shang treated HMG with acupuncture points such as the Tsusanli, Taichong, Tanzhong, Qimen, Wuyi, Hegu, and Sanyinjiao. Apply pressure to auricular points such as the breast, endocrine, Shenmen, adrenal, sympathetic, liver, subcortical, and Tri-jiao. Conclusion: The thickness of the mammary glands was reduced and the glandular nodules disappeared[9]. Lan selected 80 patients with HMG and performed acupuncture on body points such as Fenglong, Rugen, Taichong, Tanzhong, Hegu, Qimen, Tsusanli and Sanyinjiao. The auricular points were selected: breast, ovary, chest,

endocrine, liver and sympathetic. Conclusion: A total of 32 patients were cured, accounting for 40% of all cases; 35 patients were significantly effective, accounting for 43.8% of all cases; 12 patients were effective, accounting for 15% of all cases; 3 patients were ineffective, accounting for 3.8% of all cases. The overall effective rate was 96.3%[10].

5. Conclusion

A comprehensive analysis of the literature reveals that the use of auricular acupressure alone or in combination with other TCM treatments for HMG can effectively reduce the symptoms of HMG patients. If used in conjunction with other TCM therapies, the therapeutic effect can be more pronounced and the course of treatment can be shortened, thus achieving the patient's treatment expectations and making it more suitable for clinical promotion and application. Because auricular acupuncture points have some reference significance for the early diagnosis of HMG and other diseases, auricular plaster therapy can also be used as a routine health care modality to preventative intervention for diseases that have not yet reached diagnostic criteria, thus achieving the goal of treating the undiagnosed disease, if this treatment method can be promoted and popularized in the medical and healthcare system.

However, there are still some shortcomings in the clinical use of auricular plaster therapy for the treatment of HMG, for example, the lack of standardized principles for the selection of acupuncture points for the prevention and treatment of HMG by different experts using auricular acupressure therapy. Therefore, in the future, we need to further standardize the selection criteria of auricular acupressure therapy for the treatment of HMG, so that it can be more effectively used in clinical practice.

References

[1] WU, T., Chen, X.M., Qu, M.R., et al. (2023). Research status on the pathogenesis of breast hyperplasia and topical treatment of traditional Chinese medicine. Journal of Liaoning University of Chinese Medicine, pp.1-12.

[2] Xu, Y.N. and Zhang, F.Z. (2004). Progress in TCM treatment of breast hyperplasia. Clinical Journal of Traditional Chinese Medicine, no.6, pp.605–608.

[3] Qiu, P. (2018). Research progress in the treatment of breast hyperplasia in traditional Chinese medicine. Yunnan Journal of Traditional Chinese Medicine, no.2, pp.85–88.

[4] Wang, H.L. (2000). Observation of the short-term efficacy of auricle pressure in the treatment of breast hyperplasia. Journal of Practical Medicine, no.6, pp.511–512.

[5] Shen, B.Q. (2003). Ear pressure therapy treated breast hyperplasia in 112 cases. Shaanxi Traditional Chinese Medicine, no.7, pp.649.

[6] Zhu, Y.Y., Lu, S.X. and Zhu, M. (2015). Observation and nursing experience of the efficacy of ear point bean pressure in the treatment of 89 cases of breast hyperplasia. Inner Mongolia Traditional Chinese Medicine, no.2, pp.175.

[7] Feng, X.Y. and Jiang, C. (2000). Observation of the efficacy of ear acupoint pressure combined with traditional Chinese medicine in the treatment of breast hyperplasia. Clinical Journal of Acupuncture, no.2, pp.47-48.

[8] Xing, H., Huang, L.N. and Zhang, T. (2017). The effect of Rupi Sanjie Capsules combined with ear point pressure on breast hyperplasia. Southwest Defense Medicine, no.2, pp.123-125.

[9] Shang, Y.H. and Shen, P.F. (2012). Acupuncture combined with ear acupoint compression therapy for the treatment of breast hyperplasia was one case. Clinical Journal of Acupuncture, no.2, pp.47-48.

[10] Lan, Y.J. (2014). Acupuncture combined with ear acupoint pressure was used to treat 80 cases of breast hyperplasia. Chinese Practical Medicine, no.9, pp.246.

A Case of Severe Pleural Effusion and Pulmonary Dysfunction Associated with Occupational Exposure to Asphalt Tar Smoke is Reported

Yipiao Liu, Wentao Wang, Yuan Zhang, Xiao Fu*

Department of Thoracic Surgery and lung Transplantation, the First Affiliated Hospital of Zhengzhou University, Zhengzhou 450052, China.

Abstract: Asphalt and tar transportation personnel are often exposed to the polluted air environment of asphalt fumes, tar and diesel exhaust. This long-term occupational exposure can adversely affect lung function, causing fibrosis, pleural effusion, and inflammation. This paper reports a case of pleural effusion in a 35-year-old male who had been engaged in asphalt paving and transportation for 5 years. There was no occupational exposure protection during the working period. The patient had dyspnea, expectoration, and pleural effusion for more than 1 month. After admission, thoracic drainage and pleural cauterization dissection were performed, and the symptoms were relieved. However, pulmonary fibrosis and visceral pleural thickening are challenging to reverse, and patients still have pulmonary dysfunction and the risk of continuing to develop lung consolidation. Therefore, the personnel engaged in asphalt and tar transportation should be well-protected to reduce occupational exposure.

Keywords: Asphalt Fumes; Pleural Effusion; Pulmonary Function; Occupational Exposure

1. Background

Workers engaged in asphalt transportation and paving are exposed to asphalt smoke through inhalation and skin contact throughout their working life, which is one of the main occupational groups most often exposed to toxic and harmful chemical pollutants[1]. Bitumen is a black, highly viscous organism that is a liquid or semisolid product extracted from petroleum[2]. It plays a role in cementing stones and gravel in road construction. Bitumen contains a variety of chemical and biological pollutants, including volatile organic compounds (VOCs), polycyclic aromatic hydrocarbons (PAH), naphthene, inhalable particulate matter (PM), nitrogen oxides and sulfur compounds[3]. When the asphalt is treated at a high temperature in the electrode roller, the above toxic and harmful substances will volatilize a large amount of asphalt smoke[4]. Because the bitumen contains carcinogenic substances, 3, 4-benzo (a) pyrene, the content of which is as high as 2.5%-3.5%, evaporates with the flue gas. PAH can be inhaled and deposited in the respiratory system, causing lung fibrosis, pleural adhesion, pleural effusion, and even lung cancer[5]. Therefore, this paper reports a case of a patient with severe pleural effusion, pleural adhesion, and pulmonary dysfunction due to long-term exposure to asphalt. It is hoped to reduce misdiagnosis and organ damage caused by such occupational exposure in the future.

2. Case presentation

The patient was a 35-year-old male who had been engaged in asphalt tarmac paving and transportation for 5 years. The chief complaint of the patient was dyspnea and expectoration for more than 1 month, with occasional bloody sputum. In the

local hospital, it was misdiagnosed as malignant pleural effusion (neoplastic). Later, closed thoracic drainage was performed in our hospital, and the daily drainage volume was 500ml for 7 consecutive days, draining red-brown pleural effusion. The exfoliative cytology of pleural effusion showed some inflammatory cells and some exfoliated tracheal epithelial cells. A Blood routine test after admission showed that the white blood cell count was 6.34×10^9 g /L, the absolute value of monocytes was 0.76, and the other indicators were standard. The tumor marker CA125 was 81.2 KU /L, and the tumor abnormal glycan protein TAP was 131.185μm^2. Contrast-enhanced CT of the chest 13 days before surgery showed large area of atelectasis in the right lung, multiple patchy high-density shadows in the right lung, patchy soft tissue shadows beside the mediastinum of the lower lobe of the right lung, which seemed to be mildly enhanced, and a large amount of effusion in the right pleural cavity. There was a flocculent high-density shadow in the lower lobe of the left lung (Fig.1A). Symptomatic and supportive treatment including anti-infection, antitussive and expectorant treatment was continued, and pleural effusion was drained. Contrast-enhanced CT of the chest 2 days before surgery showed large area of atelectasis in the right lung, multiple patchy high-density shadows in the right lung, and patchy soft tissue shadows beside the mediastinum of the lower lobe of the right lung, which seemed to be mildly enhanced. There was a large amount of effusion shadow in the right pleural cavity, and the drainage tube shadow was visible. Multiple cystic low-density shadows were found in the posterior mediastinal esophagus and cardia, and the edge of the lesions was enhanced on a contrast-enhanced scan. There was a flocculent high-density shadow in the lower lobe of the left lung (Fig.1B). Pulmonary function tests one day before surgery showed that TLC-SB% was 58.7%, FRC-SB% was 76.6%, and DLCO-SB% was 31.3%, indicating severe restrictive ventilation dysfunction, a severe reduction in pulmonary diffusion capacity, and reduction in alveolar diffusion capacity.

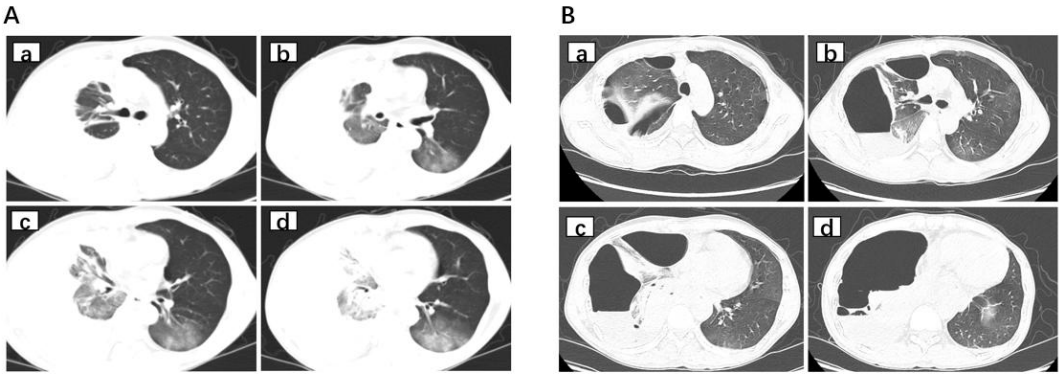

Figure 1. A Massive right pleural effusion with right lung atelectasis; Inflammation of the right lung. Localized emphysema in the apex of the right lung. Inflammation in the lower lobe of the left lung. **B** Massive pleural effusion in the right lung with right atelectasis, right lung inflammation and pulmonary fibrosis, pleural adhesion, and right pneumothorax.

For further treatment, cauterization of pleural adhesion and decortication were performed in the right thoracic cavity under the thoracic cavity. The surgical procedure was as follows: the pleural adhesion was separated under thoracoscopy, the pus was aspirated, the necrotic material was cleaned, and the thickened pleural fibrous plate was stripped. Intraoperative findings: extensive adhesion of the right pleura, consolidation of the right lower lung without expansion, yellow necrosis and fibrinous necrosis on the surface of the right lower lung near the costophrenic angle (Fig.2A). Postoperative pathology showed that the grey-red chest wall and pleural tissue were inflammatory exudation and bleeding tissue. The size of the capsule was about 4.5 × 3.5 × 1.0cm in total, the inner wall of the capsule was grey-red and smooth, and the wall thickness was about 0.1-0.3cm (Fig.2B).

CT examination on the third day after the operation showed that the brightness of both lungs was normal and the texture was disordered. The right lung showed postoperative changes, with large patches of high density shadow and fluid low density shadow in the right thoracic cavity, and local thickening of the pleura. Gas shadow and drainage tube shadow were

found in the right thoracic cavity. In the left lower lobe, there was a small high-density nodule shadow and a cord-like high-density shadow (Fig.2C). The patient's symptoms were relieved after surgery, but his pulmonary fibrosis and consolidation were challenging to reverse, and he still had pulmonary dysfunction. He needed to continue to exercise in the later stage and stay away from asphalt smoke.

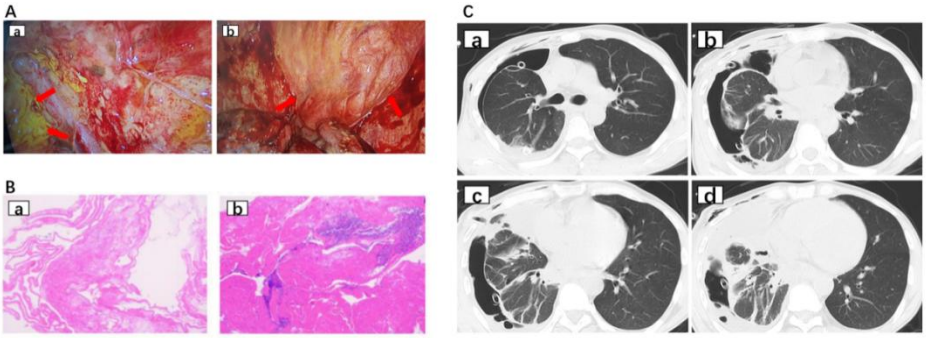

Figure 2. A Intraoperative thoracoscopic findings. **a** Yellow necrosis and fibrinoid necrosis (red arrows) on the lower right lung surface near the costophrenic Angle; **b** Showed pleural thickening, pulmonary fibrosis, and consolidation in the lower right lung layer (red arrows). **B** Chest wall and pleural tissue, all of which showed inflammatory exudation and bleeding tissue. **C** Postoperative changes of the right lung, right lung and left lower lobe inflammation.

A small nodule in the lower lobe of the left lung was recommended for follow-up. Right fluid pneumothorax. There was localized thickening of the right pleura. There was gas in the right chest wall.

3. Discussion

The patient had been engaged in asphalt pavement and transportation for 5 years, and had no daily occupational exposure protection. The patient developed massive pleural effusion, pleural adhesions, and pulmonary dysfunction due to long-term exposure to pitch smoke. There are still pleural thickening and pulmonary consolidation after operation, and long-term pulmonary function exercise is needed in order to obtain better recovery. Regular use of personal protective equipment (PPE) may therefore reduce this health risk. Personal protective equipment shall be strictly used at work, and pollution from construction projects and the emission of toxic substances shall be reduced as far as possible in accordance with regulations. Early assessment of occupational exposure susceptibility biomarkers in workers to reduce adverse health consequences of bitumen related workers**.**

References

[1] McClean MD, Rinehart RD, Ngo L, et al. Inhalation and dermal exposure among asphalt paving workers[J]. Ann Occup Hyg, 2004, 48(8):663-671.

[2] Ulvestad B, Randem BG, Skare Ø, et al. Lung function in asphalt pavers: a longitudinal study[J]. Int Arch Occup Environ Health, 2017, 90(1):63-71.

[3] Shukla S, Khan R, Bhattacharya P, et al. Concentration, source apportionment and potential carcinogenic risks of polycyclic aromatic hydrocarbons (PAHs) in roadside soils[J]. Chemosphere, 2022, 292:133413.

[4] Hrdina A, Kohale IN, Kaushal S, et al. The Parallel Transformations of Polycyclic Aromatic Hydrocarbons in the Body and in the Atmosphere[J]. Environ Health Perspect, 2022, 130(2): 25004.

[5] Díaz de León-Martínez L, Grimaldo-Galeana JM, Alcántara-Quintana LE, et al. Evaluation of cytokines in exhaled breath condensate in an occupationally exposed population to pneumotoxic pollutants[J]. Environ Sci Pollut Res Int, 2022, 29(39): 59872-59884.

The First Author: Yipiao Liu , MD, Department of Thoracic Surgery and lung Transplantation, the First Affiliated Hospital of Zhengzhou University, Zhengzhou 450052, China.

*** Correspondence Author:** Xiao Fu, MD, PhD, Department of Thoracic Surgery and lung Transplantation, the First Affiliated Hospital of Zhengzhou University, Zhengzhou 450052, China.

Predictive Effect of Pelvic Floor Ultrasound Parameters on Stress Urinary Incontinence After Cesarean Section

Liang Mu, Shuliang Nan*, Li Liu
Shaanxi Provincial People's Hospital, Xi'an 710068, China.

Abstract: Objective: To explore the predictive effect of pelvic floor ultrasound parameters on stress urinary incontinence after cesarean section. Methods: The pregnant women who underwent cesarean section in our hospital from April 2021 to April 2022 were selected as the study subjects. Fifty pregnant women with SUI within 6 months after delivery were selected as the study subjects in the experimental group. However, 50 patients who underwent cesarean section for 6 months after delivery and did not initially choose SUI were selected as the control group study subjects. The experimental content was to observe the probability of PUA, BNS, LHA, BND, URA in two groups of pregnant women under resting state. To analyze the predictive effect of ultrasound parameters on SUI after cesarean section. Results: There was no significant difference in PUA and LHA between the two groups of pregnant women at rest (P>0.05); The BNS in the resting state and the maximum Valsalva state in the experimental group were significantly lower than those in the control group. Through comprehensive collection of six data, it is possible to summarize the predictive role of pelvic floor ultrasound parameters for stress urinary incontinence after cesarean section. The data obtained by the combined diagnosis method is significantly higher than the single prediction data. Conclusion: Basin ultrasound parameters have a high predictive value for postpartum SUI after cesarean section, and combining ultrasound parameters can improve the diagnostic efficacy of postpartum SUI after cesarean section.

Keywords: Pelvic Floor Ultrasound; Cesarean Section; Stress Urinary Incontinence; Forecast

1. Data and Methods

1.1 Information

The pregnant women who underwent cesarean section in our hospital from April 2021 to April 2022 were selected as the study subjects. Fifty pregnant women who developed SUI six months after cesarean section were selected as the experimental group, and 50 pregnant women who did not develop SUI six months after cesarean section were selected as the control group. The diagnostic standard for SUI is that changes in abdominal pressure occur when the patient's posture changes such as laughter, cough, sneezing, and exercise, ultimately leading to uncontrollable urinary leakage in the pregnant woman. Parturients participating in the experiment need to complete some tests, first of all, the bladder neck lift test and pressure induced test are both positive, and the urodynamic test confirms the diagnosis of postpartum stress urinary incontinence. The patient was determined to undergo a cesarean section in our hospital. Before delivery, the patient did not have any congenital diseases, especially urinary system diseases, etc. At the same time, the patient and their family members should sign an informed consent form. Exclusion criteria: Natural spontaneous childbirth women do not participate in the research experiment. "A woman with a urinary system may also cause urinary incontinence in the patient. It is not possible to determine whether the woman has postpartum urinary incontinence or urinary incontinence caused by the urinary system, so

she cannot participate in the experimental study.". A woman who has cognitive impairment such as mental, visual, and hearing impairment. Maternal women with severe pelvic diseases; Women with urinary incontinence due to infection, trauma, neurological abnormalities, and other reasons; A pregnant woman who cannot complete the Valsalva action.

1.2 Method

All the subjects underwent pelvic floor ultrasound examination using GE Voluson E10 and Voluson S8 ultrasound diagnostic instruments from the United States. The three-dimensional volume probes RM6C and RIC5-9W-RS were used, with a probe frequency of 4-8MHz. Instruct the subject to urinate 10 to 20 minutes before testing to empty the bladder. Take the bladder lithotomy position, apply an appropriate amount of coupling agent to the probe surface, apply a sterile isolation sleeve, and then apply an appropriate amount of coupling agent to the isolation sleeve. Place the probe on the midsagittal section of the lower edge of the pubic symphysis at the pelvic floor for scanning, and sequentially display the urethra, bladder, and vagina. The posterior vesicourethral angle (PUA), the horizontal and vertical distance (BNS) from the bladder neck to the lower edge of the pubic symphysis, and the area of the levator ani fissure (LHA) under the resting state and the maximum Valsalva state were collected, as well as the difference between the distance between the bladder neck and the lower edge of the pubic symphysis (BND) under the two states, and the difference between the urethral inclination angle under the two states, namely, the urethral rotation angle (URA). The ultrasound examination and measurement of all subjects were performed by the same physician.

1.3 Statistical analysis

SPSS23.0 statistical software was used for data processing and analysis. The number of use cases (percentage) of counting data is expressed as [example (%)], and the comparison between groups is performed using χ 2 Inspection; The measurement data were expressed as mean ± standard deviation (x ± s) and compared between groups using a t-test; Draw the ROC curve, calculate the area under the ROC curve of pelvic floor ultrasound parameters to predict SUI, and use logistic regression analysis to determine independent risk factors for SUI after cesarean section. $P<0.05$ indicates a statistically significant difference.

2. Results

2.1 Comparison of general information between two groups of pregnant women

There were no statistically significant differences in age, body mass index, gestational week, parity, alcohol consumption during pregnancy, and educational level between the two groups ($P>0.05$), which were clinically comparable.

2.2 Comparison of pelvic floor ultrasound parameters between two groups of pregnant women

There was no significant difference in PUA and LHA between the two groups in resting state ($P>0.05$); The resting state BNS and maximum Valsalva state BNS in the observation group were significantly lower than those in the control group, while the maximum Valsalva state PUA, LHA, BND, URA were significantly higher than those in the control group, with significant differences ($P<0.05$).

3. Discussion

With the continuous improvement of people's requirements for quality of life, there is currently a high level of attention paid to the recovery of pregnant women after childbirth. After childbirth, there is a certain probability that women will experience stress induced urinary incontinence. For SUI, although it will not have an impact on the life and health of patients, due to long-term urinary incontinence in patients, these can have an impact on their mental and psychological health. In the long run, patients cannot control the excretion of urine from the body by themselves. The most serious situation is patients' feelings such as inferiority complex and depression. It seriously affects the daily life and mental health of female patients. Normal urinary control in the human body mainly depends on the patient's urethra and bladder neck. When the urethra or bladder is damaged by surrounding supporting structures, it is unable to resist the increase in abdominal pressure, resulting in uncontrollable urinary incontinence.

The main predisposing factors for SUI are generally believed to be childbirth injury and estrogen decline, while about 16% to 34% of women experience SUI after childbirth, mainly due to pelvic floor muscle damage caused by pregnancy and childbirth. A 2016 meta study showed that delivery methods are closely related to the occurrence of postpartum SUI among women, with the risk of SUI occurring during vaginal delivery being approximately twice that of cesarean section. Currently, there is a lack of recognized gold standards for the diagnosis of SUI. The widely recognized clinical test method is urodynamic examination. However, this method is expensive, cumbersome, and belongs to invasive examination. More importantly, it cannot provide the shape of the lower urinary tract. Ultrasound diagnosis is widely used in the diagnosis of clinical SUI and the evaluation of the efficacy of rehabilitation treatment due to its non radiation, strong real-time, and simple operation. Transabdominal ultrasound is easily affected by pubic and intestinal qi, and the pelvic floor structure is often not clearly displayed. Transrectal and vaginal ultrasound can cause changes in the structural position and morphology of pelvic floor organs, resulting in false negatives. The conventional examination method for SUI evaluation is transperineal ultrasound, which can clearly display the position, shape, and movement of female pelvic floor organs in the midsagittal plane. Therefore, three-dimensional ultrasound examination of the pelvic floor in postpartum women is of great significance for the diagnosis of female SUI and pelvic floor muscle dysfunction.

Through this study, it can be determined that the accuracy of predicting stress urinary incontinence after cesarean section through pelvic floor ultrasound parameters is higher. Studies have shown that the position of the urethra and bladder in women with SUI will move downward and begin to move backward. Defective supporting structures such as urethra. The urethral wall, bladder, pubic muscle, and surrounding fascia form the supporting structure of the urinary tract. The pelvic floor is supported by the levator ani muscle complex. When the supporting structure or muscle group of the urinary tract is damaged or defective, it will not be able to lift the urethra and bladder, resulting in a higher internal pressure in the bladder than in the urethra, which can lead to excessive urination. The reason for this may be that under resting state, the more parallel the human body's gravity is to the direction of the urethra, the more susceptible it is to the influence of intra-abdominal pressure and gravity. In Valsalva state, subjects are required to cooperate with breathing movements to make their abdominal muscles contract and increase intra-abdominal pressure. Ultrasound can detect the position and morphological changes of pelvic floor supporting structures such as the female postpartum urethra and bladder neck.

4. Summary

In summary, basin ultrasound parameters have a good effect on disease prediction for women with SUI after cesarean section. By combining multiple ultrasound parameters to complete the prediction of SUI diagnosis after cesarean section, they can be effectively used in clinical evaluation of SUI diagnosis and rehabilitation treatment effects.

References

[1] Pei HG. The value of brain blood flow ultrasound parameters combined with cardiac ultrasound parameters in the diagnosis and prognosis of patent ductus arteriosus in premature infants [J]. Chinese Journal of Practical Medicine, 2022 (09).

[2] Ma YC. Clinical application value of serology combined with ultrasound parameters in predicting preeclampsia [J]. Contemporary Medicine, 2021 (07).

[3] Niu J. Application of ultrasound parameters in predicting cesarean scar pregnancy and massive bleeding [J]. Medical Theory and Practice, 2021 (13).

[4] Huang H, Li XY. Progress in the study of umbilical vascular ultrasound parameters and their clinical significance [J]. Guangxi Medicine, 2021 (11).

[5] Liu XX, Liu Y, Chen X. Analysis of pelvic floor ultrasound parameters and diagnostic value in patients with stress urinary incontinence [J]. Heilongjiang Medical Science, 2022 (06).

Pelvic Floor Ultrasound Evaluation of the Impact of Delivery Times and Delivery Methods on the Anterior Pelvic Cavity

Shuliang Nan, Liang Mu*, Li Liu
Shaanxi Provincial People's Hospital, Xi an 710068,

Abstract: Objective: To evaluate the impact of delivery frequency and delivery method on the anterior pelvic cavity using pelvic floor ultrasound. Method: 200 women who gave birth in our hospital from January 2019 to January 2022 were selected as the research subjects, including 100 first-time vaginal delivery women, 50 second-time vaginal delivery women, and 50 cesarean section women each. The control group consisted of 100 women who underwent a 15 day follow-up examination after the first artificial abortion surgery in our hospital during the same period. The patients were divided into a control group, a first-time delivery group, a second-time delivery group, and a cesarean section group. Observing the changes in the anterior pelvic structure during resting state and maximum Valsalva movement through perineal ultrasound examination. Result: The distance from the bladder neck to the reference line in the resting state was significantly different between the control group, cesarean section group, first vaginal delivery group, and second vaginal delivery group ($P<0.05$); During the maximum Valsalva maneuver, the detection rate of bladder neck mobility, urethral rotation angle, posterior angle of bladder, and funneling of internal urethral orifice, the second vaginal delivery group, the first vaginal delivery group>the cesarean section group>the control group, and the difference between each group was statistically significant ($P<0.05$). During the maximum Valsalva maneuver in the first and second vaginal delivery groups, the lowest point of the bladder was located below the reference line, and there was no statistically significant difference between the two groups ($P>0.05$); During the maximum Valsalva maneuver in the cesarean section group and control group, the lowest point of the bladder was located on the reference line, and there was no statistically significant difference between the two groups ($P>0.05$); The difference between the vaginal delivery group and the cesarean section and control group was statistically significant ($P<0.05$). Conclusion: Different birth times and delivery methods have varying degrees of impact on the anterior pelvic cavity of women. Pelvic floor ultrasound can early evaluate these structural changes and provide reliable basis for the screening and diagnosis of pelvic floor dysfunction disease (PFD).

Keywords: Pelvic Floor Ultrasound; Anterior Pelvic Cavity; Delivery Method; Parity

1. Materials and Methods

1.1 Data sources

A questionnaire survey and pelvic floor ultrasound examination were conducted on 200 women who underwent routine postpartum examinations for 42-60 days from January 2019 to January 2022 in our hospital. 100 cases in the first vaginal delivery group; 50 cases in the second vaginal delivery group, with both fetuses delivered via vagina; The cesarean section group consists of 50 primiparous women. Exclusion criteria: (1) Have a history of premature birth and induced labor; (2) Have a history of abdominal surgery; (3) Individuals with large pelvic masses; (4) People with chronic diseases such as diabetes and hypertension. The control group consists of 100 women who underwent the first artificial abortion in our

hospital at the same time and underwent a follow-up examination 15 days after delivery. The exclusion criteria are the same as above.

1.2 Method

1.2.1 Questionnaire survey

A general questionnaire survey was conducted among the selected subjects, including age, height, pre pregnancy and pre delivery quality, pelvic floor ultrasound body mass (that is, 42~60 days after delivery), delivery frequency and mode, newborn birth body mass, whether there is abnormal defecation and previous history (chronic cough, hypertension, diabetes, pelvic surgery, preterm delivery, induced labor history, etc.). Body mass index measurement: Body mass index (BMI)=body mass (kg)/height 2 (m2).

1.2.2 Inspection methods and anterior pelvic measurement indicators

Before the examination, the examinee was instructed to empty the stool. The bladder capacity was about 50~100ml. The structures of the bladder, urethra, vagina and anal canal were clearly displayed on the median sagittal plane plane. The pelvic floor ultrasonic reference line adopts the human horizontal line passing through the posterior lower edge of the pubic symphysis, that is, a 135 ° straight line passing through the posterior lower edge of the pubic symphysis and the central axis of the pubic symphysis. Measurement indicators under resting state: (1) The position of the bladder neck, i.e. the distance from the bladder neck to the reference line; (2) The posterior angle of the bladder, which is the angle between the posterior wall of the bladder triangle and the proximal urethra; (3) Urethral inclination angle refers to the angle between the proximal urethra and the longitudinal axis of the human body. Observation and measurement indicators during the maximum Valsalva action: (1) Bladder neck mobility, which is the difference between the position of the bladder neck during the maximum Valsalva action and the resting state position; (2) Urethral rotation angle, difference in urethral inclination angle between resting state and maximum Valsalva action; (3) The lowest point of the bladder (bladder neck or posterior wall), which is the vertical distance from the lowest point of the bladder to the reference line; (4) If the internal urethral orifice is funnel shaped, observe whether the internal urethral orifice is open and funnel shaped. The bladder neck or lowest point of the bladder is located on the head side of the reference line, defined as the reference line, represented by a positive number; If located on the foot side of the reference line, it is defined as below the reference line and represented by a negative number.

1.2.3 Instruments

The Mindray Resona8 color Doppler ultrasound diagnostic instrument has an intracavity volume probe frequency of 3-9MHz and a volume scanning angle of 120 °.

SPSS17.0 statistical software was used to analyze the data, with econometric data expressed in ($x \pm s$) and inter group differences analyzed using analysis of variance; The counting data is represented by [example (%)], and comparison is made using $\chi 2$ Inspection. $P<0.05$ indicates a statistically significant difference.

2. Results

2.1 Data sources

There was no statistically significant difference in pre pregnancy, pre delivery, and post partum BMI, as well as newborn birth weight among the groups of second vaginal delivery, first vaginal delivery, and cesarean section (all $P>0.05$). There was a statistically significant difference in age between the groups ($P<0.05$), with the second vaginal delivery group

and the first vaginal delivery group being higher than the cesarean section group and higher than the control group. However, there was no statistically significant difference between the first vaginal delivery group and the cesarean section group (P>0.05).

2.2 Observation indicators of anterior pelvic cavity

Compare the distance between the bladder neck and the reference line in a resting state. The difference between the control group, cesarean section group, first vaginal delivery group, and second vaginal delivery group was statistically significant (P<0.05); There was no statistically significant difference in the posterior horn of the bladder between the groups (P>0.05). The bladder neck movement, urethral rotation angle, and posterior bladder angle during the maximum Valsalva maneuver were significantly higher in the second and first vaginal delivery groups than those in the cesarean section group and control group (P<0.05); The lowest point of the bladder during the maximum Valsalva maneuver in the first and second vaginal delivery groups was below the reference line, and there was no statistically significant difference between the two groups (P>0.05); The lowest point of the bladder during the maximum Valsalva maneuver in the cesarean section group and control group was located on the reference line, and there was no statistically significant difference between the two groups (P>0.05); The differences between the first and second vaginal delivery groups, the cesarean section group, and the control group were statistically significant (all P<0.05). The detection rate of funneling of the internal urethral orifice of the urethra during the maximum Valsalva maneuver: the second vaginal delivery group, the first vaginal delivery group>the cesarean section group>the control group. There was no significant difference between the cesarean section group and the control group (P>0.05), and there was significant difference between the other groups (P<0.05).

3. Discussion

The hormone changes in women's body during pregnancy, the estrogen level decreases, and the nourishing effect on levator ani muscle decreases, resulting in atrophy of levator ani muscle. The enlarged uterus compresses the iliac vein, causing blood reflux disorders, resulting in insufficient blood supply to pelvic floor tissue and metabolic imbalance. In the non pregnancy state, the force of the uterine center of gravity points to the sacrococcygeal bone. The increased uterine center of gravity during pregnancy changes, and the force points to the levator ani muscle. Under the downward pressure, the levator ani muscle is overstretched for a long time, or even exceeds the stretch limit of nerve fibers and loses control of the divine channel. In the process of vaginal delivery, the coronation of the fetal head and the delivery of the fetus mechanically compress the pelvic floor tissues such as the levator ani muscle and ligament fascia, causing extreme tissue expansion, directly leading to myogenic injury. These factors can all lead to damage to the pelvic floor support structure, which may persist until postpartum or even be irreversible.

Therefore, both pregnancy and delivery can cause damage to the pelvic floor supporting tissue in women, leading to changes in pelvic floor structure and being two independent risk factors for PFD. The main manifestations of anterior pelvic PFD are stress urinary incontinence (SUI) and bladder prolapse. Some studies suggest that the prevalence of SUI is higher in pregnant and postpartum women. In patients with SUI, including asymptomatic women, the formation of funneling of the internal urethral orifice can be observed by pelvic floor ultrasound during Valsalva movement and even at rest. This phenomenon is caused by insufficient urethral closure pressure, and is the most relevant indicator with SUI. Morphologically, when the internal urethral orifice is funneled, there is a lower position of the bladder neck and a larger posterior bladder angle, which may be a pathological change formed under the condition of urethral detrusor reflex, detrusor contraction and pressure, suggesting that the supporting structure around the bladder neck and proximal urethra is weakened, leading to the descent of the bladder neck and proximal urethra.

References

[1] Wu Y, Li WJ; Shen FX et al. The application of pelvic floor electrophysiological assessment in postpartum pelvic floor dysfunction [J]. China Maternal and Child Health, 2019 (07).

[2] Xu YZ, Tang HL and Feng ZY. Observation of the recent effects of secondary natural childbirth on female pelvic floor structure through pelvic floor ultrasound examination [J]. Chinese Journal of Medical Ultrasound (Electronic Edition), 2018 (03).

[3] Liu FF, Yan YL, GaoYB, Cui GH, Ying T. Analysis of the differences in ultrasound features and clinical manifestations between type II and type III bladder prolapse [J]. Chinese Journal of Ultrasound Medicine, 2017 (09).

[4] Peng LL. The clinical application value of pelvic floor ultrasound in evaluating anterior pelvic disorders [J]. Imaging Research and Medical Application, 2019 (12).

A Review of Studies on the Treatment of Severe Acute Pancreatitis

Hang Ren [1,a], Ting Lei[2], Jianfei Sun[2,*]

1. Shaanxi University of Chinese Medicine, Xianyang 712046, China.

2. Affiliated Hospital of Shaanxi University of Chinese Medicine, Xianyang 712000, China.

Abstract: Acute pancreatitis (AP) is one of the common acute abdominal diseases in clinic, and the main mechanism is due to a variety of triggers that activate pancreatic enzymes in the pancreas, and then cause the inflammatory reaction of pancreatic tissue self digestion, edema, hemorrhage and even necrosis, with many complications and a high case fatality rate. Among them, especially severe acute pancreatitis (SAP), often leads to severe complications and even death in patients due to various factors such as prompt medical treatment and misdiagnosis, which is a clinically intractable disease.

Keywords*:* Pancreatitis; Treatment; Review

1. Introduction

Severe acute pancreatitis (SAP), also known as acute hemorrhagic necrotizing pancreatitis, is a special type of AP with an insidious course, severe complications, and high case fatality rate, accounting for approximately 5% - 10% of AP overall [1] 740. Further deterioration of the condition of acute edematous pancreatitis will produce organ failure and last for 48h and above [2], using the new version of the Atlanta classification criteria as a reference, which is based on the diagnosis of SAP with a high mortality rate of 36% - 50% [3], is a recognized and intractable acute and critical illness in the world. Common etiologies include biliary stones, hepatopancreatic sphincter dysfunction, alcohol abuse or overeating. Fever, nausea and vomiting, persistent mid - and upper abdominal drilling pain with radiating to the back are typical clinical findings. The treatment of SAP is mainly performed using the multidisciplinary comprehensive therapy collaborative group (MDT) mode [1] 741, and the clinical routine treatment means are fasting without drinking, gastrointestinal decompression, fluid resuscitation, pancreatic enzyme inhibition, surgical treatment, and so on.

2. Conventional western medicine for the treatment of SAP

Modern Western medicine the diagnosis and treatment of SAP requires the adoption of the multi-disciplinary team (MDT) model, disease stage classification, complex pathophysiological processes and the goal guidance of treatment are different, which all raise higher requirements for the diagnosis and treatment of SAP. Especially, the diagnosis and treatment of SAP, which is characterized by the main features of early organ dysfunction and late infectious complications, means the intersection of multi-disciplinary fields, aims to give advanced life support to patients with SAP, maximize the relief of patient suffering, and reduce complications to symptomatic support treatment.

3. Conservative treatment in Western Medicine

Early onset to week 2 was the first " peak of death " of SAP, diagnosis and treatment strategies and focus points were different between national and international guidelines, Chinese guidelines emphasized the importance of maintaining

function with alternative organs, taking ICU as the main body, nonsurgical treatment as the main body, and the early comprehensive rescue system aimed at preserving organ function was gradually shaped. Lactated Ringer's fluid and normal saline are preferred, the rate of fluid replacement is controlled [4], and the application of a goal-directed fluid therapy pattern in the early stages of the disease is beneficial for the improvement of tissue perfusion and the guidance of fluid intake [5]. Routine use of non steroids, opioids, etc., multimodal combination analgesia such as epidural analgesia, self-controlled analgesia etc. should maximize pain symptoms and potentially improve clinical outcomes in mechanically ventilated patients with SAP. Recent years related studies have shown that enteral nutrition support therapy at the early stage has a promoting effect on the recovery of patients with AP, which is beneficial to the protection of gastrointestinal mucosal barrier, the inhibition of intestinal bacterial translocation, and then reducing the risk of infectious pancreatic tissue necrosis and the occurrence of systemic inflammatory reactions [6-8]. This further shakes up the traditional treatment perspective of Western medicine as " requires strict prohibition of diet so that food can enter the gastrointestinal tract and then further stimulate the secretion of pancreatic juice ", so the new edition of the guidelines recommends that in the event of regaining tolerance of gastrointestinal function, oral or enteral nutrition should be initiated as early as possible (24-72 h after admission). Once again, the treatment means such as gastrointestinal decompression, puncture and drainage, and analgesia can effectively reduce the intra-abdominal pressure, so that the compliance of the abdominal wall increases, to some extent, alleviating the early severe complications in SAP " increased intra-abdominal pressure and organ dysfunction as an important cause of death ", the disease progression of abdominal compartment syndrome (ACS).

4. Surgical treatment in Western Medicine

Surgery still has an irreplaceable leading role in the management of specific types of pancreatitis and severe complications such as infection, necrosis, hemorrhage, and abscess. Mastering the timing and indications of surgery and the choice of appropriate surgical approach has great clinical significance for the treatment of SAP. The Atlanta criteria in 2013 concluded that 3-4 weeks after the onset of SAP, and timely removal of pancreatic and perinecrotic tissue should be performed until the borders of the necrotic tissue parcels have formed. The new surgical principles, while reducing the risk of bleeding and local trauma, also reduce the risk of sepsis occurrence and systemic inflammatory response after surgery [9]. Concurrent infectious pancreatic necrosis in SAP is the first indication for surgery and the need for surgical intervention has become industry consensus. Patients with persistent multiorgan failure and fulminant acute pancreatitis refractory to conservative treatment are surgical indications for debridement of necrotic tissue. Likewise ACS also requires aggressive surgical intervention, the surgical goal of which is in line with reducing intra-abdominal hypertension and increasing abdominal wall compliance. In recent years, new minimally invasive surgical modalities have emerged in layers and a mosaic, gradually gaining mainstream consensus and becoming a research hotspot. Percutaneous catheterization drainage is one of the most widely used minimally invasive techniques. Relevant studies have shown that puncture and drainage can achieve remission of the disease in 62.5% of sepsis cases and 36.6% of cases with organ failure [10]. The trauma transmission therapy, which is based on the step-by-step operation of puncture, endoscopy, endoscopy, and laparotomy, is now the guiding concept of emerging treatment modes for SAP, which minimize the occurrence of local exudation and systemic inflammatory response, maximize debridement, maximize the retention of viable pancreatic tissue, and guarantee exudate drainage and the patency of established channels. But today, where emerging technologies continue to evolve, there will also be concomitant production of new complications, and the modalities of all types of surgical treatment still have their "" sight out of sight. "".

5. Integrative medicine in the treatment of SAP

On the background of possessing modern scientific and technological treatment means such as dialysis, peritoneal lavage, drainage, laparoscopy and intervention, combined traditional Chinese medicine (TCM) treatment technology and the theory of prescription medicine have unique advantages in the therapeutic effect of SAP, and also become a current research hotspot of SAP, which has been sought by many researchers. Weiwei Wang [11], in a clinical randomized controlled trial, applied dahchai Hu Tang combined with continuous blood purification to treat SAP compared with that of Western medicine alone, and found that the biochemical parameters amylase, creatinine, IL-6, TNF in the observation group-α, Serum creatinine and serum amylase levels were significantly lower than those of the control group, and the patients' abdominal distension, disappearance time of abdominal pain, bowel sounds, recovery time of bowel function, defecation time, as well as hospital stay were significantly shorter after treatment than those of the control group. Guo long [12] and others applied a combination of acupuncture and a TCM Decoction, Qing pancreatong Fu Tang, to treat 28 patients with SAP, and the conclusions of the study obtained after treatment by an adequate course of treatment were basically consistent with Weiwei Wang's, and the patients' abdominal symptom disappearance time and related biochemical indexes were shorter and lower than those of the control group treated with western medicine alone.

6. Summary

SAP is a relatively common class of acute abdomen in clinical hepatobiliary pancreaticosplenic diseases, characterized by an acute onset, severe disease, rapid progression, many systemic and local complications, and an extremely high mortality rate, therefore, there is no delay in the development and application of preventive and therapeutic measures for this disease.

References

[1] Pancreatic surgery group, division of external science, Chinese Medical Association. Diagnosis and treatment guidelines for acute pancreatitis in China (2021) [J]. Chinese Journal of Practical Surgery, 2021, 41 (7): 739-746.

[2] Sarr MG, Banks PA, Bollen TL,et al.The new revised classification of acute pancreatitis 2012[J]. Surg Clin North Am, 2013, 93(3): 549-562.

[3] Vege SS, Gardner TB, Chari ST, et al. Low mortality and high morbidity in severe acute pancreatitis without organ failure:a case for revising the Atlanta Classification to include “moderately severe acute pancreatitis”. Am J Gastroenterol, 2009; 104(3): 710-715.

[4] Iqbal U, Anwar H, Scribani M. Ringer's lactate versus normal saline in acute pancreatitis:A systematic review and metaanalysis[J], 2018, 19(6): 335-341.

[5] Crockett SD, Wani S, Gardner TB, et al.American Gastroenterological Association Institute Guideline on initial management of acute pancreatitis[J].Gastroenterology, 2018, 154(4):1096-1101.

[6] Boxhoorn L, Voermans RP, Bouwense SA, et al.Acute pancreatitis[J].Lancet, 2020, 396(10252): 726-734.

[7] Arvanitakis M, Ockenga J, Bezmarevic M, et al.ESPEN guideline on clinical nutrition in acute and chronic pancreatitis[J].Clin Nutr, 2020, 39(3):612-631.

[8] Li XY, He C, Zhu Y, et al.Role of gut microbiota on intestinal barrier function in acute pancreatitis[J].World J Gastroenterol, 2020, 26(18):2187-2193.

[9] Bello B, Matthews JB. Minimally invasive treatment of pancreatic necrosis. World J Gastroenterol, 2012,18:6829-6835.

[10] Gooszen HG, Besselink MG, Van Santvoort HC, et al.Surgical treatment of acute pancreatitis.L angenbecks Arch Surg, 2013, 398. 799-806.

[11] Wang WW, Wang ZY. Efficacy of dahchaihu decoction combined with continuous blood purification for the treatment of acute severe pancreatitis and effects on serum biochemical parameters, immune function and inflammatory factors [J]. Modern Journal of integrated traditional Chinese and Western medicine, 2020, 29 (4): 426-429.
[12] Guo L, Wang J, Bai M, et al.. the role of acupuncture combined with Qing pancreatong Fu Tang in the treatment of severe acute pancreatitis [J]. Inner Mongolia Medical Journal, 2012, 44 (07): 845-846.

Professor Wang Xiaoyan's Experience in Treating Dementia

Miaomiao Tian[1], Jiao Zhang[1], Xiaoyan Wang[2,*]

1. Shaanxi University of Traditional Chinese Medicine, Xianyang 712046, China.

2. Xi'an Hospital of Traditional Chinese Medicine, Xi'an 710021, China.

Abstract: Dementia is a common Psychiatric disease, especially in the elderly group of high incidence, Professor Wang Xiaoyan thinks that the pathogenesis of this disease is the deficiency of upper qi, Yang qi can not access the brain body, the etiology is divided into two categories, including deficiency syndrome is divided into weak temper, kidney essence deficiency, positive syndrome is divided into phlegm turbidity and upper confusion, Yang Ming dry heat, etc.Clinical patients are mostly mixed with deficiency and reality, need to distinguish the primary and secondary, dialectical treatment, remarkable effect.

Keywords: Dementia; Experience of Famous Doctors; Wang Xiaoyan; Dialectical Treatment

Introduction

Jiebin Zhang made a systematic discussion on the etiology, pathogenesis and symptoms of dementia in the Book of Jingyue · Miscellaneous Syndrome Mo [1], "Dementia, usually without phlegm, gradually leads to dementia by stagnation, failure, deliberation, confusion, or panic. The words are reversed, the actions are irregular, or excessive sweating, or suffering from anxiety, and the symptoms are numerous and strange.Pulse will be or string, or number, or large, or small, change is not often ".Shiduo Chen analyzed the etiology of dementia in "Record of Syndrome Differentiation · Volume 4", "About its beginning, from the depression of liver qi;In the end, because of the failure of the stomach qi.Liver depression is wood soil, and phlegm can not be transformed;Stomach failure is soil water, and phlegm can not be eliminated.So phlegm accumulation in the chest, entrenched in the heart, so that the gods are not clear, and into the disease."The treatment method of "opening Yu to expel phlegm and strengthening stomach ventilation" was put forward.Qingren Wang put forward in "Medical Forest Correction · Brain Theory" that "children have no memory, the brain is not full;High years have no memory, brain gradually empty ".It is believed that the cause of infantile dementia and senile dementia is the empty myeloid sea.The dementia of Chinese medicine is a broad dementia with idiocy as the main clinical manifestation.Including modern medicine of congenital brain hypoplasia, vascular dementia, Alzheimer's disease, intracranial organic diseases and due to infection, poisoning, trauma, metabolic diseases caused by central nervous diseases caused by cognitive disorders.

Xiaoyan Wang , master supervisor of Shaanxi University of Traditional Chinese Medicine, a famous TCM in Shaanxi Province, the first famous TCM in Xi 'an, and the discipline leader of encephalopathy in Xi 'an Hospital of Traditional Chinese Medicine, has engaged in more than 30 clinical and scientific research works, especially in the field of encephalopathy and internal injuries and miscellaneous diseases.The author has the honor to learn from Professor Wang, with the teacher clinic, teacher Cheng carefully taught, now Professor Wang's experience in the treatment of dementia is summarized as follows.

In traditional Chinese medicine, Professor Wang believes that the pathogenesis of this disease is always due to deficiency of upper qi, Yang Qi cannot access the brain, and the disease location is mainly in the brain, and the causes of

deficiency of upper qi are divided into two categories, among which the deficiency syndrome is divided into weakness of temper, deficiency of kidney essence, and the positive syndrome is divided into phlegm turbidness and upper confusion, Yang Ming dry heat and so on.The general treatment is qi lifting, reinforcing deficiency and reducing deficiency.Virtual is filled successively two days, fill kidney essence, tonifying temper;In fact, dispelling cold and dehumidification, clearing Yang and Ming desiccation heat, etc. Clinically, patients are often mixed with deficiency and substance, deficiency and substance, so at the same time, attention should be paid to not hurt Zhengqi and solidified to protect Benqi.

1. Syndrome of weak temper

The spleen and stomach is the source of acquired Qi and blood biochemistry."Plain ask · Meridian" said: "Drink into the stomach, overflow qi, on the spleen, spleen loose essence, on the lung, through the channel, the bladder, water essence four cloth, five parallel."A Treatise on the Secret Scriptures of the Plain Man Linglan" says, "The spleen and stomach are the officials of granary storage, and the five flavors are out."The spleen and stomach is located in the middle coke, the main receiving, rotting water, produce fine matter, constantly nourish the whole body.The subtle substances of the spleen and stomach are injected upward into the brain through the meridians to fill the brain and make it play the normal role of the main spirit and wisdom.Professor Wang Xiaoyan used Lizhong Decoction and Shengjin decoction for dementia with syndrome of temper weakness.Lizhong decoction focuses on the jiao spleen and stomach in the center of the circle, warms and vibrates the jiao Yang qi in the middle, eliminates the cold and dampness in the middle earth, makes the central axis run, the axis moves the wheel, the four wheels rotate accordingly, and the whole circle movement can proceed normally, so that the evil that has left its position can return to its position and the body can restore the circular motion state.The stomach often declines, the spleen often rises, the stomach qi drops, the upper qi drops, the temper rises, the lower qi rises, the middle qi rises and rises, and all the diseases are cured [2].

2. Syndrome of insufficient kidney essence

"Lingshu · Meridia" said: "The beginning of human life, the first to become essence, essence and brain marrow.The essence of the kidney is to nourish the bone marrow.Kidney essence foot, the pulp function is strong, pulp Wang brain marrow enrichment, Shenji intelligent;The deficiency of kidney Yin leads to insufficient production of qi, while the deficiency of pith sea and air leads to the loss of brain and the loss of divine machinery [3].The brain is the blood of the five Zang Qi, and the pith is gathered in the brain, which is the gathering place of the essence.The formation of the brain depends on the synthesis of the congenital essence, the replenishment of the kidney essence, and the replenishment of the pulp sea."The head is the house of wisdom", the brain is empty, God has no return, memory decay.Professor Wang used Sini Decoction combined with kidney Siwei for dementia with syndrome of kidney deficiency.Sini Decoction warming Shaoyin deficiency cold, Yang Qi to warm nourishing kidney essence.Kidney four from "Li Ke old Chinese medicine acute severe difficult disease experience album", wolfberry, cuscuta sex flat, psoralea, epimedium sex temperature.The whole four kinds of medicine is slightly warm.From the effect point of view, psoralea, epimedium, cuscuta seed three medicines tonifying kidney Yang, wolfberry tonifying kidney Yin.Yin and Yang double complement, with Yang as the main, reflects the concept of seeking Yang in Yin, seeking Yin in Yang, Yang master Yin from.The four medicines are used in combination, as Li Lao said, "The four medicines enter the liver and kidney with peaceful properties, warm but not dry, moist but not greasy.Tonifying kidney essence, drumming kidney qi, warming Yang without the disadvantages of cinnamon, nourishing Yin without the disadvantages of ripe land "[4].

3. Syndrome of turbid phlegm and upper disturbance

Phlegm turbidized for the human body water and liquid transport disorders, its good cohesion, easy to confuse the mind,

disturb the gods and show symptoms of dementia.Among the many risk factors that lead to dementia, drinking and smoking are easy to help fire burning jin to phlegm, and hypertrophy is easy to trap the spleen Yang so that the spleen is lost and the phlegm is turbidized, thus obstructing the brain's qi machinery and blinding the Qingqiao.In the Secret Record of the Stone Room, Shiduo Chen of Qing Dynasty summed up the pathogenesis of stupor disease as "phlegm potential is the highest and stupor is the deepest".Professor Wang used Sansheng Yin for dementia with phlegm turbid and upper disturbance syndrome.This kind of patient sputum turbid upper disturbance as the standard, Yang qi weakness as the basis, this prescription to expel phlegm to warm Yang, first remove its standard, then solidified its roots.

4. Hot and desiccant syndrome of Yangming

"Su Wen · Yin Yang yin xiang Big Treatise" cloud: "Strong fire qi decline, little fire qi strong.Strong fire food Qi, Qi food less fire.Strengthen fire and dissipate air, and reduce fire and anger."[5] "Zhuang Huo" is the fire of overactivity in the body, pathological evil fire, burnt burning of healthy qi, and then dissipating kidney essence.Insufficient Qi, blood and body fluid can not be filled with brain orifice.Because Qing reduces the dry heat of Yang Ming, Yang Ming restoration of the main acceptance, rot function.Professor Wang ses Baihu plus ginseng soup to reduce the dry heat of Yang Ming and protect the middle Qi from damage.

5. Summary

At present, conservative treatment is still the main treatment for dementia at home and abroad. The current therapeutic means, whether drug or surgical treatment, can only improve the symptoms of patients, but can not stop the development of the disease, let alone cure.TCM has excellent curative effect on the treatment of dementia. Professor Wang guides the syndrome differentiation and treatment of dementia with the theory of "Qi monism" through syndrome differentiation and treatment, which can effectively guide the clinical diagnosis and treatment of TCM.

References

[1] Yang JX, Kang Y, Zhai W, et al. The development of traditional Chinese medicine understanding of senile dementia [J]. Renren Health, 2022, No.582(25):78-80.

[2] Zhang LM. Round movement and clinical application of Lizhong Decoction [J]. Modern Distance Education of Chinese Traditional Medicine,202,20(11):78-80.

[3] Zhao FY, Li CH. Exploring the etiology and pathogenesis of dementia from the perspective of kidney deficiency [J].Chinese medicine miscellaneous of yunnan, China, 2012 (9) : 10 to 11.

[4] Li K. Li Ke's experience album of Acute Critical and Difficult Diseases of Traditional Chinese Medicine [M]. Shanxi Science and Technology Press. 2001.

[5] Jiang L, Zhang YF, Meng FZ, et al. Discussion on the pathogenesis of diabetics' fiery injury of Qi based on the thought of "strengthening fire and eating Qi" in Huangdi Neijing[J]. Tianjin Traditional Chinese Medicine, 202, 39(01): 45-48.

Comparison of Neostigmine-Atropine Administration Methods for Hemodynamic Parameters in Patients Undergoing Elective Surgery: A Randomized Control Trial

Junbei Wu, Huixuan Zhou*

Department of Anesthesiology, The First Affiliated Hospital of Nanjing Medical University, Nanjing 210029, China.

Abstract: **Objective:** The aim of this study is to compare the hemodynamic effects of neostigmine-atropine in the reversal of muscle relaxants when administered either sequentially or simultaneously. **Methods:** Patients undergoing noncardiac surgery were recruited and randomly allocated to either a sequential or a simultaneous administration of neostigmine (0.04 mg kg^{-1}) and atropine (0.02 mg kg−1) at the end of surgery. Sequential group (SEQ group): Neostigmine and 1/3 dose of atropine were administered first minute, followed by another 2/3 dose of atropine 3 minutes later. Simultaneous group (SIM group): Neostigmine and atropine mixture was finished in 4 minutes. The primary outcome was the area under the curve (AUC) of the heart rate difference within 15 minutes of administration. The secondary outcome was the heart rate at each time point and the heart rate difference. **Results:** The AUC of heart rate difference within 15 minutes after administration in the SEQ group was 13.05±9.57 versus 43.56±10.54 in the SIM group (P<0.05). SIM group had a significantly lower heart rate when compared to SEQ group at 9, 10, 11, 12, 13, 14, and 15 minutes after administration (P<0.05). Heart rate difference was significantly smaller at 9, 10, 11, 12, 13, 14, and 15 minutes after administration in the SEQ group (P<0.05). **Conclusion:** Sequential administration, when atropine was administered later, induced smaller heart rate variability. Atropine and neostigmine should be administered in this order: neostigmine combined with small doses of atropine was administered first, followed by the remaining atropine.

Keywords: Neostigmine; Atropine; Heart Rate

Introduction

Postoperative residual curarization is a common problem in post-anaesthesia care units (PACUs) and a risk factor for postoperative complications [1]. Aspiration, airway obstruction, hypoxemia, and postoperative pulmonary complications (PPCs) may be increased by residual curarization..Reversal of neuromuscular blocking agents at the end of surgery is recommended in the guidelines [2]. Neostigmine is commonly administered. Although it is a frequent practice to use the combination of neostigmine and atropine for the reversal of neuromuscular block, heart rate fluctuations are common. Atropine has a more rapid onset than neostigmine, resulting in an initial tachycardia. We performed the present study comparing the hemodynamic effects of two different administration methods for the reversal of residual neuromuscular block in anesthetized patients.

Methods

Study population

Between November 2022 and March 2023, patients having elective non-cardiac surgery at the First Affiliated Hospital of Nanjing Medical University were evaluated for eligibility. Written informed consent was obtained from all patients. All subjects, aged 18 to 75 years, with a BMI in the range of 18.5 to 25.0 kg m^{-2}, who met the criteria for ASA physical status classification I to II, and of expected duration of more than 1 hour under general anesthesia were recruited. We excluded patients with underlying cardiovascular or respiratory diseases, pregnancy, emergent or urgent surgery, contraindication to any study drug or scheduled anesthetic drug.

Randomization and blinding

Based on a computer-generated random distribution sequence (1:1 assignment ratio), participants were randomly assigned to "Sequential group (SEQ group)" or "Simultaneous group (SIM group)". A staff member of the department who was not engaged in the study devised the randomization order prior to the study. Either "SEQ group" or "SIM group" was inscribed on a piece of paper, which was then enclosed in a sealed opaque envelope. The envelopes were then shuffled and labeled.

Study protocol

Standard ASA monitors (electrocardiogram, pulse oximetry, blood pressure, end-tidal CO_2) were applied. Anesthesia was induced with midazolam (0.05 mg kg^{-1}), etomidate (0.3 mg kg^{-1}), sufentanil (0.3 ug kg^{-1}) followed by cis-atracurium (0.2 mg kg^{-1}) intravenously. Anesthesia was maintained with a propofol infusion and/or sevoflurane. Train of four (TOF) was performed for neuromuscular monitoring continuously with the time interval of 30 minutes. During the procedure, a dosage of 0.05-0.07 mg kg-1 of cis-atracurium was administered for intraoperative neuromuscular blockade to keep TOF 0–1.

When the anesthesia team was ready for reversal, they paged the research team to deliver the envelope containing the randomization assignment. The i.v. study drug (neostigmine 0.04 mg kg^{-1} with atropine 0.02 mg kg^{-1}) was administered at the end of surgery once two responses to TOF nerve stimulation were present. SEQ group: Neostigmine and 1/3 dose of atropine were administered first minute, followed by another 2/3 dose of atropine 3 minutes later. SIM group: Neostigmine and atropine mixture is finished in 4 minutes. If the patient's heart rate was below 45 bpm, atropine 0.5mg was administered.

Index

Demographics and clinical characteristics that included age, sex, height, weight, BMI, American Society of Anesthesiologists (ASA) classification were documented before the surgery. Duration of surgery was also recorded. The primary outcome was the area under the curve (AUC) of the heart rate difference (heart rate difference = heart rate - baseline) within 15 minutes of administration. The secondary outcome was the heart rate at each time point within 15 minutes of administration and the heart rate difference.

Statistical analysis

Statistical software SAS was used for data processing. Data were expressed as mean ± standard deviations for continuous variables or n of patients (%) for categorical data. Variance analysis between groups was compared using the two-sample Student’s t-test for continuous variables. The Pearson’s chi-squared or Fisher’s exact test was used to analyze categorical data. The one-way ANCOVA (analysis of covariance) was used to analyze AUC. We used a P value threshold of 0.05 for

statistical significance.

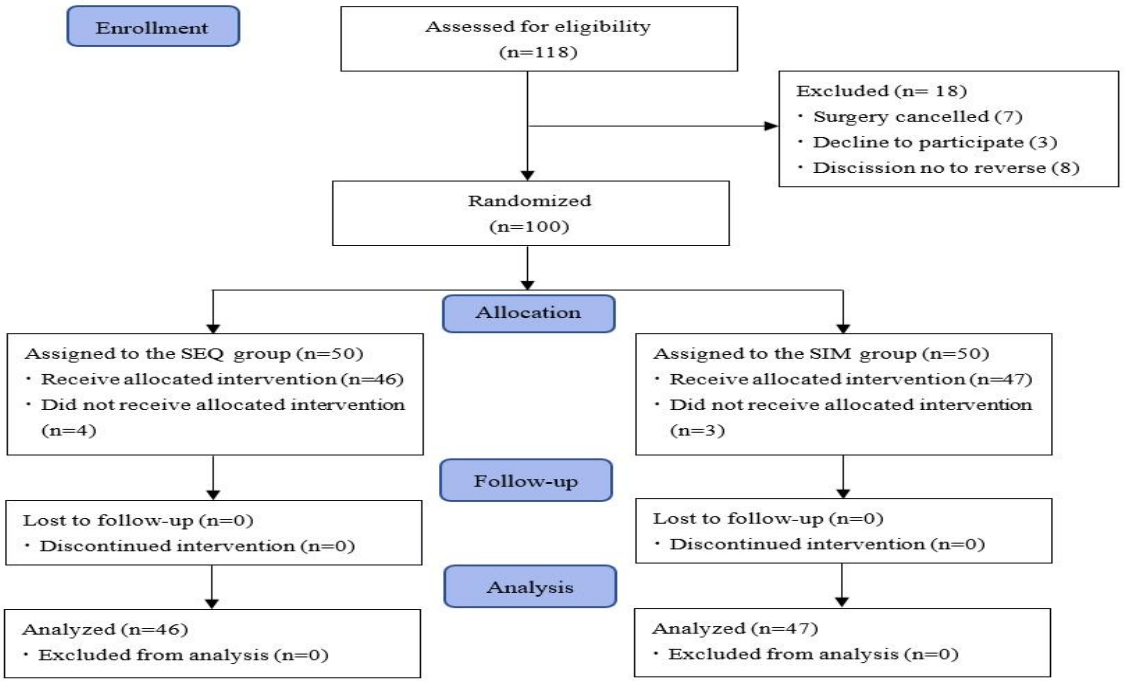

Figure 1. Consort flow diagram of the trial design

Results

(Figure 1) shows the trial design according to Consolidated Standards of Reporting Trials (CONSORT) guidelines. Ninety-three patients (n = 46 SEQ; n = 47 SIM) were finally analyzed. There was not any significant difference between groups in terms of demographic features and duration of surgery (P > 0.05) (Table 1).

Table 1. Demographic and clinical features

	Group	Group	p-value
Age (years)	47.8±11.2	47.0±11.4	0.75
Gender M/F (n)	25/21	20/27	0.26
ASA classification I/II (n)	13/33	18/29	0.31
Height (cm)	165.1±7.3	166.2±8.1	0.48
Weight (kg)	63.8±9.0	65.8±9.2	0.29
BMI (kg/m^2)	23.4±2.7	28.8±2.9	0.47
Duration of Surgery (min)	85.1±18.7	91.2±19.2	0.13

No significant difference was found in baseline heart rate. The AUC of heart rate difference within 15 minutes after administration in the SEQ group was 13.05±8.82 versus 43.56±10.54 in the SIM group (P<0.05). No differences were found in heart rate between the two groups at 1, 2, 3, 4, 5, 6, 7, and 8 minutes after administration (P>0.05). SIM group had a significantly lower heart rate when compared to SEQ group at 9, 10, 11, 12, 13, 14, and 15 minutes after administration (P<0.05) (Figure 2). There was no significant difference in heart rate difference at 1, 2, 3, 4, 5, 6, 7, and 8 minutes after administration (P>0.05). Heart rate difference was significantly smaller at 9, 10, 11, 12, 13, 14, and 15 minutes after administration in the SEQ group (P<0.05) (Figure 3).

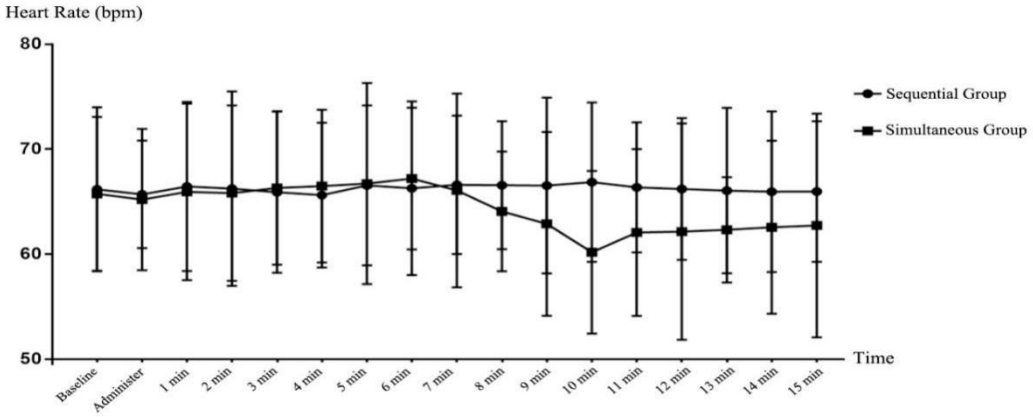

Figure 2. Comparison of heart rate.

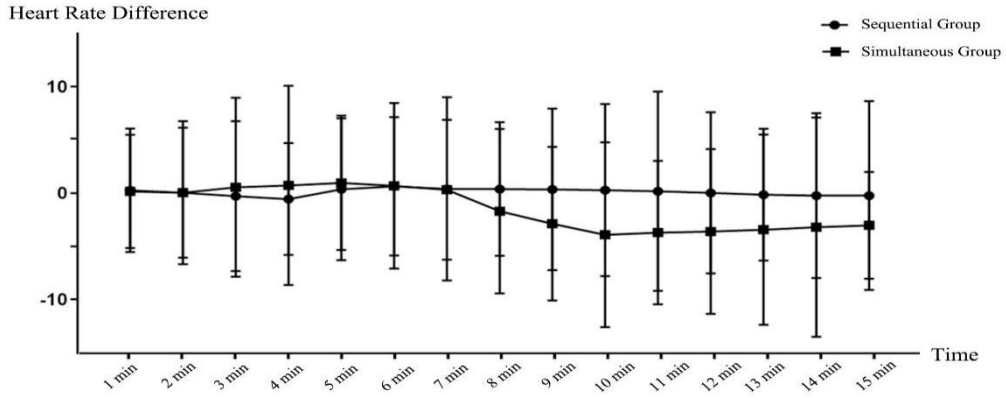

Figure 3. Comparison of heart rate difference

Discussion

By suppressing parasympathetic impacts on the heart, atropine raises the heart rate and improves atrioventricular conduction. The neostigmine-induced bradycardia is correlated with cholinesterase inhibition, or activating cholinergic receptors within the cardiac parasympathetic pathway [3]. the optimal administration mode has not been evaluated.

The effects of atropine develop more quickly than those of neostigmine. The degree and duration of tachycardia were significantly greater when atropine was administered first, followed by neostigmine, than simultaneous administration [4]. When atropine and neostigmine were provided in this order—neostigmine combined with small doses of atropine was administered first, followed by the remaining atropine—no early tachycardia was observed; later bradycardia could be prevented; and no serious arrhythmias had been encountered.

Conclusion

In our study, we observed that there was no significant tachycardia in either group. However, the simultaneous administration of the atropine-neostigmine mixtures subsequently reduced heart rate. Sequential administration, when atropine was administered later, induced smaller heart rate variability. Therefore, we suggest that sequential administration of neostigmine-atropine might be a safe option to reverse neuromuscular blockage. Atropine and neostigmine should be administered in this order: neostigmine combined with small doses of atropine was administered first, followed by the remaining atropine.

References

[1] Naguib M, Kopman AF, Ensor JE. Neuromuscular monitoring and postoperative residual curarisation: A meta-analysis. BJA. [J] British Journal of Anaesthesia. 2007;98:302-316.

[2] Thilen SR, Weigel WA, Todd MM, et al. 2023 american society of anesthesiologists practice guidelines for monitoring and antagonism of neuromuscular blockade: A report by the american society of anesthesiologists task force on neuromuscular blockade. [J] Anesthesiology. 2023;138:13-41.

[3] Backman SB, Stein RD, Blank DW, et al. Different properties of the bradycardia produced by neostigmine and edrophonium in the cat. [J] Canadian Journal of Anaesthesia. 1996;43:731-740.

[4] Ovassapian A. Effects of administration of atropine and neostigmine in man [J], Anesthesia & Analgesia. 1969;48:219-223.

Practical Application of Bayesian Network and Genetic Algorithm for Optimizing Antibiotic Management in Hospital Settings

Wenyan Zhu[1,*], Huiliang Zhai[2]

1. Department of Medical Record, Weishan People's Hospital, Jining 277600, China.

2. CVIC Software Engineering Co., Ltd. (CVICSE), Jinan 250014, China.

Abstract: With the widespread use and misuse of antibiotics, there's a lot of talk about antibiotic resistance crisis these days. Researching the antibiotic resistance crisis have become pressing. In the first five years, the market share of antibiotics and anti-drugs increases, while that of other drugs declines. However, after the first five years, the trend of anti-drugs and other drugs decreases, that of antibiotics blooms up meanwhile. If development of market is supported , early rising share of antibiotics and other drugs, not containing antibiotics continue to decline, in twentieth years the market is stable, with antibiotics having the advantage over others.

Keywords: Antibiotic Management System; Hospital Settings; Advanced Healthcare

1. Introduction

Since penicillin was used in clinic, a variety of antimicrobial agents have emerged, so that the global mortality of infectious diseases can be reduced. Yet with the widespread use and misuse of antibiotics, antibiotic resistance crisis has become the focus of global attention. Resistant bacteria could lead to serious consequences and some researchers are worried that we will enter a postantibiotic age, in which we are infected by bacteria that can defeat every drug medicine has to offer.

Actually, in 1945, Alexander Fleming warned that penicillin might become useless. Nevertheless, Scientists thought it just didn't seem to matter very much. Nowadays, the true threat of antibiotic resistance was growing even clearer. Because of the antibiotic resistance crisis, the United Nations will convene a highlevel meeting to coordinate the global fight against these invisible enemies. And our team,the ICMFDA will help develop a better understanding of the factors involved with antibiotic resistance crisis.

The misuse of antibiotics results from treatment of diseases and animal feed. The existence of the interest chain of antibiotic intensifies the antibiotic resistance crisis. Thereby to develop a model that provides a interest chain for use of antibiotics and the sensitivity of parties is needed. It is important to consider the dynamic nature of the factors that affect both supply and demand in our modeling process. The interest chain can determine reform targets and the sensitivity can help us realize how to cope with antibiotic resistance crisis. Perfect competitive market is a market structure in which competition is adequate without any hindrance or interference. It is critical to predict the developing trend towards the crisis under perfect competitive markets by set a model. By analyzing data, the trend towards the crisis with no government intervention and the trend can reflect the importance of the government intervention is gained.

Because of the emergence of super-bacterium, how to control the use of antibiotics has threatened the social health. And our term is asked to design a portable management system for the use of antibiotics which is the most urgent affair for

super-bacterium. Besides, it is a must to write a report on our model and propose a set of policies.

2. Materials and Methods

2.1 Bayesian Network

Let G≝IE represents a directed acyclic graph (DAG), which sets the I represents all the nodes in the graph, and E represents a connection to a collection of line segments, and let X=XiI and I for the random variable I of a node in the directed acyclic graph the representative, if the joint probability distribution of node X can be expressed as:

$$P(X)=i\in IPXiXpa(i) \quad (1)$$

Then X is called a Bayesian network with respect to acyclic graph G.

For arbitrary random variables, the joint distribution can be obtained by multiplying the local conditional probability distribution:

$$P(X1=x1,\cdots, Xn=xn)=i=1nPXi=xiXi+1=xi+1,\cdots, Xn=xn \quad (2)$$

In accordance with the above formula, a joint probability distribution of a Bayesian network could be assigned:

$$P(X1=x1,\cdots, Xn=xn)=i=1nPXi=xiXj=xj \quad (3)$$

The above two said of difference is that the conditional probability of the part in the Bayesian network, if its “cause” variables are known, some nodes with “because” and “only independent variables, dependent variable nodes will” conditional probability of existence. Markov blanket is a minimal feature subset that satisfies the following characteristics: a feature in its Markov blanket condition, and all other features in the feature domain

are independent. A Markov blanket feature of T MB(T), then this can be expressed as:

$$PTMB(T)=PTY,MB(T) \quad (4)$$

The Y for all non Markov blanket node characteristics in the domain. This is the most direct definition of Markov blanket. Form a Markov blanket feature in Bayesian network is the feature (i.e. the nodes) parent nodes, child nodes and child nodes of the parent node.

The maximum likelihood estimation method (MLE) is used to get the parameters. Its log likelihood function is:

$$L=1Ns=1ni=1slogPXipa(Xi),Di \quad (5)$$

Where pa(Xi)represents the Xi dependent variable, Di represents the first observation, N represents the total number of observations data.

2.2 Results

2.2.1 Genetic Algorithm and Its Characteristics

Genetic algorithm is a kind of reference biological evolutionary laws (survival of the fittest, survival of the fittest genetic mechanism) evolved random search method. This method aims to optimize the fitting function and get the result we need.The main characteristic is to operate directly on the structure of the object, there is no derivation and limited function continuity with global internal implicit parallelism and better optimization ability using probability optimization methods,automatically obtain and optimize the search space and adaptively adjust the search direction, not need to determine the rules. Finally, genetic algorithm is used to optimize the results.

Its steps are as follows:

1. Chromosome coding. Using binary code to encode the independent variables.
2. Initialization groups. The fitness value of the chromosome is calculated.
3. Copy operation.

4. Crossover operation.

5. Mutation operation.

6. Stop criterion.

2.2.2 Solving Bayesian Network

We construct the above relationship, each factor and the success rate will be one of the factors influencing the success, so we think that each factor of only two possible values: T (success) or F (failure).

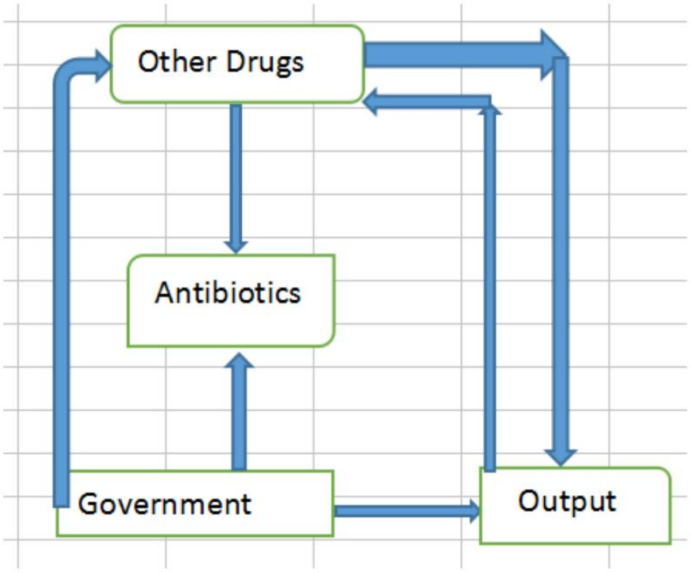

Figure 1 This caption shows the results of relationship between various factors.

The structure and parameters of Bayesian network is known, it is a must to use the maximum likelihood estimation method to calculate the probability of each node, and this probability is the degree of impact. Based on the data we have previously obtained, these probabilities is not difficult to get:

$$PX1=x1X2=x2=0.63 \quad (1)$$

$$PX2=x2X3=x3=0.45 \quad (2)$$

$$PX3=x3X1=x1=0.52 \quad (3)$$

Where X1 is for government, X2 for other drugs X3 for output.

3. Conclusion

With the development of science and technology,antibiotics has been widely used in the animal husbandry.Nowadays,the misuse of antibiotics in the animal husbandry is an important factor that effect the antibiotic resistance crisis. So we need to solve the problem of antibiotic abuse. Through the above analysis, we know that government intervention makes an important impact.

1.Encourage people to use antibiotic substitutes. Antibiotics can be regarded as growth stimulant and drugs. Many people misuse antibiotics to get more interest. Government has to find the antibiotic substitutes, and then set a reward policy. Generally, the antibiotic substitutes are more expensive, so the government must subsidize price differences. In order to encourage more farmers to use antibiotic substitutes, they should be given extra reward.

2.Control the dosage of antibiotics. The amount is also important. When antibiotic is used as growth stimulant, we can determine a specialized range. We know that growth cycle and profit are inversely proportional, and we should reward

farmers who use antibiotic in specialized range. In another hand, when it is used as drugs, farmers can increase the initial dose appropriately.

3.Control the usage of antibiotics. That is to say, we should determine the objects, usage, use period and withdrawal time. Proper usage and withdrawal time can not speed up the antibiotic resistance crisis. As for antibiotic drug residues, if it reach the standard, people should be rewarded.

4.Control the type of antibiotics. The government should divide illicit drugs and common drugs. If people use illicit drugs,they will be punished.

References

[1] Song TZ, Zhen XC, Gao W, Zhu W. Identification of potential driving genes in prostatic cancer using complex network analysis. Computer Methods in Biomechanics and Biomedical Engineering: Imaging & Visualization. 2022 Nov 2;10(6):616-21.

[2] Sun Z, Liu Y, Yu Y. China's carbon emission peak pre-2030: Exploring multi-scenario optimal low-carbon behaviors for China's regions. Journal of cleaner production. 2019 Sep 10;231:963-79.

[3] Song Z, Sun Z. Representing Functions in H 2 on the Kepler Manifold via WPOAFD Based on the Rational Approximation of Holomorphic Functions. Mathematics. 2022 Aug 2;10(15):2729.

[4] Sun Z. Total Energy Consumption Control based on Environmental ZSGDEA. Metallurgical & Mining Industry. 2015 May 1(5).

Tumor-Associated Macrophages in the Progression of Hepatocellular Carcinoma

Dingjie Liu, Yong Li

Zhuhai Interventional Medical Center, Zhuhai Precision Medical Center, Zhuhai Hospital Affiliated With Jinan University, Zhuhai Hospital Affliated With Jinan University (Zhuhai People's Hospital), Zhuhai 519000, China.

Abstract: Hepatocellular carcinoma (HCC) contains many immune cell matrices, which constitute the tumor microenvironment (TME). Tumor-associated macrophages (TAM) are the main compartments of immune cell matrix in HCC, which play an important role in the pathogenesis of HCC, including immunosuppression, angiogenesis, tumor invasion and metastasis, and malignant transformation of HCC stem cells. At present, targeted TAM therapy for HCC has achieved promising results by eliminating existing TAMs, blocking the recruitment of TAMs, reprogramming TAMs polarization, regulating TAMs products and restoring TAMs phagocytosis. This review summarizes our understanding of TAMs and HCC, and discusses the role of TAMs in the development of HCC.

Keywords: Tumor-Associated Macrophages; Immunotherapy; Hepatocellular Carcinoma

1. Introduction

Liver cancer is the fourth most common cause of cancer-related death worldwide, and its incidence is on the rise worldwide[1] . HCC is the most common type of liver cancer, accounting for about 90% of all cases. Compared with other common solid tumors, the prognosis of patients with HCC was poor, and the overall 5-year survival rate was 18%. Patients with early and medium-term HCC can receive a variety of effective treatments, including surgical hepatectomy, liver transplantation, ablation and transcatheter arterial chemoembolization.However, The main treatment for advanced HCC is systematic therapy, including tyrosine kinase inhibitors sorafenib, lamvatinib and immune checkpoint blockers (ICBS) [2].However, suppression of immune checkpoints with anti-EGFR antibodies atrizumab and bevacizumab has become a first-line treatment for patients with advanced liver cancer [2] . TME consists of many components that coexist and interact with each other, including tumor-associated macrophages, CD4 and CD8 T cells, dendritic cells (DC), natural killer (NK) cells, tumor-associated endothelial cells (EC), abnormal tumor vascular system, cancer-associated fibroblasts (CAF) and myelogenic immunosuppressive cells (MDSC). TME is a dynamic environment coordinated by multiple cells and non-cells, and each component or component hopefully represents a potential indicator of re-editing TME [3] . However, as one of the most abundant immune cells in infiltrating TME, TAM exists in all stages of liver cancer progression.

As far as we know, the interaction, potential mechanism and therapeutic effect of TAMs on HCC regulation have not been fully understood and rarely reported. In this review, we aim to provide the latest and comprehensive updates on TAM in HCC. And focuses on the role of TAMs in HCC, to provide a solid theoretical basis for the discovery of related targeted drugs.

2. Activation and activation of TAM in microenvironment of hepatocellular carcinoma

TAM is recruited and activated by different chemokines in the TME of HCC and differentiates into specific polarization forms related to specific pathological conditions. According to the state and function of macrophage activation, macrophages can be divided into two different polarization states: classical activated M1 macrophages and alternately activated M2 macrophages[4]. The two forms of polarization are interchangeable under certain circumstances and in the presence of certain stimuli. M1 macrophages usually play a pro-inflammatory role and secrete a large number of pro-inflammatory cytokines. Classical macrophage activation occurs when cells are stimulated by:1) lipopolysaccharide, a component of the cell wall of Gram-negative bacteria; 2) IFN- γ released by NK cells and type 1 T helper cells (Th1);3) tumor necrosis factor (TNF); 4) granulocyte macrophage colony stimulating factor (GM-CSF) ; 5) Toll-like receptor (TLR) ligands [5] . Activated M1 macrophages secrete some interleukines, chemokines and TNF- α to induce pro-inflammatory effects.

In contrast, M2 macrophages usually perform the opposite function as M1 macrophages. Cytokines IL-4, IL-10, IL-13 and transforming growth factor β (TGF- β) are secreted by Th2 cells and tumor cells. CSF1 and prostaglandin E2 (PGE2) can induce alternative activation of macrophages and lead to M2 polarization phenotype. M2 macrophages can secrete several complex immunosuppressive factors, cytokines and growth factors, regulate Th-2 immune response, promote tumor cell growth and participate in tumor angiogenesis [6] .

3. M1-TAM and liver cancer

Classical activated macrophages show anticancer properties. In HCC, M1 can inhibit tumor progression through various mechanisms. Expression of sirtuin1 in hepatoma cells regulates M1 polarization through NF- κB pathway[7].In addition, monocytes overexpressing IL-12 can down-regulate phosphorylated signal transducers and activators of transcription 3 (p-STAT-3) and c-Myc to differentiate into M1 and inhibit HCC growth. However, M1 also shows a positive correlation with cancer, and this abnormal mechanism is relatively rare. For example, M1 macrophages secrete IL-1 β to activate hepatoma cells and induce PD-L1 expression through transcription factors IRF1 and NF- κB [8] . Therefore, M1-TAM and M2-TAM are not always mutually exclusive; On the contrary, these two types of cells often coexist in TME. So these two types of macrophages cannot be considered to be completely different macrophage populations. The preferred function of mixed TAMs phenotype depends on the balance between macrophage activation and inhibition and immune microenvironment.

4. M2-TAM and HCC

4.1 M2-TAM promotes proliferation, invasiveness and metastasis of cancer cells

Although most studies have focused on tumor-derived exosomes, the existence of TAM-derived exosomes is necessary for tumor progression and metastasis. Alternatively, activated (M2) macrophages can secrete cytokines CCL2 to enhance tumor invasion and induce epithelial mesenchymal transformation (EMT) through Smad2/3 and Smad1/5/8 activation and snail upregulation[9] . In addition, CCL2 secreted by M1 macrophages is closely related to tumor dryness and EMT in TGF-β 1 and Wnt/ β catenin signaling pathways [10]. In vitro data show that M2-TAMs coordinates the immune microenvironment of iCCA by secreting various cytokines (such as TNF- α, ICAM-1,IL-6) and regulating EMT of cancer cells [10] . Interestingly, enhanced communication between TAM and tumor-related cells also promotes cancer invasion and metastasis.

The above studies show that macrophages play an exciting role in tumorigenesis. Therefore, an attractive therapeutic strategy for HCC may be to block the communication between M2-TAM and HCC cells, such as the use of non-coding RNA inhibitors and TAMs receptor inhibitors.

4.2 M2 TAM stimulates angiogenesis of HCC

Because of the angiogenic nature of most HCC tumors, angiogenesis is very important for the occurrence and metastasis of HCC. Angiogenesis in HCC is a multidimensional process coordinated by HCC cells and a series of tumor-associated stromal cells, including TAM and its bioactive products. In recent years, monocyte / macrophage subsets characterized by tyrosine kinase receptor Tie-2 expression have attracted much attention. TEM is mainly concentrated in the perivascular area of tumor tissue and participates in HCC angiogenesis.Macrophage population and phenotype were positively correlated with angiogenesis and clinical prognosis of HCC. CCR+2TAM is more abundant in the margin of highly vascularized HCC, while the lack of CCR2TAM infiltration can reduce pathogenic vascularization [11] . A case-control study showed that CD14 inflammatory macrophages secrete a large amount of IL-23 after stimulation of hepatitis virus-infected hepatocytes, accompanied by up-regulation of IL-23 receptors and strong macrophage-associated angiogenesis [12].

The angiogenic characteristics of TAMs and the angiogenic mimics in TME are the root causes of poor prognosis of tumor patients. In the preclinical model, the accumulation of macrophages is related to the emergence of drug resistance to anti-VEGF therapy [13]. The escape of VEGF targeted therapy may be due to the down-regulation of VEGFR-1 and VEGFR-3 and the up-regulation of angiogenesis-promoting genes. This key finding suggests that the use of VEGF blockers in combination with macrophage blockers, such as CSF1 or CCR2 inhibitors, can enhance the anti-VEGF therapeutic response.

5. Future and prospect

Although the preclinical and clinical studies of TAM provide encouraging results, there are still some challenges in using macrophages as targeted therapy for liver cancer. First, most TAM studies are limited to animal models. There is considerable heterogeneity between mouse model and human in pathogenesis and response to drug treatment. Secondly, due to the diversity of the origin of macrophages and the heterogeneity after differentiation, TAM shows different characteristics in different stages. It seems that the use of specific blockers is not sufficient to overcome liver malignant tumors,such as CSF1 blocking for all macrophages, resulting in systemic toxicity. Third, checkpoint blocking on the surface of macrophages is currently limited to PD-L1. Several novel immune checkpoints are expressed on the surface of macrophages, such as SIRP α and Tim-3. Finally, the elimination of TAM seems to lead to the compensatory appearance of other immunosuppressive cells. Therefore, TAM elimination also requires compensation for other immunosuppressive cells, such as Tregs and MDSC, which are only resistant to targeted TAM.

This article describes the origin of TAMs, the communication between TAMs and surrounding cells and the latest progress in treatment, which provides more options and substantial evidence for targeted macrophage therapy for patients with HCC. In the future, drugs targeting macrophages in the specific immune environment of the liver and more stable, safe and efficient immunotherapy can promote the further development of immunotherapy for HCC.

References

[1] Vogel A, Meyer T, Sapisochin G, et al. Hepatocellular carcinoma [J]. Lancet, 2022, 400(10360): 1345-62.

[2] Foerster F, Gairing SJ, Ilyas SI, et al. Emerging immunotherapy for HCC: A guide for hepatologists [J]. Hepatology, 2022, 75(6): 1604-26.

[3] Cheng K, Cai N, Zhu J, et al. Tumor-associated macrophages in liver cancer: From mechanisms to therapy [J]. Cancer Commun (Lond), 2022, 42(11): 1112-40.

[4] Li Z, Wu T, Zheng B, et al. Individualized precision treatment: Targeting TAM in HCC [J]. Cancer Lett, 2019, 458(86-91.

[5] Ivashkiv LB. IFNγ: signalling, epigenetics and roles in immunity, metabolism, disease and cancer immunotherapy [J]. Nat Rev Immunol, 2018, 18(9): 545-58.

[6] Mantovani A, Marchesi F, Malesci A, et al. Tumour-associated macrophages as treatment targets in oncology [J]. Nat Rev Clin Oncol, 2017, 14(7): 399-416.

[7] Zhou B, Yang Y, Li C. SIRT1 inhibits hepatocellular carcinoma metastasis by promoting M1 macrophage polarization via NF-κB pathway [J]. Onco Targets Ther, 2019, 12(2519-29.

[8] Zong Z, Zou J, Mao R, et al. M1 Macrophages Induce PD-L1 Expression in Hepatocellular Carcinoma Cells Through IL-1β Signaling [J]. Front Immunol, 2019, 10(1643.

[9] Zhu F, Li X, Chen S, et al. Tumor-associated macrophage or chemokine ligand CCL17 positively regulates the tumorigenesis of hepatocellular carcinoma [J]. Med Oncol, 2016, 33(2): 17.

[10] Sun D, Luo T, Dong P, et al. M2-polarized tumor-associated macrophages promote epithelial-mesenchymal transition via activation of the AKT3/PRAS40 signaling pathway in intrahepatic cholangiocarcinoma [J]. J Cell Biochem, 2020, 121(4): 2828-38.

[11] Bartneck M, Schrammen PL, Möckel D, et al. The CCR2(+) Macrophage Subset Promotes Pathogenic Angiogenesis for Tumor Vascularization in Fibrotic Livers [J]. Cell Mol Gastroenterol Hepatol, 2019, 7(2): 371-90.

[12] Zang M, Li Y, He H, et al. IL-23 production of liver inflammatory macrophages to damaged hepatocytes promotes hepatocellular carcinoma development after chronic hepatitis B virus infection [J]. Biochim Biophys Acta Mol Basis Dis, 2018, 1864(12): 3759-70.

[13] Dalton HJ, Pradeep S, Mcguire M, et al. Macrophages Facilitate Resistance to Anti-VEGF Therapy by Altered VEGFR Expression [J]. Clin Cancer Res, 2017, 23(22): 7034-46.

*:Correspondence: Yong Li

Telescoping Tubridge flow diverter treatment in giant middle cerebral artery fusiform aneurysm

Hetai Lai
Zhuhai Hospital Affiliated With Jinan University (Zhuhai People's Hospital), Zhuhai 519000, China.

Abstract: Giant fusiform aneurysm of the middle cerebral artery is a rare lesion with a high risk of rupture and high mortality, which is more difficult to treat either surgically or endovascularly. We report a case of a giant middle cerebral artery (MCA) M1 segmental fusiform aneurysm treated with the Tubridge Flow Diverter (TFD) telescoping technique alone without coil embolization. The patient had a single TFD implanted initially after the accidental discovery of a giant left MCA fusiform aneurysm, and after 3 months of postoperative shortening of the proximal end of the TFD and no significant healing of the aneurysm, a second TFD was implanted in the second stage by Telescoping technique. the aneurysm healed completely at 6 and 18 months after procedure, with no significant complications during follow-up.

Keywords: Flow Diverter; Endovascular Treatment; Middle Cerebral Artery; Fusiform Aneurysm; Tubridige

Introduction

Intracranial fusiform aneurysms are characterized by low morbidity, high bleeding rate, high mortality and technical difficulty.[1, 2] Flow diverters (FD) have gradually become one of the best options for the treatment of fusiform aneurysms,[3, 4]of which, the most used are Pipeline embolization diverters (PED) and Tubridge flow diverters (TFD). The treatment is mostly coil embolization combined with a single FD implant. However, fusiform MCA aneurysms are at greater risk of penetrating infarction and generally heal less efficiently than posterior circulation aneurysms due to their origin in the penetrating ductus arteriosus.[5] In addition, fusiform aneurysms have long necks and may have incomplete coverage with a single FD length. Thus, Liu et al. reported cases of fusiform aneurysms treated by telescoping FD technique, the majority of which were combined with coil embolization and were predominantly located in the posterior circulation.[6] In this case, we report the successful treatment of MCA fusiform aneurysm with telescoping FD without coil embolization, and the patient has a good prognosis.

Case report

A 29-year-old man with no previous history of underlying medical conditions had a left middle cerebral artery fusiform aneurysm (Figure1 A) discovered unexpectedly during the completion of cranial magnetic resonance (MR) in the course of treatment for a middle ear cholesteatoma, followed by the completion of magnetic resonance artery (Figure1 B). A digital subtraction angiogram (DSA) was performed, which showed a cloacal aneurysm (Figure1 C, D) measuring 35.4 × 10.6 mm in the left M1 segment of the MCA.

Before treatment, the CYP2C19 genetic test showed a good response to aspirin (ASA) and clopidogrel. The patient was given ASA (100mg daily) and clopidogrel (75mg daily) five days before the procedure. Thromboelastograms (TEGs) was performed in the patient to evaluate the efficacy of platelet inhibition. A 8F Cordis, Fremont, California, USA) was placed at the C1 end of the left internal carotid artery. With the cooperation of a 5F MidAccess catheter(125 cm, Passageway, CHINA)

and 0.014 micro-guide wire (200 cm, Stryker, USA), a T-track stent catheter (MicroPort, Shanghai) was introduced in the ipsilateral MCA M3. A Tubridge stent (4.0 × 45 mm, MicroPort, China) was released from the MCA M2 segment to the M1 segment (Figure2 A～D). No significant abnormality was seen on the 24h postoperative reexamination of the Computed Tomography. The patient was discharged without complication and the mRS score: 0. Regular medication was taken after discharge.

Three months later, DSA showed no healing of the MCA fusiform aneurysm (Figure3 A), shortening of the proximal end of the stent, and visible stenosis of the distal vessel (Figure3 B). Further treatment by TFD bridging was decided after discussion. During the procedure, a Tubridge FD (4.0 × 45 mm) was released in the M1 segment of the MCA (Figure3 C). The stent was released completely and the contrast was visible on imaging with significant retention of contrast (Figure3 D). The patient was discharged without any complication.

Six months after telescoping, DSA showed that the fusiform aneurysm was significantly reduced and the distal stenosis was improved (Figure4 A, B). And the DSA was reexamined at 18 months, showing complete healing of the aneurysm (Figure4 C, D).

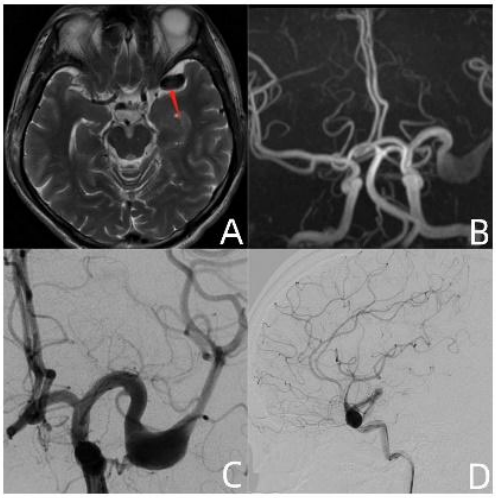

Figure1: (A) and (B) magnetic resonance of the giant middle cerebral artery fusiform aneurysm. (C) and (D) before the procedure, anteroposterior and lateral angiography of the left internal carotid artery.

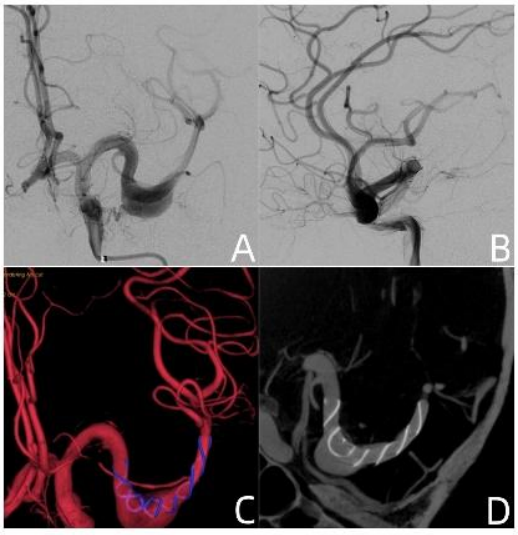

Figure2:（A）and (B) after the procedure, anteroposterior and lateral angiographies of the left internal carotid artery. (C) and

(D) the FD was completely opened and released well.

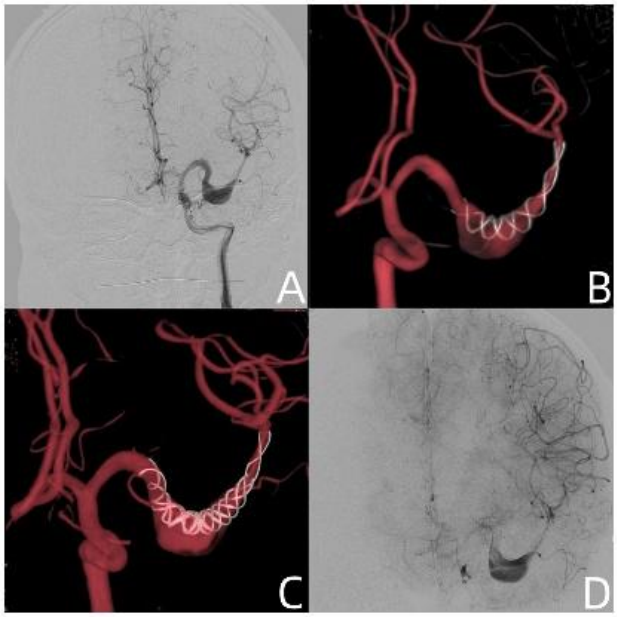

Figure3: （A）no significant healing of the aneurysm. (B) shortening of the proximal end of the stent, and visible stenosis of the distal vessel. (C) after the treatment of telescoping FD. (D) significant contrast stagnation within the aneurysm can be seen.

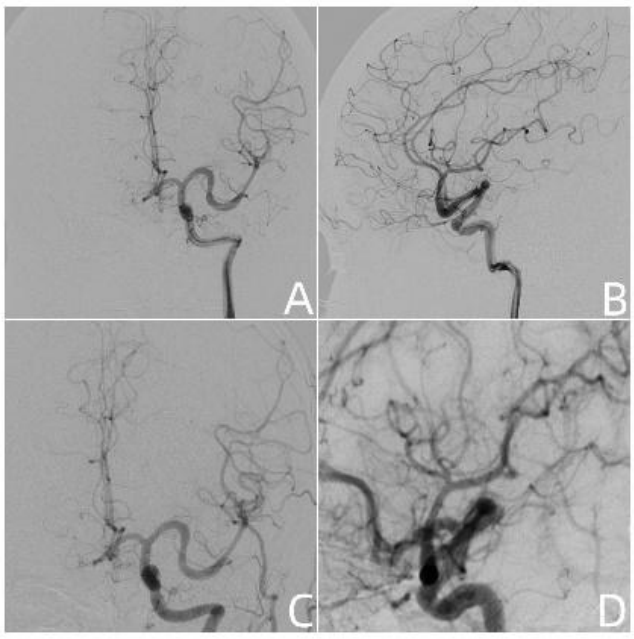

Figure4: (A) and (B) 6 month later, anteroposterior and lateral angiographies of the left internal carotid artery. (C) and (D) the angiographies still showed a complete healing.

Discussion

MCA giant fusiform aneurysms are relatively rare in clinical practice, and there is no standard treatment option. The healing efficiency of conventional stent-assisted embolization for fusiform aneurysms is low because of the long aneurysm

neck that is difficult to embolize densely, as well as the low metal coverage of conventional stents and slow intra-aneurysm thrombus formation. FD is generally safe and effective when applied to fusiform aneurysms, with neurological morbidity/mortality ranging from 4 to 8% and aneurysm occlusion rates of 59-75%.[3, 4, 7] Chalouhi et al. reported that the application of multiple FD to the same unruptured aneurysm would not only increase the technical difficulty of the procedure but also further increase the rate of complications.[8] However, limited by the size of the FD and the potential for shortening, not all fusiform aneurysms can be well occluded by a single FD. In addition, the telescoping FD technique increases metal coverage, which can reduce intra-aneurysmal flow velocity by up to 30%, accelerating aneurysm healing and reducing the risk of rupture bleeding. [9, 10]

The application of telescoping FD techniques to MCA fusiform aneurysms is currently reported to be limited and is mostly based on coil embolization. Ikeda et al. reported the successful treatment of M2 segment fusiform aneurysms with 3 telescopic PEDs. [2] Although Liu et al. reported 2 cases related to MCA aneurysms, one of them used coil embolization and the other case was unknown. To our knowledge, this is the first report of a giant fusiform aneurysm of MCA treated with telescoping TFD alone. In this report, we chose TFD mainly because of the large size of this aneurysm and the fact that the stent is more likely to shorten or even fall off intraoperatively or during the follow-up period when FD is applied to shuttle aneurysms, resulting in incomplete coverage of the aneurysm and preventing intra-aneurysmal thrombosis. [6, 11] The TFD has longer dimensions, stronger radial force and higher metal coverage than the PED, and its safety and effectiveness have been proven. [12] In telescoping technology, it is important to understand the characteristics of FD.

It has been shown that FD apposition is associated not only with aneurysm healing efficiency, but also with in-stent restenosis during the follow-up period. [13, 14] Our experience is that after the telescope technique, there may be poor apposition between the two FD's. Therefore, a "J" wire technique is used to promote apposition, and balloon dilation is used when necessary. In addition, the extent of FD telescope should be increased as much as possible to ensure coverage of the aneurysm neck, which is beneficial for improving metal coverage and the healing process. It has been suggested that the overlapping FD technique will greatly increase the incidence of occlusion of the penetrating artery or in-stent thrombosis , [3] which may be due to a wide aneurysm neck (>20 mm) or insufficient dual anti-platelet aggregation effect. In this case, we followed the approach and extended the patient's time on dual antiplatelet agents until complete healing of the aneurysm, which may be the reason why we were able to keep the patient free of ischemic complications during the follow-up period.

Overall, we report a case of a giant fusiform aneurysm in MCA treated with TFD telescoping technique alone. Future multicenter, large sample, prospective cohort studies are needed to confirm this finding.

References

[1] Xu F, Xu B, Huang L, et al. Surgical Treatment of Large or Giant Fusiform Middle Cerebral Artery Aneurysms: A Case Series [J]. World Neurosurg, 2018, 115(e252-e62.

[2] Ikeda DS, Marlin ES, Shaw A, et al. Successful endovascular reconstruction of a recurrent giant middle cerebral artery aneurysm with multiple telescoping flow diverters in a pediatric patient [J]. Pediatr Neurosurg, 2015, 50(2): 88-93.

[3] Griffin A, Lerner E, Zuchowski A, et al. Flow diversion of fusiform intracranial aneurysms [J]. Neurosurg Rev, 2021, 44(3): 1471-8.

[4] Monteith SJ, Tsimpas A, Dumont AS, et al. Endovascular treatment of fusiform cerebral aneurysms with the Pipeline Embolization Device [J]. J Neurosurg, 2014, 120(4): 945-54.

[5] Xu C, Wu P, Zou L, et al. Anterior Circulation Fusiform Aneurysms Have a Lower Occlusion Rate After Pipeline Embolization Device Treatment Than Posterior Circulation Fusiform Aneurysms: A Multicenter Cohort Study [J]. Front Neurol, 2022, 13(925115.

[6] Tang H, Shang C, Hua W, et al. The 8-year single-center experience of telescoping flow diverter for complex

intracranial aneurysms treatment [J]. J Clin Neurosci, 2022, 100(131-7.

[7] Fischer S, Perez M A, Kurre W, et al. Pipeline embolization device for the treatment of intra- and extracranial fusiform and dissecting aneurysms: initial experience and long-term follow-up [J]. Neurosurgery, 2014, 75(4): 364-74; discussion 74.

[8] Chalouhi N, Tjoumakaris S, Phillips JL, et al. A single pipeline embolization device is sufficient for treatment of intracranial aneurysms [J]. AJNR Am J Neuroradiol, 2014, 35(8): 1562-6.

[9] Damiano RJ, Ma D, Xiang J, et al. Finite element modeling of endovascular coiling and flow diversion enables hemodynamic prediction of complex treatment strategies for intracranial aneurysm [J]. J Biomech, 2015, 48(12): 3332-40.

[10] Uchiyama Y, Fujimura S, Takao H, et al. Hemodynamic Investigation of the Effectiveness of a Two Overlapping Flow Diverter Configuration for Cerebral Aneurysm Treatment [J]. Bioengineering (Basel), 2021, 8(10).

[11] Miyachi S, Hiramatsu R, Ohnishi H, et al. Usefulness of the Pipeline Embolic Device for Large and Giant Carotid Cavernous Aneurysms [J]. Neurointervention, 2017, 12(2): 83-90.

[12] Xie D, Zhao L, Liu H, et al. Tubridge Flow Diverter for the Treatment of Unruptured Dissecting Cerebral Aneurysms [J]. World Neurosurg, 2023.

[13] Liu JM, Zhou Y, Li Y, et al. Parent Artery Reconstruction for Large or Giant Cerebral Aneurysms Using the Tubridge Flow Diverter: A Multicenter, Randomized, Controlled Clinical Trial (PARAT) [J]. AJNR Am J Neuroradiol, 2018, 39(5): 807-16.

[14] Aquarius R, De Korte A, Smits D, et al. The Importance of Wall Apposition in Flow Diverters [J]. Neurosurgery, 2019, 84(3): 804-10.

Summary of Experimental Studies on the Effects of RDPR on the Cardiovascular System

Wen Bao
People's Country Peptide Group Co. LTD, Beijing 100000, China.

Abstract: As a special diet, it has a relatively large number of study compared with other health foods. The scope includes basic and animal experiments, studies in healthy populations, people with cardiovascular risk factors, and patients with vascular diseases. Related studies show that erythrospinal peptide has certain effects of antiplatelet aggregation, dissolving thrombosis in vitro, lowering blood pressure, lowering blood lipid, and enhancing immunity.

Keywords*:* Red Myelpeptide Cardiovascular System Immune Function; Clinical Application

Foreword

In order to scientifically and specifically reflect the safety and effectiveness of peptide, and better regulate and guide the application of peptide, people's Peptide Group and experts continuously tracked and collected the latest basic and clinical research results of peptide to complete this article.

This article focuses on three issues: concepts related to blood peptide, red myelpeptide and yak bone peptide, suitable population for red myelpeptide, and clinical trials of red myelpeptide on cardiovascular system risk factors.

This article uses scientific methods to evaluate the safety and effectiveness of erythropeptide in people at risk of vascular disease, so as to provide scientific basis for clinicians' recommendation, marketing and public science popularization.

1. Research background

As a special diet, it has relatively many research results compared with other special meals, and these research results become the basis and basis of this article.

There are many kinds of special dietary markets in China, but most of them lack scientific and standardized evaluation of their safety and effectiveness, which puzzles the recommendation of clinicians and nutrition experts, marketing and public selection. This article expounds the scientific research process and methods of health food at home and abroad, which can not only help domestic clinicians and nutrition experts to understand and guide the public to use red marrow peptide more objectively, but also provide methodological reference for future research of similar products. As a research method, the experimental study of the effect of red marrow peptide on the cardiovascular system will continuously absorb the latest research results of the product, continuously update the content, and provide comprehensive, latest and objective research ideas and evidence.

2. Concept related to blood peptide, red oid peptide and yak bone peptide

Red peptide peptide was extracted from the bone marrow of young yaks. The total amount of a single young yak was 1800 grams, the proportion of living extraction was 10%, the proportion of red peptide was 1%, and the total amount of a

single young yak was only 1.8 grams. However, red marrow peptide is very easy to be inactivated by high temperature, and the development of new secret technology can better maintain the activity of peptides. The active substance was stored in more than 97% after encountering water. After expert research, red myelin peptide can supplement red bone marrow and activate hematopoietic function.

Blood peptide is a kind of active peptides with biological function obtained after enzymatic processing of animal blood.

Animal blood is rich in protein, and protein is one of the important nutrients needed by human, animal blood after centrifugal separation, enzyme, decolorization, filtration, sterilization and other steps of biological active peptides, with general active peptides has involved in nerve and immune regulation, antihypertensive, remove free radicals, improve the function of food flavor, heme peptide heme called high iron, is an important iron channel, has been proved by the pharmacological experiments that heme against anemia function curative effect is better, and heme iron can be directly absorbed by intestinal mucosal cells, high biological utilization. Polypeptide fragments with antibacterial activity in blood peptide can improve immunity and accelerate the healing ability of wounds. The superoxide dismutase (SOD) contained in blood peptide is an excellent free radical scavenger, which has anti-radiation and anti-inflammation effects.

Yak bone peptide has promoted the effect of the collagen in the body, and can regulate the metabolism and growth of bone, can participate in bone calcium absorption and release, promote due to dysplasia or trauma, and caused by osteoporosis and damage, promote the formation of callus, and attached around the formation of new blood vessels, can promote its healing, give adequate nutrition.

Yak bone peptide is mainly a kind of nutrient purified from the plateau yak. It is very rich in amino acids, collagen, a variety of trace elements and minerals, and is very rich in nutrients.

3. Suitable population for erythrospinal peptide

In 2016, the European Food Safety Agency (European Food Safety Authority, EFSA) recommended blood peptide as a food supplement with a maximum recommended intake of 10g for healthy men and women aged> 35 years, excluding pregnant and lactating women.

In the study, erythromyelpeptide had anticoagulation, antiplatelet aggregation, reducing blood pressure and blood lipid, and also had a certain role in stroke patients. Therefore, this paper expanded the adaptive population to those with risk factors for vascular disease and patients with vascular disease.

Expert proposes

① Erymyelpeptide can be used in healthy people> 35 years, except pregnant and lactating women.(B ， IIc)

② Hempeptide is used in people with vascular disease risk factors, including hypertension, hyperlipidemia, atherosclerosis and stroke patients may benefit.

4. Clinical application

There are three main types of thromboembolic diseases: (1) thrombosis in coronary artery disease, mainly referring to acute myocardial infarction (AMI); (2) thrombosis in cerebrovascular diseases, that is, cerebral thrombosis and stroke; (3) thrombosis in peripheral arteriovenous diseases, that is, vascular embolism.

Ischemic encephalopathy Ischemic encephalopathy (ischemic stroke) includes transient ischemic attack, cerebral thrombosis and cerebral infarction, and its incidence and disability rate are the first of all diseases. It has been established that the high viscosity syndrome is an important factor inducing hemiplegia.

Red marrow peptide, is a kind of composed of blood peptide, red marrow peptide and yak bone peptide products, blood peptide is considered more institutions are more suitable for purify blood peptide substances, red marrow peptide has added

red bone marrow and activate hematopoietic function and yak bone peptide has repair blood environment, reduce blood lipids, restore elastic blood pressure, 2 it is with special affinity, can combine with fibrin fibrin can degrade quickly, but also can reduce the blood viscosity, improve blood oxygen saturation, improve microcirculation, is a way of prevention and restore cerebral infarction safer good choice. In order to prevent or reduce cerebral thrombosis, erythrospinal peptide was used for intervention, and the expert group observed more than 200 patients with cerebral infarction, and the treatment effect was certain. Compared with coenzyme Q10 and natto kinase verkinase mixture alone (Table 1), the effective rate and significant efficiency were significantly improved compared with the control group, with the total effective rate reaching 41.21% and the significant efficiency reaching 31.01%, which was difficult to achieve for other equivalent substances. Erymyelpeptide has obvious effect on the recovery of multiple functions of the blood system. To reduce the plaque area, improve the indicators of blood rheology, and improve ester metabolism, especially the decrease of triglyceride is the most optimal, therefore, erymyelpeptide has the effect of anticoagulation thrombolysis and anti-atherosclerosis formation.

Table 1 Red myelpeptide and coenzyme Q10 and nattokinase vermikinase mixture before and after administration

control group	cholesterol total (TC)	Triacylglycerol (TC)	High-density lipoprotein cholesterol (HDL-C)	Low-density lipoprotein cholesterol (LDL-C)	Apo A 1 (Apo A1)	Apolipoprotein B (ApoB)
Red medullary peptide	5.71 mmol/L	1.64 mmol/L	1.38 mmol/L	3.4 mmol/L	1.59 g/L	1.06 g/L
Coenzyme Q10	7.23mmol/L	1.71 mmol/L	1.39 mmol/L	4.33 mmol/L	1.60 g/L	1.05 g/L
Nattokinase lumbrokinase mixture	6.91 mmol/L	1.76 mmol/L	1.55 mmol/L	3.4 mmol/L	1.60 g/L	1.10 g/L

Acute myocardial infarction combined with hyperfibrinogenemia fibrinogen and its degradation products can act on the vascular wall, thus making the smooth muscle cells attached to it, aggravating atherosclerosis, and can directly participate in the formation of plaque and thrombosis. Therefore, it is very important to correct the hyperfibrinogenemia of coronary heart disease. The myocardial infarction was treated with Hpeptide in 24 cases, and blood fibrinogen was measured before and after medication. It was found that the blood fibrinogen content decreased significantly after 2 weeks and further decreased after 3 weeks. There was also a difference between the group and the control group ($P < 0.07$). And no obvious adverse reactions, can be considered as a prevention product of coronary heart disease.

Carotid atherosclerotic plaque involvement of the carotid artery leads to artery stenosis or even occlusion, resulting in cerebral ischemia and stroke symptoms, severe hemiplegia aphasia and even life-threatening. In 26-assisted statins administered before and after peptide administration, studies were shown to reduce plaque volume by approximately 10%. And concluded that statin-assisted Hpeptide can reverse atherosclerosis and plaque. Clinically, after taking, the vascular plaque is reversed and the vascular lumen stenosis is reduced, and there is no obvious adverse reactions, but it must be matched with a healthy lifestyle.

Platelets in diabetic patients are in an activated state, and platelet adhesion and aggregation function increase, which is one of the reasons for the early occurrence and high incidence of arteriosclerosis in diabetic patients and the easily complicated microvascular lesions. Plasma GMP140 is one of the activation and release products of platelets or endothelial cells. Studies have shown that the determination of GMP140 content in plasma can also reflect the activation degree and thrombosis tendency of platelets in vivo, while TXB 2 is the metabolic end product of TXA 2, which has a strong effect on

promoting platelet aggregation and vasoconstrictor. Studies have shown that erythromyelpeptide has some effect in inhibiting platelet activation in diabetic patients.

Erymyelpeptide can significantly improve hematological indexes in patients after stroke. In a randomized double-blind, placebo-controlled prospective study, experts randomized 18 patients with ischemic cerebrovascular disease into 9 patients in treatment group and 9 patients in control group. Oral erymyelpeptide was measured twice daily before administration, 3 months and 6 months. Results After administration, whole blood viscosity, plasma viscosity, platelet aggregation rate, red blood cell aggregation index and fibrinogen content were the most significant at 6 months, with no change in the control group.

Special attention

This product must be taken before meals, in order to play a good effect, and pregnant women and lactating women with caution.

In conclusion, erythromyelin is thrombolytic in clinical oral administration. Subject coagulation activity and in vitro thrombosis has a trend of decrease or inhibition, and no obvious effect on platelet quantity and aggregation rate, is a safe, effective special diet, with the understanding of intestinal absorption mechanism, the deepening of gene structure and function research, for the clinical application and dosage form improvement provide theoretical basis, shows its better application prospects.

5. Conclusion

The effects of red myeloid peptide on cardiovascular disease are multifaceted and multi-target. This active polypeptide is of great help to the renewal of cardiovascular and cerebrovascular vessels and blood vessels and the improvement of anemia. Among them, the red myeloid cells play an irreplaceable role in the human immunity and the replacement and supplement of blood system.

References

[1] Muthuraju S, Maiti P, Solanki P, et al. Acetylcholinesterase inhibitors enhance cognitive functions in rats following hypobaric hypoxia[J]. Behavioral Brain Research, 2009, 203: 114.

[2] Shukitt-Hale B, Stillman MJ, Welch DI, et al.Hypobaric hypoxia impairs spatial memory in an elevation-depen dent fashion[J]. Behavioral Neural Biology, 1994, 62: 244-252.

[3] Master S, Gottstein J, Blei AT. Cerebral blood flow and the development of ammonia-induced brain edema in rats after portacaval anastomosis[J]. Hepatology, 1999, 30: 876880.

[4] Bailey DM, Davies B. Acute mountain sickness: prophylactic benefits of antioxidant vitamin supplementation at high altitude[J]. High Altitude Medicine and Biology, 2001, 2(1): 21-29.

[5] Fan PC, Ma HP, Jing LL, et al.The antioxidative effect of a novel free radical scavenger 4’-hydroxyl-2-substituted phenylnitronyl nitroxide in acute high-altitude hypoxia mice[J] .Biological & Pharmaceutical Bulletin, 2013, 36(6): 917 -924.

About the Author:

Bao Wen (1987.04-), male, Han nationality, born in Harbin, Heilongjiang Province, bachelor, Beijing Meiyan Biotechnology Co., LTD. Position: Director of Research and Development Center.

Special dietary bioactive peptides for anti-aging. Participated in a number of small molecule active peptide product project development, raw material research and other work, China special diet small molecule active peptide expert, special research under the scientific ratio of polypeptide mixing, fight against human aging direction.

Research Progress of Platelets, Lymphocytes and Neutrophils in Sepsis

Anxin Chen, Dong Wan*

Department of Emergency & Critical Care Medicine, The First Affiliated Hospital of Chongqing Medical University, Chongqing 400016, China.

Abstract: Sepsis is a life-threatening organ dysfunction syndrome caused by the body's disregulated response to infection [1]. Platelets, lymphocytes and neutrophils are important cells in the immune response process of sepsis and play an important role in the progression of sepsis. Recently, research has found that platelet can inhibit bacteria, mediate inflammatory reaction process and secrete pro-inflammatory factors in addition to coagulation function. Lymphocytes act as adaptive immune cells, and low lymphocyte count can be a manifestation of immunosuppression. Neutrophils are important innate immune cells and represent the first barrier of immunity. Moreover, neutrophils, platelets and lymphocytes are common clinical indicators, which can be obtained in blood routine examination. As a new inflammatory index, Platelet-lymphocyte ratio and Neutral-lymphocyte ratio have gradually become the focus of the inflammatory index in the immune response process. In this paper, the value of platelet, lymphocytes and neutrophils in sepsis is reviewed.

Keywords: Sepsis; Platelet; Lymphocyte; Neutrophil; Immune Response

1. Introduction

Sepsis is a life-threatening organ dysfunction syndrome caused by a dysregulated body response to infection[1]. Innate immune cells, such as neutrophils, macrophages, and dendritic cells, are the first responders to infection and play a critical role in initiating the inflammatory response. Adaptive immune cells, such as T and B lymphocytes, are important for providing long-term protection against infection. The purpose of this review is to find out the important immune cells involved in the immune response process in sepsis, to better understand the development process of sepsis.

2. Immune cells in sepsis

2.1 Platelets are involved in the immune response process of sepsis

The role of platelets on coagulation function has been recognized. In recent years, studies have found that platelets have various functions besides hemostasis[2]: platelets have been shown to inhibit bacterial growth and spread; platelets can affect the recruitment and function of leukocytes, inhibit cytokines and affect the activated of vascular endothelial coagulation reaction; Platelets help to maintain vascular integrity, especially in a strongly proinflammatory environment. Platelets play an important role in the process of immune regulation and inflammation by inducing the release of inflammatory cytokines, and with different types of bacteria and immune cells (including neutrophils, T lymphocytes, natural killer cells (NK) cells and macrophages) interaction, which lead to the start of the inflammatory process or intensified[3]. In the progress of sepsis, a low platelet count may be associated with an adverse outcome. In a large study including 931 patients with sepsis, Claus Hughes et al reported that patients with lower platelet counts at the ICU admission had higher disease severity and an increased risk

of mortality[4]. In addition, low thrombocytopenia is the most common cause of coagulopathy in septic patients, associated with platelet consumption and also with higher mortality.

Platelets originate from megakaryocytes. When pathogens invade the body, platelets can rapidly activate and release substances that promote the death of pathogens, and activate the innate and adaptive immune system, such as reactive oxygen species, antimicrobial proteins, kallikrein and other antibacterial molecules, to directly kill the pathogen[5]. Among them, the platelet antimicrobial protein, stored in platelet granules and platelet cells, is a small cationic polypeptide that kills the pathogen. CD40L, generated on the surface of activated platelets, can directly stimulate B cell proliferation and release antibodies, and enhance the cell killing ability of cytotoxic T cells. Meanwhile, CD40L interacts with CD40 of immune cells and can serve as a regulatory mechanism of inflammation, participating in helper T cell-driven activation, proliferation, and differentiation[6]. The trigger receptor-1 (triggering receptors expressed on myeloid cells-1, TREM-1) expressed by myeloid cells is an important molecule used to amplify the inflammatory response. It is selectively expressed on various cell surfaces, such as neutrophils, CD14 + monocytes / macrophages. Activated platelets were found to produce ligands for TREM-1, which combined with TREM-1 to enable its activation. Activated TREM-1 upregulates pro-inflammatory factors and suppresses the expression of anti-inflammatory factors. Ligand levels of TREM-1 were correlated with sepsis severity. Neutrophil extracellular traps (neutrophil extracellular traps, NETs), as another mechanism to control the pathogen, also involve platelets. NETs have a control disease.

2.2 Lymphocytes participate in the sepsis immune response process

Acquired immunity of the body is mainly mediated by lymphocytes, and the lymphocytes expand rapidly when stimulated by cytokines and specific antigens to produce a specific immune response. Normally, lymphocyte apoptosis removes itself or maintains immune cell activation; while lymphocyte apoptosis during sepsis significantly increases low lymphocyte count, which partly represents the degree of immunosuppression and inflammatory response [7, 8]. There are also reports in the literature associated with inflammatory diseases, such as cardiovascular disease and type 2 diabetes[7, 8].

Based on these findings, the Platelet-lymphocyte ratio (PLR) is suggested as a new indicator of systemic inflammation, and has gradually become a research hotspot. Yanfei Shen et al found that high PLR (> 200) was associated with poor outcome in sepsis outcomes, while low PLR was not associated with poor outcome[11].

2.3 Neutrophils are the first line of defense in the immune response process

As an indicator of inflammation, NLR has also attracted much attention in recent years. Neutrophils, as the first line of defense to provide rapid warning and elimination of pathogens, play a crucial role in innate immunity. Of the lymphocyte response-specific immune processes. NLR is a rapid and simple parameter reflecting systemic inflammation and stress, which can indicate the severity of disease in critically ill patients and is clinically an important clinically accessible inflammatory marker. Neutrophilic lymphocyte ratio reflects indicators of systemic inflammation and stress status, and is associated with the degree of critical illness, often appearing in symbiosis with PLR. The NLR reflects the balance between innate and adaptive immunity. Moreover, NLR is also a readily accessible biomarker that can be analyzed based on the whole blood count and has been reported to be associated with various diseases, including inflammation, cerebral infarction, cancer and traumatic[12].

2.4 Progress on the value of Platelet-lymphocyte ratio (PLR) and Neutrophil-lymphocyte ratio (NLR) in sepsis

PLR and NLR in sepsis . NiJ, Wang H et al found that NLR could act as an independent predictor of death in patients

with sepsis[12]. Can E， Emrah MD et al in a cross-sectional study including 122 neonates found a statistically significant positive association between NLR and neonates with early-onset sepsis[13]. The physiological immune response of leukocytes to many stress events in the circulatory system is characterized by an increased neutrophil count and a decreased lymphocyte count. The inflammatory response leads to an increase in the total number of leukocytes and neutrophils caused by microbial infection. Therefore, these counts may be used as diagnostic markers for microbial infection. The NLR is becoming a more valuable marker for inflammation than neutrophil or lymphocyte counts alone for predicting bacterial infection [14, 15]. NLR and PLR have become inflammatory markers of sepsis due to changes in neutrophil, platelet, and lymphocyte counts due by inflammation.

The neuroinflammatory hypothesis suggests that the inflammatory response of central nervous cells is the underlying pathogenesis leading to confusion and cognitive dysfunction. Is a more popular hypothesis. Theory suggests that acute peripheral inflammatory stimuli, glial activation, and overexpression of proinflammatory cytokines can lead to apoptotic neuronal cell apoptosis and synaptic dysfunction. Promote the occurrence and development of brain dysfunction. It is well known that delusion is a common manifestation of the organ dysfunction induced in sepsis. Martin et al found that psychosis was the most common cause of psychosis in the ICU, and sepsis and psychosis were closely related[16]. Moreover, systemic inflammation may be an important trigger. Increasing evidence suggests that prostst, IL-8, IL-6, and S100 β play an important role in the development of confusion. Furthermore, C-reactive protein levels were found to predict the severity and duration of the postoperative delusion. Overall, inflammation is the underlying mechanism of encephalopathy. Xuandong Jiang[17]. A retrospective study found that high ICU admission PLR (> 100) was associated with a higher incidence of delusion and that high PLR (> 100) was an independent risk factor for delusion. Therefore, the study concluded that PLR could be a useful predictor of developing disturbance of consciousness in critically ill patients. It is also confirmed that the inflammatory response may be an important cause of brain dysfunction in septic patients. There are no studies on neutrophil lymphocyte ratio and platelet lymphocyte ratio in predicting sepsis-related encephalopathy.

3. Conclusion

Sepsis is a life-threatening organ dysfunction syndrome caused by the imbalance of the immune response to infection, and its core process is the imbalance of the immune response. Platelets, lymphocytes and neutrophils all have important roles in the process of immune inflammatory response. Platelets mediate proinflammatory responses in sepsis immune regulation and participate in the injury process of multiple organ dysfunction in sepsis. In sepsis, common lymphocytes decrease, representing the trend of immunosuppression in the process of immune regulation. Neutrophils are the first line of defense of immunity and are a commonly used indicator of the inflammatory response and stress status of the body. In recent years, NLR and PLR have often entered the research hotspot field as a new inflammatory indicator, and their ratio reflects the balance between innate immunity and adaptive immunity, and between proinflammatory response and antiinflammatory response. This index has been clinically verified for the diagnosis and prognosis evaluation of sepsis and the evaluation of organ function damage, but whether there is an association with sepsis-related encephalopathy still needs further verification.

References

[1] Singer M, Deutschman CS, Seymour CW, et al. The Third International Consensus Definitions for Sepsis and Septic Shock (Sepsis-3)[J]. JAMA, 2016,315(8):801.

[2] Maclullich AM, Ferguson KJ, Miller T, et al. Unravelling the pathophysiology of delirium: a focus on the role of aberrant stress responses[J]. J Psychosom Res, 2008,65(3):229-238.

[3] Gill P, Jindal NL, Jagdis A, et al. Platelets in the immune response: Revisiting platelet-activating factor in anaphylaxis[J]. J Allergy Clin Immunol, 2015,135(6):1424-1432.

[4] Wang YQ, Zhi QJ, Wang XY, et al. Prognostic value of combined platelet, fibrinogen, neutrophil to lymphocyte ratio and platelet to lymphocyte ratio in patients with lung adenosquamous cancer[J]. Oncol Lett, 2017,14(4):4331-4338.

[5] Alharbi A, Thompson JP, Brindle NP, et al. Ex vivo modelling of the formation of inflammatory platelet-leucocyte aggregates and their adhesion on endothelial cells, an early event in sepsis[J]. Clin Exp Med, 2019,19(3):321-337.

[6] Verschoor A, Neuenhahn M, Navarini AA, et al. A platelet-mediated system for shuttling blood-borne bacteria to CD8alpha+ dendritic cells depends on glycoprotein GPIb and complement C3[J]. Nat Immunol, 2011,12(12):1194-1201.

[7] Atterton B, Paulino MC, Povoa P, et al. Sepsis Associated Delirium. [J]. Medicina (Kaunas, Lithuania), 2020,56(5).

[8] Manzoli TF, Delgado AF, Troster EJ, et al. Lymphocyte count as a sign of immunoparalysis and its correlation with nutritional status in pediatric intensive care patients with sepsis: A pilot study[J]. Clinics (Sao Paulo), 2016,71(11):644-649.

[9] Felmet KA, Hall MW, Clark RS, et al. Prolonged lymphopenia, lymphoid depletion, and hypoprolactinemia in children with nosocomial sepsis and multiple organ failure[J]. J Immunol, 2005,174(6):3765-3772.

[10] Bao X, Borne Y, Johnson L, et al. Comparing the inflammatory profiles for incidence of diabetes mellitus and cardiovascular diseases: a prospective study exploring the 'common soil' hypothesis[J]. Cardiovasc Diabetol, 2018,17(1):87.

[11] Otton R, Soriano FG, Verlengia R, et al. Diabetes induces apoptosis in lymphocytes. [J]. The Journal of endocrinology, 2004,182(1):145-156.

[12] Liu S, Wang X, She F, et al. Effects of Neutrophil-to-Lymphocyte Ratio Combined With Interleukin-6 in Predicting 28-Day Mortality in Patients With Sepsis[J]. Front Immunol, 2021,12:639735.

[13] Can E, Hamilcikan S, Can C. The Value of Neutrophil to Lymphocyte Ratio and Platelet to Lymphocyte Ratio for Detecting Early-onset Neonatal Sepsis[J]. J Pediatr Hematol Oncol, 2018,40(4):e229-e232.

[14] Wyllie D H, Bowler I C, Peto T E. Relation between lymphopenia and bacteraemia in UK adults with medical emergencies[J]. J Clin Pathol, 2004,57(9):950-955.

[15] Yoon N B, Son C, Um S J. Role of the neutrophil-lymphocyte count ratio in the differential diagnosis between pulmonary tuberculosis and bacterial community-acquired pneumonia[J]. Ann Lab Med, 2013,33(2):105-110.

[16] Maclullich A M, Ferguson K J, Miller T, et al. Unravelling the pathophysiology of delirium: a focus on the role of aberrant stress responses[J]. J Psychosom Res, 2008,65(3):229-238.

[17] Jiang X, Shen Y, Fang Q, et al. Platelet-to-lymphocyte ratio as a predictive index for delirium in critically ill patients: A retrospective observational study[J]. Medicine (Baltimore), 2020,99(43):e22884.

Head-to-Head Comparison of TB-LAMP, Mycobacterial Culture and Adenosine Deaminase for Diagnosis of Pleural Tuberculosis in China

Lei Chen,[1#] Aiyan Wang,[2#] Juan Cheng,[1] Shouhua Han,[1] Guangfu Liu,[1] Zhaobao Pan[1,*]

1. Department of Laboratory Medicine, The Second People's Hospital of Weifang, Weifang 261041, China.

2. Department of Laboratory Medicine, People's Hospital of Fangzi District, Weifang 261041, China.

Abstract: **Objectives:** The objective of the prospective single-center study was to investigate the diagnostic performance of Loop-Mediated Amplification test (TB-LAMP), mycobacterial culture and adenosine deaminase (ADA) for diagnosing pleural tuberculosis (TB) from the pleural effusions in a TB-endemic setting. **Methods:** We retrospectively analyzed patients suspected of having pleural TB in Weifang between March 2018 and October 2019. The PE samples were evaluated by smear microscopy, mycobacterial culture, TB-LAMP and ADA assay. **Results:** Overall, 170 patients with suggestive of pleural TB were retrospectively reviewed in this study, of which 125 were diagnosed as pleural TB. Among 125 pleural TB cases, 52 cases were identified by TB-LAMP, resulting in a sensitivity of 41.6%. When combing MGIT and TB-LAMP, 13 additional positive cases were detected compared to MGIT culture alone, demonstrating a sensitivity of 56.8%. The mean ADA levels were corelated with age, and the mean ADA value of <35 years group was significantly higher than that of ≥70 years group (p=0.0214). **Conclusion**: In conclusion, our data demonstrate the promising effectiveness of TB-LAMP in detection of MTB in concentrated PE specimens. The ADA levels are decreased with advanced age, highlighting the urgent need for confirmation of different cut-off values for various age group.

Keywords: Pleural Tuberculosis; Diagnosis; Lamp; Adenosine Deaminase

Introduction

Pleural tuberculosis (TB) is one of the most common forms of extrapulmonary tuberculosis across different regions around the world, as well as a common cause of pleural effusions (PEs) in TB-endemic countries (Pang et al., 2019). Because of the paucibacillary nature of TBP in pleural effusions, it remains a diagnostic challenge highlighting the urgent need of highly accurate tools for correctly diagnosing TBP patients (Solari et al., 2018). The Loop-Mediated Amplification test for TB (TB-LAMP) is endorsed by the World Health Organization to facilitate the detection of pulmonary TB patients (WHO, 2016). However, the current data is restricted to sputum samples only, which hamper the potential use of TB-LAMP in various EPTB samples. Therefore, the prospective single-center study was conducted to investigate the diagnostic performance of TB-LAMP, mycobacterial culture and adenosine deaminase (ADA) for diagnosing pleural TB from the pleural effusions in a TB-endemic setting.

Materials and Methods

We retrospectively analyzed patients suspected of having pleural TB in the Second People's Hospital of Weifang

between March 2018 and October 2019. The pleural effusion (PE) samples were evaluated by Ziehl-Neelsen smear microscopy, mycobacterial culture in the the Mycobacterial Growth Indicator Tube (MGIT) 960 automated system (Becton Dickinson), TB-LAMP and adenosine deaminase assay as previously described (Liu et al., 2020). The clinically diagnosed pleural TB was used as the reference standard to assess the sensitivity, specificity, positive predict value (PPV), and negative predictive value (NPV).

Results

Overall, 170 patients with suggestive of pleural TB were retrospectively reviewed in this study, of which 125 were diagnosed as pleural TB based on laboratory, histology and/or clinical evidence. Among 125 pleural TB cases, 58 were detected by MGIT culture testing, yielding a sensitivity of 46.4% (95% confidence interval (95% CI: 37.7%-55.1%). For TB-LAMP, 52 cases were identified as pleural TB cases, resulting in a sensitivity of 41.6% (95% CI: 33.0%-50.2%). There was no significant difference observed in sensitivity between MGIT culture and TB-LAMP (p=0.45). When combing MGIT and TB-LAMP, 13 additional positive cases were detected compared to MGIT culture alone, demonstrating a sensitivity of 56.8% (95% CI: 48.1%-65.5%). In addition, 44 out of 45 non-pleural TB cases could correctly identified by TB-LAMP, yielding a specificity of 97.8% (95% CI: 93.5%-100.0%) (Table 1).

Table 1.Comparison of diagnostic efficacy between MGIT culture and TB-LAMP in the diagnosis of tuberculous pleurisy

Method	Clinical diagnosis		Sensitivity （%）	Specificity （%）	Positive predictive value （%）	Negative predictive value （%）
	Tuberculous pleurisy （125）	Non tuberculous pleurisy （45）				
LAMP						
Positive	52	0	41.6%	100%	100%	38.1%
Negative	73	45				
MGIT culture						
Positive	58	0	46.4%	100%	100%	40.2%
Negative	67	45				
LAMP and MGIT culture						
Positive	71	0	56.8%	100%	100%	45.5%
Negative	54	45				

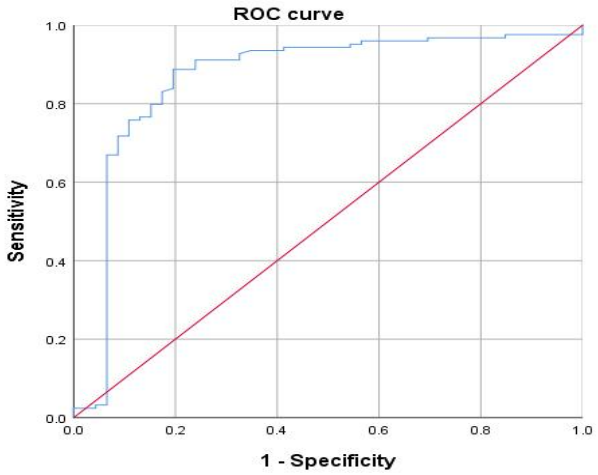

Figure 1A depicts the ROC curve calculated for the cut-off value for distinguishing pleural TB and non-pleural TB cases. A threshold of 17.85 U/l was determined to best differential diagnosis of pleural TB. Using this temporary value, the ADA assay had a sensitivity of 91.2% and a specificity of 66.7%. We further analyzed the ADA concentrations stratified to different age groups (Fig. 1B). The mean ADA level was decreased with advanced age, ranging from 42.11±16.24 for <35 years group to 29.95±23.17 for ≥70 years group. Statistical analysis revealed that the mean ADA value of <35 years group was significantly higher than that of ≥70 years group (p=0.018).

Figure 1A.the ROC curve calculated for the cut-off value for distinguishing pleural TB and non-pleural TB cases

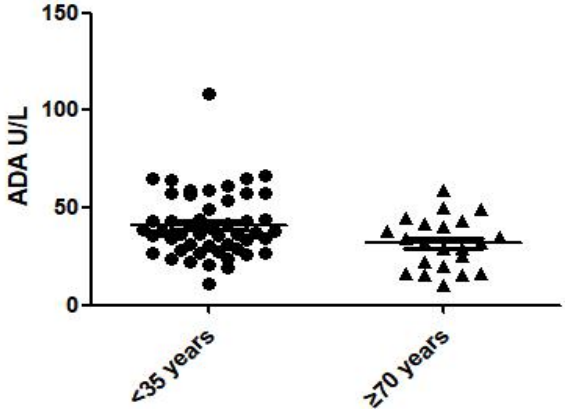

Figure. 1B. the ADA concentrations stratified to different age groups

Discussion

In this study, our data firstly demonstrate the promising performance of TB-LAMP in detection of MTB in PE specimens. A meta-analysis of recent evaluation studies reported that the pooled sensitivity of Xpert was low at 17.0% for diagnosis of pleural TB compared with a composite reference standard, which was significantly lower than that of TB-LAMP (WHO, 2013). In contrast, a serial of pervious reports have repeatedly confirmed that Xpert outperforms TB-LAMP in detecting MTB from sputum specimens (WHO, 2013; WHO, 2016). Compared with the Xpert assay using hemi-nested PCR, the TB-LAMP had higher amplification efficiency, with DNA amplified 10^9-10^{10} times in 30 min (Parida et al., 2008). A study of analytic sensitivity demonstrated that the detection limit of Xpert was 131 CFU/ml (Blakemore et al., 2010), whereas the combined use of isothermal amplification and fluorescence assay yielded a detection limit of 5-50 CFU/ml for TB-LAMP (Iwamoto et al., 2003). Despite the higher analytic sensitivity, TB-LAMP loads the maximal 60 μl of clinical specimens, only one twentieth of that loaded in Xpert (approximate 1 mL). The sampling issues may contribute to

the decreased efficacy of TB-LAMP in sputum samples. In the present study, the concentrated PE samples rather than the original samples were used for TB-LAMP, which may be a potential explanation for these conflicting evaluation results. In addition, we also observe that a proportion of pleural TB cases missed in automated MGIT system yielded positive results by TB-LAMP, reflecting the paucibacillary nature of PE samples. Our results indicate that the parallel use of mycobacterial culture and TB-LAMP will bring additional benefit of correctly diagnosing pleural TB patients.

The ADA in pleural effusion is considered as a useful maker for the differential diagnosis of pleural TB (Abrao et al., 2014). In our analysis, using a cut-off level of 18 U/l, the pleural TB cases yielded a specificity of 67%, which was significantly lower than previous observations (Keng et al., 2013). Notably, we found that the ADA levels were decreased with advanced age. Similar results were reported by Abrao and colleagues that age was correlated with pleural ADA levels in the Brazil population (Abrao et al., 2014). As a common biochemical indicator, the ADA production appears to be influenced by factors associated with the anti-TB immune. In view of the fact that aging is associated with declines in immune system function (Weyand and Goronzy, 2016), the immunosenescence in both innate and adaptive immunity may be an important reason for the decreased ADA production in the old age group. Therefore, the different cut-off levels should be set for various age groups to help clinicians interpret the ADA results.

In conclusion, our data demonstrate the promising effectiveness of TB-LAMP in detection of MTB in concentrated PE specimens. The ADA levels are decreased with advanced age, highlighting the urgent need for confirmation of different cut-off values for various age group. Further studies are warranted to evaluate the performance of TB-LAMP in other forms of concentrated extrapulmonary specimens.

Funding

This work was supported by the Science and Technology Project of Weifang Health Committee (WFWSJK-2020–063, WFWSJK-2020-011).

Ethical approval statement

This study was approved by the Ethics Committee of the Second People's Hospital of Weifang. All data were kept anonymous in analysis process.

References

[1] Abrao FC, De Abreu IR, Miyake DH, Busico MA, Younes RN. Role of adenosine deaminase and the influence of age on the diagnosis of pleural tuberculosis. Int J Tuberc Lung Dis 2014;18(11):1363-9.

[2] Blakemore R, Story E, Helb D, Kop J, Banada P, Owens MR, et al. Evaluation of the analytical performance of the Xpert MTB/RIF assay. J Clin Microbiol 2010; 48(7): 2495-501.

[3] Iwamoto T, Sonobe T, Hayashi K. Loop-mediated isothermal amplification for direct detection of Mycobacterium tuberculosis complex, M. avium, and M. intracellulare in sputum samples. J Clin Microbiol 2003; 41(6): 2616-22.

[4] Keng LT, Shu CC, Chen JY, Liang SK, Lin CK, Chang LY, et al. Evaluating pleural ADA, ADA2, IFN-gamma and IGRA for diagnosing tuberculous pleurisy. J Infect 2013;67(4):294-302.

[5] Liu R, Li J, Tan Y, Shang Y, Li Y, Su B, et al. Multicenter evaluation of the acid-fast bacillus smear, mycobacterial culture, Xpert MTB/RIF assay, and adenosine deaminase for the diagnosis of tuberculous peritonitis in China. Int J Infect Dis 2020;90:119-24.

[6] Pang Y, An J, Shu W, Huo F, Chu N, Gao M, et al. Epidemiology of Extrapulmonary Tuberculosis among Inpatients, China, 2008-2017. Emerg Infect Dis 2019; 25(3):457-64.

[7] Parida M, Sannarangaiah S, Dash PK, Rao PV, Morita K. Loop mediated isothermal amplification (LAMP): a new

generation of innovative gene amplification technique; perspectives in clinical diagnosis of infectious diseases. Rev Med Virol 2008;18(6):407-21.

[8] Solari L, Soto A, Van der Stuyft P. Development of a clinical prediction rule for the diagnosis of pleural tuberculosis in Peru. Int J Infect Dis 2018;69:103-7.

[9] Weyand CM, Goronzy JJ. Aging of the Immune System. Mechanisms and Therapeutic Targets. Ann Am Thorac Soc 2016;13 Suppl 5:S422-S8.

[10] World Health Organization. The use of loop-mediated isothermal amplification (TB-LAMP) for the diagnosis of pulmonary tuberculosis. Geneva: World Health Organization, 2016.

[11] World Health Organization. Xpert MTB/RIF assay for the diagnosis of pulmonary and extrapulmonary TB in adults and children. Policy update. Geneva: World Health Organization, 2013.

[#]These authors contributed equally to this study.

*Corresponding author. Mailing address for Zhaobao Pan: The Second People's Hospital of Weifang, No.7, Yuanxiao, Kuiwen District, Weifang 26104, China.

Application of Nursing Risk Management in Patients with Cardiovascular Emergencies

Linping Dong[1], Xiaojuan Wang[1], Juan Chang[1], Linhuan Dong[2]

1. Department of Cardiovascular Medicine Shandong Second People's Hospital, Jinan 250022, China.

2. Department of emergency, The First Affiliated Hospital of Shandong First Medical University &Shandong Province Qianfoshan Hospital, Jinan 250014, China.

Abstract: **Objectives:** To study the nursing effect of nursing risk management in patients with acute cardiovascular disease. **Methods:** A total of 62 acute and critical cardiovascular patients admitted to the Second People's Hospital of Shandong Province from November 2021 to January 2023 were selected as the study objects, and the patients were randomly divided into control group and observation group. The control group adopted conventional nursing methods, while nursing risk management measures were carried out in the observation group. The nursing effects of the two groups were compared, and the incidence rate and patient satisfaction were analyzed according to the time. **Results:** The effective rate of the observation group was 93.55%, significantly higher than 61.29% of the control group, and the difference was statistically significant($P<0.05$). The occurrence of risk events in observation group was significantly less than that in control group, and patient satisfaction was significantly higher than that in control group ($P<0.05$). **Conclusion:** Nursing risk management could significantly improve the nursing effect of patients, reduce the occurrence of risk events, improve patient satisfaction, has a certain application value.

Keywords: Nursing Risk Management; Acute Cardiovascular Disease; Nursing Effect; Risk Event; Patient Satisfaction

Introduction

Cardiovascular and cerebrovascular system is a kind of chronic disease which is very harmful to health and affects the quality of life [1], The disease covers a lot of contents and has a high risk. With the continuous progress of society and the improvement of people's living standards, the rate of cardiovascular and cerebrovascular diseases is also rising year by year, and the risk of nursing is intensifying [2]. Therefore, strengthening nursing risk management is of great clinical significance to ensure patient safety and promote recovery.

1. Materials and Methods

1.1 Research object and grouping

A total of 62 critical cardiovascular patients admitted to the Second People's Hospital of Shandong Province from November 2021 to January 2023 were selected as the study subjects. The patients were randomly divided into a control group and an observation group, with 31 patients in each group. In the observation group, there were 17 males and 14 females, aged 50-78 years old, with an average age of 62.81±6.64 years old. In the control group, there were 19 males and 12 females, aged 52-76 years old, with an average age of 63.87±7.23 years old.

1.2 Inclusion and exclusion criteria

Inclusion criteria: 1)Meeting the admission criteria for cardiovascular diseases, age<80 years old; 2)Signed informed consent.

Exclusion criteria: 1)Severe mental illness; 2)Lose the ability to take care of oneself and be completely taken care of by others; 3)Very poor compliance.

1.3 Nursing method

The patients in control group were treated with routine nursing methods, nursing staff should follow the doctor's advice and clinical pharmacists for rational drug use for patients, establish a reasonable communication channel between doctors and patients [3]. The observation group adopted nursing risk management measures:1) Establishing a nursing risk management team: The head nurse with rich experience was selected to play the role of group leader in the group. The group leader need to organize regular inter-group discussion among the group members, mainly for the problems existing in the nursing process and the occurrence and causes of the previous nursing risks were investigated. According to the actual situation, the nursing plan was formulated for each patient in line with it; 2) Improve the professional competence of nursing staff: Strengthen the training of professional abilities of nursing staff to ensure that every nursing staff can handle these dangerous situations in a timely manner when encountering patients falling off the bed, falling down, and unplanned extubation; 3) Risk management implementation: Doing a good job of daily equipment management and maintenance, nursing staff in the use of special instruments need to carry out professional training and assessment and obtain relevant qualifications before use. At the same time, it was also necessary to strengthen the training of medical knowledge for nursing staff and improve the rules and regulations in the department.

1.4 Evaluation indexes

The nursing effect of the two groups was compared, and the nursing effect evaluation was divided into obvious, effective and ineffective: Significant effective——The patient's symptoms completely disappeared and the indicators returned to normal; effective——The patient's symptoms and indicators were beginning to show good signs; invalid——The patient's symptoms and indicators did not improve, and even increasingly aggravated. The occurrence of inter-group risk events was analyzed and their incidence rates were compared. Risk events mainly included complications, nurse-patient disputes and medical accidents. The difference in satisfaction before and after care was observed and compared between the two groups.

2. Statistical analysis

Measurement data were expressed using mean ± standard deviation ($\bar{x} \pm s$) and analyzed using a t-test. Counting data were represented by % and was compared by chi-square test. $P<0.05$ indicated statistically significant difference.

3. Results

3.1 Comparison of nursing effect between two groups

After nursing, 17 patients were significantly effective, 12 were effective, and 2 were ineffective in the observation group. In the control group, 11 patients were significantly effective, 8 were effective, and 12 were ineffective. The nursing effective rate of observation group was significantly higher than that of control group($P<0.05$, Table 1).

Table 1. Comparison of nursing effect between two groups

Groups	Significant effective	Effective	invalid	total effective rate(%)
Observation group(n=31)	17(54.84%)	12(38.71%)	2(6.45%)	93.55%
Control group(n=31)	11(35.48%)	8(25.81%)	12(38.71%)	61.29%
P				<0.001

3.2 Comparison of the incidence of risk events between the two groups

As shown in Table 2, the occurrence of risk events in the observation group was significantly less than that in the control group, and the difference was statistically significant(P<0.05, Table 2).

Table 2. Comparison of the incidence of risk events between the two groups

Groups	complications	nurse-patient disputes	Risk event rate(%)
Observation group(n=31)	5(16.13%)	2(6.45%)	22.58%
Control group(n=31)	12(38.71%)	9(29.03%)	67.74%
P			<0.001

3.3 Comparison of nursing satisfaction between the two groups

After investigation, the satisfaction rate of patients in the observation group was significantly higher than that in the control group (P<0.05, Table 3).

Table 3. Comparison of nursing satisfaction between the two groups

Groups	satisfaction	dissatisfaction	Nursing satisfaction rate (%)
Observation group(n=31)	24	7	77.42%
Control group(n=31)	12	19	38.71%
P			<0.001

4. Discussion

Nursing risk has strong unpredictability, often is an emergency, if the nursing risk is relatively low will bring adverse effects on the normal treatment of patients, if the nursing risk is high, will lead to death of patients. In the course of acute and critical care in cardiovascular medicine, nursing risks mainly come from three aspects: hospital, medical staff and patients [4, 5].Therefore, in the nursing of acute and severe cardiovascular patients, we should pay attention to the risk factors, strengthen nursing risk management, provide efficient and high-quality services, improve the nursing effect of patients.

In this study, patients were divided into two groups according to the characteristics of patients. Nursing risk management and routine nursing management were respectively implemented. As a consequence, the nursing effective rate of patients with nursing risk management could reach 93.55% and the incidence of nursing risk events was also significantly reduced, and the patient satisfaction was higher. It showed that the nursing quality of patients can be improved comprehensively through nursing risk management, and the effect of nursing intervention can be significantly improved.

To sum up, nursing risk management is worthy of clinical promotion and application because of its pertinence, comprehensiveness and systematization, which can reduce the risk incidence and improve the nursing effect and patient satisfaction.

References

[1] Wu GH, Chu HJ, & Hu W. Application effect analysis of nursing risk management in the nursing of severe

patients in cardiovascular medicine [J]. Capital Food and Medicine,2019; 26(03): 153.

[2] Ding XR, & Ma J. Application and effect analysis of nursing risk management in nursing of cardiovascular patients with severe disease [J]. Electronic Journal of Practical Clinical Nursing Science,2019; 4(49): 18.

[3] Gao Y. Nursing risk Management of severe patients in cardiovascular Medicine [J]. Electronic Journal of Clinical Medicine Literature,2018; 5(A0): 135-136.

[4] Lv JJ. Risk assessment and prevention in acute and critical care of cardiovascular medicine [J]. Frontiers of Medicine,2020.

[5] Zheng GY. Analysis of the impact of risk nursing awareness on nursing safety and patient nursing satisfaction in operating room [J]. Lingnan Journal of Emergency Medicine,2019; 1): 3.

*Corresponding author: Linhuan Dong, Department of emergency. The First Affiliated Hospital of Shandong First Medical University &Shandong Province Qianfoshan Hospital, Jinan, 250014, China.

Photothermally Induced Alkyl Radicals and Pyroptosis Synergistically Inhibit Breast Tumor Growth

Yang Du[1,2], Lili Niu[1,2,3], Nannan Li[1,2,3], Huishu Guo[1,2] *

1. Central Laboratory, First Affiliated Hospital, Dalian Medical University, Dalian 116021, China.

2. The Institute of Integrative Medicine, Dalian Medical University, Dalian 116021, China.

3. Center for Medical Research and Innovation, Shanghai Pudong Hospital, Fudan University Pudong Medical Center, Shanghai 201399, China.

Abstract: Photothermal therapy (PTT) is an emerging local tumor ablation technique with clinical translation potential. After the NIR-II laser irradiates the tumor, the photothermal agent Hu-Kaiwen ink (Ink) converts light energy into hyperthermia and maintains the temperature at 42-45°C, thus achieving a low-temperature photothermal therapy. Alkyl radicals can kill tumor cells by overcoming the hypoxic microenvironment of the tumor. The photothermal reaction can induce the conversion of alkyl radicals from 2,2′-azobis[2-(2-imidazolin-2-yl) propane] dihydrochloride (AIPH) and thus have a synergistic tumor inhibition effect. the DNA methyltransferase inhibitor decitabine (DCT) can induce pyroptosis and cause inflammation and immune response to achieve systemic immunity. In this way, a synergistic combination of photothermal, alkyl radicals and pyroptosis could be used to kill breast tumor cells. Sodium alginate (ALG) was used as a carrier to form a hydrogel structure, which can improve the stability and duration of action of the mixed drugs. The significant tumor growth inhibitory effect of composite hydrogels has been demonstrated in both in vitro and ex vivo studies.

Keywords: Alkyl radical; Pyroptosis; Low-temperature photothermal therapy; Hydrogel; Breast cancer

1. Introduction

In 2020, there was nearly 2.3 million new cases of breast cancer in women around the world, making it the leading cancer in the world in terms of new cases [1]. Currently, the most common clinical treatments for breast cancer are surgery, chemotherapy, targeted therapy, immunotherapy and endocrine therapy. For the past few years, combination therapies have more applications in cancer treatment.

Alkyl radicals have received much attention in anti-tumor because this approach can kill tumor cells in a hypoxic microenvironment within the tumor [2]. In this subject, 2,2′-azobis[2-(2-imidazolin-2-yl) propane] dihydrochloride (AIPH) was used as an alkyl radical donor, which is capable of generating alkyl radicals at high temperatures. Even under hypoxic conditions, alkyl radicals could be generated and induce apoptosis by increasing intracellular lipid peroxidation [3].

Photothermal therapy (PTT) was used as a synergistic treatment to induce the conversion of alkyl radicals within the tumor. A photothermal agent with high photothermal conversion efficiency was used in PTT to convert exogenous light energy into hyperthermia under near-infrared (NIR) laser irradiation, resulting in localized hyperthermia at the tumor site, which in turn kills tumor cells [4]. The subject used low-temperature photothermal therapy (<45°C) by NIR-II laser irradiation to produce hyperthermia that inhibited tumor growth while inducing rapid conversion of AIPH to generate cytotoxic alkyl radicals [5]. Hu-Kaiwen ink (Ink) with good photothermal conversion rate was adopted as a photothermal agent.

As AIPH and Ink are fluid and easily degradable when administered as a liquid, it is important to select a suitable biomaterial as a drug carrier to improve stability and prolong drug release [6]. Sodium alginate (ALG) is a commonly used hydrogel material because of its low toxicity, good biocompatibility and biodegradability [7]. Moreover, ALG has the ability to exchange ions with multivalent cations and forms hydrogels under mild physiological conditions [8]. In view of the good drug-carrying capacity and gel-forming properties, ALG was adopted to immobilize the drug mixture in the tumor for a long time.

Pyroptosis is a form of programmed cell death and the onset of pyroptosis releases contents with inflammatory characteristics. The Gasdermin family is the main executor of pyroptosis. One of the most recently discovered mechanisms of pyroptosis is that Caspase-3 is able to cleave the DMLD sequence in GSDME, thereby inducing pyroptosis [9]. In this subject, photothermal therapy and cytotoxic radicals were used to activate caspase-3 to cleave the sensitive sequence of GSDME and induce pyroptosis. Most tumor cells express much lower GSDME than normal cells due to in vivo Deafness Autosomal Dominant 5 (DFNA5) promoter methylation [10,11]. DNA methyltransferase (DNMT) inhibitors can deregulate DNA methylation modifications and restore normal expression of functional proteins. In this study, the DNMT inhibitor decitabine (DCT) was used to demethylate the promoter of the methylated DFNA5 gene and to increase the expression of GSDME in tumor. Caspase-3 were activated by photothermal treatment and alkyl radicals, which can cleave the sensitive sequence of GSDME and induce pyroptosis. Finally, pyroptosis could cause an inflammatory response and an immune response to achieve a systemic immune response that completely kills tumor cells and prevents metastasis and recurrence.

2. Materials and experimental

2.1 Animals

BALB/c mice (female, 6−8 weeks of age) were acquired from Chang Sheng Biotechnology Corporation (Liaoning, China). Animal experiments were performed in accordance with the Guidelines for Animal Experiments of Dalian Medical University.

2.2 Preparation and characterization of hydrogel

Free Ink solution and Ink+ ALG (ALG 5 mg/mL；Ink 0.2 mg/mL) were Separately injected into $CaCl_2$ (Aladdin, China) solution (1.8 mmol/L). Successive photographs were taken to determine the synthesis of the composite hydrogel.

The Ink (Hu-Kaiwen, China) and ALG mixture, AIPH (Aladdin, China) and ALG mixture and DCT (Aladdin, China) and ALG mixture were prepared separately. Each mixture was injected into $CaCl_2$ (1.8 mmol/L) solution and photographs of each group were taken at 0 h and 24 h. The UV absorption of the supernatant of each group was detected using UV-vis to determine drug release.

2.3 Photothermal effects

H_2O, ALG, AIPH, DCT, Ink, DCT+ AIPH+ Ink+ ALG solutions were separately irradiated with laser (1064 nm, 0.5 W/cm^2, 10 min) and the temperatures were recorded by infrared thermal imager (Filr, USA).

2.4 Generation of intracellular free radicals

Different compositions including AIPH (50 μg/mL), Ink (25 μg/mL), ALG (1 mg/mL), DCT (10 μg/mL) and were added to 4T1 cells, with or without 1064 nm laser (0.5 W/cm^2, 10 min). DCFH-DA (Sigma-Aldrich, USA) working solution and DAPI staining were added sequentially to each group of confocal culture dishes, respectively. Confocal microscopy was used for observation.

2.5 Morphology of pyroptosis

After administration of the drug as in the previous method, the cells were placed under an inverted fluorescent microscope (Olympus, Japan) and photographed in white light for cell morphology.

2.6 Release of lactate dehydrogenase (LDH)

After administration of the drug as in the previous method, the prescribed amount of LDH releaser and the assay working solution were added to the corresponding cell samples in turn according to the procedure of the LDH cytotoxicity assay kit (Beyotime, China). Incubate for the prescribed time and measure the absorbance at 490nm.

2.7 Release of intracellular Ca^{2+}

After administration of the drug as in the previous method, Fluo-3 AM Calcium fluorescent probe working solution and DAPI solution were added to each group of cells in turn. Confocal microscopy was used for observation.

2.8 Cytotoxicity in vitro

AIPH, Ink, DCT and AIPH+ Ink+ DCT+ ALG composite hydrogel (ALG 1 mg/mL, Ink 25 μg/mL, AIPH 20 μg/mL, DCT 10 μg/mL) were added to 4T1 cells, with or without 1064 nm laser (0.5 W/cm^2, 10 min). Cell viability was assessed using the Cell Counting Kit-8 (CCK-8, KeyGen, China) after 24 hours of incubation.

2.10 In vivo synergistic cancer therapy

Thirty female BALB/c mice were inoculated with 0.1 mL of 4T1 cell suspension (1×10^7 cells) on their breast pads and experiments were performed when tumors grew to 100 mm^3.

50μL of the corresponding reagent in each group were injected into the tumor. After different administration for each group of mice, weight and subcutaneous tumor size were measured every other day throughout the treatment. And the tumors in each group were removed after 15 days of treatment. Tumor volume and tumor growth inhibition rate (IR) were calculated using the following formulae.

$$V\ (mm^3) = 0.5\times W^2\times L$$

$$IR= (W_{blank}- W_{treat})/W_{blank}\times 100\%$$

2.11 Data analysis and statistics

Statistical differences between the two groups were assessed with the unpaired student t-test. Multiple group comparisons were performed by the Bonferroni test for two-way ANOVA. *$p< 0.05$ was considered statistically significant. All data are expressed as mean± standard deviation.

3. Results and discussion

3.1 Preparation and characterization of hydrogel

As illustrated in Fig. 1A, the free Ink instilled into the Ca^{2+} solution diffused rapidly, which couldn't achieve controlled release of the drug. When the composite hydrogels were injected into the Ca^{2+} solution, a black hydrogel was seen among the solution and no significant diffusion of the black Ink solution occurred. After 24 h, the form of hydrogel was intact and black ink was released, proving that the composite hydrogels could play a good role in controlled drug release. In addition, according to our previous experiments, ALG concentration of 5mg/mL resulted in a better state of gel formation [12].

Fig. 1.

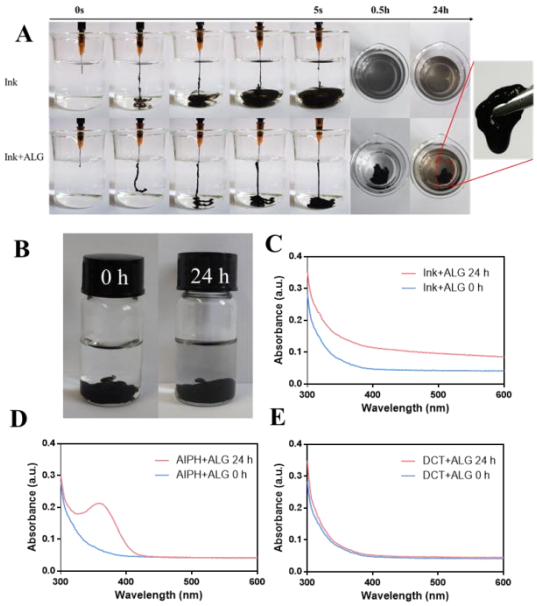

Subsequently, the release behaviors of the components in the composite hydrogels were investigated. After 24 h of constant temperature shaking experiment, the solution of the composite hydrogel changed from colorless to black, demonstrating the release of the drug from the ALG and Ca^{2+} cross-linkage (Fig. 1B). To further investigate the drug release capacity, the UV-vis spectra of the components in the composite hydrogels were analyzed (Fig. 1C-E). Compared to the absence of UV-visible absorption at 0 h, the supernatants of all groups exhibited varying degrees of absorbance after 24 h, indicating the release of Ink, AIPH and DCT from the hydrogels.

3.2 Photothermal effects of composite hydrogel

It was found that the H2O, ALG, AIPH and DCT in the composite hydrogels did not change in temperature after 10 min of laser irradiation by a 1064 nm laser, proving that they had no photothermal properties. Only when Ink was present in the composite hydrogels, its temperature rose gradually with time after laser irradiation, proving that only Ink had photothermal conversion properties in the composite hydrogels (Fig. 2A-B). What's more, the concentration of 25 μg/mL of Ink was selected for the subsequent study according to our previous experiments [12].

Fig. 2.

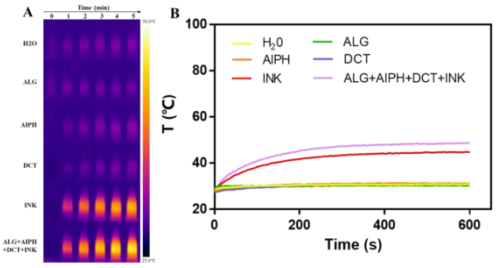

3.3 Detection of intracellular alkyl radicals

As indicated in Fig. 3, strong green fluorescence was visible under confocal microscopy in the DCT+ AIPH+ Ink+ ALG+ laser, DCT+ AIPH+ Ink+ laser and AIPH+ Ink+ ALG+ laser groups, while the green fluorescence signal was weak in the other groups. The experimental groups that included both AIPH and Ink and used laser irradiation could generate a

variety of free radicals, demonstrating that the heat generated by photothermal treatment could cause rapid conversion of cytotoxic alkyl radicals from AIPH. DCFH-DA was used to detect the alkyl radicals in 4T1 cells, as it can be oxidized by intracellular free radicals to produce green fluorescence [13].

Fig. 3.

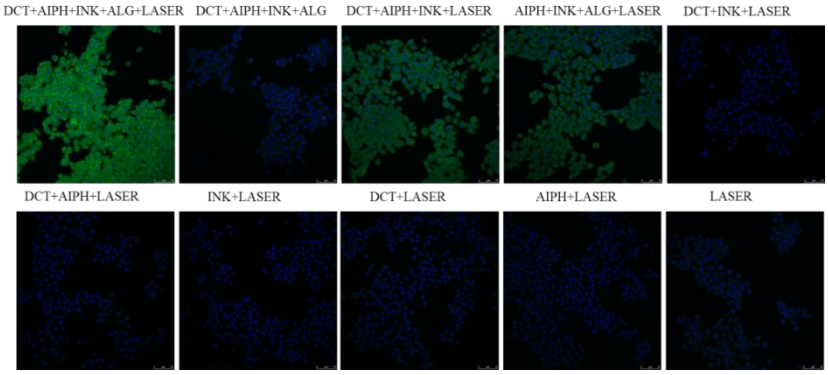

3.4 Pyroptosis caused by composite hydrogels

As shown in Fig. 4A, cells in the DCT+ AIPH+ Ink +ALG+ Laser group, DCT+ AIPH+ Ink+ Laser group and DCT+ Ink+ Laser group showed typical morphological changes of pyroptosis: cells bulged and produced bubbles. Some cells in the AIPH+ Ink+ Laser group and Ink+ Laser group showed apoptotic morphology such as smaller cell size, deformation and crumpling. The cell morphology of the other groups did not change significantly. It has been reported that the Gasdermin-N structural domain binded to membrane phospholipids and perforated the cell membrane after pyroptosis occurs, disrupting the osmotic potential and leading to cell swelling and the production of large bubbles [14]. In addition, the apoptotic morphology of the cells appeared in AIPH+ Ink+ Laser group and Ink+ Laser group in the experiments presumably related to apoptosis caused by photothermal toxicity and the release of cytotoxic alkyl radicals from AIPH during the photothermal transition.

Loss of cell membrane integrity results in the release of cell contents into the culture medium, including LDH in the cytoplasm [15]. So LDH release is seen as an important indicator of the integrity of the cell membrane. As shown in Fig. 4B, the LDH release rates of DCT+ AIPH+ Ink+ ALG+ Laser group and DCT+ AIPH+ Ink+ Laser group were 30.31% and 32.74% respectively, which were significantly different from the 2.62% in the PBS control group. The high release rate of LDH demonstrated that the integrity of the cell membrane was disrupted by the administration of these two groups.

High levels of Ca^{2+} are not detected when the cells are intact. In contrast, pyroptosis punctures the cell membrane, which causes high levels of Ca^{2+} to flow outside the cell. As shown in Fig. 4C, a large amount of green fluorescence appeared around the cells in the DCT+ AIPH+ Ink+ ALG+ Laser group and the DCT+ AIPH+ Ink+ Laser group, demonstrating that there was a large Ca^{2+} efflux and the integrity of the cell membrane was disrupted.

In summary, the occurrence of pyroptosis after DCT+ AIPH+ Ink+ ALG+ Laser composite hydrogel administration could be inferred from the typical morphology of pyroptosis and the disruption of cell integrity.

Fig. 4.

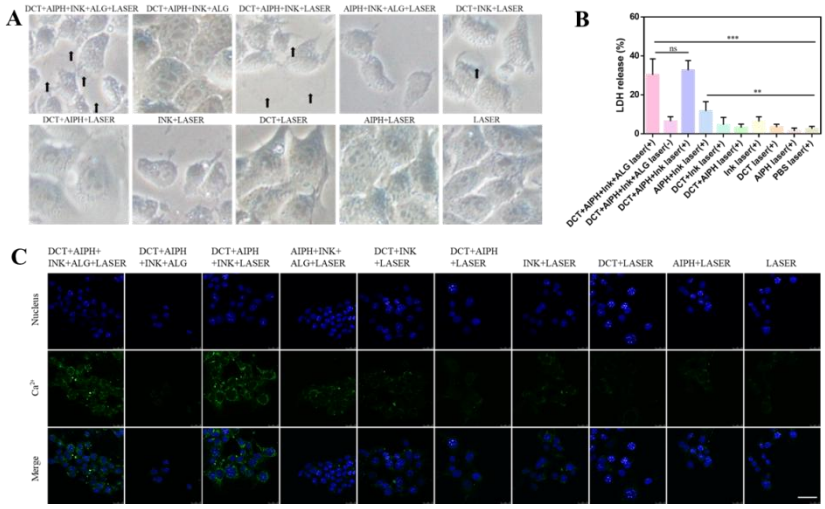

3.5 In vitro cytotoxicity of composite hydrogels

As illustrated in Fig. 5A-B: After incubation with different concentrations of DCT (0-40 μg/mL) and AIPH (0-50 μg/mL) solutions, cell viability values were high with or without laser irradiation, indicating that AIPH and DCT had no photothermal properties and had no cytotoxic to 4T1 breast cancer cells within the concentration range tested. As shown in Fig. 5C, cell viability values were high in the group without laser irradiation after incubation with different concentrations of Ink (0-100 μg/mL) solution. In the laser-irradiated group, the cell viability values were high in the concentration range of 0-50 μg/mL. but when 100 μg/mL of Ink was incubated with laser irradiation, the cell viability values decreased significantly and the cell survival rate was only 20.07%.

Two groups of composite hydrogels with different concentrations of AIPH were used in parallel to incubate 4T1 cells for 24 h. As shown in Fig. 5D, the group without laser irradiation showed good cell activity. Only when the AIPH concentration was increased to 100 μg/mL, the cell viability values decreased slightly. However, in the laser irradiated group, the cell viability decreased significantly with the increase of AIPH concentration. The cell viability value decreased sharply to 15.28% when the AIPH concentration was increased to 100 μg/mL. As a result, it could be proved that the synergistic administration of photothermal, alkyl radical and pyroptosis remarkably inhibited the growth of 4T1 breast cancer cells.

Fig. 5.

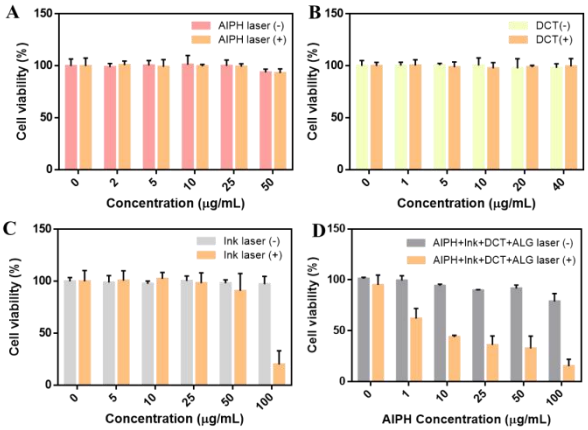

3.6 Antitumor effect and biocompatibility of composite hydrogels

The experimental protocol was shown in Fig. 6A. Fig. 6B showed the representative in situ tumor photographs peeled on day 15 of treatment, which demonstrated that DCT+ AIPH+ Ink+ ALG+ Laser composite hydrogel had the most significant tumor suppression effect. Fig. 6C showed the change curves of tumor growth volume in 4T1 tumor-bearing mice after administration of different treatment groups. After 15 days of treatment, the DCT+ AIPH+ Ink+ ALG+ Laser composite hydrogel group had the slowest tumor volume growth and the smallest tumor volume. Meanwhile, Fig. 6D showed the tumor inhibition rate of mice after administration of different treatment groups. The DCT+ AIPH+ Ink+ ALG+ Laser composite hydrogel administration group had the highest tumor inhibition rate of 85.81%. However, the tumor inhibition rate of the DCT+ AIPH+ Ink+ Laser administration group was only 47.56%, indicating that the loss of the hydrogel structure caused rapid metabolism of the drug in vivo, making it difficult to achieve a good therapeutic effect. Notably, none of the groups of mice showed significant fluctuations in body weight (Fig. 6E), indicating high biological safety of composite hydrogels. In summary, we concluded that the DCT+ AIPH+ Ink+ ALG+ Laser composite hydrogel had a highly synergistic tumor suppression effect.

Fig. 6

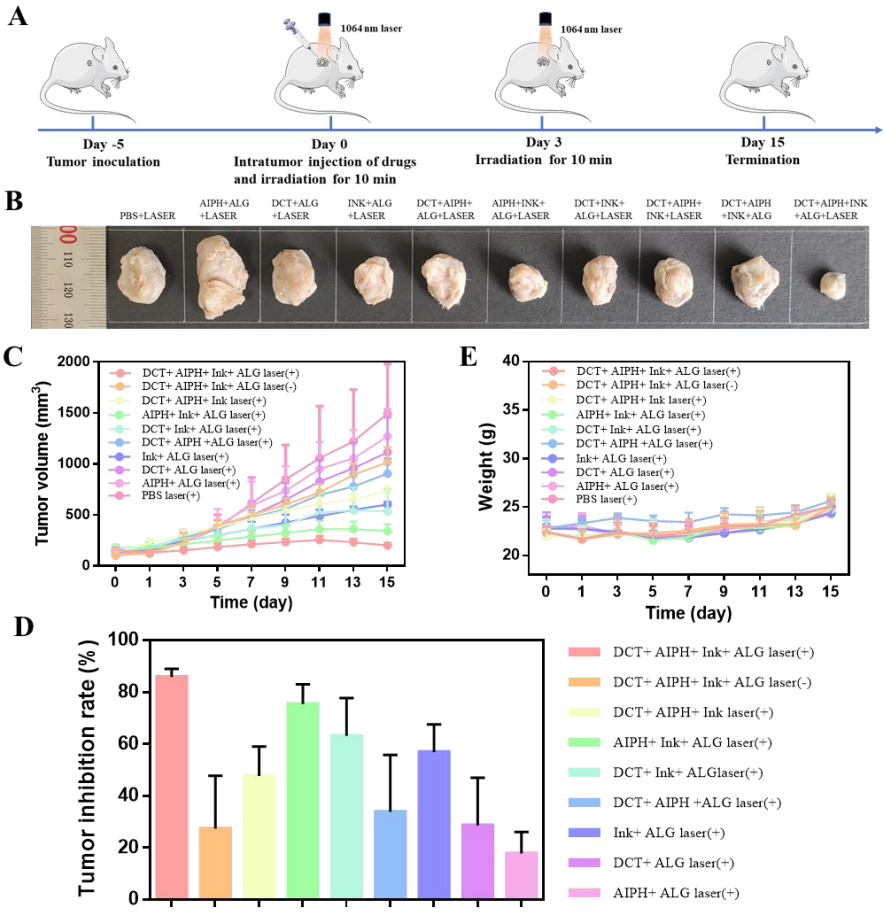

4. Conclusion

A composite hydrogel with sodium alginate as carrier was successfully established in this project. The treatment of breast tumors was achieved in a synergistic way with photothermal therapy, alkyl radicals and pyroptosis in combination.

The significant tumor growth inhibitory effect of DCT+ALG+ Ink+ ALG+ Laser composite hydrogel has been demonstrated in both in vitro and ex vivo studies. Additionally, this composite hydrogel strategy had a highly effective tumor suppression effect and high biological safety, which would pave a new route for the controllable, accurate, and coordinated tumor treatments.

5. Acknowledgements

This work was supported by the Key R&D Projects of Liaoning Province (2020JH2/10300046).

References

[1] Sung H, Ferlay J, Siegel RL, Laversanne M, Soerjomataram I, Jemal A, Bray F. Global Cancer Statistics 2020: GLOBOCAN Estimates of Incidence and Mortality Worldwide for 36 Cancers in 185 Countries[J]. CA Cancer J Clin, 2021, 71(3).

[2] Xiang H, Lin H, Yu L, Chen Y. Hypoxia-Irrelevant Photonic Thermodynamic Cancer Nanomedicine[J]. ACS Nano, 2019, 13(2).

[3] Chen ZH, Saito Y, Yoshida Y, Niki E. Effect of oxygen concentration on free radical-induced cytotoxicity[J]. Biosci Biotechnol Biochem, 2008, 72(6).

[4] Jaque D, Martinez Maestro L, Del Rosal B, Haro-Gonzalez P, Benayas A, Plaza J L, Martin Rodriguez E, Garcia Sole J. Nanoparticles for photothermal therapies[J]. Nanoscale, 2014, 6(16).

[5] Liao W, Ning Z, Chen L, Wei Q, Yuan E, Yang J, Ren J. Intracellular antioxidant detoxifying effects of diosmetin on 2,2-azobis(2-amidinopropane) dihydrochloride (AAPH)-induced oxidative stress through inhibition of reactive oxygen species generation[J]. J Agric Food Chem, 2014, 62(34).

[6] Cai Y, Si W, Huang W, Chen P, Shao J, Dong X. Organic Dye Based Nanoparticles for Cancer Phototheranostics[J]. Small, 2018, 14(25).

[7] Maity C, Das N. Alginate-Based Smart Materials and Their Application: Recent Advances and Perspectives[J]. Top Curr Chem (Cham), 2021, 380(1).

[8] Pan H, Zhang C, Wang T, Chen J, Sun S K. In Situ Fabrication of Intelligent Photothermal Indocyanine Green-Alginate Hydrogel for Localized Tumor Ablation[J]. ACS Appl Mater Interfaces, 2019, 11(3).

[9] Wang Y, Gao W, Shi X, Ding J, Liu W, He H, Wang K, Shao F. Chemotherapy drugs induce pyroptosis through caspase-3 cleavage of a gasdermin[J]. Nature, 2017, 547(7661).

[10] Akino K, Toyota M, Suzuki H, Imai T, Maruyama R, Kusano M, Nishikawa N, Watanabe Y, Sasaki Y, Abe T, Yamamoto E, Tarasawa I, Sonoda T, Mori M, Imai K, Shinomura Y, Tokino T. Identification of DFNA5 as a target of epigenetic inactivation in gastric cancer[J]. Cancer Sci, 2007, 98(1).

[11] Kim MS, Chang X, Yamashita K, Nagpal JK, Baek JH, Wu G, Trink B, Ratovitski EA, Mori M, Sidransky D. Aberrant promoter methylation and tumor suppressive activity of the DFNA5 gene in colorectal carcinoma[J]. Oncogene, 2008, 27(25).

[12] Ouyang B, Liu F, Ruan S, Liu Y, Guo H, Cai Z, Yu X, Pang Z, Shen S. Localized Free Radicals Burst Triggered by NIR-II Light for Augmented Low-Temperature Photothermal Therapy[J]. ACS Appl Mater Interfaces, 2019, 11(42).

[13] Huang G, Qiu Y, Yang F, Xie J, Chen X, Wang L, Yang H. Magnetothermally Triggered Free-Radical Generation for Deep-Seated Tumor Treatment[J]. Nano Lett, 2021, 21(7).

[14] Wu D, Wang S, Yu G, Chen X. Cell Death Mediated by the Pyroptosis Pathway with the Aid of Nanotechnology: Prospects for Cancer Therapy[J]. Angew Chem Int Ed Engl, 2021, 60(15).

[15] Feng Y, Xiong Y, Qiao T, Li X, Jia L, Han Y. Lactate dehydrogenase A: A key player in carcinogenesis and

potential target in cancer therapy[J]. Cancer Med, 2018, 7(12).

Figure Legends

Fig. 1. Characterization of composite hydrogels. (A) Photographs of hydrogel formation at different time points after Ink and Ink+ ALG were injected into $CaCl_2$ solution respectively (ALG 5 mg/mL). (B) Changes in the appearance of drug release from composite hydrogels in $CaCl_2$ solutions for 24 h. (C)-(E) UV-vis absorption spectra of Ink, AIPH and DCT in the supernatant of the composite hydrogel after 24 h in $CaCl_2$ solution.

Fig. 2. Photothermal properties of composite hydrogels. (A) Infrared thermograms of different components of the composite hydrogel under 1064 nm laser irradiation (0.5 W/cm^2, 10 min). (B) Photothermal curve corresponding to Fig. 2A.

Fig. 3. Confocal images of alkyl radical in 4T1 breast cancer cells after different dosing treatments, bar= 75 μm.

Fig. 4. Pyroptosis induced by composite hydrogel. (A) Morphology of cells after different treatments. (B) LDH release after different treatments. (C) Intracellular Ca^{2+} concentration after different treatments, bar= 50 μm. P values: * $p < 0.05$; ** $p < 0.01$; *** $p < 0.001$.

Fig. 5. In vitro cytotoxicity of composite hydrogels. Relative cell viabilities of 4T1 cells after 24 h incubation with or without laser irradiation for different concentrations of (A) AIPH, (B) DCT and (C)Ink, respectively. (D) Relative cell viabilities of 4T1 cells after 24 h incubation with or without laser irradiation in composite hydrogels at different AIPH concentrations and constant concentrations of other components.

Fig. 6. In vivo synergistic therapeutic effect of composite hydrogels. (A) Schematic diagram of the therapeutic experiment. (B) Representative photographs of the in situ tumor removed after day 15 of treatment. (C) Tumor growth curves in 4T1 tumor-bearing mice after various treatment, n= 5. (D) Body-weight changes during 15 days, n= 5. (E) Tumor growth inhibition after various treatment, n= 5.

Effect of Mechanical Ventilation Combined with Budesonide Suspension on Pulmonary Function Indices in the Treatment of Severe Asthma

Rong Fan, Wei Xiao, Weihua Hu, Wu Zhu*
Jingzhou First People's Hospital, Jingzhou 434000, China.

Abstract: Objective: To observe the effectiveness of different methods in the treatment of severe asthma. Methods: Ninety patients admitted from 2020.2 to 2022.8 were divided into groups A and B, 45 patients each, and all were given basic symptomatic treatment, group A was given nebulized inhalation of budesonide suspension, group B was mechanically ventilated on the basis of group A's protocol, and the treatment was compared between groups. Results: After 3 weeks of continuous treatment, the lung function (FEV1, PEF, FEV1/FVC) levels of patients in group B were higher than those in group A, and the difference reached a significant level ($P < 0.05$). The incidence of adverse reactions in groups A and B was 8.89% and 6.67% respectively, which was not statistically significant ($P > 0.05$). Conclusion: In patients with severe asthma, early mechanical ventilation with inhalation of budesonide suspension can improve lung function more rapidly and with higher safety, and is worth promoting.

Keywords: Severe Asthma; Mechanical Ventilation; Budesonide; Lung Function; Adverse Effects

Introduction

The elderly are at high risk of severe asthma, with symptoms such as coughing and dyspnoea, which can significantly reduce the quality of daily life, and can lead to emphysema and respiratory failure if not treated in a timely manner. Budesonide mixed suspension has anti-inflammatory and antispasmodic effects, thus reducing the patient's symptoms, but the long-term effect of monotherapy is not good, so many doctors recommend that patients receive a combination of treatment, the author's department combined mechanical ventilation and budesonide treatment of severe asthma disease, and achieved more satisfactory results, the following analysis of treatment.

1. Data and methods

1.1 General information

The data of 90 patients with severe asthma filed in the Department of Pathology from 2020.2 to 2022.8 were extracted and analyzed. All the above selected patients had a clear diagnosis of severe asthma disease23], were conscious, could cooperate with the instructions given by the medical staff, knew the purpose of this study and cooperated actively to complete it. The groups were divided as follows.

Group A (n=45): (m/f) 28/17, age 33-74 (54.7±5.2) years, duration of illness 3-6 (4.2±1.5) d.

Group B (n=45): (m/f) 26/19, age 31-78 (55.4±5.5) years, duration of illness 2-8 (4.5±1.3) d.

The above baseline data of patients in groups A and B were not statistically significant ($P > 0.05$).

1.2 Methods

The basic treatment consisted of nutritional support, anti-infection and correction of acid-base disorders. Group A received 2 ml of budesonide suspension + 2 ml of saline by nebulised inhalation twice a day. Group B was treated with a BiPAP (positive pressure ventilator) in addition to the control group, with the inspiratory and expiratory pressures set at 8~18 ㎝ H2O and 4~10 ㎝ H2O respectively.

Patients in each group were treated continuously for 3 weeks.

1.3 Observation indexes

(1) Pulmonary function: [maximal expiratory volume in the 1st s (FEV1), maximal peak expiratory flow rate (PEF), FEV1/exertional spirometry (FVC)].

(2) Adverse effects.

1.4 Statistical processing

SPSS 33.0 software was used to process the data, and, rate (%) indicated the measurement and count data respectively, X^2 test. It was calculated that if $P < 0.05$, the difference reached the level of significance.

2. Results

2.1 Pulmonary function

After treatment, all the patients in group B had higher values of lung function index test than group A, and the difference reached the significance level ($P < 0.05$). Table 1.

Table 1 Comparison of lung function indicators before and after treatment between groups of patients $(\bar{x} \pm s)$

Time	Group（n）	FEV1（L）	PEF(L/s）	FEV1/FVC（%）
Before treatment	Group B（45）	1.48±0.18	2.07±0.56	45.94±3.14
	Group A（45）	1.50±0.14	2.11±0.54	45.81±3.22
After treatment	Group B（45）	2.23±0.16	3.03±0.59	67.21±4.33
	Group A（45）	1.74±0.20	2.28±0.65	53.17±3.37

2.2 Adverse reactions

In terms of adverse reaction rate, the difference between Group A vs Group B was 8.89% vs 6.67%, which was not significant ($p>0.05$). Table 2.

Table 2 Comparison of adverse reactions in patients between groups

Group（n）	sound of shouting	Facial discomfort	Rash	Total occurrence（%）
Group B（45）	1	0	2	3（6.67）
Group A（45）	2	1	1	4（8.89）

3. Discussion

The occurrence and development of asthma disease is strongly associated with the action of a variety of cytokines, and epidemiological surveys have revealed that there are currently 30 million diagnosed cases of asthma in China, and that the incidence of the disease will increase progressively in the context of a deteriorating atmospheric environment. Patients with severe asthma commonly suffer from airway smooth muscle spasm, airflow obstruction and increased functional residual air volume, so treatment of these patients requires early clearance of airway secretions, reduction of the inflammatory response, relief of airway obstruction and restoration of lung function.

In this study, after 3 weeks of continuous treatment, the FEV1, PEF and FEV1/FVC test values of patients in Group B were all greater than those in Group A, suggesting that patients in this group had better lung function improvement. The inhalation of budesonide by nebulisation allows the drug to reach the disease site directly, acting precisely on the airway mucosa, producing a significant inhibitory effect on the activity of immune cells, gradually relieving the spasm state and reducing the secretion of inflammatory substances, thus achieving good local anti-inflammatory effect and increasing the bioavailability of the drug. In practice, however, patients with severe asthma commonly have symptoms associated with respiratory muscle fatigue and their own poor sensitivity to budesonide, making it difficult to effectively control symptoms in around 10% of patients, and therefore requiring combined mechanical ventilation therapy. Non-invasive positive pressure ventilation is a reliable connection between the patient and the mask or nasal mask, which artificially simulates the normal breathing process, with a high level of inspiratory pressure, overcoming high airway resistance, reducing respiratory muscle fatigue symptoms, lowering oxygen consumption, reasonably regulating the ventilation and blood flow ratio, and thus improving alveolar ventilation and blood gas exchange efficiency [3]. The safety of treatment is an issue of great concern to the majority of patients, therefore, this topic observed the occurrence of adverse reactions, 8.89% and 6.67% in groups A and B respectively, the difference is not significant, which shows that the implementation process of the treatment plan in group B is safer and the majority of patients can participate in the treatment with confidence.

In conclusion, for patients with severe asthma, early mechanical ventilation and inhalation of budesonide suspension can improve lung function more rapidly and with a higher safety profile, which is worthy of popular application.

References.

[1] Ren W. Clinical observation of budesonide nebulized inhalation combined with methylprednisolone in the treatment of severe bronchial asthma [J]. China Pharmaceutical Guide, 2019,17(01):92-93.

[2] Lv P. Clinical effects of interferon combined with budesonide in the treatment of pediatric asthma [J]. Journal of Clinical Rational Drug Use,2022,15(29):129-132.

[3] Xie H, Wan QQ, Lin HY, Gan HL. Study on the efficacy of high-flow humidified oxygen therapy in the adjunctive treatment of severe asthma[J]. Heilongjiang Medicine, 2021, 34(05):1129-1131.

Author Bio

First author

Fan Rong (1980.1.10-), F, Han, Place of origin: Hubei. Jingzhou, MA, Title: Attending, Unit: Jingzhou First People's Hospital, Department: Department of Respiratory and Critical Care, Major research interests: Chronic obstructive pulmonary disease, interstitial lung disease, pulmonary embolism, pulmonary hypertension, ECMO life support, etc.

Corresponding author

Wu zhu (1982.5.14-), Male, Han Nationality, Place of Origin: Xiangtan, Hunan Province, Master's Degree, Title: Attending Physician, Unit: Jingzhou First People's Hospital, Department: Breast Surgery, Main Research Interests: Comprehensive treatment of breast cancer, diagnosis and treatment of non-lactating mastitis, postoperative reconstruction of

breast tumors, etc.

Second author

Xiao Wei (1969.9.8-), Male, Ethnicity: Han, Origin: Jingzhou, Hubei Province, Highest Education: Master, Title: Chief Physician, Unit: Jingzhou First People's Hospital, Department: Department of Respiratory and Critical Care, Main research interests: chronic obstructive pulmonary disease; bronchial asthma; lung cancer; pulmonary embolism; interstitial lung disease, etc.

Third author

Hu Weihua (1977.10.12-) Female, Ethnicity: Han, Place of origin: Jingzhou, Hubei, Highest education: Master, Title: Chief Physician

Unit: Jingzhou First People's Hospital, Department: Department of Respiratory and Critical Care Main research interests: chronic obstructive pulmonary disease; bronchial asthma; lung cancer; interstitial lung diseases, etc.

Exploration of the Shared Gene Signatures and Molecular Mechanisms Between Diabetic Foot Ulcer and Diabetic Microvascular Disease

Zhuodong Fu, Junwei Zong, Shouyu Wang

Department of Orthopedic Surgery, the First Affiliated Hospital of Dalian Medical University, Dalian 116011, China.

Abstract: Background: Diabetic foot ulcer (DFU) is a serious complication of diabetes caused by multiple factors. Diabetic microvascular disease has a close linkage with DFU. However, the inter-relational mechanisms between them are still unclear. This article aimed to explore the shared gene signatures and potential molecular mechanisms in DFU and diabetic microvascular disease. Methods: In the GEO database, DFU microarray datasets (GSE80178, GSE68183) and diabetic microvascular disease microarray datasets (GSE43950) were downloaded. After data standardization processing, we used R software to analyze the transcriptome sequencing data of each data set to find the differentially expressed genes (DEGs) of DFU and diabetic microvascular disease. Then obtained the overlapped DEGs in DFU and diabetic microvascular disease database by Jvenn. Finally, the shared DEGs were enriched by pathway enrichment and protein-protein interaction (PPI) analysis, and the hub gene was found by node analysis. Results: Totally, 1007 DEGs were identified in the GSE80178 dataset, 338 DEGs were identified in the GSE68183 dataset, 1154 were identified in the GSE43950 dataset, Venn diagram analyses showed that there were 14 shared DEGs in these datasets. Enrichment analysis shows that the shared DEGs were mainly associated with chronic inflammatory response, leukocyte migration, cellular transition metal ion homeostasis, vascular wound healing, collagen-containing extracellular matrix and Toll-like receptor binding. Involved pathways were mainly enriched in IL-17 signaling, glycosaminoglycan degradation, and calcium signaling. PPI analysis of these shared DEGs shows that S100A9, S100A8, CSTA, ADAP2, CD34 and FGL2 were the hub gene whose plays a pivotal role in DFU.Conclusion: Our work has identified several new DFU candidate genes that can be used as biomarkers or potential therapeutic targets.

Keywords: Diabetic Foot Ulcer; Diabetic Microvascular Disease; Differential Gene Analysis

1. Introduction

Diabetes mellitus (DM) has become one of the most serious public health problems worldwide. According to the latest data, the global prevalence of DM has reached 10.5% in 2021 and this number is expected to reach 12.2% in 2045, approximately 783.2 million people[1].

Poorly controlled diabetes lead to variety of chronic complications, such as microvascular disease, diabetic foot ulcer (DFU) and peripheral neuropathy. DFU is a disease caused by many factors, which is defined as the destruction of skin and its deep tissue far away from the ankle in patients with DM, always complicated with infection and (or) arterial occlusion of the lower extremities, and in severe cases involving muscle and bone tissue[2]. It is one of the most common and serious complications of DM. Microvascular disease are mainly characterized by thickened capillary basement membrane and

microthrombosis. Under the action of multiple factors, the morphological function and metabolic function of microvessels and microblood flow are seriously impaired, which leads to organ and tissue damage. Currently, there are many clinical studies on the association between DFU and diabetic microvascular disease, but mainly limited to the histological and functional levels, fewer at the molecular level.

Using the published gene expression data from the Gene Expression Omnibus (GEO) (http://www. ncbi.nlm.nih.gov/geo/), we identified the shared gene between DFU and diabetic microvascular disease, explored the underlying molecular mechanisms. It may help us to explore new diagnostic markers or therapeutic targets for DFU.

2. Materials and Methods

2.1 Dataset Download

We downloaded the DFU and diabetes-related microvascular complications gene expression profiles in the Gene Expression Omnibus (GEO, http://www.ncbi.nlm.nih.gov/ geo) database. The following criteria filter the downloaded dataset: First, the gene expression profiling must include cases and controls. Second, these datasets must provide the processed data or raw data that could be used for reanalyzation. Finally, the GEO dataset numbered GSE80178, GSE68183 and GSE43950 were selected. The GSE80178 and GSE68183 datasets were tested on the platform of Affymetrix Human Gene 2.0 ST Array. The GSE43950 dataset was tested on the Rosetta/Merck Human RSTA Custom Affymetrix 2.0 microarray platform.

2.2 Identification of Shared and Unique Gene Signatures in DFU and Diabete Microvascular Disease

The “limma” package (version3.50.1) in R software (version4.1.2) was used to normalize the gene expression data and identify the differentially expressed genes (DEGs) between the case and control group. The FDR < 0.05, $|logFC| > 0.5$ (GSE80178, GSE43950) and $|logFC| > 1$ (GSE68183) were considered to be threshold values. The “pheatmap” package (version 1.0.12) in R software was used to perform the hierarchical clustering heat maps that reveal the expression patterns of these DEGs. The overlapped DEGs in DFU and diabetes-related microvascular complications database were obtained using Jvenn.

2.3 GO and KEGG Analyses

The biological functions of identified DEGs of interest were assessed using the Database for Annotation, Visualization, and Integrated Discovery version (DAVID) Bioinformatics Resources (v6.8). Briefly, shared DEGs were imported into DAVID, and Gene Ontology (GO) and KEGG enrichment analyses were then conducted. For GO analyses, enriched biological processes (BPs), molecular functions (MFs), and cellular components (CCs) were assessed. The “GOplot” R package was used to visualize the results of these enrichment analyses.Then, DEGs were imported into Search Tool for the Retrieval of Interacting Genes (STRING) to construct the protein-protein interaction (PPI) network. The TSV file of PPI network was imported into Cytoscape 3.7.1. The interactions between enriched KEGG pathways were calculated and visualized by Cytoscape 3.7.1.

2.4 Common miRNAs-Target Genes Network Construction

The miRTarbase is an experimentally validated miRNA-target interactions database (http://mirtarbase. mbc.nctu.edu.tw/ php/index.php), which included 4,076 miRNAs and 23,054 target genes supported by experimental evidence (reporter assay, Western blot, microarray, or pSILAC). The intersection of target genes of common miRNAs and shared genes in DFU and

diabete microvascular disease were used to construct the miRNAs–mRNAs regulated network. Cytoscape software was used to visualize the network.

3. Result

3.1 DEG Identification

The GSE80178, GSE68183 and GSE43950 gene expression datasets were obtained from the GEO database. The GSE80178 dataset included 9 diabetic foot biopsy samples and 3 biopsy samples from normal individuals, GSE68183 dataset included 3 diabetic foot biopsy samples and 3 biopsy samples from normal individuals, whereas the GSE43950 dataset included 5 diabetic microvascular disease biopsies and 9 biopsies from healthy individuals. In total, 1007 DEGs were identified in the GSE80178 dataset (296 upregulated, 711 downregulated), 338 DEGs were identified in the GSE68183 dataset (135 upregulated, 203 downregulated), while 1154 were identified in the GSE43950 dataset (821 upregulated, 333 downregulated). The volcano plot and the heatmap of all DEGs were visualized respectively (Figure 1). Totally, 14 DEGs were shared between these three datasets, as identified through Venn diagram analyses (Figure 2).

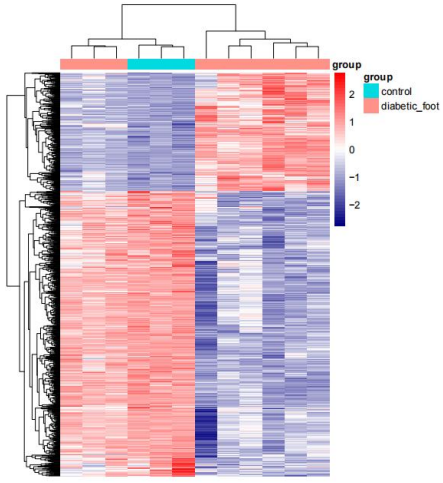

(a)

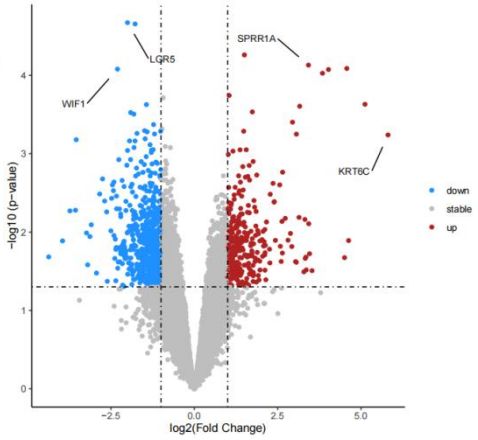

(b)

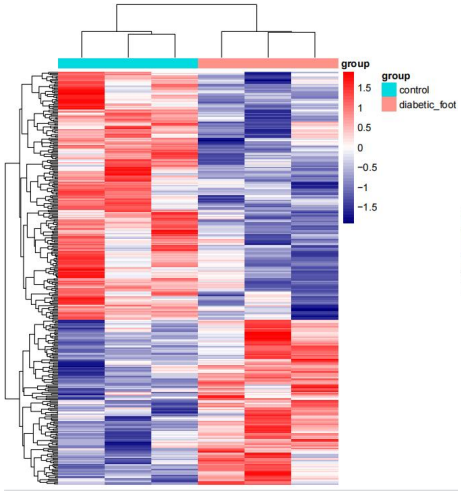

(c)

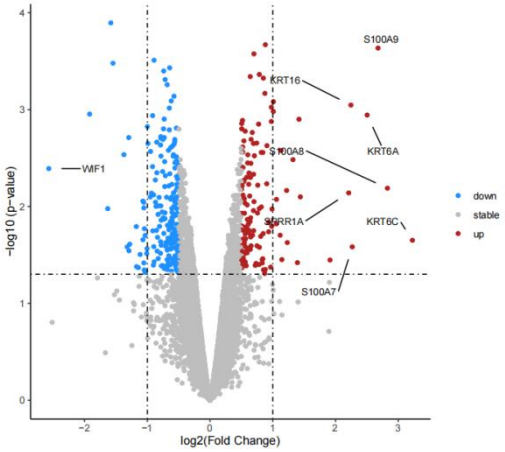

(d)

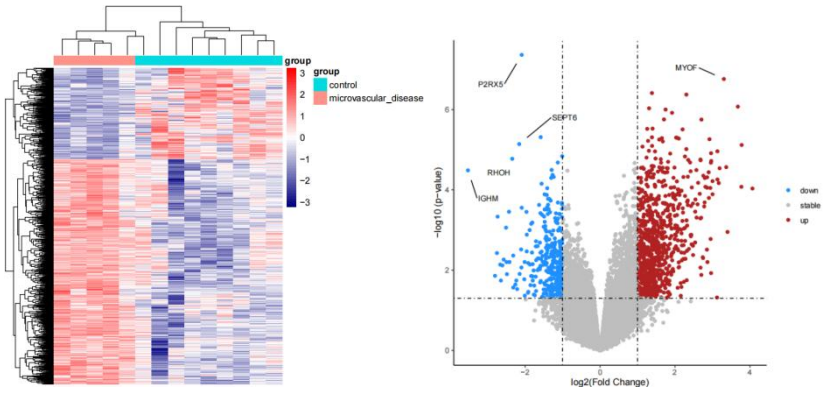

(e) (f)

Figure 1: Detection of differentially expressed genes (DEGs) in the GSE80178, GSE68183 and GSE43950 datasets. (a) An expression heat map of all the DEGs in the GSE80178 dataset, as determined based upon P values. (b) A volcano plot corresponding to the GSE80178 dataset. (c) An expression heat map of all the DEGs in the GSE68183 dataset, as determined based upon P values. (d) A volcano plot corresponding to the GSE68183 dataset. (e) An expression heat map of all the DEGs in the GSE43950 dataset, as determined based upon P values. (f) A volcano plot corresponding to the GSE43950 dataset.

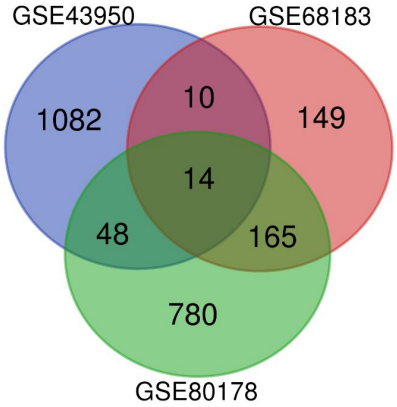

Figure 2: Identification of shared DEGs in GSE80178, GSE68183 and GSE43950.

3.2 GO and KEGG Analyses

The biological functions and pathways analyses were conducted using R package clusterProfifiler. The three GO categories (BP, CC, MF) of the shared DEGs were enriched respectively (Figure 3). The shared DEGs were mainly associated with chronic inflammatory response, leukocyte migration, cellular transition metal ion homeostasis, vascular wound healing, collagen-containing extracellular matrix and Toll-like receptor binding. As shown in Figure 4, the involved pathways were mainly enriched in IL-17 signaling (hsa04657), glycosaminoglycan degradation (hsa00531), and calcium signaling (hsa04020).

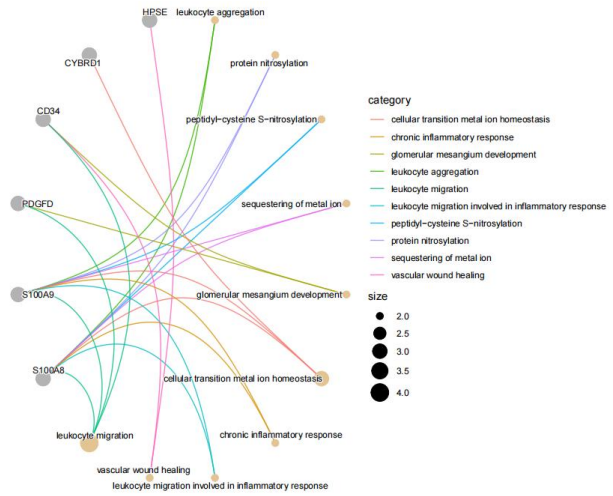

(a)

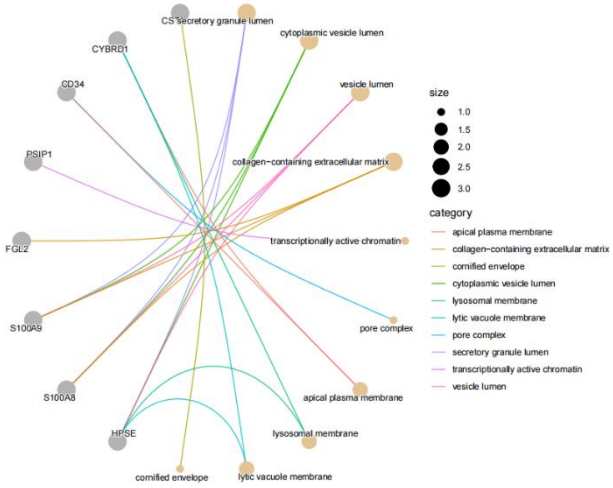

(b)

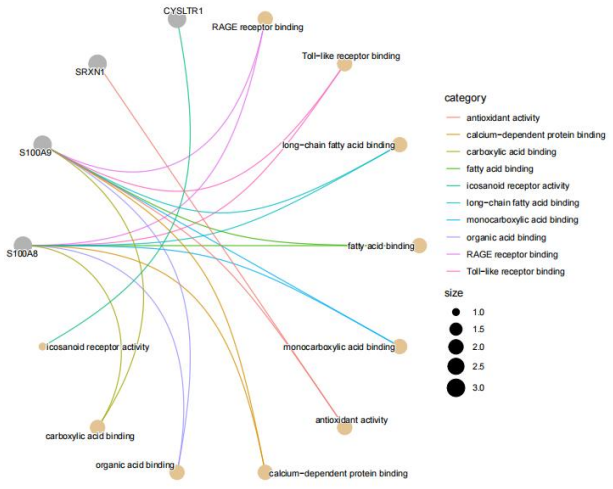

(c)

Figure 3: The top 10 terms of GO categories. (a) Biological process (BP). (b) Cellular component (CC). (c) Molecular function (MF).

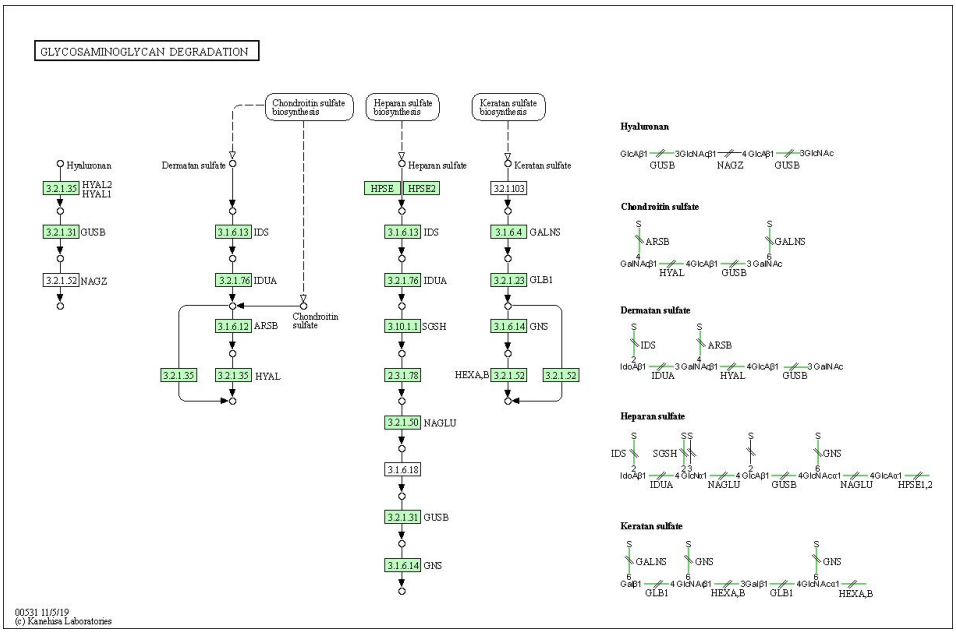

Figure 4: KEGG pathway analysis of the shared DEGs.

3.3 PPI Network Construction

The STRING database was next used to construct a gene PPI network (Figure 5). After the isolated nodes were removed by Cytoscape 3.7.1, a PPI network of shared DEGs between GSE80178, GSE68183 and GSE43950 was generated, which contained 6 hub genes (Figure 5).

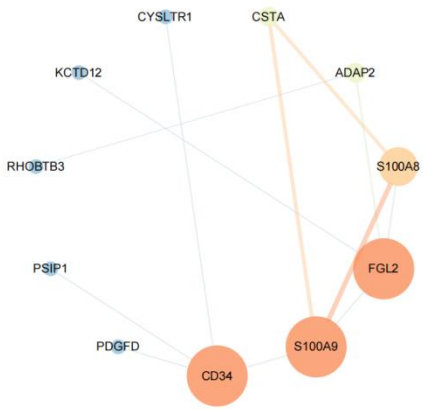

Figure 5: PPI network of shared DEGs between GSE80178, GSE68183 and GSE43950

4. Discussion

DFU is one of the most serious complications of DM, with high recurrence rate, amputation rate and mortality rate, which brings a serious burden to patients and society. DFU wounds usually show the characteristics of ischemia, hypoxia and chronic inflammation[3], which are difficult to cure[4,5]. Although researchers have carried out some studies on the pathogenesis of DFU, but the understanding of it is still relatively limited. Therefore, it is necessary to have a deeper understanding of its pathogenesis in order to find potential treatment targets and provide more treatment options.

In this study, the gene expression profile of GSE80178, GSE68183, GSE43950 were downloaded and analyzed by bioinformatics methods. Finally, 14 shared DEGs between DFU and diabetic microvascular disease were identified for

subsequent GO functional enrichment. Enrichment analysis showed that these genes were mainly associated with chronic inflammation, cell migration, immune response and extracellular matrix, which containing chronic inflammatory response, leukocyte migration, cellular transition metal ion homeostasis, vascular wound healing, collagen-containing extracellular matrix and Toll-like receptor binding. These annotation results provided valuable clues to reveal molecular interactions in the development of DFU. Clinical and experimental evidence suggests that DFUs fail to follow an orderly and selflimited progression of healing events and are characterized by a sustained inflammatory phase, which leads to permanent residence of inflammatory cells in the wound microenvironment, thereby chronically upregulating proinflammatory cytokines and transforming wounds into nonhealing chronic wounds[6]. Liu et al. reported that enhanced neutrophil extracellular traps in diabetic wounds triggered nod-like receptor protein 3 (NLRP3) inflammasome activation and IL-1β release in macrophages via the toll-like-receptor TLR-4/TLR-9 signaling pathway which are involved in the sustained inflammatory phase in DFUs[7]. Chang et al. found that monocytes come to the DFU and become macrophages (a type of white blood cells that digest microbes and cell debris through phagocytosis) and secrete transforming growth factor (TGF)-β1 and vascular endothelial growth factor (VEGF) for angiogenesis, results in production of collagen, hyaluronic acid, and fibronectin to form the new extracellular matrix[8]. As shown in the KEGG pathway analysis， genes were enriched in pathways such as “IL-17 signaling”, “glycosaminoglycan degradation” and “calcium signaling”. It is suggested genes or pathways relating to pro-inflammatory cytokines, glycosaminoglycan degradation and calcium channel might have important roles in the pathophysiology of DFU.

In order to further explore the potential hub genes between DFU and diabetic microvascular disease, we also screened the hub gene through PPI analysis. The results show that S100A9, S100A8, CSTA, ADAP2 (upregulation) and CD34, FGL2 (downregulation) may be the hub gene whose plays a pivotal role in DFU. In physiological function, S100A8 and S100A9 can be combined into homodimers or to bind in a non-covalent to form a willing dimer. When the concentration of Ca^{2+} changes, they also have other trimer or tetramer forms, and participate in the regulation and metabolism of cytoskeleton, arachidonic acid metabolism and anti-infective immune process in different ways. S100A8 and S100A9 can also recruit inflammatory cytokines to participate in anti-inflammatory response[9,10], so it has a certain value to reflect the intensity of inflammatory response. Singh et al. reported that the upregulation of bone marrow-derived pro-inflammatory cytokine S100A8 is one of the mechanisms leading to wound healing disorders and chronic ulcers in T2DM subjects[11]. ADAP2 is a member of the protein family with ADP ribose factor GTP enzyme activating protein domain. The protein encoded by this gene can bind to beta- tubulin and increase the stability of microtubules. It has been proved to be an important interferon stimulating gene in the immune system[12].CD34 is a transmembrane protein that is selectively expressed on the surface of mammalian hematopoietic stem or progenitor cells. When the cells gradually mature, the expression of CD34 decreases until it disappears. It is one of the main indicators for monitoring the microvessel density of new blood vessels[13], and is closely related to the biological process vascular wound healing. The downregulation of this gene may be related to the long-term nonunion of DFU. CSTA is a cysteine protease inhibitor that inhibits a variety of proteases, such as papain and cathepsin B, H and L, and is involved in cell adhesion, epidermal development and maintenance[14]. FGL2 is a membrane protein with prothrombinase at the N-terminal, expressed in a variety of cells, such as macrophages, dendritic cells, and endothelial cells, and can be induced robustly and exclusively in macrophages in response to stimulation with cytokines (IFN or TNF-α), viral infection, and lipopolysaccharide[15]. This suggests that FGL2 itself is a critical mediator of inflammation in that the interaction between inflammation and coagulation is reciprocally exacerbated in terms of inflammatory cytokine production and tissue factor secretion[16]. However, the role of CSTA and FGL2 in DFU needs to be further studied.

5. Conclusion

In this study, we analyzed the data sets of DFU and diabetic microvascular disease by bioinformatics, the co-expression

genes were identified and their functions were analyzed. It is shown that S100A9, S100A8, ADAP2 and CD34 are potential biomarkers for predicting DFU, which can provide ideas for follow-up research and treatment.This study still has some limitations, such as the small number of samples and the lack of clinical sample verification. More in-depth experiments are needed to verify the results of this study in the future.

References

[1] Sun H, Saeedi P, Karuranga S, et al. IDF Diabetes Atlas: Global, regional and country-level diabetes prevalence estimates for 2021 and projections for 2045. Diabetes Research and Clinical Practice, 2022, 183: 109119.

[2] Cruciani M, Lipsky BA, Mengoli C, et al. Granulocyte-colony stimulating factors as adjunctive therapy for diabetic foot infections. Cochrane Database of Systematic Reviews, 2013, 8(8).

[3] Vieceli Dalla Sega F, Cimaglia P, Manfrini M, et al. Circulating Biomarkers of Endothelial Dysfunction and Inflammation in Predicting Clinical Outcomes in Diabetic Patients with Critical Limb Ischemia. Int J Mol Sci. 2022, 23(18):10641.

[4] Catrina SB, Zheng X. Hypoxia and hypoxia-inducible factors in diabetes and its complications. Diabetologia. 2021, 64(4):709-716.

[5] Deng L, Du C, Song P, et al. The Role of Oxidative Stress and Antioxidants in Diabetic Wound Healing. Oxid Med Cell Longev. 2021, 2021:8852759.

[6] Yang S, Hu L, Han R, et al. Neuropeptides, Inflammation, Biofilms, and diabetic Foot Ulcers. Exp Clin Endocrinol Diabetes. 2022, 130(7):439-446.

[7] Liu D, Yang P, Gao M, et al. NLRP3 activation induced by neutrophil extracellular traps sustains inflammatory response in the diabetic wound. Clin Sci (Lond). 2019, 133(4):565-582.

[8] Chang M, Nguyen TT. Strategy for Treatment of Infected Diabetic Foot Ulcers. Acc Chem Res. 2021, 54(5):1080-1093.

[9] Argyris PP, Slama Z, Malz C, et al. Intracellular calprotectin (S100A8/A9) controls epithelial differentiation and caspase-mediated cleavage of EGFR in head and neck squamous cell carcinoma. Oral Oncol. 2019, 95:1-10.

[10] Pruenster M, Vogl T, Roth J, et al. S100A8/A9: From basic science to clinical application. Pharmacol Ther. 2016, 167:120-131.

[11] Singh K, Agrawal NK, Gupta SK, et al. Increased expression of TLR9 associated with pro-inflammatory S100A8 and IL-8 in diabetic wounds could lead to unresolved inflammation in type 2 diabetes mellitus (T2DM) cases with impaired wound healing. J Diabetes Complications. 2016, 30(1):99-108.

[12] Bist P, Kim SS, Pulloor NK, et al. ArfGAP Domain-Containing Protein 2 (ADAP2) Integrates Upstream and Downstream Modules of RIG-I Signaling and Facilitates Type I Interferon Production. Mol Cell Biol. 2017, 37(6):e00537-16.

[13] Marcianò A, Ieni A, Mauceri R, et al. CD34 and CD105 Microvessels in Resected Bone Specimen May Implicate Wound Healing in MRONJ. Int J Environ Res Public Health. 2021, 18(21):11362.

[14] Blaydon DC, Nitoiu D, Eckl KM, et al. Mutations in CSTA, encoding Cystatin A, underlie exfoliative ichthyosis and reveal a role for this protease inhibitor in cell-cell adhesion. Am J Hum Genet. 2011, 89(4):564-71.

[15] Ju C, Tacke F. Hepatic macrophages in homeostasis and liver diseases: from pathogenesis to novel therapeutic strategies. Cell Mol Immunol. 2016, 13(3):316-27.

[16] Ju C, Reilly TP, Bourdi M, et al. Protective role of Kupffer cells in acetaminophen-induced hepatic injury in mice. Chem Res Toxicol. 2002, 15(12):1504-13.

Identification of Potential Therapeutic Targets Inducible Co-Stimulator (ICOS) in Cancer Immunotherapy Using Bioinformatics Analysis

Qingjie Guo
ZIBO Vocational Institute, Zibo 255314, China.

Abstract: Clinical trials testing Inducible Co-Stimulator (ICOS) agonists in cancers are under way. However, Co-expression and Interaction of ICOS at the Gene and Protein Levels, the correlations of ICOS to prognosis and tumor-infiltrating lymphocytes in different cancers remain unclear. ICOS expression was analyzed via the Oncomine database and Tumor Immune Estimation Resource (TIMER) site. Analysis of the expression difference of ICOS shows that the expression of ICOS is significantly increased in BRCA, ESCA, HNSC, KIRC, KIRP, LIHC, STAD and UCEC. We evaluated the influence of ICOS on clinical prognosis using Kaplan-Meier plotter and Gene Expression Profiling Interactive Analysis (GEPIA). This analysis confirmed that low ICOS expression was significantly correlated with poor overall survival (OS) and progression-free survival (PFS) in ovarian cancer. The correlations between ICOS and cancer immune infiltrates were investigated via TIMER. Metascape and Protein-protein interaction (PPI) analysis suggest that ICOS plays an important role in the process of immune activation. ICOS is a potential target for the development of antibody drugs.

Keywords: ICOS; Cancer; Lymphocytes; Immunotherapy; Prognosis

1. Introduction

In the past decade, it has been widely recognized that the immune system can control the occurrence and development of tumors. ICOS is one of the members of the CD28 family. It has attracted interest as a T-cell enhanced costimulatory receptor. Hutloff et al. first described ICOS as a T cell-specific costimulatory molecule that enhances T cell responses to foreign antigens. ICOS is a complex central immune response and homeostasis center. Whether ICOS can be used as a drug target needs to be further determined.

Here, we evaluated the expression level of ICOS mRNA in different types of cancer and evaluated the association with the prognosis of various types of cancer in a common database (e.g., Oncome, Kaplan-Meier plotter, GEPIA). We also use the Metascape and String database to reveal the important role of ICOS in the biological process, and provide the current situation of anti ICOS antibody agonists.

2. Material and methods

2.1 Oncomine database analysis

ICOS mRNA expression levels in different types of human cancers were identified in the Oncomine database (https://www.oncomine.org/resource/login.html) [1]. The threshold was a P-value of 0.001, a fold change of 1.5, a top 10% gene ranking, and the data had to be from mRNA.

2.2 TIMER database analysis

We analyzed ICOS expression and the correlation of ICOS expression with the abundance of 6 types of infiltrating immune cells (B cells, CD4+ T cells, CD8+ T cells, neutrophils, macrophages, and dendritic cells) in in different types of human cancers via The Tumor IMmune Estimation Resource (TIMER) algorithm database (https://cistrome. shinyapps. io/timer/) [2].

2.3 Co-expression and Interaction Analysis

COXPRESdb database was used to predict the co expression genes of ICOS. The Metascape database (http://metascape.org) is used to analyze the functional enrichment relationship of ICOS [3]. String database (https://string-db.org/cgi/input.pl) was used to predict the biological process and function of ICOS protein, and analyze protein-protein interaction [4].

3. Results

3.1 The mRNA Expression Levels of ICOS in Different Types of Human Cancers

In order to determine the difference of ICOS expression between tumor and normal tissues, the Oncomine database were used to analyze the level of ICOS mRNA in different tumor and normal tissues of multiple cancer types (Figure 1A). The Oncomine database analysis revealed that ICOS mRNA expression was lower in sarcoma. Higher expression was observed in breast cancer, kidney cancer, Melanoma.

For further evaluate ICOS expression in human cancers, we examined ICOS expression using TCGA RNA-sequencing data by TIMER. The differential expression of tumor and adjacent normal tissue for ICOS in all TCGA tumors is shown in Figure 1B. ICOS expression was significantly lower in LUAD (lung adenocarcinoma), LUSC (Lung squamous cell carcinoma), THCA (thyroid carcinoma) compared with adjacent normal tissues. However, LAYN expression was significantly higher in BRCA (breast invasive carcinoma), ESCA (Esophageal carcinoma), HNSC (head and neck cancer), KIRC (kidney renal clear cell carcinoma), KIRP (Kidney renal papillary cell carcinoma), LIHC (liver hepatocellular carcinoma), STAD (stomach adenocarcinoma) and UCEC (uterine corpus endometrial carcinoma) compared with adjacent normal tissues.

3.2 Co-expression and Interaction Analyses of ICOS at the Gene and Protein Levels

We used the COXPRESdb database to analyze the genes co-expressed with ICOS. The results showed that the gene treasure co-expressed with ICOS included CTLA4, ITK, CD28, TRAT1, CD2, SH2D1A, CD3D, CD3G, UBASH3A, SIRPG, IFNG, THEMIS and TIGIT. The functions of ICOS and genes co-expressed were predicted by analyzing GO and KEGG in Metascape. Metascape analysis found that the following processes were affected by ICOS gene alterations: Lymphocyte activation; T cell receptor signaling pathway; Hematopoietic cell lineage; Cytokine-cytokine receptor interaction; Cell adhesion molecules (CAMs); negative T cell selection; regulation of lymphocyte differentiation (Figure 2A and B). These results indicate that ICOS plays an important role in immune regulation.

For further investigate the molecular function and biological process of ICOS, String database is used to analyze the

Protein-protein interaction (PPI) of ICOS. String predicted functional partners included ICOL, RC3H1, CD40LG, B7RP1, PIK3R1, PIK3CB, PIK3CD, PIK3R3, PIK3R2 and PIK3CA. As shown in Figure 4C, these functional molecules form a PPI network in String database. The biological process analysis of ICOS shows that ICOS plays an important role in positive regulation of immune system process, phosphatidylinositol phosphorylation, T cell costimulation, phosphatidylinositol-3-phosphate biosynthetic process (Figure 2D). The molecular function analysis of ICOS shows that phosphatidylinositol 3-kinase activity, 1-phosphatidylinositol-3-kinase activity, phosphatidylinositol-4, 5-bisphosphate 3-kinase activity, 1-phosphatidylinositol-3-kinase regulator activity, 1-phosphatidylinositol-4-phosphate 3-kinase activity, phosphotransferase activity, alcohol group as acceptor are important molecular functions of ICOS (Figure 2E). These results suggest that ICOS plays an important role in the process of immune activation.

4. Discussion

Nowadays, immunotherapy has become an important means of cancer treatment. The clinical manifestations of anti-CTLA-4 and anti-PD-1 antibodies also provide a basis for immunotherapy. Combined immunotherapy is an effective method to improve the effect of immunotherapy monotherapy. Therefore, we provide three development strategies: 1) develop bispecific antibody related to ICOS; 2) develop fusion protein with agonist function based on ICOSL gene sequence; 3) combine anti-ICOS antibody agonist with other drugs for tumor treatment

In addition, it is worth noting that ICOS can activate both killer T cells and regulatory T cells. Autoimmune disease is a kind of chronic disease with multiple organs and systems damage caused by the disorder of the body's autoimmune system, such as systemic lupus erythematosus (SLE), rheumatoid arthritis (RA), Sjogren's syndrome (SS), polymyositis and dermatomyositis (DM). The development of ICOS antagonists is expected to be a therapeutic drug for autoimmune diseases.

Conflict of interest

The authors declare that there are no conflicts of interest.

Fig. 1. ICOS expression levels in different types of human cancers. (A) ICOS in data sets of different cancers in the Oncomine database. (B) Human ICOS expression levels in different tumor types from TCGA database were determined by TIMER (*$p < 0.05$, **$p < 0.01$, ***$p < 0.001$).

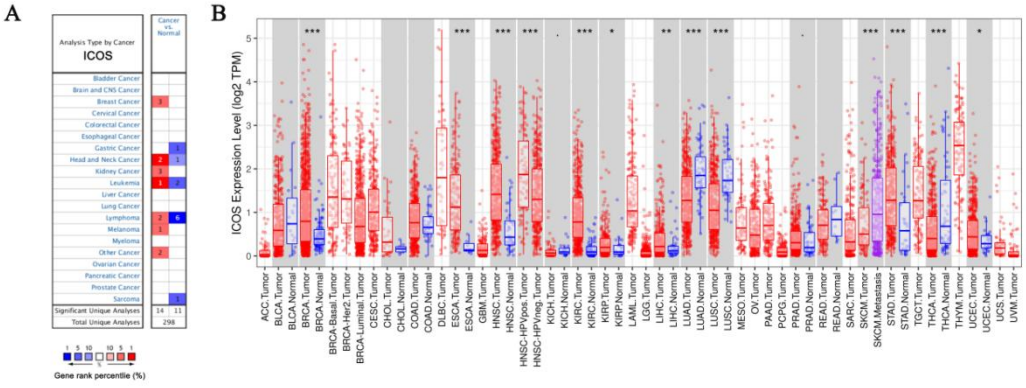

Fig. 2. Co-expression and Interaction Analyses of ICOS at the Gene and Protein Levels. (A) Metascape bar graph and (B) Metascape enrichment network visualization showing the functions of ICOS and genes co-expressed by analyzing GO and KEGG. (C) Protein–protein interaction network of ICOS in the String database. (D) biological process and (E) molecular function of ICOS enrichment analyses. The x-axis represents the −log10 (p value), and the y-axis represents the GO term. The GO terms were measured by the rich factor, p value and number of genes enriched. The greater the Rich factor is, the greater the degree of enrichment and the greater the p value [0, 1]. The brighter the color of red is, the more significant

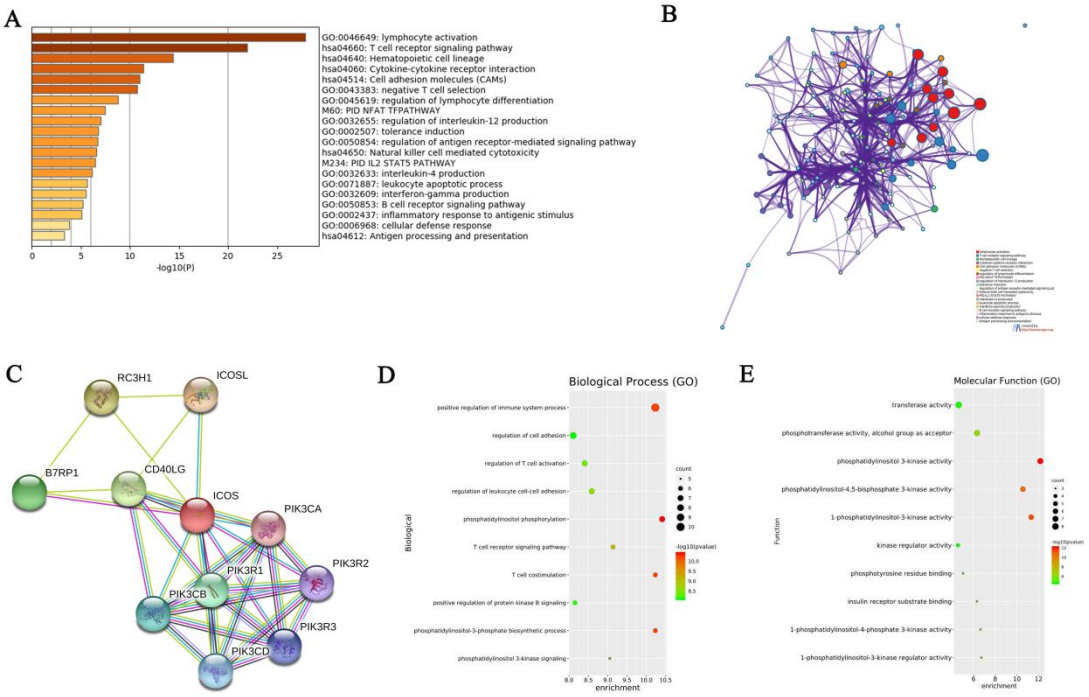

the term.

References

[1] Rhodes DR, Kalyana-Sundaram S, Mahavisno V, et al, Chinnaiyan AM (2007) Oncomine 3.0: genes, pathways, and networks in a collection of 18,000 cancer gene expression profiles. Neoplasia (New York, NY) 9 (2):166-180.

[2] Li T, Fan J, Wang B, et al. (2017) TIMER: A Web Server for Comprehensive Analysis of Tumor-Infiltrating Immune Cells. Cancer research 77 (21):e108-e110.

[3] Tang Z, Li C, Kang B, et al. (2017) GEPIA: a web server for cancer and normal gene expression profiling and interactive analyses. Nucleic acids research 45 (W1):W98-w102.

[4] Franceschini A, Szklarczyk D, Frankild S, et al. (2013) STRING v9.1: protein-protein interaction networks, with increased coverage and integration. Nucleic acids research 41 (Database issue):D808-815.

Research Progress of CD73 in Cancer

Shuang Guo[1], Hongli Liu[1,2*]

1. School of Medical Technology, Shaanxi University of Chinese Medicine, Xianyang 712000, China.

2. Clinical Laboratory Center of Xi'an People's Hospital (Xi'an Fourth Hospital), Xi'an 710000, China.

Abstract: CD73 (NT5E, extracellular 5' nucleotidase) is a multifunctional glycoprotein encoded by the NT5E gene with a relative molecular weight of 70 kD that can be anchored to the outer surface of cell membranes by glycosyl phosphatidylinositol (GPI).CD73 expression levels are aberrant in breast, colorectal, head and neck squamous cell carcinomas, gastric and hepatocellular carcinomas. However, the possible role and mechanism of CD73 in gastric carcinogenesis and development has not been clarified. In this paper, we will review the multiple roles of CD73 in tumour development, including the clinical significance of CD73, the promotion of tumour growth, metastasis and angiogenesis by CD73, the suppression of immune response by CD73, the regulatory mechanisms of CD73 expression, and the current status of CD73 anti-tumour therapy, with a view to providing a reference for subsequent studies.

Keywords*:* CD73; Cancer; Antitumor Therapy; Regulatory Mechanism

Introduction

The development, progression and metastasis of malignant tumours in vivo are intricate and complex, involving rapid proliferation of mutant cells in an uncontrollable manner, inhibition of programmed cell death, massive angiogenesis, escape from immune surveillance, invasion and colonisation to distant organs. In addition, many signalling pathways have been identified in relation to cancer progression[1].It is now clear that adenosine is one of the most important immunosuppressive regulatory molecules in the tumour microenvironment[2].

CD73 is a glycosylphosphatidylinositol (GPI)-anchored cell surface protein with a molecular weight of 70 kD, encoded by the NT5E gene, also known as extracellular 5'-nucleotidase (Ecto-5'-nucleotidase), which plays a crucial role in the switching of adenosinergic signalling. A growing body of evidence confirms that CD73 is a key regulatory molecule in cancer development. It has a promising role in the study of rheumatoid mouse models, and although it has not yet been studied in clinical patients, ANTICD73 therapy has emerged as a promising approach for the future treatment of cancer patients[3-4] . This article provides a review of the role of CD73 in cancer development, including the clinical significance of CD73 in cancer patients, the role of CD73 in promoting tumour growth, metastasis and angiogenesis , the suppressive effect of CD73 on the immune system in the tumour microenvironment, the regulatory mechanisms of CD73 expression, and the prospects for antiCD73 therapy.

1. Clinical significance of CD73 in cancer patients

There is increasing evidence that NT5E is highly expressed in tumor tissues such as lung[5] , breast[6] , colorectal[7] , pancreatic[8] , gallbladder[9] , prostate[10] , thyroid[11] , and head and neck[12] . In addition, Inoue et al. found that CD73

overexpression was associated with gender, smoking and histological classification in patients with non-small cell lung cancer[5].in breast cancer patients, Turcotte et al.found that CD73 overexpression predicted trastuzumab resistance in breast cancer patients[13].Cushman et al. also found It has been shown that high CD73 expression was observed in gastric cancer tissues and serum compared to normal human gastric mucosal tissues and healthy human serum[14], respectively, and that high CD73 expression was positively associated with poor differentiation, depth of tumour infiltration, more lymph node metastases, number of distant metastases and clinical advanced stage in gastric cancer patients. However, its molecular mechanism is not clear.

2. Promotion of tumour growth, metastasis and angiogenesis by CD73

Recently, Lu et al. evaluated the clinical significance and prognostic value of CD73 in human gastric cancer tissues in digestive system cancers:CD73 expression was analysed by immunohistochemistry (IHC) and CD73 overexpression was found to be positively correlated with tumour differentiation, depth of infiltration, lymph node morphology, metastasis and cancer stage, and overall survival was lower in patients with high CD73 expression[15] . In addition to gastric cancer, Serra et al. evaluated the clinical significance of CD73 in chronic lymphocytic leukaemia and found that high CD73 expression was associated with more aggressive clinical behaviour[16], while another study showed that CD73 expression had no prognostic value in children (aged 1-18 years) with acute lymphoblastic leukaemia In other cancers, Yang et al. reported that CD73 in prostate cancer Overexpression of CD73 in prostate cancer was associated with lymph node metastasis[17].Taken together, these results reveal that CD73 is an important clinical or prognostic biomarker in several types of cancer, suggesting its potential value in clinical diagnosis and prognosis.

3. Regulatory mechanisms of CD73 expression

CD73 plays an important role in the progression of malignancies and has been found to be overexpressed in many types of cancer. CD73 expression was found to be negatively regulated by the estrogen receptor (ER) in breast cancer, and ER deficiency significantly increased CD73 expression. Thus,CD73 is highly expressed in ER-negative breast cancer patients than in ER-positive breast cancer patients and may be a promising target for clinical treatment of ER-negative breast cancer patients[18].In contrast to ER, thyroid hormones are thought to synergistically promote CD73 expression in several cell types of the nervous and cardiovascular systems (glioma cells, vascular smooth muscle cells and ventricular myocytes)[19-20].It was found that CD73 expression was positively correlated with cell sphere-forming capacity and was highly expressed in hepatocellular carcinoma cells. downregulation of CD73 impeded cell clone formation, whereas overexpression of CD73 produced the opposite effect[21].

4. The future of CD73 anti-tumour therapy

The role of CD73 in tumour growth and metastasis, particularly as a key immunosuppressor in the tumour microenvironment, offers a potential opportunity for the development of anti-CD73 therapies for various human cancers.Cancer immunotherapy has become increasingly interesting in recent years. Drugs such as anti-pd1 monoclonal antibodies and anti-CTLA-4 monoclonal antibodies that block programmed death-1 (PD-1) and cytotoxic T-lymphocyte antigen (CTLA-4) receptors have shown very impressive objective responses in patients[22].Interestingly, Allard found that in mouse models, anti-cd73 monoclonal antibody significantly enhanced the activity of anti-ctla -4 and anti-PD-1 monoclonal antibodies against MC38-OV A (colon) tumours, RM-1 (prostate) subcutaneous tumours and metastatic 4T1.2 breast cancer[23].

5. Summary and perspectives

The relationship between CD73 overexpression and cancer subtype, prognosis, and patient response to drugs has been significantly correlated. CD73 is a potential target for cancer therapy. Some researchers have also shown good anti-tumour effects in mouse tumour models treated with inhibitors or monoclonal antibodies targeting CD73. It is believed that in the future, CD73 blockers and immunotherapeutic agents will be developed that are safe, effective and can be used in the treatment of clinical patients, providing a good opportunity to treat some cancer patients.

References

[1] Burnstock G, Di Virgilio F. Purinergic signalling and cancer. Purinergic Signal. 2013 Dec; 9(4): 491-540.

[2] Bours MJ, Swennen EL, Di Virgilio F, *et al*. Adenosine 5'-triphosphate and adenosine as endogenous signaling molecules in immunity and inflammation. Pharmacol Ther. 2006 Nov;112(2):358-404.

[3] Zhang B. Opportunities and challenges for anti-CD73 cancer therapy. Immunotherapy. 2012 Sep;4(9):861-5.

[4] Stagg J. The double-edge sword effect of anti-CD73 cancer therapy. Oncoimmunology. 2012 Mar 1;1(2):217-218.

[5] Inoue Y, Yoshimura K, Kurabe N, et al. Prognostic impact of CD73 and A2A adenosine receptor expression in non-small-cell lung cancer [J]. Oncotarget, 2017, 8(5): 8738-51.

[6] Yu J, Wang X, Lu Q, et al. Extracellular 5'-nucleotidase (CD73) promotes human breast cancer cells growth through AKT/GSK-3beta/beta-catenin/ cyclinD1 signaling pathway [J]. Int J Cancer, 2018, 142(5): 959-67.

[7] Xie M, Qin H, Luo Q, et al. MicroRNA-30a regulates cell proliferation and tumor growth of colorectal cancer by targeting CD73 [J]. BMC Cancer, 2017, 17(1): 305.

[8] Wu R, Chen Y, Li F, et al. Effects of CD73 on human colorectal cancer cell growth in vivo and in vitro [J]. Oncol Rep, 2016, 35(3): 1750-6.

[9] Haun RS, Quick CM, Siegel ER, et al. Bioorthogonal labeling cell-surface proteins expressed in pancreatic cancer cells to identify potential diagnostic/ therapeutic biomarkers [J]. Cancer Biol Ther, 2015, 16(10): 1557-65.

[10] Yang Q, Du J, Zu L. Overexpression of CD73 in prostate cancer is associated with lymph node metastasis [J]. Pathol Oncol Res, 2013, 19(4): 811-4.

[11] Bertoni APS, Bracco PA, De Campos RP, et al. Activity of ecto-5'-nucleotidase (NT5E/CD73) is increased in papillary thyroid carcinoma and its expression is associated with metastatic lymph nodes [J]. Mol Cell Endocrinol, 2019, 479(54-60.

[12] Song Y, Song C, Yang S. Tumor-Suppressive Function of miR-30d-5p in Prostate Cancer Cell Proliferation and Migration by Targeting NT5E [J]. Cancer Biother Radiopharm, 2018, 33(5): 203-11.

[13] Turcotte M, Allard D, Mittal D, et al. CD73 Promotes Resistance to HER2/ErbB2 Antibody Therapy [J]. Cancer Res, 2017, 77(20): 5652-63.

[14] Cushman SM, Jiang C, Hatch AJ, et al. Gene expression markers of efficacy and resistance to cetuximab treatment in metastatic colorectal cancer: results from CALGB 80203 (Alliance) [J]. Clin Cancer Res, 2015, 21(5): 1078-86.

[15] Zhao J, Soto LMS, Wang H, Katz MH, Prakas. *et al*. Overexpression of CD73 in pancreatic ductal adenocarcinoma is associated with immunosuppressive tumor microenvironment and poor survival. Pancreatology. 2021 Aug;21(5):942-949.

[16] Serra S, Horenstein AL, Vaisitti T, *et al*. CD73-generated extracellular adenosine in chronic lymphocytic leukemia creates local conditions counteracting drug-induced cell death. Blood. 2011 Dec

1;118(23):6141-52.

[17] Yang Q, Du J, Zu L. Overexpression of CD73 in prostate cancer is associated with lymph node metastasis. Pathol Oncol Res. 2013 Oct;19(4):811-4.

[18] Loi S, Pommey S, Haibe-Kains B, *et al*. CD73 promotes anthracycline resistance and poor prognosis in triple negative breast cancer. Proc Natl Acad Sci U S A. 2013 Jul 2;110(27):11091-6.

[19] Wink MR, Tamajusuku AS, Braganhol E, *et al*. Thyroid hormone upregulates ecto-5'-nucleotidase/CD73 in C6 rat glioma cells. Mol Cell Endocrinol. 2003 Jul 31; 205(1-2):107-14.

[20] Tamajusuku AS, Carrillo-Sepúlveda MA, Braganhol E, *et al*. Activity and expression of ecto-5'-nucleotidase/CD73 are increased by thyroid Activity and expression of ecto-5'-nucleotidase/CD73 are increased by thyroid hormones in vascular smooth muscle cells. Mol Cell Biochem. 2006 Sep; 289(1-2): 65-72.

[21] Ma XL, Hu B, Tang WG, *et al*. CD73 sustained cancer-stem-cell traits by promoting SOX9 expression and stability in hepatocellular carcinoma. j Hematol Oncol. 2020 Feb 5;13(1):11.

[22] Pardoll DM. The blockade of immune checkpoints in cancer immunotherapy. Nat Rev Cancer. 2012 Mar 22;12(4):252-64.

[23] Allard B, Pommey S, Smyth MJ, *et al*. Targeting CD73 enhances the antitumor activity of anti-PD-1 and anti-CTLA-4 mAbs. Clin Cancer Res. 2013 Oct 15;19 (20):5626-35.

Risk Factors for Artificial Kidney Failure During Continuous Renal Replacement Therapy

Wen Guo, Xuemei Chen*

Emergency Department, The First Affiliated Hospital of Chongqing Medical University, Chongqing 400042, China.

Abstract: **Objective** To explore the influencing factors of artificial kidney failure (AKF) during continuous renal replacement therapy (CRRT). **Methods** We conducted a retrospective observational study on 70 patients undergoing 199740 minutes of CRRT comprising 143 circuits at the Department of Intensive Care Medicine of First Affiliated Hospital of Chongqing Medical University from August 2021 to August 2022. **Results** The occurrence rate and total time of access outflow dysfunction (AOD) in AKF group increased significantly than those in nAKF group. Receiver Operating Characteristic (ROC) Curve analysis showed the optimal cutoff value of AOD total time (AODTT) was 7 minutes. Logistic regression analysis further showed that AODTT≥7 min was an independent predictor of AKF. **Conclusion** The presence of AOD was related to AKF. AODTT≥7 min during CRRT was an independent risk factor for AKF.

Keywords: Continuous Renal Replacement Therapy; Artificial Kidney Failure; Access Outflow Dysfunction

Introduction

Continuous renal replacement therapy (CRRT), which can continuously and slowly remove extra water and solutes retained, has become an effective multiple organ support therapy, widely used to manage renal and extra-renal problems such as fluid overload or severe acidosis in intensive care unit (ICU)[1]. However, CRRT prescription is not always fully delivered. Many factors could hinder CRRT delivery generating a gap between prescription and delivery. Maintaining extracorporeal circuit (ECC) function is important for safe and effective CRRT delivery[2]. ECC includes a double-lumen catheter, its vascular access outflow and inflow lumen, filter, pre-filter and post-filter tubing, air-trap chamber and pre-vascular inflow tubing. When dysfunction occurs at any part of the ECC, it can cause the failure of the entire artificial kidney (AKF)[3], leading to unexpected treatment interruptions, inefficient blood purification, blood loss, more waste and cost[4].

CRRT modality, dilution type, anticoagulation mode and catheter function highly influence ECC life[5,6]. Modern CRRT equipment can automatically monitor circuit pressure at intervals of 1 minute, including access outflow pressure (AOP), pre-filter pressure (PFP), effluent pressure (EP) and return inflow pressure (RIP)[7]. The transmembrane pressure (TMP) can be estimated by the following formula: TMP=(PFP+RP)/2-EP[8]. Automated monitoring circuit pressure at different points during CRRT may contribute to early identify where and how ECC dysfunction occurs, prompt to modify the settings, avoid unplanned CRRT interruptions or avoidable downtime[9]. The current study aims to explore the influencing factors of AKF during CRRT.

1. Materials and methods

1.1 Study subjects

We conducted a retrospective observational study of patients who underwent CRRT in the Department of Intensive Care Medicine of the First Affiliated Hospital of Chongqing Medical University from August 2021 to August 2022. The exclusion criteria were as follows: CRRT connected to an ECMO circuit, pressure data could not be obtained and incomplete data. Due to its retrospective observational nature, written informed consent was not required.

1.2 Data collection

General information including age and sex, and CRRT-related parameters were collected. Pressure of extracorporeal circulation circuit during CRRT was downloaded, decompressed and extracted.

1.3 Definition

AKF was defined by the following criteria: 1)TMP ≥ 450mmHg, blood does not return due to complete clotting of filter; 2)TMP ≥ 250mmHg in hour prior to circuit cessation; 3)AP and RP extremes (AP≤-250mmHg or RP≥+350mmHg in hour preceding circuit cessation)[10]; 4) unscheduled CRRT cessation due to dysfunctional ECC. Access outflow dysfunction (AOD) was defined as AOP<-200mmHg[3].

1.4 Statistical analysis

Statistical analysis was performed using SPSS 26.0 statistical software. All numeric data with a normal distribution were presented as means±SD and analyzed using Student's t-test. Numeric variables with skew distribution were expressed as median (interquartile range) and compared using Mann-Whitney U test. Categorical variables were expressed as percentages and analyzed using chi-square test. Receiver-operating characteristic (ROC) curve analysis and binary logistic regression analysis were conducted to predict risk factors for AKF. $P<0.05$ was considered statistically significant.

2. Results

2.1 Changes of CRRT-related parameters

In total, 70 patients including 98 males and 45 females aged 14–90 years, undergoing 199740 min of CRRT comprising 143 CRRT circuits were enrolled in this study. According to whether AKF occurs, CRRT circuits were divided into AKF group and nAKF group. We explored the risk factors for AKF and found significantly increased AOD occurrence and AOD total time (AODTT) in the AKF group compared with the non-AKF group ($p<0.05$). No differences in CRRT modalities, anticoagulation mode, vascular access and dilution mode were noted between the two groups (Table 1).

Table 1 Comparison of CRRT-related parameters in AKF group and nAKF group

	nAKF (n=94)	AKF (n=49)	*P*
Modality			
CVVHDF	84(89.36)	41(83.67)	0.33
CVVH	10(10.64)	8(16.33)	
Anticoagulation			
Citric acid	75(79.79)	44(89.80)	0.07
Low molecular weight heparin	16(17.02)	2(4.08)	

Non-anticoagulant	3(3.19)	3(6.12)	
Dilution			
Post-dilution (CVVHDF)	84(89.36)	41(83.67)	0.33
Pre- and post-dilution (CVVH)	10(10.64)	8(16.33)	
Vascular access			
Internal jugular vein	5(5.32)	1(2.04)	0.35
femoral vein	89(94.68)	48(97.96)	
AOD	51(54.26)	39(79.59)	0.00
AOD total time	1(0,7)	17(1,55)	0.00

2.2 Risk factors for AKF during CRRT

Because longer AODTT was found to be associated with AKF, we performed ROC analysis to assess the predictive value of this variable for AKF. The area (95% CI) under ROC of AODTT to predict AKF was 0.69 (0.57~0.80). The optimal cutoff value, sensitivity and specificity of AODTT were 7 min, 65% and 77%, respectively. Logistic regression analysis further showed that AODTT≥7 min was an independent predictor of AKF (P<0.05).

Table 2 Independent risk factors for AKF during CRRT

	P	OR	95% CI
Presence of AOD (versus absence)	0.91	1.07	0.35 ~ 3.28
AODTT≥7min (versus<7min)	0.00	5.44	1.78~ 16.65

3. Discussion

Today, CRRT has been widely used in critically ill patients to optimize fluid and solutes management[11]. Maintaining ECC patency and filter performance is crucial to ensure CRRT delivery in a safe and high-quality manner[3]. In fact, dysfunctional vascular access and ECC clotting remain the main reasons for unscheduled treatment cessation and circuit replacement, which may reduce CRRT efficacy, increase blood loss, workload and costs[9]. Early identifying risk factors for AKF might help to adjust settings, increase circuit life and efficiency.

Vascular access plays a significant role in determining ECC life. Catheter bending, collapse of a central vein around the catheter, and sudden catheter position changes usually leading to intermittent occlusion, and progressive thrombus or fibrous sheath in the lumen of a catheter, inducing circuit blood flow rapid decrease or even flow cessation were reported to be related to shortened circuit life[12]. Baldwin et al. used ultrasound to monitor circuit blood flow and found that blood flow reductions occurred frequently without machine alarms alerting the operator, and then no corrective responses were made, eventually inducing stasis and circuit failure[13]. Automated electronic monitoring ECC pressure at different points is helpful for early identifying vascular access dysfunction, making corrective response, and then preventing AKF. We found 62.94% circuits experienced AOD similar to 56.96% reported by Zhang et al.[9]. It is reported AOD events could shorten circuit life[3], our study also showed the occurrence of AOD in circuits with AKF (79.59%) was higher than circuits without AKF (54.26%). We further found total time of AOD in AKF group increased significantly than those in nAKF group, and AODTT≥7 min was an independent risk factor for AKF, suggested an alarming level of AODTT≥7 min could be set to alert the operator, then make corrective response to prevent circuit failure. However, this is a single center, retrospective observational study, further multicenter prospective randomized controlled studies are needed to corroborate our findings.

CRRT-related parameters including treatment modality, dilution and anticoagulation modes, and vascular access sites are also related to circuit life. It is reported CVVHDF/CVVHD provided longer filter life compared to CVVH[14,15]; the filter life in Pre-dilution CVVH might be longer than post-dilution CVVH because the blood is diluted prior to entry into the

filter[12]; citrate anticoagulation (RCA) might improve filter life compared with systemic heparin anticoagulation[16]. Whereas, our study included 87.41% circuits in CVVHDF with post-dilution group, only 18 (12.59%) circuits in CVVH with pre-dilution and post-dilution group, no circuit in CVVH with post-dilution group; 83.22% circuits in RCA group, only 18(12.59%) and 6 (4.2%) circuits in low molecular weight heparin group and non-anticoagulant group, respectively, we didn't find significant differences between AKF group and nAKF group in CRRT treatment modality, anticoagulation and dilution mode. A study showed better filter life with femoral vein access compared with internal jugular vein and subclavian vein catheterization; no difference was detected between internal jugular and subclavian vein catheterization[17]. However, no difference in catheter dysfunction rates was found between femoral and internal jugular sites[18].This study included 95.81% circuits in femoral vein group, only 6 circuits in internal jugular vein group and no circuits in subclavian vein group, showed no significant difference between AKF group and nAKF in vascular access sites. We need to enlarge sample size to further explore risk factors for AKF.

In summary, this retrospective observational study showed that the presence of AOD was related to AKF, and AODTT≥7 min was an independent risk factor for AKF.

Funding

This study was supported by grant from Clinical Medicine Postgraduate Joint Training Base of Chongqing Medical University-the First Affiliated Hospital of Chongqing Medical University (lpjd202001).

References

[1] Schiffl H, Lang SM, Fischer R. Daily hemodialysis and the outcome of acute renal failure. N Engl J Med. 2002; 346(5): 305-310.

[2] Neyra JA, Tolwani A. CRRT prescription and delivery of dose. Semin Dial. 2021; 34(6):432-439.

[3] Zhang L, Tanaka A, Zhu G, et al. Patterns and Mechanisms of Artificial Kidney Failure during Continuous Renal Replacement Therapy. Blood Purif. 2016; 41(4): 254-263.

[4] Gattas DJ, Rajbhandari D, Bradford C, et al. A randomized controlled trial of regional citrate versus regional heparin anticoagulation for continuous renal replacement therapy in critically ill adults. Critical Care Medicine 2015;43(8):1622-9.

[5] Tsujimoto H, Tsujimoto Y, Nakata Y, et al. Pharmacological interventions for preventing clotting of extracorporeal circuits during continuous renal replacement therapy. Cochrane Database Syst Rev. 2020;3(3):CD012467.

[6] Tsujimoto Y, Miki S, Shimada H, et al. Non-pharmacological interventions for preventing clotting of extracorporeal circuits during continuous renal replacement therapy. Cochrane Database Syst Rev. 2021;9(9):CD013330.

[7] Zhang L, Baldwin I, Zhu G, et al. Automated electronic monitoring of circuit pressures during continuous renal replacement therapy: a technical report. Crit Care Resusc. 2015;17(1):51-54.

[8] Michel T, Ksouri H, Schneider AG. Continuous renal replacement therapy: understanding circuit hemodynamics to improve therapy adequacy. Curr Opin Crit Care. 2018; 24(6): 455-462.

[9] Li P, Zhang L, Lin L, et al. Effect of Dynamic Circuit Pressures Monitoring on the Lifespan of Extracorporeal Circuit and the Efficiency of Solute Removal During Continuous Renal Replacement Therapy. Front Med (Lausanne). 2021;8:621921.

[10] Sansom B, Sriram S, Presneill J, et al. Circuit Hemodynamics and Circuit Failure During Continuous Renal Replacement Therapy. Crit Care Med. 2019; 47(11): e872- e879.

[11] Tandukar S, Palevsky PM. Continuous Renal Replacement Therapy: Who, When, Why, and How. Chest. 2019;155(3):626-638.

[12] Kim IB, Fealy N, Baldwin I, et al. Premature circuit clotting due to likely mechanical failure during continuous renal replacement therapy. Blood Purif. 2010; 30(2): 79-83.

[13] Baldwin I, Bellomo R, Koch B. Blood flow reductions during continuous renal replacement therapy and circuit life. Intensive Care Med. 2004;30(11):2074-2079.

[14] Mann L, Ten Eyck P, Wu C, et al. CVVHD results in longer filter life than pre-filter CVVH: Results of a quasi-randomized clinical trial. PLoS One. 2023; 18(1): e0278550.

[15] Davies HT, Leslie G, Pereira SM, et al. A randomized comparative crossover study to assess the affect on circuit life of varying pre-dilution volume associated with CVVH and CVVHDF. Int J Artif Organs. 2008; 31(3):221–7.

[16] Poh CB, Tan PC, Kam JW, et al. Regional Citrate Anticoagulation for Continuous Renal Replacement Therapy - A Safe and Effective Low-Dose Protocol. Nephrology (Carlton). 2020; 25(4):305-313.

[17] Crosswell A, Brain MJ, Roodenburg O. Vascular access site influences circuit life in continuous renal replacement therapy. Crit Care Resusc. 2014;16(2):127-130.

[18] Parienti JJ, Mégarbane B, Fischer MO, et al. Catheter dysfunction and dialysis performance according to vascular access among 736 critically ill adults requiring renal replacement therapy: a randomized controlled study. Crit Care Med. 2010; 38(4): 1118-1125.

Analysis of Ophthalmic Examination Results of 7364 Cases in Kunming Regional Health Management Center

Han Hu, Ting Liu, Shubin Fan*, Xuekui Duan
Kunming First People's Hospital Province, Kunming 650000, China.

Abstract: Objective To understand the distribution of eye diseases in the tested population, and to provide a reference basis for the prevention, diagnosis and treatment of eye diseases. **Methods** A total of 7, 364 patients in the Health Management Center from June 2022 to September 2022 underwent eye examination, and the statistical analysis of their eye examination results was conducted by retrospective analysis. **Results** Of the 7, 364 patients, 6, 202 cases(84. 22%) had a history of eye disease or eye surgery, and the top five eye diseases were refractive error(75. 35%), cataract(18. 06%), pterygium(4. 09%), pinguecula(3. 57%), fundus tigre(2. 70%). **Conclusion** In the tested population, the prevalence of refractive error was the highest, followed by cataract, pterygium and so on in men Blebral spot, ptosis. More cataracts and fundus arteriosclerosis, and more women suffer from corneal diseases and trichiasis. There is no obvious difference between men and women, and middle-aged and elderly people have a higher probability of cataract and fundus diseases.

Keywords: Ophthalmic Examination; Prevalence

Introduction

About 210 million people in China suffer from eye diseases, the largest in the world[1]. As one of the countries with a large number of blind people in the world, the task of eye disease prevention and treatment is arduous[2]. The health management center is the front line of eye disease screening for the physical examination population. Through the analysis of the results of the eye examination, it can better understand the situation of eye disease in the physical examination population, and provide reference for the prevention, diagnosis and treatment of eye disease.

1. Data and methods

1. 1 Data

Selected ophthalmic examination results of 7364 patients of Kunming Health Management Center from June 2022 to September 2022.

1. 2 Methods

A retrospective analysis was used to conduct the statistical analysis of the examination results.

1. 3 Specific examination

①Past history: ocular trauma and surgical history; ②vision examination; ③external eye examination: eyelid, e ye position, eye appearance, etc. ; ④slit lamp examination: conjunctiva, cornea, sclera, iris, anterior room, crystal, vitreous,etc.;⑤fundus examination: macular, optic disc, retina, etc.

1. 4 Diagnostic

Criteria are mainly based on *Ophthalmology* (3rd edition/8-year system) and *Ophthalmology* (9th edition /undergraduate clinic), and *Fundonology* (2nd edition) as reference.

2. Results

2. 1 Sex and age distribution of the subject population

Table 1 Sex and age

age	man constituent ratio [(%)]	woman constituent ratio [(%)]	amount to
Under 30	636(50. 4%)	635(49. 96%)	1271
And 31- -59 years old	2667(55. 98%)	2097(44. 02%)	4764
Over 60 years old	809(60. 87%)	520(39. 13%)	1329
amount to	4112(55. 83%)	3252(44. 16%)	7364

Of the 7364 patients, Men have 4, 112 cases(55. 83%), Women have3, 252 cases(44. 16%), Most ages were 31-59 years old(4764 cases, 64. 69%).

2. 2 Prevalence of eye diseases in the tested population

Table 2 Prevalence of eye diseases

eye disease	Number of detected cases (prevalence)
ametropia	5549（75. 35%）
Disease of cornea	55(0. 75%)
trichiasis	60(0. 81%)
pterygium	301(4. 09%)
pinguecula	263(3. 57%)
ptosis	40(0. 54%)
The new life of the eyelid	46(0. 62%)
cataract	1330(18. 06%)
postcataract	151(2. 05%)
glaucoma	12(0. 16%)
Maculopathy, and retinopathy	52(0. 71%)
Fundus artery hardening	131(1. 78%)
fundus tigre	199(2. 70%)
Postoperative myopia	145(1. 97%)
eye traumas	19(0. 26%)

In the examined population, the top five eye diseases in the prevalence rate were the refractive error 5, 549 cases (75. 35%), cataract 1, 330 cases(18. 06%), pterygium 301 cases (4. 09%), pinguecula 263 cases(3. 57%), fundus tigre 199 cases (2. 70%). In addition, other eye diseases are 55 cases of corneal diseases(0. 75%), trichiasis 60 cases(0. 81%), ptosis 40cases(0. 54%), The eyelid new organism 46 cases(0. 62%), glaucoma 12 cases(0. 16%), Macular disease, retinopathy, 52 cases(0. 71%), 131 cases of fundus arteriosclerosis(1. 78%), 19 ocular injuries (0. 26%), postcataract151 cases(2. 05%), 145 cases after myopia surgery(1. 97%).

2. 3 The relationship between the eye disease status and gender in the tested population

Table 3 Eye diseases and gender

eye disease	man constituent ratio [(%)]	woman constituent ratio [(%)]	amount to
ametropia	3063(55. 20%)	2486(44. 80%)	5549
Disease of cornea	25(45. 45%)	30(54. 55%)	55
trichiasis	29(48. 33%)	31(51. 67%)	60
pterygium	163(54. 15%)	138(45. 85%)	301
pinguecula	168(63. 88%)	95(36. 12%)	263
ptosis	28(70. 00%)	12(30. 00%)	40
The new life of the eyelid	21(45. 65%)	25(54. 35%)	46
cataract	809(60. 83%)	521(39. 17%)	1330
postcataract	87(57. 62%)	64(42. 38%)	151
glaucoma	8(66. 67%)	4(33. 33%)	12
Maculopathy, and retinopathy	27(51. 92%)	25(48. 08%)	52
Fundus artery hardening	97(74. 05%)	34(25. 95%)	131
fundus tigre	109(54. 77%)	90(45. 23%)	199
Postoperative myopia	59(40. 69%)	86(59. 31%)	145
eye traumas	14(73. 68%)	5(26. 32%)	19

With the following eye diseases, the male proportion is significantly higher than the female:eyelid fissure spot (63. 88% male, 36. 12%f emale), ptosis (70. 00% male, 30. 00% female), cataract (60. 67% male, 39. 17% female), glaucoma(66. 67% male, 33. 33% female), fundus arteriosclerosis (74. 05% male, 25. 95% female), and ocular trauma (73. 68% male, 26. 32% female).

With the following eye diseases, women accounted for higher proportion than men: corneal diseases(female54. 55%, male 45. 45%), trichiasis (female51. 67%, male 48. 33%), eyelid neobiology (female54. 35%, male45. 65%), and myopia (female 59. 31%, male 40. 69%).

2. 4 The relationship between eye diseases and age in the tested population

Table 4 Eye diseases and age

inspection result	Under 30 constituent ratio [(%)]	31-59 Years old constituent ratio [(%)]	Over 60 years old constituent ratio [(%)]	amount to
ametropia	1036(18.67%)	3505(63.16%)	1008(18.17%)	5549
Disease of cornea	10(18.18%)	24(43.64%)	21(38.18%)	55
trichiasis	15(25.00%)	33(55.00%)	12(20.00%)	60
pterygium	2(0.66%)	142(47.18%)	157(52.16%)	301
pinguecula	0	189(71.86%)	74(28.14%)	263
ptosis	2(5.00%)	8(20.00%)	30(75.00%)	40
The new life of the eyelid	7(15.22%)	32(69.57%)	7(15.22%)	46

cataract	11(0.83%)	439(33.01%)	880(66.17%)	1330
postcataract	0	14(9.27%)	137(90.73%)	151
glaucoma	0	4(33.33%)	8(66.67%)	12
Maculopathy, and retinopathy	1(1.92%)	15(28.85%)	36(69.23%)	52
Fundus artery hardening	0	23(17.56%)	108(82.44%)	131
fundus tigre	54(27.14%)	79(40.20%)	65(32.66%)	199
Postoperative myopia	34(23.45%)	111(76.55%)		145
eye traumas	3(15.79%)	12(63.16%)	4(21.05%)	19

The majority of the subjects were 31-59 years old, including those under 30 years old (27. 14%), trichiasis (25. 00%), relatively high prevalence after myopia (23. 45%). 31-59, eyelid fissure (71. 86%), eyelid organism (69. 57%). After myopic surgery (76. 55%). The prevalence rate is relatively high. Patients over 60 years, pterygium 157 (52. 16%), Pptosis(75. 00%), Cataract(66. 17%), After cataract surgery (90. 73%), Glaucoma(66. 67%), Maculopathy, retinopathy(69. 23%), The arterial stiffness of the fundus(82. 44%)The prevalence rate is relatively high.

3. Discussion

This study showed that the top five prevalence rates were refractive error (75. 35%), cataract (18. 06%), pterygium (4. 09%), pinguecula (3. 57%), Leopard grain pattern fundus (2. 70%).

Among them, men suffer from the following eye diseases more than women:eyelid fissure spot, For ptosis, cataract, glaucoma, fundus arteriosclerosis, eye trauma, the above conditions are considered to accept more ultraviolet light, faster eyelid aging, relatively poor control of basic diseases, and more vulnerable to external forces. And women suffer from more eye diseases: corneal disease, trichiasis, eyelid new biology, myopia, which is related to the relatively loose eyelid structure, hormone secretion fluctuations, more strong willingness to remove the mirror and so on factors. Most of the remaining eye diseases, there was no obvious difference between men and women.

In this study, the highest prevalence of refractive error was observed (75.35%), Leopard grain pattern fundus (2.70%). It also cannot be ignored. In this study, people under the age of 30 had the leopard pattern fundus (27.14%) relatively high, considering related to high myopia;proportion of population after myopia surgery 1. 97%, Mainly aged 30-59 (76.55%), this is related to the high cost of myopia surgery, which can bear more young and middle-aged people with stable income, and myopia surgery has certain requirements for eye conditions, so it is relatively low at present. At present, myopia is incurable, and the probability of high myopia is higher to suffer from fundus related diseases. It is urgent to protect the vision, improve the awareness of loving eyes, wear glasses correctly, and actively control the development of myopia.

Cataract ranks first among many blind eye diseases in the world. At present, China has the largest number of cataract blindness in the world[3]. In developing countries, the incidence of cataract in people aged over 40 is about 11. 8% -18. 8%[4]. The prevalence of cataract is 18. 06%, Relatively high, and the prevalence of people over 60 years old is reached 66. 17%, This is related to the plateau of Yunnan Province, with relatively strong ultraviolet light and relatively low education level;people after cataract surgeryAccounting for 2. 05%, Mainly concentrated in those over 60 years old(90. 73%), This shows that age-related cataract is still the focus of the prevention and treatment of blindness. The prevalence rate of pterygium(4. 09%) and pinguecula(3. 57%) is higher, which is also related to the above geographical location and education level of the population in Yunnan Province. Enhance the population's awareness of eye love, advocate the elderly ultraviolet protection, regular eye examination, timely cataract surgery is more key.

China has entered the aging process, and the prevalence of age-related eye diseases has increased accordingly by[5]. In this study, The prevalence of pterygium, ptosis, cataract, after cataract surgery, glaucoma, macular disease, retinopathy, and

fundus arteriosclerosis is relatively high. This is related to the elderly suffering from "three high" and other basic diseases, most of them do not realize that eye disease is closely linked with the whole body, and weak awareness of eye love. It is the key to the prevention and treatment of the elderly to enhance the understanding of fundus diseases, comprehensively manage the basic diseases, and advocate the early detection, diagnosis and treatment of the elderly, and the key to guarantee the living vision of the elderly.

4. Summary

The study showed that the prevalence of refractive errors was the highest, followed by cataract and pterygium, among menBlebral fissure spot, ptosis, More cataracts and fundus arteriosclerosis, and more women suffer from corneal diseases and trichiasis. There is no obvious difference between men and women, and middle-aged and elderly people have a higher probability of cataract and fundus diseases. China has entered an aging society, is a big country of myopia, the relevant departments and ophthalmologists, should actively advocate universal eye care, widely popularize eye love knowledge, improve the health awareness of the population, Promote the development of eye health and ophthalmology in China to benefit more patients with eye diseases.

References

[1] Chen BB, Lou LX, Ye J. Current situation and change trend of eye disease burden over 30 years in China[J]. Journal of Zhejiang University (Medical edition), 2021(8): 420-421.

[2] Gao H, Chen XN, Shi WY. Analysis of the prevalence of blindness and the status of major blinding diseases in China[J]. Chinese Journal of Ophthalmology, 2019, 55(8):625-628.

[3] Pascolini D, Mariotti SP. Global estimates of visual impairment:2010[J]. Br J Ophthalmol, 2012, 96(5):614-618.

[4] Xu JJ, Zhang Y, Yao K, Chen XJ, research progress in the pathogenesis and prevention strategies of cataract[J]. Chinese Science Journal, 2022, 52(12):1807-1814. [5] Li YP. The cataract disease status and influencing factors, service demand and utilization in people aged 50 years and above in central and western China [D]. Nanchang: Nanchang University, 2020.

Research Progress on Integrated Traditional Chinese and Western Medicine in the Treatment of Post-Cholecystectomy Syndrome

Xiaoqing Huang[1], Xingwu Yang[2,*], Xin Wang[1], Guocang Chen[1*corresponding author]

1. Shaanxi University of Chinese Medicine, Xianyang 710246, China.

2. Affiliated Hospital of Shaanxi University of Chinese Medicine, Xianyang 712000, China.

Abstract: Laparoscopic cholecystectomy (LC) is a highly accepted treatment at this stage, with the increasing incidence of biliary tract disease and the development of endoscopic technique in recent years However, some patients after cholecystectomy still have symptoms similar to preoperative symptoms, such as abdominal pain, diarrhea, indigestion and so on. This series of syndromes has become a common clinical problem at present.This article reviews the research progress of etiology, pathogenesis, diagnosis and treatment of post-cholecystectomy syndrome by reading related literatures.

Keywords*:* Postcholecystectomy Syndrome; Traditional Chinese Medicine Treatment; Research Progress

Introduction

The term post cholecystectomy syndrome (PCS) refers to a syndrome in which, after surgical removal of the gallbladder, the original clinical symptoms have not disappeared or, on this basis, new symptoms have developed, such as discomfort with abdominal tightness and distension, abdominal pain, shoulder and back pain, dyspepsia, nausea or vomiting with vomiting, eructation, and increased frequency of stools, and specific biliary symptoms such as severe right upper quadrant pain, biliary colic, fever, jaundice, etc. [1]The onset can occur from within days postoperatively to years postoperatively. Genera "abdominal pain ", " jaundice ", "biliary distension " in Chinese medicine.

1. Pathogenesis of post cholecystectomy syndrome

1.1 Pathogenesis of traditional Chinese Medicine

The traditional chinese medicine holds Dan as the province of “Qiheng”, which is also the first of “six Fu” organs.The liver and bile are mutually episodic. [2] The clinical symptoms of PCS can be assigned to the categories of "flank pain ", " jaundice ", "biliary distension ", and " fullness " in Traditional Chinese Medicine . According to Prof. Zhengxue Pei, after damage to the human body by the scalpel, the human Qi is made deficient, which causes qi stagnation and blood stasis, liver stagnation, and transverse spleen stomach, so that after cholecystectomy, more gallbladder stumps and gastrointestinal infections exist. [3] Traditional Chinese medicine believed that the disease location was still hepatobiliary, and involved the spleen and stomach, and the disease mechanism was an adverse effect of Shaoyang main and collateral channels. [4]

1.2 Pathogenesis of Western Medicine

The current western medical pathogenesis of PCS is not very clear, and it is currently believed that the etiology of PCS is related to bile duct stones before operation, and about half of the patients with bile duct stones develop PCS after cholecystectomy, and the statistical significance of PCS in this category of patients after open or laparoscopic cholecystectomy reaches 4.76-7.34%. [5-6] The predisposing factor is either related to the damage caused by the operating instruments during the operation or to the residual gallbladder, part of the bile duct, bile that accumulates in the stump predisposing to inflammation or stone formation again triggering PCS. [7] Duodenal parapapillary diverticula were present in 38.5% of the patients with PCS. [8] Therefore, some authors believe that duodenal parapapillary diverticulum is also a common pathogenic factor of PCS. Jiaqing Wu [9] suggested that the onset of PCS is closely related to the thickness of the gallbladder wall, the number and size of stones, the patients' emotions and life habits. When the gallbladder is surgically removed and the function of the bile duct is not fully compensated to replace gallbladder function.After cholecystectomy, bile is discharged into the bile duct, duodenum, after losing the concentration effect of the gallbladder, causing abdominal discomfort and other gastrointestinal symptoms. [10]

2. Diagnosis of post cholecystectomy syndrome

Among the imaging examinations, hepatobiliary and pancreatic spleen color ultrasound, endoscopic ultrasound (EUS), computed tomography (CT), magnetic resonance cholangiography (MRCP), and endoscopic retrograde cholangiopancreatography (ERCP) were performed. Color ultrasound is easy, fast and noninvasive in the clinic, and is usually used as the initial screening test to exclude gallbladder and bile duct diseases, but it can be disturbed by feeding conditions, gases and other factors, so it is often used as the initial screening test for hepatobiliary pancreaticosplenic diseases. CT is relatively good for stones, bile duct dilatation, pancreatitis, tumours, but may be too small a diameter of the stone to make a missed diagnosis. MRCP, ERCP are widely used in clinical departments, and both have high-definition development ability and can clearly present stone number, size, and location. EUS can be used to find distal common bile duct and ampullary lesions, and also has a high diagnostic yield of 88.9% for stones less than 4 mm in diameter. [11]

3. Management of post cholecystectomy syndrome

3.1 Traditional Chinese medicine treatment

Traditional Chinese medicine (TCM) has not uniformly developed a syndrome type classification for PCS, and based on clinical experience, various doctors make an approximate classification of the disease.Clinically, Yangyang Wu [12] applied Chaihu Shugan powder plus and minus formula to treat PCS with remarkable efficacy.Zhengxue Pei[13] believed that the treatment of PCS should be Shu-gan- Li-dan, and Chai-hu-Shu-gan-San are often used to treat the disease in clinic. At the same time, acupuncture can be combined, however, Xiran Su[14] selected acupuncture points such as Dan Shu, Yang ling quan, and Taichong in clinical studies and applied electroacupuncture, which make Qi and blood in the meridians smooth to improve symptoms with significant efficacy.

3.2 Western medicine treatment

When patients experience stomach discomfort and regurgitant acid after surgery, proton pump inhibitors are used to inhibit the secretion of gastric acid and relieve the symptoms of stomach pain and regurgitant acid. Jiali Wei [15] when the patient developed functional dyspepsia postoperatively, deanxit combined with Mosapride was given, compared with the effect of Mosapride alone was prominent. Since more than half of patients with bile duct stones develop PCS postoperatively,

Because many symptoms occur after cholecystectomy, the etiology can be found in most cases by the ERCP technique, and the technique has many advantages such as safety, little patient suffering, and few complications, ERCP treatment should be considered the first choice for PCS patients with indications for endoscopic treatment. [16]In patients with PCS sphincter of Oddi dysfunction was observed in some patients, and after LC operation, bile normally secreted by the liver loses the space for concentration and storage, bile drained into the bile duct thereby causing the intra biliary pressure to rise, and irregularly drained into the duodenum through sphincter of Oddi, affecting its normal physiological function. [17-19] However, conservative treatment is still the generally recommended treatment with symptomatic supportive treatment, such as acid suppression and promotion of gastrointestinal motility, maintenance of water electrolyte balance, administration of vitamins and hepatoprotective treatment, and administration of antiviral and antispasmodic and sedative treatment if necessary. [20]

4. Summary

When a cholecystectomy is performed, it is an invasive procedure that is traumatic, and more or less has an impact on the autonomic function of the patient, with a range of postoperative symptoms occurring. [21] In Traditional Chinese Medicine treatment, it is important to emphasize that treatment based on syndrome differentiation and postoperative peace of mind and a light diet are effective means, establishment of a standardized TCM treatment regimen for PCS [22] In the treatment of Western medicine, PCS revisited prevention,a clear preoperative diagnosis, intraoperative attention to protect the surrounding normal anatomical structures, avoid accidental damage are effective steps in the prevention of PCS.

References

[1] Rasić S, Kulenović I, Haracić A, Catović A. Left ventricular hypertrophy and risk factors for its development in uraemic patients. Bosn J Basic Med Sci 2004; 4: 34-40.

[2] Yin HH. Basic theory of traditional Chinese medicine [M]. Shanghai: Shanghai Science and Technology Press, 1983:52.

[3] Li RR, Ma Q, Ma QQ, et al. professor Xue Zheng Pei for post cholecystectomy syndrome [J]. Asia Pacific traditional medicine, 2018, 14 (7): 131-132.

[4] Du YW, Gu Q, Hong Shan Dai [PubMed: 201709] and Shaoyang recipe for the treatment of postoperative Gallbladder Syndrome [J]. Global traditional Chinese medicine, 2017, 10 (1): 39-41.

[5] Hong L, Xiang HP. A comparison of two different surgical modalities for the treatment of chronic lithiasis cholecystitis presenting post cholecystectomy syndrome [J]. Hepatobiliary Surg 2016, 24 (3): 206-208.

[6] Huang JP. Current treatment of gallbladder postoperative syndrome [J]. Modern remote education in Chinese traditional medicine, 2017, 15 (2): 151-152.

[7] Lan JL, Dong XY, Chang WL, et al.diagnosis and treatment of bile duct injury during laparoscopic cholecystectomy [J]. Chinese Journal of general surgery, 2017, 26 (8): 1076-1080.

[8] Wu SD, Tian Y, Su Y, et al.study of the relationship between biliary disease and duodenal peripapillary diverticulum [J]. Surgical theory and practice, 2007, 12 (4): 342-344.

[9] Wu JQ. Current status of syndrome after cholecystectomy and clinical study of syndrome differentiation and differentiation [D]. Nanjing: Nanjing University of traditional Chinese medicine, 2018.

[10] Yu DG, Zhao LJ, Cai ZF, et al Integrated traditional Chinese and Western medicine in the treatment of post cholecystectomy syndrome in 56 patients [J]. Modern Journal of integrated traditional Chinese and Western medicine, 2006, 25 (1): 61-62.

[11] Karakan T, Cindoruk M, Alagozlu H, et al. EUS versus endoscopic retrograde cholangiography for patients with intermediate probability of bile duct stones: a prospective randomized trial[J].Gastrointest Endosc,2009,69(2): 244-252.

[12] Wu YY. Example case report of a postoperative syndrome treated with Chaihu Shugan Lidan Decoction [J]. Journal of practical Gynecological Endocrinology (ePub), 2016, 3 (10): 57-59.

[13] Li RR, Ma Q, Bao QQ, et al. Professor Pei Zheng subtyping for post cholecystectomy syndrome [J]. Asia Pacific traditional medicine, 2018, 14 (7): 131-132.

[14] Su XR. Traditional Chinese and Western medicine in the treatment of post cholecystectomy syndrome in 52 patients [J]. Practical integration of traditional Chinese and Western medicine clinical, 2008, 8 (4): 28-29.

[15] Wei JL. Clinical analysis of a functional dyspepsia selected mosapride combined with delixin treatment [J]. EPub 2018, 5 (97): 175-176.

[16] Bi YL, Zhu T, Pan XF, et al. ERCP in the etiologic diagnosis and treatment of post cholecystectomy syndrome. [J]. Chinese Journal of general surgery, 2008, 17 (2): 120-123.

[17] Hu YT, Xu YF, Zhao N, et al. Study of post cholecystectomy syndrome [J], 2021, 33(2):144-147.

[18] Schofer JM. Biliary causes of postcholecystectomy syndrome[J]. J Emerg Med, 2010, 39(4): 406-410.

[19] Madacsy L, Fejes R, Kurucsai G, et al. Characterization of functional biliary pain and dyspeptic symptoms in patients with sphinc- ter of Oddi dysfunction: Effect of papillotomy[J].World J Gastroen- terol,2006,12(42) : 6850-6856.

[20] Liu HH, Tian Y, Peng Y, et al Diagnosis and prevention of post cholecystectomy syndrome [J]. Journal of clinical hepatobiliary disease, 2018, 34 (11): 2464-2468.

[21] Huang GR, Guo SZ, Sun W. Effecet of laparoscopic surgery on stress and immune function in patients with cholecystolithiasis com- plicated with acute cholecystitis[J]. Clin J Med Offic, 2018,46 (3) : 354-355.

[22] Yuan XQ, Lei PJ. Progress in the treatment of postcholecystectomy syndrome with traditional Chinese medicine [J]. Clinical Research of Traditional Chinese Medicine, 2015,7(7):142-144.

Advances in the ADAMTS Family in Cardiovascular Disease

Tianying Jin, Zhaohui Meng*

Laboratory of Molecular Cardiovascular Disease, Department of Cardiology, The First Affiliated Hospital of Kunming Medical University, Kunming 650032, China.

Abstract: Cardiovascular disease is a serious threat to human life and health. The number of people who die from cardiovascular disease is up to 15 million every year, ranking the first cause of all causes of death. ADAMTS family (A Disintegrin and Metalloproteinase With Thrombospondin Motifs, ADAMTSs) are matrix-associated zinc metallopeptidases with secretory function. It has diverse roles in tissue morphogenesis, pathophysiological remodeling, inflammation, and vascular biology. Controlling the structure and function of the Extracellular Matrix (ECM) is the central theme of the biology of ADAMTSs. ADAMTSs mainly play a biological role by regulating the structure and function of extracellular mechanisms, and the abnormal expression or dysfunction of some family members is associated with cardiovascular diseases. ADAMTS family plays an important role in the occurrence and development of various cardiovascular diseases. This paper aims to study the role of ADAMTS family in cardiovascular diseases.

Keywords: ADAMTSs; Dilated Cardiomyopathy; Acute Coronary Syndrome; Atherosclerosis

Introduction

The world's leading cause of death is now cardiovascular disease (CVD) : it kills more people each year than any other cause. More than three quarters of CVD-related deaths occur in low - and middle-income countries. According to the statistical study in the 2020 Report on Cardiovascular Health and Disease in China [1], the prevalence of cardiovascular disease in China is still on the rise. The report clearly estimated that the total number of cardiovascular diseases now reached 330 million, of which 13 million were stroke patients, 11.39 million were coronary heart disease patients, 8.9 million were heart failure patients, 4.87 million were atrial fibrillation patients, about 5 million were pulmonary heart disease patients, and 2.5 million were rheumatic heart disease patients. Congenital heart disease affects 2 million people, lower extremity arterial disease affects 45.3 million people, and hypertension affects up to 245 million people [1]. At present, the etiology of many cardiovascular diseases is not clear, and many patients have insidious onset without seeking medical treatment or being diagnosed, which poses a great threat to human health. At present, a large number of clinical and basic researches on various cardiovascular diseases have been carried out in clinical and scientific research, with the purpose of seeking efficient diagnosis and treatment methods, improving the prognosis of cardiovascular diseases, and summarizing the early prevention of cardiovascular diseases.

ADAMTS family is a secreted protease belonging to the Zn2 + -dependent metalloproteinase family [2]. The mammalian genome contains a total of 19 ADAMTS genes numbered 1 to 20, of which code 11 was not used because it was assigned to the gene previously identified as ADAMTS5. The ADAMTSs protease family shares the same structural domain, which includes a propeptide region, a metalloproteinase domain, a disintegrin-like domain, and a thrombospondin type 1 (TSP1) motif. It is only that individual members of this family differ in the number of C-terminal TSP1 motifs, with some having unique C-terminal domains [3]. The proprotein encoding ADAMTS has proteolytic processing function, which can

eventually form the mature procollagen N protease. This protease excises the N-propeptide of type I-III and type V protofibrillar collagen. ADAMTS and ADAM(A Disintegrin and Metallo pro-teinase) family activities can be inhibited by The Tissue Inhibitor of metalloproteinases Metallop-roteinases, TIMPs) and other endogenous inhibitors, whose activity can also be inhibited by synthetic small molecule inhibitors [4]. ADAMTS and ADAM have been shown to be potential therapeutic targets and important diagnostic biomarkers for cardiovascular diseases. [5] Among various proteinases in the human body, ADAMTS, Matrix Metallo proteinase (MMP) and ADAM play a crucial role in cardiovascular diseases. [5] Therefore, it is urgent to explore the role and related pathophysiological mechanism of ADAMTS family in the occurrence and development of cardiovascular diseases, which may bring new progress in the early diagnosis, targeted treatment, improvement of prognosis and long-term survival rate of cardiovascular diseases.

1. ADAMTSs and the occurrence and development of cardiovascular diseases

1.1 ADAMTSs and dilated cardiomyopathy and heart failure

Dilated Cardiomyopathy (DCM) is characterized by enlargement of the left or right ventricle or both ventricles with systolic dysfunction. Some patients may have congestive heart failure during the process of the disease, and most of them have ventricular or atrial arrhythmias. The etiology of DCM is unknown, and the disease is progressive, and death can occur at any stage of the disease. At present, there is no targeted treatment for DCM. According to the 2021 China Cardiovascular Health and Disease Report, the prevalence of dilated cardiomyopathy (DCM) in China was 19/100 000 according to the survey of 9 provinces (autonomous regions) [6]. Recent studies have shown that the imbalance of ADAMTS1 and MMP2/TIMP1 ratio interferes with the synthesis of extracellular matrix and participates in ventricular remodeling in terms of collagen degradation and angiogenesis, which may promote the further development of myocarditis into dilated cardiomyopathy [7]. In the same year, Huang et al. [8] found that ADAMTS7 could degrade cartilage matrix protein (COMP) in cardiomyocytes, thereby promoting the migration of vascular smooth muscle cells (VSMC) and participating in the process of myocardial remodeling, proving that ADAMTS7 plays an important role in the occurrence and development of DCM. Subsequent studies found that ADAMTS2 expression was up-regulated in the failing human heart and hypertrophic mouse heart, and ADAMTS2 gene could also drive isoproterenol induced cardiac hypertrophy in mice [9]. ADAMTS2 attenuated endothelin (ET) -induced cardiomyocyte hypertrophy in neonatal rat cardiomyocytes. Blocking the phosphoinositide 3-kinase (PI3K)/Akt pathway can improve the hypertrophic response caused by ADAMTS2 deficiency [10]. Based on the above studies, it is hypothesized that ADAMTS1, 2, and 7 are abnormally important in the ventricular remodeling process of DCM.

Heart failure (HF) is a clinical syndrome caused by structural or functional diseases of the heart, which leads to impaired filling and/or ejection function, insufficient cardiac output to meet the metabolic needs of body tissues, congestion of pulmonary and/or systemic circulation, and insufficient blood perfusion of organs and tissues. Omura[11] et al. found that ADAMTS8 knockout mice exhibit improved right ventricular failure under conditions of chronic hypoxia, enhanced angiogenesis, and reduced right ventricular ischemia and fibrosis. This suggests that ADAMTS8 may be associated with the occurrence and development of HF.

1.2 ADAMTSs and atherosclerosis and acute coronary syndrome

Atherosclerosis is characterized by the accumulation of lipids and complex saccharides in the intima of the involved arteries, followed by hemorrhage, thrombosis, fibrous tissue hyperplasia and calcinosis. Over time, the middle layer of the

arteries gradually changes and calcifications. If the lesion progresses to occlusion of the arterial lumen, ischemia and necrosis will occur in the area supplied by the artery. Acute Coronary Syndromes (ACS) refers to the rupture or erosion of unstable plaques, incomplete or complete occlusion of coronary arteries, and acute myocardial ischemia on the basis of coronary atherosclerotic lesions. At present, ACS is clinically divided into 3 categories: Unstable angina, ST-segment elevation acute myocardial infarction, and non-ST-segment elevation acute myocardial infarction.

Studies have found that ADAMTS1, 4, 5 and 13 can be expressed in carotid plaques, especially in smooth muscle cells and macrophages, while ADAMTS1 expression is higher and ADAMTS4 and 5 expression is slightly increased in unstable plaques [12]. Jonsson-Rylander [13] et al. found through immunohistochemistry and other experiments that ADAMTS1 may promote the occurrence of atherosclerosis by cutting extracellular matrix proteins and inducing vascular smooth muscle cell migration. Pehlivan[14] et al. showed that ADAMTS1 was diffusely distributed in the myocardium of individuals who died of myocardial infarction or trauma, as analyzed by staining of cardiomyocytes from postmortem patients. Another study showed that the immune response area of ADAMTS2, 3 and 13 was very large in acute myocardial infarction, and subsequently ADAMTS2, 3, 13 and 14 were listed as the culprit of acute myocardial infarction [15]. ADAMTS4 can generally diffuse into the plasma after cardiovascular injury. Elevated plasma ADAMTS4 levels have been found in patients with ACS[16-19] and atherosclerosis [19-23]. Some of these studies have linked elevated plasma levels of ADAMTS4 to increased ACS severity [18-21] and plaque instability [23]. Elevated ADAMTS4 levels have also been found in macrophage-rich regions of human atherosclerotic plaques and unstable coronary plaques [20-23]. Plasma ADAMTS4 levels are significantly increased in acute coronary syndrome, and continue to increase with the progression from stable angina to UA, NSTEMI, and STEMI. Studies have shown that continuous measurement of plasma ADAMTS4 may be a marker of plaque instability in acute coronary syndrome [19].

Studies in mice have shown that ADAMTS7 acts early in the development of atherosclerosis, possibly in response to TNF in an inflammatory environment [24]. Corresponding analyses of human atherosclerotic lesions have shown that ADAMTS7 localizes to smooth muscle cells, but not macrophages in lesions, and localizes them to their cell surface and pseudopodia [25]. ADAMTS7 colocalizes with macrophages and smooth muscle cells in coronary and carotid atherosclerotic plaques and stains throughout the plaque, including the shoulder, cap, and core [26,27]. Plasma ADAMTS7 is elevated in patients with severe obstructive coronary artery disease [27]. Various findings suggest that ADAMTS7-related advanced atherosclerosis may be associated with the degradation of cartilage oligomeric matrix protein (COMP), a protein secreted by vascular smooth muscle cells [28-30]. Previous studies have shown that ADAMTS7 can promote vascular muscle cell migration and intimal thickening after vascular injury, and can also degrade COMP, so it plays an important role in atherosclerosis and restenosis after atherosclerosis [31-34]. Bengtsson[35] et al. analyzed the expression of ADAMTS7 in human carotid plaques by immunohistochemical method and analyzed its correlation with the components of plaque vulnerability. The results showed that ADAMTS7 levels were increased in plaques of symptomatic patients compared with those of asymptomatic patients.

Subsequently, in animal model experiments, it was found that ADAMTS13-deficient mice had a larger myocardial infarction area when myocardial ischemia was induced than wild-type mice [36-38]. Another small case-control study showed that ADAMTS13 may also play a role in coronary atherosclerotic heart disease [39]. Using a meta-analysis approach, Maino[40] et al. also demonstrated that low ADAMTS13 levels increased the risk of myocardial infarction.

In summary, we found that ADAMTS1, 2, 3, 4, 7, 10, 13, 14, 17 were all more or less related to atherosclerosis or acute coronary syndrome, which provided evidence for us to study the relationship between ADAMTSs and atherosclerosis and acute coronary syndrome.

1.3 ADAMTSs and hypertension

Hypertension is a cardiovascular syndrome characterized by elevated systemic arterial pressure, defined as office systolic blood pressure ≥140mmHg and/or diastolic blood pressure ≥90mmHg. Hypertension is one of the most frequent chronic diseases in the world, and it is also one of the most important risk factors for cardiovascular and cerebrovascular diseases. In 2018, Lu Chenling [41] et al. found that the G-C mutation at rs402007 site of ADAMTS1 gene may increase the risk of essential hypertension by affecting the expression of ADAMTSl protein. Other studies have shown that ADAMTS2 promotes the occurrence and development of hypertensive disorders complicating pregnancy [42]. ADAMTS7 has been shown to affect vascular remodeling and thus reduce the occurrence of PIH, and the normal expression of ADAMTS7 has a protective effect on the occurrence of severe eclampsia [42]. ADAMTSs may be closely related to the occurrence, development and treatment of hypertension.

1.4 ADAMTSs and atrial fibrillation

Atrial fibrillation (AF) is one of the most common arrhythmias, which is more common in middle-aged and elderly people. Af is the regular and orderly loss of atrial electrical activity, which is replaced by rapid and disordered fibrillation waves, forming many new atrial reentry loops, leading to atrial rhythm disorder. Severe atrial electrical rhythm disorder leads to atrial pumping dysfunction and abnormal atrioventricular junction electrical conduction, resulting in highly irregular ventricular response and impaired cardiac function. In 2012, Cervero [43] et al. showed that the expression of ADAMTS18 was down-regulated in a pig model using rapid atrial pacing to simulate atrial fibrillation, suggesting that the reduction of ADAMTS18 may play a role in the process of thrombosis in AF. Freynhofer[44] et al. reported in 2013 that a high ratio of plasma vWF /ADAMTS13 could independently predict major adverse cardiovascular events in AF patients. Recent studies have shown that ADAMTS13 gene polymorphism may be related to the progression of hypertensive atrial fibrillation, and the detection of ADAMTS13 gene polymorphism can predict the progression of the disease [45]. Therefore, vWF and ADAMTS13, 18 May play an important role in the progression of AF.

1.5 ADAMTSs and valvular heart disease

Valvulopathy is the abnormal structure (leaflet, annulus, chordae tendines, or papillary muscles) or function of single or multiple valves caused by a variety of reasons, which eventually leads to valve stenosis and/or insufficiency. The development of myxomatous mitral valves in ADAMTS5-deficient and ADAMTS9-haplodeficient mouse models suggests that alterations in complex proteolysis are the origin of abnormal valve development [46-47]. The loss of ADAMTS19 can also cause progressive, non-syndromic valvular heart disease [48]. ADAMTS19 has been identified as a new pathogenic gene of autosomal recessive valvular heart disease, mainly affecting the aortic valve and pulmonary valve [49]. In addition, 38% of homozygous ADAMTS19 knockout mice were found to exhibit progressive aortic valve disease, characterized by aortic valve stenosis and incompetence [49]. This suggests that ADAMTS5, 9 are associated with valve development, and ADAMTS19 may be a pathogenic gene for valvular heart disease.

2. Summary and Prospect

In summary, with the continuous development of technology, we have found more and more members of ADAMTS family, and have a certain understanding of its structure and function. A large number of literatures have pointed out that ADAMTSs are involved in the occurrence and development of cardiovascular diseases through a variety of ways, which provides a basis for us to understand the pathogenesis, early diagnosis, and molecular treatment of cardiovascular diseases. However, cardiovascular diseases have multiple pathogenic factors, and how ADAMTSs are involved in them still needs to

be further explored. These studies may provide new ideas for the diagnosis and treatment of cardiovascular diseases.

References

[1] Chinese Journal of Cardiovascular Health and Disease Report 2020[J]. Journal of Cardiovascular Disease,2021,40(10):1005-1009.

[2] Porter S, Clark I M, Kevorkian L, et al. The ADAMTS metalloproteinases[J]. Biochemical Journal, 2005, 386(1): 15-27.

[3] Rodríguez-Manzaneque J C, Fernández-Rodríguez R, Rodríguez-Baena F J, et al. ADAMTS proteases in vascular biology[J]. Matrix Biology, 2015, 44: 38-45.

[4] Zhong S, Khalil R A. A Disintegrin and Metalloproteinase (ADAM) and ADAM with thrombospondin motifs (ADAMTS) family in vascular biology and disease[J]. Biochemical pharmacology, 2019, 164: 188-204.

[5] Shiomi T, Lemaître V, D'Armiento J, et al. Matrix metalloproteinases, a disintegrin and metalloproteinases, and a disintegrin and metalloproteinases with thrombospondin motifs in non-neoplastic diseases[J]. Pathology international, 2010, 60(7): 477-496.

[6] Chinese Cardiovascular health and disease Report Compilation Committee. China Cardiovascular health and disease report 2021: latest summary. Biomedical Environmental Sciences, 2012,7; 35 (7) :573-603.

[7] Xie Y, Li M, Wang X, et al. In vivo delivery of adenoviral vector containing interleukin-17 receptor a r educes cardiac remodeling and improves myocardial function in viral myocarditis leading to dilated cardiomyopathy [J]. PLoS One, 2013, 8(8): e72158.

[8] Huang Y, Xia J, Zheng J, et al. Deficiency of cartilage oligomeric matrix protein causes dilated cardiom yopathy[J]. Basic research in cardiology, 2013, 108: 1-21.

[9] Rau C D, Romay M C, Tuteryan M, et al. Systems genetics approach identifies gene pathways and Ada mts2 as drivers of isoproterenol-induced cardiac hypertrophy and cardiomyopathy in mice[J]. Cell systems, 2017, 4(1): 121-128. e4.

[10] Wang X, Chen W, Zhang J, et al. Critical role of ADAMTS2 (a disintegrin and metalloproteinase with thrombospondin motifs 2) in cardiac hypertrophy induced by pressure overload[J]. Hypertension, 2017, 69(6): 1060 -1069.

[11] Omura J, Satoh K, Kikuchi N, et al. ADAMTS8 promotes the development of pulmonary arterial hypertension and right ventricular failure: a possible novel therapeutic target[J]. Circulation research, 2019, 125(10): 884-906.

[12] Pelisek J, Deutsch L, Ansel A, et al. Expression of a metalloproteinase family of ADAMTS in human vulnerable carotid lesions[J]. Journal of cardiovascular medicine, 2017, 18(1): 10-18.

[13] Jönsson-Rylander A C, Nilsson T, Fritsche-Danielson R, et al. Role of ADAMTS-1 in atherosclerosis: r emodeling of carotid artery, immunohistochemistry, and proteolysis of versican[J]. Arteriosclerosis, thrombosis, and vascular biology, 2005, 25(1): 180-185.

[14] Pehlivan S, Gurses M S, Ural M N, et al. The role of ADAMTS1 and versican in human myocardial infarction: a postmortem study[J]. Laboratory Medicine, 2016, 47(3): 205-212.

[15] Lee C W, Hwang I, Park C S, et al. Expression of ADAMTS-2,-3,-13, and-14 in culprit coronary lesio ns in patients with acute myocardial infarction or stable angina[J]. Journal of thrombosis and thrombolysis, 2012, 3 3: 362-370.

[16] Ren P, Zhang L, Xu G, et al. ADAMTS-1 and ADAMTS-4 levels are elevated in thoracic aortic aneur ysms and dissections[J]. The Annals of thoracic surgery, 2013, 95(2): 570-577.

[17] Chen L, Yang L, Zha Y, et al. Association of serum a disintegrin and metalloproteinase with thrombos podin motif 4 levels with the presence and severity of coronary artery disease[J]. Coronary artery disease, 2011, 22(8): 570-576.

[18] Uluçay S, Çam F S, Batır M B, et al. A novel association between TGFβl and ADAMTS4 in coronary artery disease: A new potential mechanism in the progression of atherosclerosis and diabetes[J]. Anatolian journal of cardiology, 2015, 15(10): 823.

[19] Zha Y, Chen Y, Xu F, et al. ADAMTS4 level in patients with stable coronary artery disease and acute coronary syndromes[J]. Biomedicine & pharmacotherapy, 2010, 64(3): 160-164.

[20] Wågsäter D, Björk H, Zhu C, et al. ADAMTS-4 and-8 are inflammatory regulated enzymes expressed in macrophage-rich areas of human atherosclerotic plaques[J]. Atherosclerosis, 2008, 196(2): 514-522.

[21] Zha Y, Chen Y, Xu F, et al. Elevated level of ADAMTS4 in plasma and peripheral monocytes from patients with acute coronary syndrome[J]. Clinical Research in Cardiology, 2010, 99: 781-786.

[22] Dong H, Du T, Premaratne S, et al. Relationship between ADAMTS4 and carotid atherosclerotic plaque vulnerability in humans[J]. Journal of Vascular Surgery, 2018, 67(4): 1120-1126.

[23] Chen Y C, Bui A V, Diesch J, et al. A novel mouse model of atherosclerotic plaque instability for drug testing and mechanistic/therapeutic discoveries using gene and microRNA expression profiling[J]. Circulation research, 2013, 113(3): 252-265.

[24] Bauer R C, Tohyama J, Cui J, et al. Knockout of Adamts7, a novel coronary artery disease locus in humans, reduces atherosclerosis in mice[J]. Circulation, 2015, 131(13): 1202-1213.

[25] Pu X, Xiao Q, Kiechl S, et al. ADAMTS7 cleavage and vascular smooth muscle cell migration is affected by a coronary-artery-disease-associated variant[J]. The American Journal of Human Genetics, 2013, 92(3): 366-374.

[26] Bengtsson E, Hultman K, Dunér P, et al. ADAMTS-7 is associated with a high-risk plaque phenotype in human atherosclerosis[J]. Scientific reports, 2017, 7(1): 3753.

[27] Yu J, Zhou B, Yu H, et al. Association between plasma ADAMTS-7 levels and severity of disease in patients with stable obstructive coronary artery disease[J]. Medicine, 2016, 95(48).

[28] Kessler T, Zhang L, Liu Z, et al. ADAMTS-7 inhibits re-endothelialization of injured arteries and promotes vascular remodeling through cleavage of thrombospondin-1[J]. Circulation, 2015, 131(13): 1191-1201.

[29] Wang L, Zheng J, Bai X, et al. ADAMTS-7 mediates vascular smooth muscle cell migration and neointima formation in balloon-injured rat arteries[J]. Circulation research, 2009, 104(5): 688-698.

[30] Riessen R, Fenchel M, Chen H, et al. Cartilage oligomeric matrix protein (thrombospondin-5) is expressed by human vascular smooth muscle cells[J]. Arteriosclerosis, thrombosis, and vascular biology, 2001, 21(1): 47-54.

[31] Wang L, Wang X, Kong W. ADAMTS-7, a novel proteolytic culprit in vascular remodeling[J]. Sheng li xue bao:[Acta Physiologica Sinica], 2010, 62(4): 285-294.

[32] Wang L, Zheng J, Bai X, et al. ADAMTS-7 mediates vascular smooth muscle cell migration and neointima formation in balloon-injured rat arteries[J]. Circulation research, 2009, 104(5): 688-698.

[33] Reilly M P, Li M, He J, et al. Identification of ADAMTS7 as a novel locus for coronary atherosclerosis and association of ABO with myocardial infarction in the presence of coronary atherosclerosis: two genome-wide association studies[J]. The Lancet, 2011, 377(9763): 383-392.

[34] Du Y, Gao C, Liu Z, et al. Upregulation of a disintegrin and metalloproteinase with thrombospondin motifs-7 by miR-29 repression mediates vascular smooth muscle calcification[J]. Arteriosclerosis, thrombosis, and vascular biology, 2012, 32(11): 2580-2588.

[35] Bengtsson E, Hultman K, Dunér P, et al. ADAMTS-7 is associated with a high-risk plaque phenotype i n human atherosclerosis[J]. Scientific reports, 2017, 7(1): 3753.

[36] De Meyer S F, Savchenko A S, Haas M S, et al. Protective anti-inflammatory effect of ADAMTS13 o n myocardial ischemia/reperfusion injury in mice[J]. Blood, The Journal of the American Society of Hematology, 2 012, 120(26): 5217-5223.

[37] Gandhi C, Motto D G, Jensen M, et al. ADAMTS13 deficiency exacerbates VWF-dependent acute myo cardial ischemia/reperfusion injury in mice[J]. Blood, The Journal of the American Society of Hematology, 2012, 1 20(26): 5224-5230.

[38] Doi M, Matsui H, Takeda Y, et al. ADAMTS13 safeguards the myocardium in a mouse model of acut e myocardial infarction[J]. Thrombosis and haemostasis, 2012, 108(12): 1236-1238.

[39] Sonneveld M A H, de Maat M P M, Leebeek F W G. Von Willebrand factor and ADAMTS13 in arte rial thrombosis: a systematic review and meta-analysis[J]. Blood reviews, 2014, 28(4): 167-178.

[40] Maino A, Siegerink B, Lotta L A, et al. Plasma ADAMTS-13 levels and the risk of myocardial infarct ion: an individual patient data meta-analysis[J]. Journal of Thrombosis and Haemostasis, 2015, 13(8): 1396-1404.

[41] Lv C L, Chen C, Zheng Z,Liu P, He X W, Jin X P,et al. Association between ADAMTS-1 gene polym orphism and essential hypertension in Chinese Han population [J]. Zhejiang Med,2018,40(01):19-22.

[42] Liu C, Wang X, Shang L X,et al. Expression of ADAMTS-2 and ADAMTS-7 in placenta with gestation al hypertension [J]. Chinese People's Armed Police Medicine,2013,24(08):695-698.

[43] Cerveró J, Segura V, Macías A, et al. Atrial fibrillation in pigs induces left atrial endocardial transcriptional remodelling[J].Thrombosis and haemostasis, 2012, 108(10): 742-749.

[44] Freynhofer M K, Gruber S C, Bruno V, et al.Prognostic value of plasma von Willebrand factor and its cleaving protease ADAMTS13 in patients wit-h atrial fibrillation[J]. International journal of cardiology, 2013, 168(1): 317-325.

[45] Wang H J, Xiao M, Zeng Z, et al.Correlation analysis between ADAMTS-13 gene polymorphism and hypertension-induced atrial fibrillation[J].Eur Rev Med Pharmacol Sci, 2020, 24(5): 2674.

[46] Dupuis L E, McCulloch D R, McGarity J D, et al. Altered versican cleavage in ADAMTS5 deficient mice; a novel etiology of myxomatous valve disease[J]. Developmental biology, 2011, 357(1): 152-164.

[47] Kern C B, Wessels A, McGarity J, et al. Reduced versican cleavage due to Adamts9 haploinsufficiency is associated with cardiac and aortic anomalies[J]. Matrix biology, 2010, 29(4): 304-316.

[48] Wünnemann F, Ta-Shma A, Preuss C, et al. Loss of ADAMTS19 causes progressive non-syndromic hear t valve disease[J]. Nature genetics, 2020, 52(1): 40-47.

[49] Massadeh S, Alhashem A, van de Laar I M B H, et al. ADAMTS19-associated heart valve defects: Nov el genetic variants consolidating a recognizable cardiac phenotype[J]. Clinical Genetics, 2020, 98(1): 56-63.

Fundprogram: National Natural Science Foundation of China (Foundation number :81860074)

Effect of FTY720 on the Tissue Microenvironments of Acute Spinal Cord Injury

Xiaotian Li[1,2], Linxuan Zou[3], Xin Han[4,5*], Zhuodong Fu[3*]

1. Department of Orthopaedics, Dalian Third People's Hospital affiliated to Dalian Medical University, Dalian 116000, China.

2. Dalian Third People's Hospital, Department of Orthopaedics, Dalian 116000, China.

3. The First Affiliated Hospital of Dalian Medical University, Department of Orthopaedics, Dalian 116000, China.

4. The Second Affiliated Hospital of Dalian Medical University, Department of Orthopaedics, Dalian 116000, China.

5. Naqu People's Hospital, Department of Orthopaedics, Naqu 852000, China.

Abstract: Objectives: To observe the effect of FTY720 on the changes of tissue microenvironment after acute spinal cord injury (ASCI) in rats. Methods: A total of 168 female SD rats were randomly divided into A, B and C groups, with 56 rats in each group. In group A (Sham-operation group), only T9 laminectomy was performed without spinal cord injury, and 0.3 ml normal saline was given by gavage immediately after suture. Group B (control group) was given 0.3 ml normal saline by gavage, group C (treatment group) was given 0.3 ml FTY720 diluted in 3mg/kg normal saline by gavage. The rats were sacrificed at 6h, 12h, 24h, 72h, 7d and 21d after operation. The injured spinal cord (the corresponding part of group A) was taken for ultrathin section, and HE staining was used to observe the necrosis of the spinal cord, inflammatory cell infiltration, glial scar formation, and the size of the syringomyelia in each group. The ratio of syringomyelia area to spinal cord area was calculated 21 days after injury. SPSS 13.0 software was used for statistical analysis. Results: HE staining showed that the morphology of the spinal cord in group A was normal at each time point: At 12h to 48h after operation, progressive edema of the spinal cord and liquefaction necrosis of the injured central area were observed, accompanied by inflammatory cell infiltration, mainly neutrophils, lymphocytes and monocytes. At 12h and 72h after operation, the degree of inflammatory cell infiltration in group B was significantly higher than that in group C ($P<0.05$). The degree of lymphocyte infiltration in group C was significantly lower than that in group B 12 hours after operation ($P< 0.05$). At 72 hours after operation, the central area of the injury had formed an unorganized structure cavity, and a large number of inflammatory cells infiltrated around the cavity, mainly microglia/monocytes. The number of glial scar cells in group B was significantly higher than that in group C ($P < 0.05$). The syringomyelia formed 21 days after operation. The syringomyelia ratio in group B was significantly higher than that in group C ($P<0.05$). Conclusions: FTY720 can significantly improve neurological function in rats after ASCI possibly by inhibiting the inflammatory response after spinal cord injury, thereby reducing the secondary injury of the spinal cord.

Keywords: FTY720; Neural Apoptosis; Acute Spinal Cord Injury

---

1. Introduction

Acute spinal cord injury (ASCI)[1] is extremely serious, with an annual incidence of about 20-40 /million people in the world[2]. The disability rate remains high[3]. Acute spinal cord injury can be divided into primary injury and secondary injury. A large number of studies have shown that the outcome of ASCI depends not only on the degree of primary injury, but also on the development of secondary injury. Therefore, the treatment of spinal cord injury is mainly aimed at secondary injury. In recent years, with the deepening of the research on a series of biochemical reactions triggered by secondary injury[4-6], the impact of autoimmune factors on spinal cord injury has received increasing attention. Improving the microenvironment of spinal cord injury and promoting functional recovery through immunosuppressive therapy has become a new approach for the treatment of spinal cord injury.[7]

After methylprednisolone[8, 9], a few immunosuppressive drugs have been found to be effective in the treatment of acute spinal cord injury[10, 11], but the systemic side effects of immunosuppressive drugs have seriously affected their clinical application.FTY720[12, 13], chemically named 2-amino-2·[2(4-octylphenyl)ethyl]-1 ， 3-propanediol hydrochloride, is synthesized by chemical modification of ISP-1 from the culture medium of Cordyceps sinensis. It is a new immunosuppressive drug different from other immunosuppressive drugs. FTY720 has little toxic and side effects on human body, and there is no significant decrease in peripheral blood neutrophils. It does not cause obvious damage to liver and kidney function, and can effectively play the role of immune regulation while maintaining the immune function of patients[14]. Recent studies have shown that FTY720 has a certain therapeutic effect on neuronal injury in brain tissue[15, 16], but the specific mechanism is still unclear. Whether FTY720 has a protective effect on neurons in acute spinal cord injury is still unknown. In this study, based on the establishment of an experimental acute spinal cord injury animal model, FTY720 was used to treat the injured animals, and the protective effect of a new immunosuppressant on spinal cord injury was explored from the perspective of neuronal microenvironment and cell apoptosis.[17-19]

2. Materials and methods

2.1 Materials

2.1.l Experimental animals

84 female Sprague-Dawley rats, weighing 180g--220g, were provided by the Animal Experimental Center of Dalian Medical University (SCXK(Liao) 2008.0002).The treatment of animals in the process of animal ethics experiments should refer to the Guiding Opinions on the Good Treatment of Experimental Animals issued by the Ministry of Science and Technology of the People's Republic of China in 2006.

2.1.2 Reagents and instruments

FTY720: purchased from Wuhan Yuancheng Technology Development Co., LTD.

Caspase-3 antibody: Caspase3(CPP32)Ab-4 was produced by NeoMarkers For Lab Vision Corporation (USA).

Tunel kit: Produced by Roche Diagnostics GmbH Mannheim, Germany.

SP kit (ready-to-use type) : contains H_20_2, 5% sheep serum, sheep anti-rabbit polyclonal antibody, peroxidase.Purchased from Beijing Zhongshan Jinqiao Biotechnology Co., LTD.

Allen's Animal Spinal Cord Crusher.

2.2 Method

2.2.1 Experimental grouping and animal model preparation

A total of 84 female SD rats were randomly divided into 3 groups: Sham-operation group (group A), model group (group B) and FTY720 treatment group (group C), including 14 rats in group A, 35 rats in group B and 35 rats in group C. The rats in the model group and the FTY720 treatment group were anesthetized intraperitoneally with 2% chloral hydrate (60mg/kg) and placed in the prone position. The skin was prepared with T9 as the center, and the skin was routinely sterilized. The spinous processes of T9 and T10 and the corresponding lamina were exposed, and the back and sides of the spinal cord were fully exposed by biting the T9 and T10 spinous processes and the corresponding lamina with a rouge. Under aseptic condition, the spinal cord of rats was hit by modified A11en's method. If the rats showed tail wagging reflex and severe contraction of lower limbs after impact, the model was successfully established. After the impact, the wound was sutured aseptically. In the Sham-operation group, only T9 and T10 pushing plate resection was performed without hitting the spinal cord, and the rest were the same as the model group. After modeling, the FTY720 treatment group was diluted with 3mg/kg normal saline and 0.3 ml was given by gavage. The Sham-operation group and the model group were given the same amount of normal saline by gavage. After operation, the rats were fed in cages with light and natural ventilation. After operation, urination was performed 2-3 times a day by manual pressing. The food intake, wound healing, and adverse reactions were observed.

2.2.2 Sampling and section preparation

The rats in each group were sacrificed at 6h, 12h, 24h, 48h, 72h, 1w, and 3w after operation, and 5 rats in each group were sacrificed at each time point. The rats were anesthetized intraperitoneally with 2% chloral hydrate (60mg/kg), then the hearts were perfused with 50ml of 4% paraformaldehyde 0.1M PH7.4 PBS solution. The injured spinal cord was about lcm long and cut into two segments from the center of the injured spinal cord. After 24 hours, the injured spinal cord was embedded in paraffin and serially sectioned with a thickness of 4μm. One section was taken every 10 minutes for HE staining. Ten sections from each specimen were taken for HE staining to observe the destruction of spinal cord tissue, inflammatory cell infiltration, the size of the syringomalacia, glial scar formation and repair of the spinal cord.

2.2.3 Detection indicators

2.2.3.1 Pathological observation of spinal cord microenvironment

The tissue sections were taken for HE staining at 6h, 12h, 24h, 72h, 1w and 3w after operation. The HE stained sections were taken by a digital camera and the images were input into a computer. The high power field images of four non-repeated spinal cord injury areas at l2h, 72h and 1w after injury were selected to calculate the cell density as M, M= the sum of the area of inflammatory nuclei in each specimen/the sum of the area of each specimen observed area ×1 00%. Inflammatory cell infiltration and glial scar formation were observed. The lymphocyte ratio at PIH 12 was calculated and recorded as L (L= lymphocyte count/total cell count ×100%).At 3w after injury, the ratio of syrinx area to total spinal cord area was calculated from the section at 20 × low power and recorded as S, S= syrinx area/spinal cord area ×100 %.

Procedure of HE staining

①Deparaffinized to water:

②Staining with hematoxylin for 2min.

③Wash back blue for 10min.

④Dye with eosin for 1.2min.

⑤Rinse with running water for 2min.

⑥Dehydrate, clear and seal

2.2.4 Image processing methods

The data were analyzed and processed by Image· pro plus 6.0 medical image analysis system.

2.2.5 Statistical methods

SPSSl3.0 software was used for statistical processing, and the data were expressed as mean 4-standard deviation. One-way analysis of variance was used for comparison among multiple groups.t test was used for comparison between the two groups, and $P<0.05$ was considered the difference was statistically significant.

3. Results

3.1 Histomorphological observation of spinal cord injury tissues by HE staining

3.1.1 Morphological changes in Sham-operation group (group A), model group (group B) and FTY720 treatment group (group C) at 6 hours are shown in Figure l Morphological changes

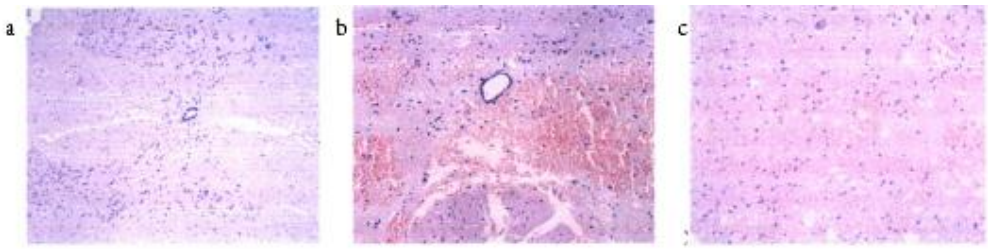

Figure 1. a: Sham-operation group (group A) b: model group (group B) c:FTY720 treatment group (group C).

In group A, the morphology of spinal cord was intact at each time point, and no destruction or liquefaction necrosis was observed. In group B and group C, obvious intraspinal hemorrhage and local hematoma were observed 6 hours after acute spinal cord injury, but the general shape of the spinal cord was still intact, the morphology of neurons was basically normal, and no obvious inflammatory cell infiltration was observed.

3.1.2 The morphological changes of the model group (group B) and FTY720 treatment group (group C) at 12 hours are shown in Figure 2

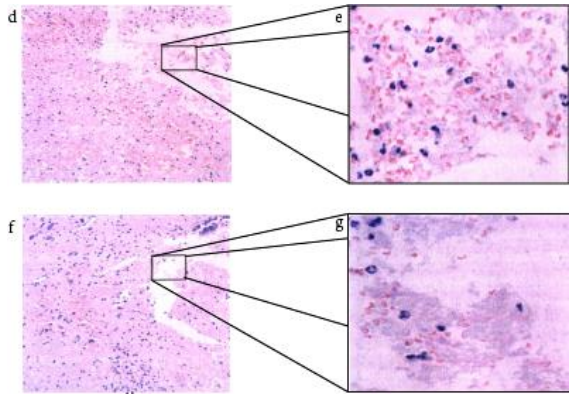

Figure 2. d, e: Model group (group B) f, g:FTY720 treatment group (group C).

At 12 hours after injury, liquefaction necrosis and inflammatory cell infiltration were observed in the spinal cord of group B and group C. Under low power field, the spinal cord tissue in group B showed obvious liquefaction necrosis, the central area of the tissue disintegrated and disappeared, and formed large cavities, and the internal hemorrhage was still obvious. The morphology of the spinal cord tissue in group C was mostly preserved, and the degree of liquefaction necrosis of the spinal cord was significantly lighter than that in group B, and small cavities were formed in some areas, and the internal hemorrhage was still obvious. In high power field, the infiltration of inflammatory cells in group B was mainly neutrophils, monocytes and lymphocytes. The infiltration of inflammatory cells in group C was mainly composed of neutrophils and monocytes, and lymphocytes were almost not seen.

3.1.3 The 24-hour morphological changes of the model group (group B) and FTY720 treatment group (group C) are shown in Figure 3

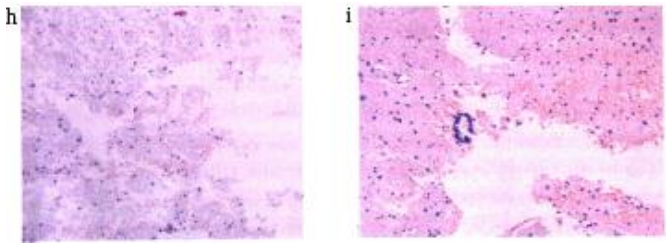

Figure 3. h: Model group (group B) i:FTY720 treatment group (group C)

At 24 hours after injury, the degree of liquefaction necrosis of spinal cord tissue in group B and group C was further aggravated, and group B was still more serious than group C. The number of neutrophils infiltration in the syringomyelia was gradually reduced, the number of microglia/monocytes around the syringomyelia was gradually increased, and the spinal cord hematoma was alleviated.

3.1.4 The morphological changes of model group (group B) and FTY720 treatment group (group C) at 72 hours are shown in FIG. 4

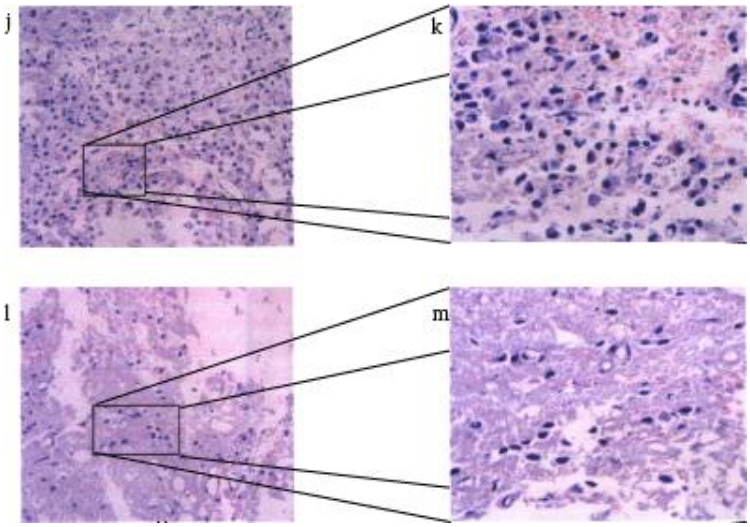

Figure 4. j, k: model group (group B) l, m:FTY720 treatment group (group C).

At 72 hours after injury, the myelomalacia area was further enlarged under low power field, and it was still more severe in group B than in group C. In group B2 and C2, the inflammatory cell infiltration was mainly microglia/monocytes, mainly located around the central area of the injury, but almost no neutrophils and lymphocytes were seen. The hemorrhage in the spinal cord still existed.

3.1.5 The morphological changes of model group (group B) and FTY720 treatment group (group C) at 1 w are shown in FIG. 5

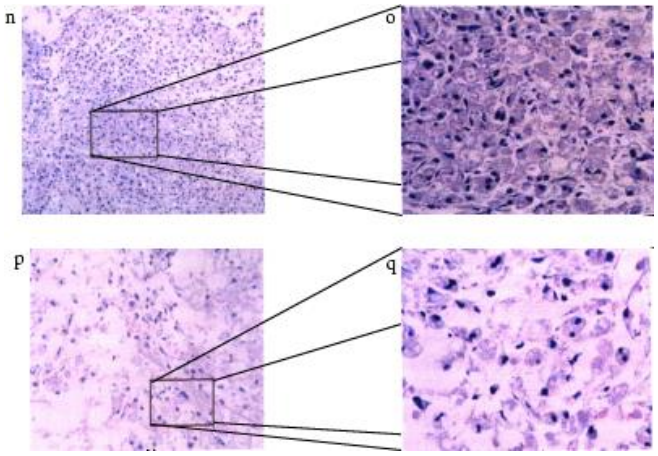

Figure 5. n, o: model group (group B) p, q:FTY720 treatment group (group C)

1 w after injury, the degree of liquefaction necrosis of the spinal cord tissue in groups B and C remained unchanged under low power field, and the hematoma in the spinal cord was almost absent. In group B, the degree of microglia/monocytes infiltration around the central area of spinal cord injury was further increased, oligodendrocytes and astrocytes proliferated, and the tissue structure was dense. In group C, the degree of microglia/monocyte infiltration around the central area of spinal cord injury was not significantly increased compared with that at 72 hours, and the proliferation of oligodendrocytes and astrocytes was not obvious.

3.1.6 The morphological changes of the model group (group B) and FTY720 treatment group (group C) at 3 weeks are shown in Figure 6

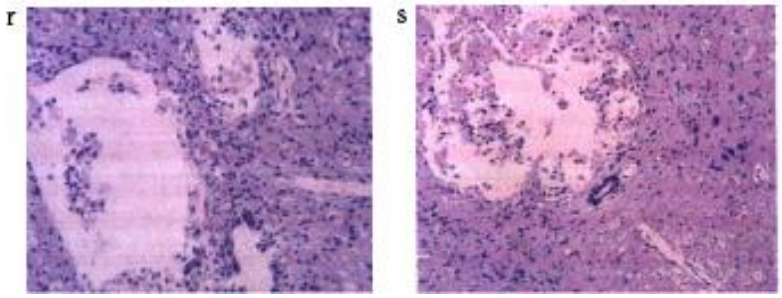

Figure 6. r: Model group (group B) s:FTY720 treatment group (group C)

At 3 weeks after injury, obvious cavities were formed in the injury center of group B and group C. In group B, there was a dense glial scar surrounding the syringomyelia and a wide transitional zone between the syringomyelia and normal spinal cord tissue. In group C, normal spinal cord tissue was observed around the syringomyelia, and there was almost no glial scar around the syringomyelia.

4. Discussion

4.1 Effect of FTY720 on tissue emblem environment in rats with acute spinal cord injury

More and more attention has been paid to the role of autoimmune response in ASCI.A large number of studies have shown that after ASCI, there will be a transient aggregation of neutrophils in the injured tissue, which means the beginning of the immune response. Antigen-specific T lymphocytes (T-LC) and antigen-nonspecific macrophage cells (MC) play a major role in the autoimmune response. The use of immunosuppressants to inhibit the local inflammatory response and improve the microenvironment of the injured neurons has become one of the new ideas for the treatment of spinal cord injury.

Current studies[20-22] have shown that FTY720 can not only promote the homing of lymphocytes to lymph nodes, but also effectively reduce the infiltration of T lymphocytes into local tissues. Therefore, FTY720 can reduce the inflammatory response by reducing the infiltration of local immune cells. In this experiment, HE staining showed that in the model group (group B), obvious blood could be seen in the spinal cord at 6 hours after acute spinal cord injury, but the morphology of the spinal cord was still roughly intact, the morphology of neuronal cells did not change significantly, and the infiltration of inflammatory cells was not obvious. However, at 12 hours after injury, liquefaction necrosis and infiltration of inflammatory cells were observed in the spinal cord tissue, mainly neutrophils, monocytes and lymphocytes. From 24 to 72 hours after injury, the liquefaction and necrosis of the spinal cord tissue were progressively aggravated. The infiltration of neutrophils and lymphocytes gradually decreased or almost disappeared, while the infiltration of microglia/monocytes gradually increased. At 1 week after injury, the infiltration of microglia/monocytes was predominant around the liquefaction necrosis area of the spinal cord, with a large number of oligodendrocytes and astrocytes. Obvious cavities could be seen in the center of the spinal cord injury area 3 weeks after injury. Although the changes of microenvironment in FTY720 treatment group (group C) were basically the same as those in model group (group B) after spinal cord injury, the degree of inflammatory

cell infiltration, especially lymphocyte infiltration, and the size of glial scar and cavity in FTY720 treatment group (group C) were significantly smaller than those in model group (group B) at all time points except 6 hours after injury. The results of quantitative analysis showed: In the model group (group B), the cell density of inflammatory cell infiltration and the cell ratio of lymphocyte infiltration at 12 hours after SCI, the density of microglia/monocytes at 72 hours, the density of glial scar cells around the first week, and the ratio of cavity area to spinal cord area at 3 weeks were significantly higher than those in the FTY720 treatment group (group C). And the difference was statistically significant ($P<0.05$).

According to the above results analysis, it can be concluded that: FTY720 alleviates secondary injury after acute spinal cord injury by reducing the infiltration of inflammatory cells and the release of related cytokines (especially T lymphocytes), reducing the area of glial scar and cavity, and retaining more normal spinal cord tissue, thus improving the microenvironment of acute spinal cord injury tissue and protecting neurons.

5. Conclusion

FTY720 can reduce the secondary injury of spinal cord by reducing the infiltration of inflammatory cells in rats with acute spinal cord injury.

References

[1] Cortez R, Levi AD. Acute spinal cord injury [J]. Critical Care Clinics, 1987, 3(2): 441-697.

[2] Tator CH, Fehlings MG. Review of the secondary injury theory of acute spinal cord trauma with emphasis on vascular mechanisms [J]. Journal of Neurosurgery, 1991, 75(1): 15-26.

[3] Tyor WR, Avgeropoulos N, Ohlandt G, et al. Treatment of spinal cord impact injury in the rat with transforming growth factor-beta [J]. Journal of the Neurological Sciences: Official Bulletin of the World Federation of Neurology, 2002, (1/2): 200.

[4] Merola A, et al. Attenuation of CNTF in ASCI treated with intravenous methylprednisolone [J]. The Spine Journal, 2002, 2(Supplement): 109.

[5] Bracken MB, Shepard MJ, Collins W, et al. Bracken M B, Shepard M J, Collins W F et alMethylprednisolone or naloxone treatment after acute spinal cord injury: I-year follow-up data. Results of the second National Acute Spinal Cord Injury Study, 1992. J Neurosurg 76: 23-31 [J]. Journal of Neurosurgery, 1992, 76(1): 23-31.

[6] Bracken M. A randomized, controlled trial of methylprednisolone or naloxone in the treatment of acute spinal cord injury [J]. N Engl J Med, 1990, 322.

[7] Beattie MS, Hermann GE, Rogers RC, et al. Cell death in models of spinal cord injury [J]. Progress in brain research, 2002: 137.

[8] John HR. Methylprednisolone for the Treatment of Acute Spinal Cord Injury: Point [J]. Neurosurgery, 2014, 61 Suppl 1(Suppl 1): 32.

[9] Bracken MB, Shepard MJ, Collins WF, et al. Methylprednisolone or naloxone treatment after acute spinal cord injury: I-year follow-up data [J]. Journal of Neurosurgery, 1992, 76(1): 23-31.

[10] Lambrechts D, Carmeliet P. VEGF at the neurovascular interface: therapeutic implications for motor neuron disease [J]. Biochimica et Biophysica Acta (BBA) - Molecular Basis of Disease, 2006, 1762(11–12): 1109-21.

[11] Ibarra A, Correa D, Willms K, et al. Effects of cyclosporin-A on immune response, tissue protection and motor function of rats subjected to spinal cord injury [J]. Brain Research, 2003, 979(1-2): 165-78.

[12] Fujita, Inoue, Yamamoto, et al. Fungal metabolites. Part 11. A potent immunosuppressive activity found in Isaria sinclairii metabolite [J]. The Journal of antibiotics, 1994.

[13] Kappos L, Antel J, Comi G, et al. Oral fingolimod (FTY720) for relapsing multiple sclerosis [J]. N Engl J Med,

2006, 355(11): 1124-40.

[14] Budde K, Schmouder R L, Brunkhorst R, et al. Budde, K. et al. First human trial of FTY720, a novel immunomodulator, in stable renal transplant patients. J. Am. Soc. Nephrol. 13, 1073-1083 [J]. Journal of the American Society of Nephrology, 2002, 13(4): 1073-83.

[15] Zhang Z, Fauser U, Schluesener HJ. Early attenuation of lesional interleukin-16 up-regulation by dexamethasone and FTY720 in experimental traumatic brain injury [J]. Neuropathology and Applied Neurobiology, 2008.

[16] Zhang, Z, et al. FTY720 attenuates lesional interleukin-17+ cell accumulation in rat experimental autoimmune neuritis [J]. Neuropathology & Applied Neurobiology, 2009.

[17] Brinkmann, V. The Immune Modulator FTY720 Targets Sphingosine 1-Phosphate Receptors [J]. Journal of Biological Chemistry, 2002, 277(24): 21453-7.

[18] Schmouder R, Serra D, Wang Y, et al. FTY720: placebo-controlled study of the effect on cardiac rate and rhythm in healthy subjects [J]. Journal of Clinical Pharmacology, 2013, 46(8).

[19] Brinkmann V, Billich A, Baumruker T, et al. Erratum: Fingolimod (FTY720): Discovery and development of an oral drug to treat multiple sclerosis (Nature Reviews Drug Discovery (2010) 9 (883-897)) [J]. 2010.

[20] Li X K, Tamura A, Fujino M, et al. Induction of lymphocyte apoptosis in rat liver allograft with ongoing rejection by FTY720 [J]. Clinical & Experimental Immunology, 2010, 123(2): 331-9.

[21] López-Vales R, García-Alías G, Forés J, et al. FK506 reduces tissue damage and prevents functional deficit after spinal cord injury in the rat [J]. Journal of Neuroscience Research, 2010, 81(6): 827-36.

[22] Nagahara Y, Ikekita M, Shinomiya T. Immunosuppressant FTY720 induces apoptosis by direct induction of permeability transition and release of cytochrome c from mitochondria [J]. Journal of Immunology, 2000, 165(6): 3250-9.

The Relationship Between Core Knowledge of Tuberculosis and Mental Health: a Cross-Sectional Study Among University Students in Xizang

Zengyan Li[1], Labasangzhu[*2,3]

1. Tibet University, Lasa 850000, China

2. Department of Preventive Medicine, Tibet University Medical College, Lasa 850000, China

3. High Altitude Medical Research Center (High Altitude Health Science Research Center) of Tibet University, Lasa 850000, China.

Abstract: The relationship between core knowledge of TB and mental health among students in a university was investigated. The results showed that the overall knowledge rate of core knowledge of tuberculosis was 71%. The main effects of coping style and standard level on mental health, anxiety, and self-denial were significant. In terms of mental health, the results had borderline significant, and the positive attitude of the "not up to standard" participants was conducive to a good mental state. This suggests that schools should not only strengthen the education of students on TB prevention and control but also cultivate positive attitudes among students.

Keywords: Awareness Rate; Mental Health

1. Introduction

Tuberculosis is mainly respiratory transmitted and is a tuberculous lesion that occurs in the lung tissue, trachea, bronchi, and pleura [1]. To effectively curb the prevalence of tuberculosis, China's 13th Five-Year Plan for the Prevention and Control of Tuberculosis aims to achieve a public awareness rate of more than 85% of the core knowledge of tuberculosis prevention and control. In June 2017, The Code of Practice for Tuberculosis Prevention and Control in Schools (2017 Edition)[2] (hereinafter referred to as the Code), which standardizes the core knowledge of TB health education in schools into eight articles. so this study first explored the knowledge of college students about the core knowledge of TB health education in the Norms.

Mental health is not only the absence of mental illness or psychopathy, but also the ability of an individual to recognize his or her potential [3][4]. Individuals who use positive coping have higher levels of psychological health[5].In the current study, the participants were selected from classes in which they had a history of TB or were found to have TB in previous screenings, and schools are characterized by high population density and mobility, so the level of knowledge about tuberculosis may affect their mental health status. In addition, considering that different coping styles may also affect mental health [5], different coping styles may lead to different levels of mental health in cases where subjects are unable to determine whether they have been diagnosed with TB and have little knowledge of this area.

2. Subjects and methods

2.1 Investigation subjects

A questionnaire based survey was conducted among university students in Xizang reported tuberculosis cases or had been diagnosed with tuberculosis in a tuberculosis screening.

2.2 Investigation content

The questionnaire includes the following four aspects: (1) general information; (2) Eight core knowledge items of TB; (3) Simple Coping Style Questionnaire (SCSQ): The scoring converts the scores of negative coping and positive coping into Z-scores, and a positive coping tendency is positive if the standard score of positive coping is subtracted from the standard score of negative coping, and negative coping if the opposite is true [6]. (4) The General Health Questionnaire (GHQ-20), including three subscales: the Self-Affirmation Scale, the Anxiety Scale, and the Depression Scale[7]. Self-affirmation scores were reverse scored to create self-denial scores. The anxiety score, depression score, and self-denial score were added to obtain the mental health score, and the higher the total score, the lower the level of mental health.

2.3 Statistical analysis

SPSS 25. 0 statistical software was used to analyze the data.

3. Results

3.1 Basic information

A total of 287 questionnaires were distributed, and the actual number of valid copies collected was 269 (93.7%)

3.2 Univariate analysis of the core knowledge of tuberculosis prevention and treatment that affects the “up to standard”knowledge

The significant differences were statistically significant ($P < 0.05$) when comparing students' professional field, area of origin, whether they have received TB-related health education, and whether they have read information about TB prevention. See Table 1.

Table 1 Awareness of the core knowledge of TB control of participants

Type Number of Participants	up to standard	Not up to standard	χ^2	P
Gender			0.006	0.937
Male（n=138）	30	108		
Female（n=131）	29	102		
Ethnicity				
Xizangan（n=154）	40	114	2.289	0.318
Han ethnic group（n=104）	32	72		
Other ethnic groups（n=11）	5	6		
area of origin			3.990	0.046*
Countryside（n=202）	33	169		

City（n=67）	16	41		
Grade			8.363	0.079
Freshman year（n=37）	13	24		
Sophomore（n=35）	6	29		
Junior（n=135）	25	110		
Senior Year（n=24）	3	21		
Grand 5th grade（n=38）	13	25		
professional field			11.298	0.001*
Medical category（n=92）	31	61		
Non-medical category（n=177）	28	149		
whether they have received TB-related health education			5.189	0.023*
Yes（n=215）	65	150		
No（n=54）	8	46		
whether they have read information about TB prevention			4.742	0.029*
Yes（n=224）	71	153		
No（n=45）	7	38		
whether they have a family history of TB			0.011	0.916
Yes（n=5）	1	4		
No（n=264）	58	206		

3.3 The Relationship between Core Knowledge of Tuberculosis and Mental Health

A two-factor ANOVA with 2 (standard level: up to standard, Not up to standard) × 2 (coping style: positive, negative) was conducted with the dependent variables of anxiety scale, depression scale, self-denial scale, and mental health score, respectively.

Firstly. On the anxiety scale, The results found that: the main effect of the standard level was significant $F(1, 266)=4.558$, $p=0.034$, $\eta_p^2=0.017$, and anxiety scores were significantly lower for people who up to standard ($M=0.356$, $SD=0.996$) than for those who did not ($M=0.938$, $SD=1.616$); the main effect of coping style was significant $F(1, 266)=9.639$, $p= 0.002$, $\eta_p^2=0.035$, and anxiety scores were significantly lower for positive coping ($M=0.306$, $SD=0.970$) than for negative coping ($M=1.164$, $SD=1.724$); the interaction between standard level and coping style was not significant $F(1, 266)=1.442$, $p=0.231$, $\eta_p^2=0.005$. Secondly, On the depression scale, the main effect of standard level was not significant $F(1, 266)=1.797$, $p=0.181$, $\eta_p^2=0.007$; the main effect of coping style was not significant $F(1, 266)=0.844$, $p=0.359$, $\eta_p^2=0.003$; the interaction between standard level and coping style was not significant $F(1, 266)=0.195$, $p= 0.660$, $\eta_p^2=0.001$.Thirdly, On the self-denial scale, the main effect of the standard level was significant $F(1, 266)=8.598$, $P=0.004$，$\eta_p^2=0.031$, and the self-denial scores were significantly lower for people who up to standard($M=4.610$, $SD=3.068$) than for those who did not ($M=6.090$, $SD=2.921$); the main effect of coping style was significant $F(1, 266)=9.459$, $P=0.002$, $\eta_p^2=0.034$, and self-denial scores were significantly lower for positive coping ($M=4.766$, $SD=3.081$) than for negative coping ($M=6.465$, $SD=2.762$); the interaction between standard level and coping style was not significant $F(1, 266)=1.354$, $P=0.246$, $\eta_p^2=0.005$. Finally, On the mental

health scores, the main effect of the standard level was significant $F(1, 266)=19.996$， $P=0.001$，$\eta_p^2=0.070$, and the mental health scores were significantly lower for people who up to standard($M=5.559$, $SD=0.385$) than for those who did not ($M=7.516$, $SD=0.209$); the main effect of coping style was significant $F(1, 266)=24.050$, $P=0.001$, $\eta_p^2=0.083$, and mental health scores were significantly lower for positive coping($M=5.464$, $SD=0.312$)than for negative coping ($M=7.611$, $SD=0.307$); The interaction between level of attainment and coping style reached borderline significant $F(1, 266)=3.645$, $p=0.057$, $\eta_p^2=0.014$, and further simple effects analysis revealed that for those who did not up to the standard, mental health scores were significantly lower with positive attitudes ($M=6.025$, $SD=3.081$) than with negative attitudes ($M=9.008$, $SD=2.053$), $t(209)=7.099$, $p=0.001$, $CI95\%$ [-3.813, -2.153]; for those who up to the standard, there was no difference in mental health scores in terms of coping style. As shown in Figure 1.

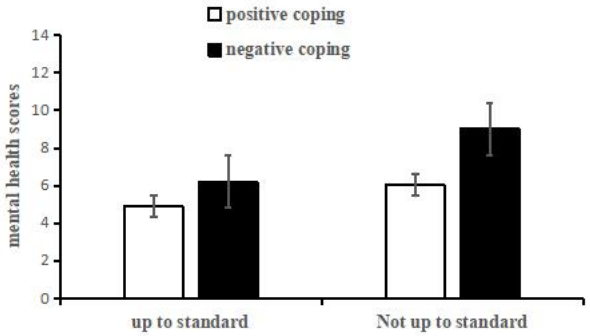

Figure 1. Mental health scores at the different standard levels under different coping styles

4. Discussion

From the analysis of this survey, the overall standard of core knowledge of TB prevention and treatment in this group was 72%, which did not reach the target of "public knowledge of TB prevention and treatment reaching over 85%" proposed in the 13th Five-Year Plan. This suggests that schools should further strengthen the dissemination of core knowledge about TB prevention and treatment to raise the awareness of students.

Our other concern is the effect of core knowledge of TB prevention and control on mental health. The main effects of standard level and coping style were found to be significant in the ANOVAs for the anxiety scale, the self-denial scale, and the total mental health scores. In terms of coping style, the results are consistent with previous studies [6], which also found lower anxiety scores and self-denial scores among active copers in the current study. possibly because individuals are more optimistic and more sure of themselves when adopting a positive attitude. Importantly, the standard levels of core knowledge of TB control were also found to influence self-denial and anxiety. This may be related to our choice of the group, as the participants had contact with the TB patients in the class and therefore became worried. At this point, when the participants had more knowledge about the core knowledge of TB control, they were able to reduce their worries, anxiety, etc. to some extent and were able to live their lives normally as usual. On the contrary, they worry about whether they are infected and thus become more upset.

However, on the depression scale, there were no differences in standard levels or coping styles. We speculate that this may be related to the content of the scale, such as "I would feel like a useless person", which may not be experienced in the current context.

It is interesting to note that in the overall mental health scores, there is a significant borderline between the coping style and the level of standard. For those who did not up to the standard, mental health scores with positive attitudes were lower than negative attitudes, suggesting that even though knowledge of core TB control knowledge did not up to the standard,

adopting attitudes such as learning from others' approaches to similar difficult situations, seek advice from relatives, friends or classmates, etc., may be able to motivate individuals to make up for their knowledge about TB and thus reduce their bad feelings.

5. Shortcomings

The current study questionnaire was collected before the PPD results were known, so it may have influenced the results, and in addition, considering the specificity of the participants group, it is necessary to continue to validate the results of this study in the next study by considering the above two reasons together.

References

[1] Diagnostic criteria for tuberculosis(WS 288—2017). *Electronic Journal of Emerging Infectious Diseases, National Health Commission of the People's Republic of China*, 2018 (01),59-61.

[2] Announcement on the issuance of norms for the prevention and control of tuberculosis in schools (2017version). *The National Health and Family Planning Commission of the People's Republic of China Bulletin*, 2017 (06),45-50.

[3] World Health Organization. Constitution of the World Health Organization, Reprinted in Basic Documents, 37thed[R]. Geneva: World Health Organization, 1946.

[4] Fu XL, Zhang K. China's national mental health development report [M]. Beijing: *Social Science Literature Press*, 2019: 1-55.

[5] Ding L, Sun GS, Zhang YQ, et al. Correlation analysis between work stress, coping style as well as anxiety and depression level among nurses in the emergency department. *Nursing Practice & Research,* 2019 (08),12-14.

[6] Xie YN, Dai XY. (2006). Practical Psychometric Tests [M]. *China Medical Science & Technology Press.*

[7] Li H, et al. (2002). Assessing Psychological Well-being of College Student: Psychometric Properties of GHQ-20. *Psychological Development & Education*(01), 75-79.

Acknowledgments

Fund Project: Everest Discipline Construction Project of Xizang University (ZF21003001); Xizang University High-level Talent Training Project (zdbs202214); Xizang University Medical College Medical Education special project.

The Application of Intracardiac Ultrasound in Atrial Septal Puncture

Qiyong Liu*
Department of Cardiology, the Third Hospital of Jinan, Jinan 250100, China.

Abstract: **Objectives:** To investigate the safety and effectiveness of atrial septal puncture assisted by intracardiac ultrasound, and to evaluate the value of intracardiac ultrasound in atrial septal puncture. **Methods:** Sixty patients who underwent radiofrequency ablation for the first time were randomly divided into two groups. Patients in experimental group underwent intraventricular ultrasound-assisted atrial septal puncture, while those in control group underwent X-ray guided atrial septal puncture. The success rate, puncture time and complications of the two groups were compared. **Results:** All atrial septal puncture was successful in the experimental group, while one-time puncture was successful in 21 cases and unsuccessful in 9 cases in the control group with a success rate of 83.33%. There was significant difference in puncture success rate between the two groups. Moreover, the puncture time of the experimental group (5.00±1.5 min) was significantly shorter than that of the control group (6.90±1.32 min). Furthermore, the complication rates of the experimental group and the control group were 10% and 13.33%, respectively, with no significant difference. **Conclusion:** Ultrasound-assisted atrial septal puncture was significantly superior to X-ray guided atrial septal puncture, with high puncture success rate, short puncture time and fewer complications.

Keywords: Intracardiac Echocardiography; X-Ray; Atrial Septal Puncture

Introduction

Radiofrequency catheter ablation for atrial fibrillation, ventricular arrhythmia, supraventricular tachycardia and other arrhythmias is increasing. Atrial septal puncture is an important surgical procedure for atrial fibrillation, ventricular arrhythmias originating from the left ventricle, superior ventricular tachycardia caused by the left atrium, and occlusion of the left atrial ear. It is also a technical approach for many cardiovascular interventions. With the recent development of radiofrequency catheter ablation for atrial fibrillation (AF), the safety of atrial septal puncture becomes particularly important [1]. There are certain risks of atrial septal puncture under the guidance of X-ray, especially for patients with abnormal atrial septal anatomy, intracardiac echocardiography (ICE) has real-time imaging of the internal structure of the heart and adjacent tissues, and real-time imaging of the process of atrial septal puncture. The position of fossa ovale and the anatomical structure of the abnormal, so as to safely guide the atrial septal puncture. As the technology continues to mature, ICE guided catheter ablation of atrial fibrillation (AF) is increasingly widely used in the clinic [2]. In this study, by comparing the effect of ICE-assisted and X-ray-guided atrial septal puncture, the existing problems in atrial septal puncture and the value of intracardiac ultrasonic-assisted atrial septal puncture are discussed.

1. Materials and methods

1.1 Object of study

Sixty patients admitted to the Department of Cardiovascular Medicine of Jinan Third People's Hospital from January 2021 to March 2023 who met the indication of atrial septal puncture were selected as the research objects. All patients received Transesophageal echocardiography (TEE) before surgery and received radiofrequency ablation for the first time. The patients were randomly divided into two groups with 30 cases in each group. All patients were excluded from the following conditions： left atrial thrombus; left atrial myxoma; severe deformities of heart, chest and spine; severe coagulation dysfunction or inability to tolerate anticoagulant therapy; thrombosis of lower limb vein, femoral vein, iliac vein, hemodynamic instability, contrast agent allergy. Informed contents were obtained in advance.

1.2 Methods

All patients had stable hemodynamics and fasting for more than 6 hours. Warfarin or rivaroxaban was stopped before surgery for 3 days, and low molecular weight heparin was used as anticoagulant. Intra-esophageal ultrasound was performed within 24 hours before surgery to exclude left atrial thrombus. Cardiac ultrasound was performed to determine cardiac function and structure, and routine biochemical examination was performed. Then an atrial septal puncture was performed.

Patients in control group received atrial septal puncture under the guidance of X – ray. Firstly, the SWARTZ or Mullins sheath tube or Preface of the puncture should be used, and the sheath tube should be fully rinsed with heparin saline before the puncture. The puncture sheath was sent to the superior vena cava through the 0.032-inch 145cm guide wire, then the guide wire was removed and sent to the atrial septal puncture needle. The puncture needle indicator was kept pointing to 12 o 'clock, and the tail was kept about 2cm away to ensure that the puncture needle tip was in the inner sheath. The left and right hands rotated the sheath and puncture needle simultaneously. The tail indicator pointed to 4-5 o 'clock, the head of the sheath turned to the atrial septum, and kept the puncture needle and the sheath retreating synchronously along the septum to the fossa ovale. After fluoroscopy, the anterior position could be used to retreat, and there were 2-3 beats at the head of the inner sheath canal during the process, indicating the right atrium and fossa ovale respectively. Before and after the puncture point was determined by the 45 degree puncture needle at RAO position and the curvature of the distal segment of the sheath canal disappeared close to a straight line, the puncture point was determined by the height of a vertebral body at the lower margin of the left atrial shadow at PA position. After the internal sheath canal tightened the atrial septum, the puncture needle rotated slightly backward along the clock to smoothly pass through the atrial septum. Contrast agent was injected, such as linear ejection of contrast agent to confirm successful introduction into the left atrium. The fixed puncture needle pushed the dilator tube so that its tip covered the puncture needle, and then pushed the outer sheath tube into the left atrium, fixed the outer sheath tube, and pulled the dilator tube and the puncture needle out of the body together.

The experimental group received intraventricular ultrasonic-assisted atrial septal puncture. The ultrasound catheter was rotated clockwise from the Home View to the left pulmonary vein fan, P curve was made to make the aortic root appear, R curve was made to make the superior vena cava appear, the long guide wire was sent to the superior vena cava, the atrial septal puncture sheath was introduced into the superior vena cava, the guide wire was withdrawn and the puncture needle was sent. Coaxial rotation makes the tail indicator point to 4-5 o 'clock. At the same time, pull down the puncture needle and sheath tube. The ultrasonic catheter is slightly bent L to track the puncture sheath head. When the puncture needle and sheath tube slip into the fossa ovalis, the "tent" sign can be seen under ultrasound; after the puncture point is determined, the puncture needle passes through the atrial septum, and the "tent" sign disappears; bright red arterial blood can be seen after extraction, and the "blister" sign of the left atrium can be seen after injection of normal saline. The puncture needle is fixed

and pushed to the dilator tube so that its tip covers the puncture needle, then the puncture needle is withdrawn, and the guide wire is sent to the left upper pulmonary vein. The catheter was sent to the atrial septal sheath along the guide wire to complete the puncture.

1.3 Evaluation index

1.3.1 Comparison of puncture success rate

Puncture failure was defined as failure of puncture for 3 times (changing the surgeon's puncture or changing to X-ray combined with ICE interatrial septal puncture) or the use of X-ray exposure during puncture.

1.3.2 Comparison of Puncture time

The time of puncture device from the beginning of superior vena cava withdrawal to the time when the sheath catheter was irrigated with heparin saline after entering the left chamber.

1.3.3 Comparison of complication rate

Complications associated with atrial septal puncture, including pericardial tamponade, aortic perforation, stroke or transient cerebral ischemia (TIA), were counted.

2. Results

2.1 Patients' general data

As shown in Table 1, there were 19 males and 11 females in the experimental group, with an average age of 60.17±3.16 years old. The left ventricular ejection fraction was 60.87±5.37%, and the anterior and posterior left atrium 39.13±2.52 mm. In the control group, there were 22 males and 8 females, with an average age of 59.07±3.45 years old. The left ventricular ejection fraction was 59.33±6.15%, and the left anterior and posterior atrial diameter was 38.83±2.25 mm. There were no significant differences in gender, age and echocardiogram parameters between the two groups, which were comparable.

Table 1. Comparison of patients' baseline data

	Experimental group（n=30）	Control group（n=30）	χ^2/t-value	P-value
Gender			0.693	0.405
Male	19	22		
Female	11	8		
Age	60.17±3.16	59.07±3.45	1.287	0.203
LVEF（%）	60.87±5.37	59.33±6.15	1.029	0.308
LAD（mm）	39.13±2.52	38.83±2.25	0.486	0.629

LVEF: Left Ventricular Ejection Fraction; LAD: Left Atrial Diameter.

2.2 Puncture time and success rate of patients in two groups

The puncture time of patients in the experimental group was 5.00±1.5 min, and the success rate of puncture was 100%, among which 28 patients were successfully pierced by the first needle and 2 patients were successfully pierced by the second needle. In the control group, the puncture time was 6.90±1.32 min, and 21 cases were successfully pierced, the success rate was 83.33%. There was significant difference in puncture success rate between the two groups ($P<0.05$).

Table 2. Puncture time and success rate of patients in two groups

Groups	Puncture time（min）	success rate（n,%）
Experimental group（n=30）	5.00±1.58	30（100%）
Control group（n=30）	6.90±1.32	21（70%）
P-value	<0.001	0.042

2.3 Comparison of complications between the two groups

As shown in Table 3, a total of 3 patients in the experimental group developed complications, of which 2 were related to femoral vein puncture (6.67%) and 1 was subcutaneous hematoma (no special treatment required). In the control group, 1 case of pericardial tamponade, 1 case of complications related to femoral venipuncture and 2 cases of stroke occurred were occurred, and the complication rate was 13.33%. There was no significant difference between the two groups（P>0.05）。

Table 3. Comparison of complications between the two groups

Groups	with complications（n,%）	without complications（n,%）
Experimental group（n=30）	3（10%）	27（90%）
Control group（n=30）	4（13.33%）	26（88.67%）
χ^2 value	0.162	
P-value	0.688	

3. Discussion

In recent years, the incidence of atrial fibrillation (referred to as atrial fibrillation) has been increasing year by year. The United States, Europe, China and other countries have successively promoted transcatheter radiofrequency ablation as the first-line treatment for paroxysmal atrial fibrillation that is difficult to control with drugs in the guidelines for the treatment of atrial fibrillation[3]， For patients with symptomatic persistent or long-duration persistent atrial fibrillation who are ineffective with antiarrhythmic drugs, Catheter ablation may also be considered to improve symptoms. The ablation method currently in routine use is to perform atrial septal puncture, location and ablation of the pulmonary venous antrum via catheter combined with X-ray images, based on a 3D model built in contact with the CARTO3, etc [4]. With the increasing number of surgical patients, the safety of this method, including the duration of intraoperative X-ray exposure, has gradually drawn attention.

Trial septal puncture is an important step in radiofrequency catheter ablation of atrial fibrillation. It is commonly used in many percutaneous interventional treatments, including left heart radiofrequency ablation, left atrial ear occlusion and percutaneous mitral valvuloplasty. CE is an ultrasound imaging technology that uses an ultrasound probe sent through the peripheral blood duct to conduct real-time high-quality imaging and/or hemodynamic determination of the heart and its adjacent tissues, and has the ability to image the structures in the heart cavity and surrounding tissues in real time [5]. ICE visualization of atrial septum is an important tool to ensure the safety of atrial septum puncture [6, 7]. In this study, patients who underwent radiofrequency ablation underwent ICE-assisted and X-ray-guided atrial septal puncture respectively, aiming to study the effect and value of the two methods. The results showed that the puncture success rate of patients with ICE-assisted atrial septal puncture was much higher than that of patients with X-ray guided atrial septal puncture, and the puncture time was greatly shortened. This suggests that ICE is effective in atrial septal puncture.

One of the most important roles of ICE technology is the timely detection and prevention of potential complications during ablation procedures. In the process of atrial septal puncture, for patients with abnormal anatomy, due to the atypical position of the atrial septal and the difficulty of puncture through the atrial septal, it cannot be accurately positioned under conventional fluoroscopy, which may lead to complications such as pericardial tamponade, puncturing of the aortic root,

arterial embolism, pulmonary vein perforation, etc. In order to reduce and avoid life-threatening complications and improve the success rate of atrial septal puncture, ICE guidance can be considered for atrial septal puncture with anatomic abnormalities [8]. In this study, it was found that the incidence of complications in both ICE-assisted and X-ray guided atrial septal puncture was low, and the difference was not significant, which may be related to the small clinical sample size and no abnormal anatomical structure of patients. But at least ICE assisted septal puncture has been shown to be safe.

In conclusion, ICE assistance can greatly improve the success rate of atrial septal puncture in patients with atrial fibrillation, shorten the puncture time, and reduce the occurrence of complications. However, the sample size of this study is small, and the results need to be further verified.

References

[1] Lin J, Li HR, Liu MX, et al. Safety and feasibility of atrial septal puncture guided by zero-ray ultrasound [J]. Advances in Cardiology 2022,43(1):93-96 .

[2] Liu HY, & Zhong JQ. Application of intracardiac ultrasound in the interventional treatment of atrial fibrillation [J]. Biomedical Engineering Research,2021; 40(4): 5.

[3] Huang H, Huang CX, Jiang H, et al. Preliminary experience of Carto3 guided radiofrequency ablation of paroxysmal atrial fibrillation [J]. 2011.

[4] Pappone C, Rosanio S, Augello G, et al. Mortality, morbidity, and quality of life after circumferential pulmonary vein ablation for atrial fibrillation: Outcomes from a controlled nonrandomized long-term study[J]. Journal of the American College of Cardiology,2003; 2).

[5] Enriquez A, Saenz LC, Rosso R, et al. Use of Intracardiac Echocardiography in Interventional Cardiology: Working With the Anatomy Rather Than Fighting It[J]. Circulation,2018; 137(21): 2278.

[6] Daoud E, Kalbfleisch S, & Hummel J. Intracardiac echocardiography to guide transseptal left heart catheterization for radiofrequency catheter ablation[J]. Journal of cardiovascular electrophysiology,1999; 10(3): 358-363.

[7] Ren JF, Marchlinski FE, Callans DJ, et al. Clinical use of AcuNav diagnostic ultrasound catheter imaging during left heart radiofrequency ablation and transcatheter closure procedures[J]. Journal of the American Society of Echocardiography Official Publication of the American Society of Echocardiography, 2002; 15(10): 1301-1308.

[8] Salghetti F, Sieira J, Chierchia GB, et al. Recognizing and reacting to complications of trans-septal puncture[J]. 2017; 15(12): 905-912.

Fundings: Medical and Health Science and Technology Development Program of Shandong Province NO.202203010368

Universe Scientific Publishing

Research Advance about Poor Response to Anti-VEGF in Neovascular Age-Related Macular Degeneration

Siyuan Nie
The Second Affiliated Hospital of Nanchang University, Nanchang 330000, China.

Abstract: Neovascular age-related macular degeneration (nAMD) has become one of the main causes of vision damage in middle-aged and elderly people, Now, anti-vascular endothelial growth factors (anti-VEGF) therapy has achieved a milestone in the treatment of nAMD, However, in clinical practice, the phenomenon of poor or even non-response of anti-VEGF drugs is still found, even maximal anti-VEGF treatment to some patients. The research on poor response to anti-VEGF therapy is also a hot topic in recent years. This article gives a brief review on diagnostic factors, This article gives a brief review on diagnostic factors, pathogenesis, characteristics of lesions and drug factors for the poor response of anti-VEGF drugs to nAMD.

Keyword: Neovascular Age-Related Macular Degeneration; Poor Response ;Anti-VEGF; Review

1. Diagnostic factors

1.1 Pseudomorphic AMD

In clinical workup, there are still many diseases that present similarly to AMD. A retrospective study showed that most patients with nAMD who were considered to have poor morphologic response to anti-VEGF medication were diagnosed with non-AMD disease by ICGA. These include chronic central serous chorioretinopathy disease, adult - onset foveomacular vitelliform dystrophy (AFVD), and drusenoid retinal pigment epithelium detachment (dPED), intraretinal inflammatory granuloma, macular capillary dilation (Mactel type 1), and others.These diseases are disguised clinically or on imaging as nAMD. The most common misdiagnosis is AFVD, which is characterized by subretinal macular-like lesions with prolonged retinal pigment epithelium (RPE) atrophy and a domed shape on early OCT. The differential diagnosis of AFVD and nAMD is difficult, especially when AFVD is accompanied by pigment epithelial detachment (PED) and choroidal neovascularization (CNV).In addition, dPED is also an important factor in the diagnosis of nAMD, which is a group of diseases that are often treated clinically with unnecessary anti-VEGF drugs. The disease is characterized by clusters of vitreous warts on the retina bilaterally and a lobular appearance in the macular center on OCT. dPED is a degenerative lesion of the macula but can be found on FFA/ICGA with normal choroidal vessels and no neovascular blood flow signal. These pseudomorphic nAMDs are often considered to have a poor response or even no response after anti-VEGF drug treatment. Therefore, it is recommended to question the original diagnosis if there is a lack of response after the initial 3-month anti-VEGF drug loading phase. In early treatment, adequate imaging data and knowledge of the patient's general condition are necessary, especially in patients with nAMD in both eyes, to ensure a more accurate identification of the disease at the first diagnosis. Of course, at this stage there are still many difficult cases that can interfere with the diagnosis.

1.2 Defining the subtypes of nAMD

Based on the anatomical location of neovascularization and vascular composition determined by OCT, MNV was classified into three subtypes, type 1, type 2, and type 3. In this typing, polypoidal choroidal vasculopathy (PCV) was classified as type 1 MNV. The study demonstrated that MNV anatomical morphological differences and BCVA outcome phenotypes can predict visual acuity changes after anti-VEGF drug treatment in different nAMD subtypes. Further examination using ICGA after poor response to anti-VEGF drug therapy in type 1 MNV revealed mostly PCV, however, PCV usually requires combination therapy to produce a response. Although it is still debated whether PCV belongs to nAMD, if the subtype of nAMD can be clarified, there will be certainty in the treatment.

2. Aspects of pathogenesis

2.1 Genetic inheritance

Anti-VEGF drug therapy is currently the first-line treatment for nAMD, but the pathogenesis of AMD is still unclear. Recently, genetic inheritance has been found to appear to play a crucial role in the pathogenesis of AMD. Several studies have identified a link between genes and susceptibility to AMD. Complement factor H gene (CFH), LOC387715 gene (HTRA1/ARMS2), complement component 2 gene (CFB/C2), Apolipoprotein E gene(APOE) and other genes have been shown to exhibit AMD susceptibility. It has been suggested that genetic factors may influence the response of nAMD to anti-VEGF drug therapy.In a meta-analysis, Hu et al showed for the first time that the G allele of the ARMS2 mutation A69S in nAMD patients had a better response to anti-VEGF drug therapy, especially in the East Asian population, and suggested that A69S could be a predictor of anti-VEGF drug therapy.Park et al suggested that there is an association between the polymorphism rs11200638 in the HTRA1 gene and response to anti-VEGF drug therapy in nAMD.However, a Meta-analysis by Zhou et albased on extensive literature showed no association between this gene and anti-VEGF drug treatment response in nAMD. Although not uniform, more studies are needed to further corroborate. Patients with a pure allelic genotype (CC) at the CFH Y402H locus have been reported to show a poorer response to anti-VEGF drug therapy in the former compared to patients carrying heterozygotes (CT) and wild-type pure heterozygotes (TT). Currently genetic testing is not necessary for ophthalmic examinations, but is it possible to predict the efficacy of nAMD anti-VEGF drugs by examining gene expression in nAMD and thus clarify treatment options at an early stage or during the course of therapy. Of course, individualized gene therapy may also hold great promise in the future.

2.2 Immune factors and inflammatory involvement

In recent years, an increasing number of experimental and clinical studies have shown that AMD is closely related to autoimmune deficiencies, immune inflammatory attacks on self-tissues, and the involvement of inflammatory cytokines; RPE cells become dysfunctional and their metabolites are deposited under the basement membrane of RPE cells, eventually causing cellular swelling and degeneration. These degenerated RPE cells become local inflammatory stimuli, synthesizing components of the vitreous wart, such as inflammatory mediators and complement components, and thus driving the AMD process. After the administration of standardized anti-VEGF drugs, some patients can be found to show early therapeutic efficacy over time, with poor or no response with continued repeated anti-VEGF drug therapy and recovery of efficacy after a period of discontinuation of drug injection. It is speculated that during the long-term course of anti-VEGF drug therapy, the choroidal substances cannot be transported to the retina due to the persistence of IRF and SRF, resulting in retinal hypoxia and initiating mechanisms such as oxidative stress, which leads to insensitivity to anti-VEGF drugs. In addition, long-term chronic inflammation may cause permanent structural damage to the vascular wall of MNV, resulting in increased

neovascular permeability and continuous exudation, so that treatment with anti-VEGF drugs is also ineffective. Finally, inflammation increases the fibrosis of the lesion, which will also result in poor response and non-response to anti-VEGF drug therapy. While in one study ,Frazin found a patient injected with bevacizumab in one eye developed aseptic uveitis in both eyes after the injection, after which the patient developed rapid resistance to anti-VEGF drugs. Similar complications have been reported after anti-VEGF drug injections. In cognition, the pathogenesis and etiology of aseptic uveitis are not clear, but most scholars believe that immunity plays an important role in its pathogenesis. Therefore, it is speculated whether after receiving anti-VEGF drugs, the body opens the immune mechanism pathway, which in turn interferes with the therapeutic effect of anti-VEGF drugs. Therefore, in the future, anti-inflammatory and anti-fibrotic therapy and immunotherapy may provide a direction for refractory AMD.

3. Drug factors

3.1 Drug regimen

In the course of anti-VEGF drug therapy, it has been argued that sufficiently regular and active treatment is required to achieve large gains in visual acuity during the first year of treatment, and that a 3-shot loading dose at the beginning of treatment in particular is essential. In actual clinical work, patients with nAMD have suffered from inadequate doses and insufficient frequency of administration in early treatment due to inconvenient follow-up and economic pressures, leading to interruptions in AMD treatment and subsequent poor response to anti-VEGF drug therapy. A study monitoring the treatment with two consecutive injections of anti-VEGF drugs found that for patients who responded poorly to anti-VEGF drug therapy, the regression of retinal fluid during the post-injection period occurred mostly in the second week after the injection, and the changes in retinal IRF/SRF fluctuated more after the injection. Therefore, the choice of the follow-up injection protocol may influence the occurrence of poor response in some patients. Of course, there is still no consensus on the length of time to determine the response. And the current anti-VEGF drug regimen includes a loading dose series of 3 consecutive months with 1 injection per month, pro re nata (PRN) or treatment and prolongation strategies. The majority of people in China are still predominantly treated with continuous 3-month loading doses with a minimum injection interval of 4 weeks. However, in foreign studies evaluating patients with nAMD who had a poor response to anti-VEGF drug therapy and were given anti-VEGF drug injections every 2 weeks, significant improvements in visual acuity and macular thickness were found in some patients.These studies also seem to suggest that high frequency of treatment may be required to achieve response in the early stages of poor response to anti-VEGF therapy. In addition, some repetors retrospectively evaluated nAMD patients with poor response to anti-VEGF therapy and found significant improvements in macular thickness when given high doses of 4 mg of abcixima. At the same time, a retrospective population-based cohort study showed that intravitreal injection of anti-VEGF drugs for nAMD was not associated with a sustained increased risk of stroke, myocardial infarction or death.

3.2 Antagonizing anti-VEGF antibody production

Ranibizumab is a human-derived monoclonal antibody that has been maximally humanized but remains immunogenic to the body and initiates the production of antibodies by the body's immune system to neutralize it. In a multicenter, double-blind, 2-year study of ranibizumab for nAMD in the Philip J study, the investigators found that serum antibodies antagonizing ranibizumab tended to increase over time in all three groups of subjects after injection, with a 0.3 mg ranibizumab group, a 0.5 mg ranibizumab group, and a sham injection group at baseline, respectively. The immune response rates were 0.9%, 0%, and 0.5% in the 0.3 mg razumab, 0.5 mg razumab, and sham injection groups, respectively, at baseline. However, by 24 months, the 0.3 mg and 0.5 mg groups had rise 4.4% and 6.3%, respectively, while the sham injection group

had only 1.1%. However, it is still debatable whether the production of antagonistic anti-VEGF antibodies affects the efficacy of nAMD response to anti-VEGF drugs.

References

[1] Song P, Du Y, Chan KY, et al.The national and subnational prevalence and burden of age-related macular degeneration in China[J].J Glob Health, 2017, 7(2):020703.

[2] De Jong PT. Age-related macular degeneration[J]. N Engl J Med, 2006, 355(14): 1474-1485.

The Application of Echocardiography in the Diagnosis of Heart Disease

Qiushan Qing, Xin Wei, Hong Zheng, Peirui Chen
Department of ultrasonography, People's Hospital of Deyangcity, Deyang 618001, China.

Abstract: Objective: To explore the application value of echocardiography in the diagnosis of hypertension-related heart disease. Methods: 88 suspected hypertension-related heart disease patients admitted to our hospital from January 2022 to February 2023 were randomly divided into a control group (n=44) and a study group (n=44) using a random number table. The control group underwent routine electrocardiogram examination, while the study group underwent echocardiography examination. The diagnostic detection rates, sensitivity, specificity, missed diagnosis rate, and misdiagnosis rate of the two examination methods were compared. Results: The detection rates of left ventricular hypertrophy, left atrial enlargement, myocardial ischemia, aortic dilation, and diffuse interventricular septal thickening in the study group were 81.82%, 88.64%, 47.73%, 79.55%, and 90.91%, respectively. In the control group, the detection rates of left ventricular hypertrophy, left atrial enlargement, myocardial ischemia, aortic dilation, and diffuse interventricular septal thickening were 61.36%, 40.91%, 29.55%, 31.82%, and 63.64%, respectively. The detection rates in the study group were significantly higher than those in the control group, and the differences were statistically significant ($P<0.05$). The sensitivity and specificity of echocardiography in diagnosing hypertension-related heart disease were higher than those of routine electrocardiography, and the missed diagnosis rate and misdiagnosis rate were lower than those of routine electrocardiography ($P<0.05$).

Conclusion: The application of echocardiography in the diagnosis of hypertension-related heart disease can effectively improve the accuracy, sensitivity, and specificity of diagnosis, reduce the missed diagnosis rate and misdiagnosis rate, and provide a reliable reference for the formulation of clinical treatment plans. It has a high application value.

Keywords: Echocardiography; Hypertension-Related Heart Disease; Diagnostic Value; Cardiac Function

Introduction

Echocardiography, also known as cardiac ultrasound, is a non-invasive imaging technique that uses high-frequency sound waves to produce images of the heart. It has become an important tool in the diagnosis of various heart diseases. Echocardiography can provide information about the size, shape, and function of the heart, as well as the movement of the heart valves and blood flow through the heart. It can also detect abnormalities such as congenital heart defects, valve disorders, and heart muscle diseases. Compared to other imaging techniques such as computed tomography (CT) and magnetic resonance imaging (MRI), echocardiography is relatively inexpensive and does not involve exposure to ionizing radiation. It can be performed in real-time, allowing the physician to observe the heart in motion. Overall, echocardiography has a high sensitivity and specificity for detecting heart disease. It is particularly useful in detecting left ventricular hypertrophy, left atrial enlargement, and aortic dilation. Additionally, echocardiography can be used to monitor the progression of heart disease and to evaluate the effectiveness of treatments.

1. Materials and Methods

1.1 General Information

88 suspected hypertensive heart disease patients admitted to our hospital from January 2022 to February 2023 were selected as the study population. Patients with a history of coronary artery bypass surgery, myocardial infarction, and mental disorders were excluded. The 88 patients were randomly divided into a control group (n=44) and a study group (n=44). The male-to-female ratio in the control group was 29/15, with an age range of 39-75 years (54.63 ± 4.57) and a BMI index ranging from 12.83-20.46 kg/m2. The male-to-female ratio in the study group was 26/18, with an age range of 40-73 years (54.79 ± 5.03) and a BMI index ranging from 13.16-21.37 kg/m2. There were no significant differences in baseline data such as gender and age between the two groups ($P > 0.05$), indicating comparability.

1.2 Methods

The control group underwent a routine electrocardiogram (ECG) examination using a Nihon Kohden 91300 device from Kenz, Japan. Patients were guided to lie on their backs during the examination, and a 12-lead ECG was performed after the equipment was calibrated. The study group underwent color Doppler echocardiography examination using a GE Vivid E9 device. The ultrasound probe frequency was set between 2 and 4.0 MHz, and patients were guided to maintain a supine position during the examination. Multiple angles were scanned starting from the left sternal edge, and the four-chamber and five-chamber apical views of the heart and the left ventricular long-axis view were carefully observed. The left ventricular wall thickness, interventricular septal thickness, and internal diameters of the aorta, left atrium, and left ventricle were recorded in detail. Both groups of patients were examined by an experienced specialist physician.

1.3 Observation indicators

The detection rates of left ventricular hypertrophy, left atrial enlargement, myocardial ischemia, aortic dilation, and diffuse interventricular septal thickening were compared between the two groups. The sensitivity, specificity, missed diagnosis rate, and misdiagnosis rate of the two examination methods were analyzed.

1.4 Statistical analysis

Measurement data were expressed as ($x \pm s$), and t-tests were used for between-group mean comparisons. Count data were expressed as frequency (n) or composition ratio (%), and the chi-square test was used for comparisons. Data analysis was conducted using SPSS 22.0 statistical software, with $P < 0.05$ indicating statistical significance.

2. Results

2.1 Comparison of the detection rates of left ventricular hypertrophy and left atrial enlargement between the two groups

The detection rates of left ventricular hypertrophy, left atrial enlargement, myocardial ischemia, aortic dilation, and diffuse interventricular septal thickening were significantly higher in the study group than in the control group, and the differences were statistically significant ($P < 0.05$). See Table 1 for details.

Table 1 Comparison of the detection rates of left ventricular hypertrophy and left atrial enlargement between the two groups (n, %)

Group	Number of cases	LV hypertrophy	LA enlargement	myocardial ischemia	aortic dilatation	diffuse thickening of the interventricular septum
Research	44	36(81. 82)	39(88. 64)	21(47. 73)	35(79. 55)	40(90. 91)
control	44	27(61. 36)	18(40. 91)	13(29. 55)	14(31. 82)	28(63. 64)

2.2 Comparison of sensitivity, specificity, missed diagnosis rate, and misdiagnosis rate between the two diagnostic methods

The sensitivity and specificity of echocardiography in diagnosing hypertensive heart disease were both higher than those of conventional electrocardiography, and the missed diagnosis rate and misdiagnosis rate were lower than those of conventional electrocardiography ($P < 0.05$). See Table 2 for details.

Table 2. Comparison of sensitivity, specificity, missed diagnosis rate, and misdiagnosis rate between the two diagnostic methods (n, %).

Examination Method	Number of cases	Sensitivity	Specificity	Missed Diagnosis Rate	Misdiagnosis Rate
Echocardiography Conventional	44	95. 00(38 /40)	75. 00(3 /4)	5. 00(2 /40)	25. 00(1 /4)
Electrocardiography	44	65. 79(25 /38)	50. 00(3 /6)	34. 21(13 /38)	33. 33(2 /6)

3. Discussion

Hypertensive heart disease is mostly caused by long-term high blood pressure, which leads to increasing left ventricular load. Echocardiography, with its high-resolution advantage, can clearly display soft tissue organs in the human body, providing assurance for obtaining precise left ventricular imaging quality and ensuring the reliability and accuracy of results for examining wall thickening and chamber enlargement. Myocardial load changes are an early response to hypertensive heart disease, initially manifested by an increase in systolic wall stress, but wall thickening stress can show a decrease during overcompensation. Therefore, for ordinary hypertensive heart disease patients, the presence of wall thickening does not necessarily indicate good systolic wall function. During echocardiography, peak stress, left ventricular end-systolic and end-diastolic volume, peak velocity ratio, left ventricular ejection fraction, and end-systolic wall stress are key parameters for diagnosing systolic heart function. However, some studies have shown that compared to peak stress, left ventricular end-systolic and end-diastolic volume and peak velocity ratio can more intuitively reflect a patient's systolic heart function, while end-systolic wall stress generally shows a negative correlation with left ventricular shortening fraction. Most hypertensive heart disease patients have an increased afterload, which is generally accompanied by increased systolic pressure and decreased left ventricular shortening fraction. The results of this study showed that the detection rates of left ventricular hypertrophy, left atrial enlargement, myocardial ischemia, aortic dilation, and diffuse interventricular septal thickening were significantly higher in the study group than in the control group, with statistically significant differences ($P <0.05$); the sensitivity and specificity of echocardiography in diagnosing hypertensive heart disease were higher than those of conventional electrocardiography, and the missed diagnosis rate and misdiagnosis rate were lower than those of conventional electrocardiography ($P <0.05$). This suggests that echocardiography can effectively determine whether a patient's heart function indicators are abnormally expressed and then make a clear diagnosis. This is due to several advantages of echocardiography in diagnosing hypertensive heart disease: (1) this examination can be performed under zero radiation, painless, and non-invasive conditions, and can clearly display the patient's left ventricular diastolic and systolic

function, left heart structure, blood flow status, etc.; (2) echocardiography has ultra-high resolution for soft tissue structures in the human body, which can clearly display the patient's body tissue and cardiac section, and can repeatedly investigate the progress of the disease, making it an important means to diagnose hypertensive heart disease and assess prognosis in real-time; (3) through the observation of the patient's echocardiographic imaging results, it is convenient for the examiner to calculate the left ventricular diastolic function index data, which more accurately and clearly reflects the changes in heart disease. In summary, the application of echocardiography in diagnosing hypertensive heart disease can effectively improve diagnostic accuracy, sensitivity, specificity, and reduce missed diagnosis and misdiagnosis rates, and is worth promoting widely.

References

[1] Li Y, Tang J. Application value and detection rate of echocardiography in the diagnosis of hypertensive heart disease. China Medical Guide, 2023, 21(07):99-101.

[2] Yang L. Application of color Doppler echocardiography in the diagnosis of adult congenital heart disease. Imaging Research and Medical Applications, 2023, 7(05):122-124.

[3] Cao Y. Comparison of diagnostic effects of echocardiography and electrocardiography in hypertensive heart disease. Primary Medical Forum, 2023, 27(05):67-69.

[4] Cai L. Clinical application of color Doppler echocardiography in the diagnosis of hypertensive heart disease. Imaging Research and Medical Applications, 2023, 7(02):80-82.

[5] Wang S. Application of real-time 3D echocardiography in the diagnosis of rheumatic mitral stenosis. Journal of Shandong Medical College, 2022, 44(05):350-351.

Effect of CASQ1 Protein Sequence Variants on Ca2+ Binding Ability

Lin Wang
University of Leeds, Leeds LS2 9JT, UK.

Abstract: Malignant hyperthermia (MH) is generally observed in people susceptible to volatile anesthetics, usually due to abnormalities in ryanodine receptor 1 (RYR1) leading to Ca^{2+} dysregulation in the sarcoplasmic reticulum (SR). CASQ1, a Ca^{2+} binding protein believed to be in the SR, also plays a regulatory role in RYR1. It has been hypothesized that mutations in CASQ1 protein may increase susceptibility to MH cases. We used the CASQ1 p.F186Y and p.I138T variants to compare Ca^{2+} binding ability with CASQ1 WT. It showed that CASQ1 F and I variants have reduced Ca^{2+} binding ability compared to CASQ1 WT.

Keywords: Microscale Thermophoresis; Ni-NTA Chromatography

1. Introduction

Malignant hyperthermia (MH) is a skeletal muscle-related genetic disorder. MH is known to be associated with uncontrolled elevation of sarcoplasmic Ca^{2+}, usually manifested by abnormalities in ryanodine receptor 1 (RYR1), uncontrolled regulation of Ca^{2+} by the sarcoplasmic reticulum (SR) in skeletal muscle, resulting in elevated sarcoplasmic Ca^{2+}, massive ATP depletion harmful to muscle membranes, and worse, life-threatening rhabdomyolysis and hyperkalemia [1].

20–30% of MH patients still do not have the RYR1 mutation, despite the fact that this gene is linked to a significant share of MH patients. Calsequestrin-1 (CASQ1), on the other hand, is an acidic protein with a molecular weight of roughly 45 kDa that is found in the SR, and its possession of glutamate and aspartate residues confers the ability to bind Ca^{2+} [2]. In fact, it has been demonstrated in further studies that CASQ1 inhibits the activity of RYR1 in the presence of junctin and triadin proteins at a low Ca^{2+} concentration of 20 μM [3]. Therefore, CASQ1 becomes one of the possible genes that play a role in MH.

Therefore, our aim in this experiment was to compare the CASQ1 p.F186Y and p.I138T variants with CASQ1 WT, and compare the binding ability of the variants with Ca^{2+} by microscale thermophoresis. Thus, the mechanism of the interaction between CASQ1 protein and MH can be better understood.

2. Methods

2.1 Induced expression of CASQ1 proteins

Small-scale expression: The single colony was picked and inoculated in 2 ml of LB media containing ampicillin at 100 μg/ml. This culture was placed in an orbital incubator (Max Q 6000) and incubated overnight at 37°C with shaking at 220 rpm. The next day, 200 μl of culture was added to LB media and incubated for 2.5 hours. Added 400 μl of autoclaved glycerol 50% (v/v), snap-freeze in liquid nitrogen, and stored at -80°C.

Large-scale expression: A stock was inoculated in 4 ml of LB medium and incubated overnight at 37 °C with shaking. The next day, the overnight culture was poured into 400 ml of 2YT medium and the culture was incubated at 37 °C with shaking until the optical density reached 0.6-0.8 at 600 nm (OD600). IPTG was added to a final concentration of 0.4 mM, then the remaining culture was incubated overnight at 18 °C. The next day, the culture was transferred to a centrifuge bottle, weight equilibrated, and centrifuged at 4000g for 30 min at 5 °C. The supernatant was discarded and the cell pellet was stored at -20 °C.

2.2 Nickel affinity chromatography

AKTA Pure FPLC system (GE Healthcare) and HisTrap HP 1 ml column (GE Healthcare) were applied in Ni-NTA chromatography. The AKTA system and column were pre-equilibrated with the low salt His-A buffer (0.02M Na H_2 phosphate pH8.0; 0.5M NaCl; 10mM imidazole). The soluble fraction was loaded onto a column using a peristaltic pump, off-line at a rate of 1 ml/min. Next, the column was washed with resuspension buffer. Wash the column with low salt His-A buffer and high salt His-B buffer (0.02 M Na H_2 phosphate pH 8.0; 0.5 M NaCl; 0.5 M imidazole), and then again with His-A buffer. Bound proteins were eluted with increasing gradients of imidazole concentration, and the elution was recorded by absorbance at 280 nm. The fractions showing a peak of absorbance at 280 nm were analyzed by SDS-PAGE.

2.3 Microscale thermophoresis

The purified protein was incubated with 3X molar excess of fluorescein isothiocyanate (FITC) on ice for 1 h. The excess FITC was removed with a NAP-5 column, and the labelled protein was eluted into A buffer (50 mM Tris pH 7.5, 150 mM NaCl), then the proteins were aspirated with NT.115 standard treated capillaries and scanned with green LED at 20% power and fluorescence values were recorded. Diluted B buffer (50 mM Tris pH7.5, 150 mM NaCl, 100 mM $CaCl_2$) in A buffer and mixed 1:1 with labelled protein and incubated for 10 min at room temperature. Protein samples were mixed 1:1 with A buffer as a control. MST was performed at MST 20% power and repeated 5 times.Graphs were made using GraphPad Prism.

3. Result

3.1 Ni-NTA Chromatography Purification of CASQ1 WT and variant proteins

To study Ca^{2+} binding ability, the CASQ1 protein was purified. The absorbance at 280 nm was monitored. The sample applied to the column caused an increase in the absorbance (Figure 1a、c、e). Selected fractions within the elution peaks were subjected to SDS-PAGE (Figure 1b、d、f).

In Figures 1a, c and e, we can see the presence of a very distinct blue peak in the range of 10-20 ml, representing the elution of CASQ1 protein. Subsequently, 9 elution fractions of CASQ1 WT (Figure 1b) were subjected to SDS-PAGE experiments, among which E4-E7 had bands apparently at the same position, and E5 had the widest and deepest band, associated with a molecular weight between 50 kDa and 60 kDa, which has been marked with a blue arrow. CASQ1 I (Figure 1d), E31 and E32 have the widest and deepest bands. CASQ1 F (Figure 1f), E14 and E15 have the widest and deepest bands.

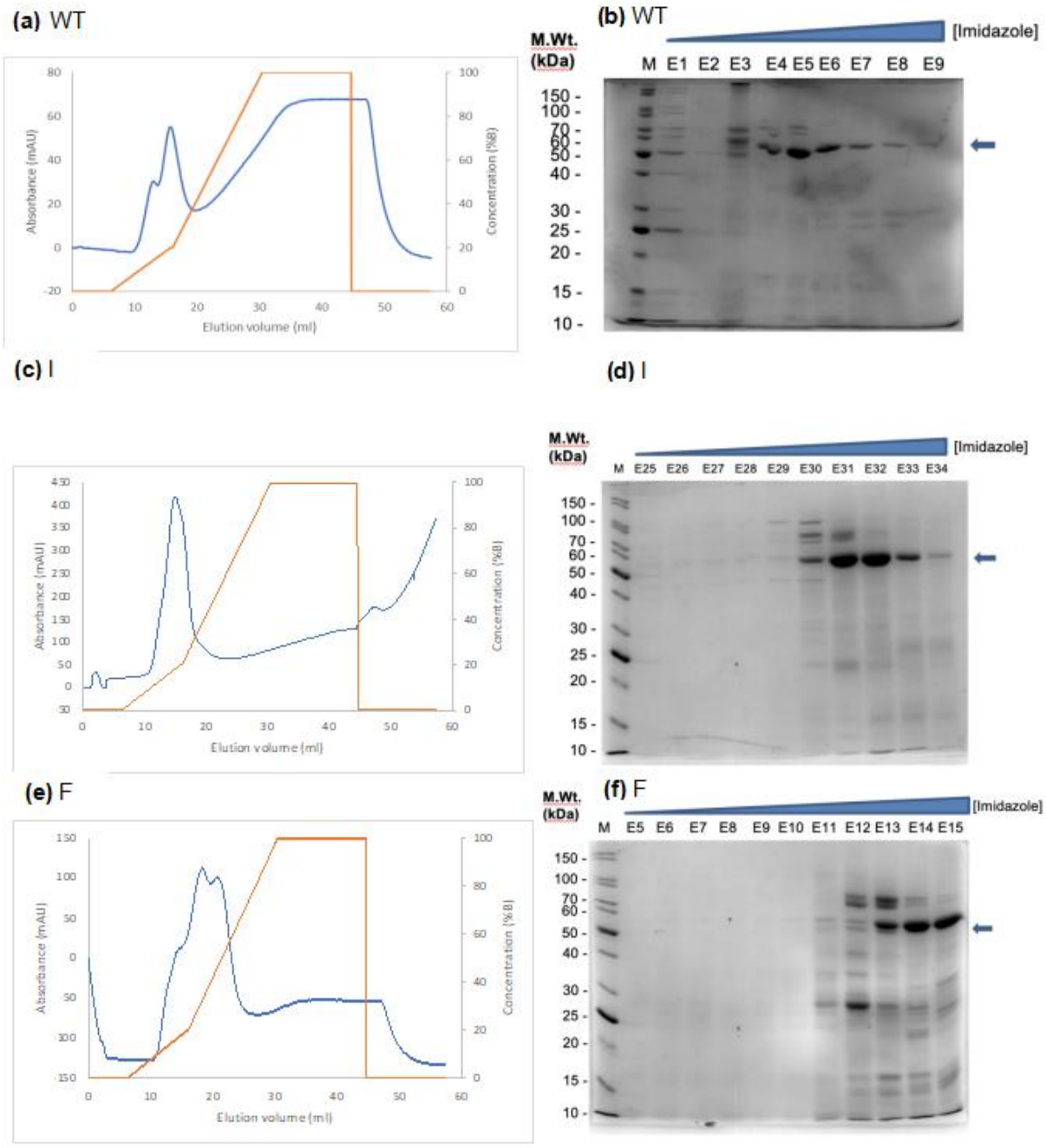

Figure 1: Ni-NTA chromatogram and SDS-PAGE analysis of CASQ1 proteins.

The absorbance at 280 nm (blue line) of eluted CASQ1 WT (a), CASQ1 I (c) and CASQ1 F (e) was measured in milli absorbance units (mAU). The concentration of elution buffer is shown by an orange line. The horizontal coordinate is the value of elution volume in ml. CASQ1 WT、I、F (Figure 1b、 d、f) proteins were subjected to SDS-PAGE. Lane 1 (M) indicates the unstained protein standard (NEB), and the molecular weight is noted on the leftmost side in kDa. The remaining lanes show the fraction of peak absorbance at 280 nm. The blue arrow represents the band matching the CASQ1 protein, blue triangle means the increase of imidazole concentration.

3.2 Microscale thermophoresis of CASQ1 WT and variant proteins

We investigated the Ca^{2+} binding ability of CASQ1 protein using microscale thermophoresis. Firstly, we labeled CASQ1 WT protein with FITC at a ratio of 1:3 with a series of Ca^{2+} concentrations. Because the higher the power of MST, the more the density and convective flow of the sample are affected, which may produce abnormal MST traces [4]. Therefore, we chose 20% power for MST experiments on CASQ1 proteins (shown in Figure 2a、b、c). However, when the Ca^{2+} concentration was at 0.1-0.4 mM, the fluorescence signal seems to be abnormal, and this phenomenon occurs in several replications, which cannot be excluded as the cause of the machine, so we did not analyze this concentration range. The fluorescence signal of CASQ1 WT protein showed an increasing tendency between Ca^{2+} concentrations of 3 mM-50 mM when the MST power was 20%. The fluorescence signal changes of CASQ1 I and F were similar to CASQ1 WT, both with an upward trend.

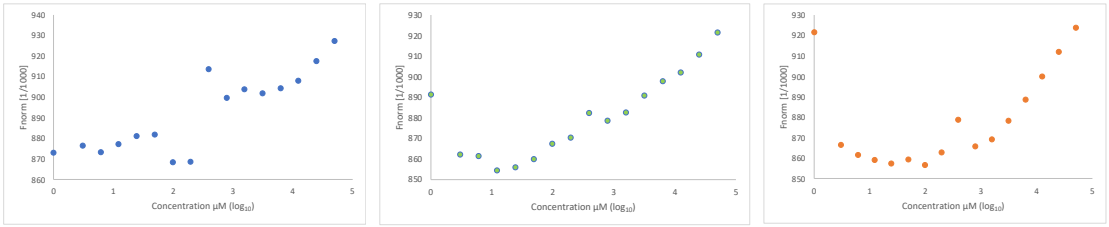

(a) **(b)** **(c)**

Figure 2: MST of CASQ1 WT (a)、I (b) and F (c) at 20% MST power.

Blue dots represent the fluorescence signal of CASQ1 WT at different Ca2+ concentrations converted to log10 in μM; green dots stand for CASQ1 I protein; orange dots indicate CASQ1 F protein. The Fnorm are shown in 1/1000 of the value.

In order to investigate the affinity of CASQ1 protein to Ca2+ binding, we performed 5 replicate MST and then calculated the average of dissociation constant (shown in Table 1). From the average of the dissociation constant, CASQ1 F protein has the highest value and CASQ1 WT protein has the lowest value. Therefore, we concluded that the CASQ1 WT protein has the highest affinity for binding Ca2+, followed by CASQ1 I. CASQ1 F has the lowest affinity.

Table 1: MST data summary table.

	CASQ1 WT	CASQ1 I	CASQ1 F
Replicate 1	1890	not fitted	not fitted
Replicate 2	not fitted	not fitted	2720
Replicate 3	not fitted	1370	2370
Replicate 4	563	4720	not fitted
Replicate 5	1910	3400	7670
Average	1454.3	3163.3	4253.3

CASQ1 WT, I and F proteins are summarized in MST replicate experiments of the dissociation constant, with the average calculated, and nonsignificant values have been labelled as not fitted.

4. Discussion

The CASQ1 proteins after IPTG induction and centrifugation were purified by Ni-NTA chromatography (shown in Figure 1). In the Nickel affinity chromatogram, we could observe the presence of single or double peaks for each protein, corresponding to molecular weights between 50 kDa- 60 kDa, which may represent our expected CASQ1 protein. The expected molecular weight (MW) of the CASQ1 protein was around 45 kDa, but the results were not as expected, probably because the acidic residues in the CASQ1 protein repel the negative charges contained in SDS, which affects the normal

electrophoretic migration [5]. Subsequently, we analyzed the Ca^{2+} binding ability of CASQ1 proteins using MST instrument. However, both CASQ1 I and F proteins appear to have reduced Ca^{2+} binding ability compared to CASQ1 WT. In the study by Kumar et al[6], Ca^{2+} binding sites in CASQ1 WT proteins have been identified with different affinities. There are also some Ca^{2+}-dependent high-affinity sites, and these sites show higher affinity with increasing Ca^{2+} concentration. Therefore, the reduced Ca^{2+} binding capacity of CASQ1 I and F variant proteins may be due to altered Ca^{2+}-dependent high-affinity sites. The conclusion that the binding capacity of CASQ1 I and F variant proteins to Ca^{2+} were reduced in our experiments is consistent with previous reports [7], but no conclusions were drawn about the strength of the affinity between CASQ1 I and F variant in Dodds' experiments, while she performed only twice MST experiments, and the data analysis was based on average values. The number of experimental repetitions was too few and the data support for the conclusion was weak. Although we still need to further explore the effects of CASQ1 I and CASQ1 F variants in terms of Ca^{2+} release at a later stage, it is reasonable to speculate that the reduced ability of the CASQ1 variant protein to polymerize has an effect on RYR1 and may lead to Ca^{2+} dysregulation as a potential aetiology of MH.

References

[1] Kim, D.-C. Malignant hyperthermia. Korean J Anesthesiol 63, 391–401 (2012).

[2] MacLennan, D. H. & Wong, P. T. S. Isolation of a Calcium-Sequestering Protein from Sarcoplasmic Reticulum. Proc Natl Acad Sci U S A 68, 1231–1235 (1971).

[3] Györke, I., Hester, N., Jones, L. R. & Györke, S. The role of calsequestrin, triadin, and junctin in conferring cardiac ryanodine receptor responsiveness to luminal calcium. Biophys J 86, 2121–2128 (2004).

[4] Rainard, J. M., Pandarakalam, G. C. & McElroy, S. P. Using Microscale Thermophoresis to Characterize Hits from High-Throughput Screening: A European Lead Factory Perspective. SLAS Discov 23, 225–241 (2018).

[5] Graceffa, P., Jancsó, A. & Mabuchi, K. Modification of acidic residues normalizes sodium dodecyl sulfate-polyacrylamide gel electrophoresis of caldesmon and other proteins that migrate anomalously. Arch Biochem Biophys 297, 46–51 (1992).

[6] Kumar, A. et al. Identification of calcium binding sites on calsequestrin 1 and their implications for polymerization. Mol Biosyst 9, 1949–1957 (2013).

[7] Dodds, R. E. Defining molecular mechanisms of calcium dysregulation in malignant hyperthermia susceptibility. (University of Leeds, 2019).

A Forecasting Analysis of Health Technicians Demand in Hainan Province based on Several Combination Forecasting Models*

Shihong Wang, Lianhua Liu
International School of Public Health and One Health, Hainan Medical University, Haikou 571199, China.

Abstract: **Objective:**Several combination models were used to forecast the demand for health technicians in Hainan Province in order to find the best combination of forecasting models and thus provide the relevant departments with a more scientific basis for their planning. **Methods:**First using ARIMA method, GM(1,1) method and trend extrapolation method to establish single forecasting models, and then based on single models, adopt equal weight method , reciprocal errors method ,odds-matrix method and artificial neural networks method to establish four kinds of combination forecasting models, finally evaluate all the prediction models and select the best model to make a short -term forecasting. **Results:**The combined forecasting model generally has a lower forecasting error than the single forecasting model. The combined artificial neural network model has the lowest forecasting error and is the relatively optimal model for forecasting health technicians. It is predicted that the demand for health technicians in Hainan Province will increase steadily from 2021 to 2023. **Conclusion:**The demand for health technicians in Hainan Province is still high, and training efforts should be further strengthened to lay a solid foundation of health care for the construction of the Hainan Free Trade Port.

Keywords: HealthTechnician; Combination Forecasting Model; Hainan

1. Introduction

As the first resource in health resources, health human resources are the key to protecting the health of citizens and promoting the healthy development of health services. Health technicians are the most important representative of health human resources, and the number of health technicians is an important indicator to measure the level of public health and medical services in a region[1]. In recent years, with the establishment of the Bo'ao Le Cheng Medical Pilot Zone and the construction of the Free Trade Port in Hainan Province, the number of migrants is increasing year by year, and the demand for medical and health services is also increasing. Therefore, it is of great importance to establish a scientific and reasonable prediction model of the number of health technicians for the rational allocation of health human resources in Hainan Province and even to guarantee the construction of the free trade port.

The issue of forecasting for health technicians has been a hot topic of research in recent years. Many researchers have used single forecasting models such as gray neural network model, ARIMA model, and gray GM(1,1) model to forecast the demand of health technicians in various provinces and cities[2-5]. However, single prediction model contains only part of the information of the predicted object, and the accuracy and stability of the prediction results are poor, while combining each single prediction model by certain rules can contain more comprehensive information of the original data,thus further improving the accuracy and stability of the prediction [6]. Therefore,many researchers have started to apply Combination Models for prediction[7-9]. However, many of these researchers have only used a certain combination of models, and most of them are linear combinations. But there are many kinds of combination prediction methods, the common ones are linear

combination methods such as equal weight method, minimum variance method, error inverse method, dominance matrix method, etc. There are also non-linear combination methods such as artificial neural network, weighted harmonic average, etc. And the prediction accuracy of different combination methods will also be different.

Therefore, this study first used the data of health technicians in Hainan Province from 2005 to 2020 to establishing three single prediction models, and then used four combined methods to establish combination prediction models. Finally, the error evaluation of all the prediction models was conducted, and the best model was selected to make a short-term prediction of the needs of health technicians in Hainan Province, in order to provide a more accurate and reliable decision-making basis for the government and health administration departments to allocate health resources.

2. Materials and methods

The data of health technicians were derived from the Statistical Yearbook of Hainan Province from 2005 to 2020.Based on the data , three single prediction methods: ARIMA, GM (1,1), and trend extrapolation method were established[10-12]. and then four combined forecasting models were established based on the single model using equal weight method, error inverse method, dominance matrix method, and artificial neural network method,and finally three forecasting accuracy evaluation indexes, MSE, MAE, and MAPE were used to evaluate the accuracy of all the prediction models.

2.1 Combination models

Combined model with equal weighting method is the simplest combined prediction method, that is, to assign the same weight to each single prediction model for linear combination [6]. For example, if there are three single prediction models, each single model has a weight of 1/3 in the combined model, and although the combined model with equal weights is simple to operate, the prediction accuracy is often higher than that of many complex combined models,This phenomenon has been regarded as the "combined prediction puzzle"[13].

The error reciprocal method is to give different weights to each single prediction model according to the error size of each single prediction model. The smaller the single prediction model error is, the larger the weight in the combined model is. For example, there are three single models, and Q_i is the sum of error squares of the ith single prediction model, so the weight of the ith single model in the combined model is: $w_i = \frac{1}{Q_i} \Big/ \sum_{i=1}^{3} \frac{1}{Q_i} \quad (i = 1,2,3)$.

The dominance matrix method is to assign weights according to the prediction accuracy of each single prediction method in each sample[14]. For example, A, B and C represent three single prediction models, n_A represents the times that error of model A is smaller than model B and C in the whole sample set, and n_B and n_C follow similar definition.s. The allocation rules of the weigh of A, B and C in the combined model is as follows:

$$w_A = \frac{n_A}{n_A + n_B + n_C}, w_B = \frac{n_B}{n_A + n_B + n_C}, w_C = \frac{n_C}{n_A + n_B + n_C}$$

Artificial neural network is a mathematical model similar to the structure of neural synaptic connections in the brain. Artificial neural network combination is a nonlinear combination method that is capable of learning a highly nonlinear mapping relationship between input and output data.

With one hidden layer, the prediction results of three single prediction methods are used as the network input layer, the

actual value as the output layer. The weights are learned by forward and back propagation to determine the weights of the neurons in each layer. Finally, the trained model is used for prediction[15].

2.2 Evaluation index

Evaluating the accuracy and reliability of prediction results is an important part of prediction analysis. and several evaluation indicators are commonly used to evaluate the prediction results, while using only one error evaluation index to evaluate the model is not reliable enough. The commonly used evaluation indexes are calculated as follows:

$$MSE = \frac{1}{n}\sum_{i=1}^{n}\left(\hat{y}_i - y_i\right)^2$$

$$MAE = \frac{1}{n}\sum_{i=1}^{n}|\hat{y}_i - y_i|$$

$$MAPE = \frac{100\%}{n}\sum_{i=1}^{n}\left|\frac{\hat{y}_i - y_i}{y_i}\right|$$

In the above equation, $\hat{y}_i$ is the predicted value, and y_i is the actual value.

3. Results

3.1 Current status of the number of health technicians

During 2005-2020, the number of health technicians in Hainan Province increased from 30,056 to 74,378 (Table 1), with an average annual growth rate of 6.20% and an average annual growth of 2,770 people.

Table 1. Raw data and predicted values of health technicians in Hainan Province from 2005 to 2020

Year	Health technicians	Three single prediction methods			Four combined prediction methods			
		ARIMA	GM(1,1)	trend extrapolation	equal weight	error reciprocal	dominance matrix	artificial neural network
2005	30056	30049	30056	29229	29778	29728	29898	29905
2006	30787	30813	31010	31078	30967	31003	30949	30814
2007	32545	32496	32972	33045	32838	32918	32807	32445
2008	33875	34566	35058	35138	34921	35004	34889	34588
2009	37857	36057	37277	37364	36899	37099	36836	37329
2010	39520	41781	39636	39732	40383	40047	40458	39684
2011	43295	43237	42144	42250	42544	42376	42574	42697
2012	44720	45284	44811	44926	45007	44939	45010	45373
2013	48192	47721	47647	47768	47712	47708	47697	47943
2014	50557	49843	50662	50785	50430	50568	50378	50752
2015	54677	54590	53868	53984	54147	54039	54160	54481
2016	57784	58034	57276	57375	57562	57447	57579	57786
2017	60579	62313	60901	60964	61393	61172	61442	60758
2018	63663	62445	64755	64761	63987	64355	63890	63441
2019	67695	66507	68853	68773	68044	68413	67958	67877
2020	74378	72095	73210	73008	72771	72936	72754	74306

3.2 Single prediction model

R4.1.0 was used for establishing the ARIMA model of health technicians. By ADF test, white noise test and model order, The optimal model is ARIMA (1,3,0). The model equation is $\nabla^3 x_t = -0.88\nabla^3 x_{t-1} + \varepsilon_t$.

Base on MATLAB7.0, GM (1,1) model of health technicians was fitted and the accuracy rating was evaluated(Table 2). With C value<0.35 and P value=1, indicate that the GM (1,1) model had a good fitting accuracy.

Table 2. The GM (1,1) model of health technicians

Index	GM(1,1)	a	μ	C	P	Evaluation results
health technicians	$x^{(1)}(k+1) = 500451.17e^{0.06k} - 470395.17$	-0.06	28223.7	0.03	1	Good

Trend extrapolation models such as linear, quadratic, cubic, logarithmic, exponential, and composite functions were fitted to the health technician data using SPSS 20.0. Among the models, the cubic function had the best effect (Table 3), and R^2 of the model was above 0.99, indicating that the trend extrapolation model is reliable and significant (P<0.05).

Table 3. Trend extrapolation model for health technicians

Index	F value	P value	R^2	Model
health technicians	1241.5	<0.001	0.997	$y = 27487.80+1688.96t+50.45t^2+1.36t^3$

3.3 Combined prediction models

based on three single prediction models, three weight assignment methods:equal weight method, error inverse method and dominance matrix method, were used to establish linear combination models (Table 4) , and also used artificial neural network method to establish nonlinear combination model. y_{1t}, y_{2t}, y_{3t} represent the predicted value of three single predicted models in t year respectively, and y_t represents the predicted value of the combined model.

Table 4. Three linear combined models

Combined models	weight of ARIMA	weight of GM（1,1）	weight of trend extrapolation model	Combined models
Equal weight method	1/3	1/3	1/3	$y_t = 1/3*y_{1t} + 1/3*y_{2t} + 1/3*y_3$
Error reciprocal method	0.174	0.431	0.395	$y_t = 0.174y_{1t} + 0.431y_{2t} + 0.395y$
Dominance matrix method	6/16	7/16	3/16	$y_t = 6/16*y_{1t} + 7/16*y_{2t} + 3/16*y$

3.4 Comparison of prediction results

The prediction values of each single prediction model and combined prediction model are shown in Table 1.The

prediction effects are shown in Table 5.The results show that among the three single prediction models, the GM (1,1) model has the smallest prediction error, followed by the trend extrapolation models. The error of the combined prediction models was generally smaller than the single prediction model, and the artificial neural network combined model has the smallest error among all the combined models. Many researchers have also proved that the combination prediction method of artificial neural network has a higher prediction accuracy[16], so we finally choose combination model of artificial neural network as the short-term prediction model for health technicians in Hainan Province.

Table 5 Comparison of the effects of the different prediction models

	MAE	MAPE	MSE
ARIMA	837.52	1.67	1316862
GM（1,1）	592.34	1.21	533562
trend extropolation	657.63	1.42	581721
Equal weight combination	569.29	1.23	477887
Error reciprocal combination	586.44	1.25	468288
dominance matrix combination	558.70	1.20	485287
Artificial neural network combination	**264.43**	**0.62**	**118133**

3.5 Prediction results of the best combined model

Combined prediction model of artificial neural network was used to make a short-term prediction of health technician needs in Hainan province from 2021 to 2023, the results are shown in Table 6.

Table 6. Short-term prediction value of health technicians in Hainan Province

Year	Predicted values by artificial neural networks model
2021	81967
2022	87193
2023	89707

4. Discussion

The combined forecasting model is, to some extent, an improvement over the single forecasting model.It improves the accuracy of a single prediction model and reduces the error of prediction.Using multiple combination methods can extract the advantages of a single model from different sides, so as to select the best combination and obtain more accurate prediction results, thus providing a more accurate and reliable decision-making basis for scientific allocation of health human resources.Later stage, the accuracy of the prediction model can be further improved from three aspects: The first is to optimize the selection strategy of single model, try to select some new single prediction models, such as SVM [17-18] and other machine learning models;the second is the selection of combination methods, whether the selection of combination methods is appropriate directly affects the combination prediction effect, so other combination methods can also be tried; the Third is other social factors should also be considered, such as the aging of the society's population, health policy, economic development and so on.

The forecast results show that from 2021 to 2023, the demand of health technicians in Hainan province will increase year by year. And with the establishment of Hainan Boao Le Cheng Medical Pilot Zone and the construction of Hainan Free Trade Port, the demand of health technicians in Hainan province will continue to increase. However, there is only one undergraduate medical college in Hainan province, and its economic development is relatively backward, so the attraction of medical talents from other provinces is weak. Therefore, it is recommended that the relevant departments use the forecast

results as a scientific basis for policy formulation and talent training, vigorously develop local medical education, and further enhance the coordination between health administration departments and education departments,adjust the scale and training direction of medical education according to the number of health technicians needed, and actively promote a balance between supply and demand of health human resources [19].

Author contributions

W-SH and L-LH contributed equally to this study and approved the final version.

References

[1] Chen Y, Xue Q. A Forecasting Analysis of Health Human resources in Inner Mongolia based on GM (1，1) Model. Medicine and Society, 2019,32 (09): 20-23.

[2] Zhang Y. A gray neural network model for predicting trends in the number of health technicians. Chinese Journal of Health Statistics, 2016,33 (02): 331-332 + 335.

[3] Sun J. Prediction Analysis on Demand of Health Workers in Guangxi Zhuang Autonomous Region Based on ARIMA Model. Modern Preventive medicine, 2017,44 (12): 2196-2201.

[4] Liu Q, Zou B, Zhu P, Zhang F, Chang R, Dong Y, Wan H. Forecast of Health Professionals Demand Based on ARIMA Model in Hubei Province. Medicine and Society, 2020,33 (02): 18-21.

[5] Li S, Liu X, Zhang X.Study on the prediction of health human resource demand in Hubei province based on grey system . Soft science of Health, 2020,34 (03): 49-53.

[6] Ling L, Zhang D. A Review of Combined Prediction Model Construction Methods and Their Applications. Statistics & Decision, 2019,35 (01): 18-23.

[7] Hou Y, Wang D, Chen Y, Zheng X, Gao Y, Zheng W. Construction and application of combination forecasting model of health human resources in Shandong Province. Soft science of Health, 2021,35 (04): 72-75 + 79.

[8] Bai Y, Wang D, Han D. Trend prediction of the number of urban and rural health technicians in China based on the combination model [J]. Chinese Journal of Health Statistics, 2019,36 (01): 111-114.

[9] Han C, Hu X, Zhao Y, Dong Z. Combination Model in Forecasting the Total Number of Health Technical Staffs of Our Country. Chinese Journal of Health Statistics, 2011,28 (04): 391-393.

[10] Zhang R, Zhao D, He S, Liu Z, Sun B, Xu X. Health human resource prediction based on Grey GM (1,1) model and ARIMA model,Sichuan Province.Modern Preventive Medicine, 2017,44 (07): 1242-1247.

[11] Yang Y, Mao S, Xue Y, Tian X, Shi X. Prediction on the Incidence rate of AIDS in China with Gray Model(1,1) and Trend Extrapolation Model. Chinese Journal of Health Statistics, 2014,31 (06): 952-954.

[12] Li W, Cui Q, Zhang L. Trend extrapolation and ARIMA forecast hospital diagnosis and hospitalization in China. Chinese Journal of Health Statistics, 2016,33 (03): 477-478 + 481.

[13] Gerder Claeskens, Jan R, Magnus, Andrey L.Vasnev,et al.The forecast combination Puzzle:A Simple Theoretical Explanation[J].International Journal of Forecasting,2016,32.

[14] Dou J, Ma H. Prediction of Building Energy Consumption Based on Ensemble Artificial Neural Networks. Computer Simulation, 2022,39 (05): 438-443.

[15] Zhang Q. Application Research on an optimal mix forecasting method on ANN. Systems Engineering-Theory & Practice, 2001 (09): 90-93.

[16] Li S, Liu L, Zhai M. Prediction for short-term traffic flow based on modified PSO optimized BP neural network. Systems Engineering-Theory & Practice, 2012,32 (09): 2045-2049.

[17] Bao X, Xiang G, Shi L, Wang D. Prediction of total health expenditure in Guangdong,based on GM(1,1)-SVM combination model. Modern Preventive medicine, 2022,49 (05): 856-859.

[18] Shen G, Wang X, Kong X. Short-term traffic volume intelligent hybrid forecasting model and its application. Systems Engineering-Theory & Practice, 2011,31 (03): 561-568.

[19] Liang S, Feng Q, Wang Y, Luo H, Qin Q, Zhang Y. Studying on the equity of health resources allocation in the minority areas sampled with Guangxi. Chinese Health Service Management, 2015,32 (09): 677-680.

Analysis of the use of minimally invasive rotary mastectomy in the treatment of multiple small nodules in the breast

Zhu Wu, Zhuo Wang, Qingqing Ye, Rong Fan*
Jingzhou First People's Hospital, Jingzhou 434000, China.

Abstract: Objective: To observe the effectiveness of different surgical excisional set-ups for the treatment of multiple small breast nodules disease. Methods: 60 patients who came to our department from 2020.10 to 2023.1 were divided into two groups A and B, 30 patients each, and were treated with conventional and minimally invasive mastectomy respectively, and the treatment status was compared between the groups. Results: Compared to group A, group B had better surgical indicators and 93.3% higher post-operative satisfaction than group A with 73.3%, forming a significant difference ($p < 0.05$). Conclusion: Minimally invasive rotary mastectomy is a minimally invasive technique for the treatment of breast nodule disease ear, which has the characteristics of short incision, less intraoperative bleeding and short operation time, which can increase the subjective satisfaction of patients and is worth promoting.

Keywords: Breast Nodules; Minimally Invasive Rotational Mastectomy; Effect Observation

Introduction

Breast nodules are a common disease among modern women, generally benign lesions, with breast swelling and pain being the typical symptoms of patients. Traditional local excision results in a large scar on the surface of the breast, making it difficult to meet the needs of patients in terms of aesthetic breast appearance [1]. In recent years, the minimally invasive concept has led to the rapid development and advancement of minimally invasive techniques, and minimally invasive rotary mastectomy is a classic type of minimally invasive technique.

1. Data and methods

1.1 General data

Sixty patients with multiple small breast nodules who were diagnosed, met the indications for surgery and voluntarily cooperated to complete the study were selected as study subjects, admitted in the time range of 2020.10 to 2023.1, and divided equally into 2 groups, with each group as follows.

Group A: minimum and maximum age 24 and 56 years, disease duration range 6 to 18 months.

Group B: minimum and maximum age 22 and 59 years, disease duration ranging from 7 to 20 months.

Patients in the above baseline data were compared between groups ($P > 0.05$) and were comparable.

1.2 Methods

Group A underwent conventional surgical treatment. Patients were placed in the supine position, under local anesthesia with 0.5% lidocaine, and an incision was made at an appropriate location according to the location of the breast nodule, and the nodule was excised individually according to its clarity, including those with a high degree of clarity, along the envelope

as a whole; for masses with an obscure envelope, they were excised together with the normal glandular tissue.

Group B was treated with a minimally invasive mastectomy. Minimally invasive mastectomy system with 11G rotary cutter and high frequency probe. The patient was placed in a supine position, under local anaesthesia, with gentian violet on the body surface to mark the extent of the mass to be removed and ultrasound instruments to assist in repositioning, and a long needle injection of local anaesthetic solution to tilt the rotary cutter to the appropriate angle for insertion deep into the lesion. After repeatedly confirming the alignment of the cutting notch with the lesion, the rotary incision is performed. After completion of the spinotomy, ultrasound is used to determine if any local tumour remains. The incision was routinely pressurized and sterile gauze was applied, and postoperative anti-infection treatment was routinely administered.

1.3 Observation indicators

(1) Surgical indicators: intraoperative blood loss, surgical time, scar and respective length of the incision.

(2) Post-operative satisfaction: questionnaire survey, very satisfied, more satisfied, unsatisfied.

1.4 Statistical processing

All data were entered into an Excel.2007 table and spss26.0 software was processed. It was calculated that if $P < 0.05$, it indicated a significant difference.

2. Results

2.1 Surgery-related indicators

The scar and incision length of patients in group B were all < group A, the intraoperative bleeding was less than group A, and the intraoperative operation took less time than group A ($P < 0.05$), Table 1.

Table 1 Comparison of surgery-related indicators between groups of patients $(\bar{x} \pm s)$

Group（n）	Incision length（mm）	Length of scar（mm）	Intraoperative blood loss（ml）	Surgery time（min）
Group B（30）	5.9±2.3	3.1±0.7	6.2±2.5	18.8±2.6
Group A（30）	17.1±3.6	11.1±2.9	17.6±4.5	34.9±3.7

2.2 Degree of satisfaction

Satisfaction in group B vs group A was 93.3% vs 73.3%, and group B was higher than group A ($P <0.05$), Table 2.

Table 2 Comparison of patient satisfaction between the groups

Group（n）	Very satisfied	More Satisfied	Not satisfied	Satisfaction（%）
Group B（30）	24	4	2	28（93.3）
Group A（30）	16	6	8	22（73.3）

3. Discussion

In recent years, the overall health care awareness of the Chinese population has increased, the level of high-frequency ultrasound technology has continued to improve and gradually achieved widespread use, and many women are found to have breast nodules during physical examination, and they are usually multiple and hidden lesions that are not palpable lumps [2]. For patients with multiple breast nodules and small, occult lesions, traditional surgery is often performed through multiple incisions or incisions, which inevitably causes great trauma to the patient, poor wound aesthetics, often delayed healing and

difficulty in locating and excising small, deep nodules with a high degree of accuracy, resulting in significant mental stress for both patient and surgeon. The resulting mental stress has a significant impact on both the patient and the surgeon.

In this study, the scar length, incision length, intraoperative blood loss and operative time were (3.1±0.7) mm, (5.9±2.3) mm, (6.2±2.5) ml and (18.8±2.6) min in group B compared to (11.1±2.9) mm, (17.1±3.6) mm, (17.6±4.5) ml and (34.9±3.7) min in group A. (34.9±3.7) min, a significant difference. As a classical minimally invasive technique, minimally invasive mastectomy has many advantages such as simplicity of operation, small scar area and minimal trauma. It uses a vacuum-assisted breast biopsy system to assist in the treatment, specifically for continuous cutting of the mass, with the possibility of adjusting the size of the blade slot and the angle of rotation to suit realistic needs, and automatically storing the pathological specimen in an airtight medical specimen box [3]. Pre-operative qualitative assessment of breast nodules is essential and minimally invasive rotary mastectomy is mainly used to treat patients whose examination is considered to be a benign lesion, while it is not recommended for those with suspected preoperative breast union or breast cancer.

In the full text, the treatment of patients with breast nodules with minimally invasive rotational mastectomy is worth promoting because of the short incision, low intraoperative bleeding, short operative time and higher subjective satisfaction.

References

[1] Zhao F. Analysis of the effect of minimally invasive rotary mastectomy in the treatment of multiple breast masses [J]. Chinese and Foreign Medical Research, 2021, 19(11):140-142.

[2] Chen YH, Li H. Effectiveness of minimally invasive rotational resection versus traditional surgery in the treatment of benign breast masses[J]. Journal of rare diseases, 2022, 29(11): 47-48.

[3] Bai H. Clinical effects of minimally invasive spinotomy versus traditional excisional surgery for benign breast masses [J]. China Modern Drug Application, 2021,15(17):42-44.

Author Bio:

First author

Name: Wu zhut (1982.5.14-), Male, Han Nationality, Place of Origin: Xiangtan, Hunan, Master, Title: Attending Physician, Unit: Jingzhou First People's Hospital, Department: Breast Surgery, Main Research Interests: Comprehensive treatment of breast cancer, diagnosis and treatment of non-lactating mastitis, postoperative reconstruction of breast tumor.

Corresponding author

Fan Rong (1980.1.10-), F, Han, Place of origin: Hubei. Jingzhou, Master, Title: Attending, Unit: Jingzhou First People's Hospital, Department: Department of Respiratory and Critical Care, Major research interests: chronic obstructive pulmonary disease, interstitial lung disease, pulmonary embolism, pulmonary hypertension, ECMO life support, etc.

Second author

Wang Zhuo (1968.10.10-), Male, Ethnicity: Han, Origin: Xiangyang City, Hubei Province, Highest Education: B.S., Title: Deputy Chief Physician, Unit: Jingzhou First People's Hospital, Department: Breast Surgery, Main Research Interests: Comprehensive diagnosis and treatment of breast diseases and breast tumors, post-operative breast reconstruction, minimally invasive treatment of breast diseases, etc.

Third author

Ye Qingqing (1979.2.23-), Female, Ethnicity: Han, Place of origin: Nanning, Guangxi, Highest education: Master, Title: Deputy Chief Physician, Unit: Jingzhou First People's Hospital, Department: Breast Surgery, Main research interests: standard treatment of breast tumours, surgical management of breast cancer.

The Value of Folic Acid Combined with Low Molecular Weight Heparin in the Treatment of Recurrent Abortion

Lingyan Zhang*
Shaanxi Provincial People's Hospital, Xi'an 710068, China.

Abstract: **Objective:** To retrospectively analyze the effect of folic acid combined with low molecular weight heparin regimen on recurrent abortion in hospital. **Methods:** The inclusion period was from February 2022 to February 2023. During this period, patients with recurrent abortion in the hospital were studied and discussed, including 70 patients. They were randomly assigned to a control group (35 patients were treated with low molecular weight heparin calcium and aspirin) and an observation group (35 patients were treated with folic acid on the basis of the control group). Relevant data were collected and sorted out, and finally processed using statistics. **Results:** The data of treatment results were processed by the statistical system, and the results ($P<0.05$) showed that the observation group had better information on various data such as hormone indicators, pregnancy outcome, and immune function indicators after treatment. **Conclusion:** The application of folic acid combined with low molecular weight heparin regimen is conducive to the smooth development of the treatment of recurrent abortion, can help patients control hormone indicators within a reasonable range, improve immune function and pregnancy outcomes, and has important significance in improving treatment effectiveness.

Keywords: Folic Acid; Low Molecular Weight Heparin; Recurrent Abortion

Introduction

Recurrent abortion is a common disease in obstetrics and gynecology, which is mainly caused by multiple factors such as chromosomal abnormalities, maternal endocrine disorders, maternal reproductive tract abnormalities, reproductive tract infections, immune dysfunction, and genetic thrombotic predisposition. Patients may experience three or more consecutive spontaneous abortions. It is necessary to attach importance to and strengthen research on the treatment of recurrent abortion, continuously improve the treatment effect, and provide a certain guarantee for the healthy development of the fetus. Clinically, drugs such as low molecular weight heparin calcium and aspirin are mainly used for treatment. Although the disease can be controlled, the treatment effect cannot be guaranteed to the maximum extent [1]. Influenced by the continuous development of modern medical and health undertakings, researchers have found that the application of folic acid in the treatment of recurrent abortion has a good effect, which provides a new direction for research on the treatment of recurrent abortion [2].

1. Data and Methods

1.1 General information

The inclusion period was from February 2022 to February 2023. Patients with recurrent abortion in the hospital during this period were studied and discussed, including 70 patients. They were randomly assigned to two groups. The control group and the observation group included 35 patients, respectively. In the control group, 25 years of age was the minimum

patient age, and 38 years of age was the maximum patient age, with an average of (32.02 ± 1.16) years; In the observation group, 25 years old was the minimum patient age, and 38 years old was the maximum patient age, with an average value of (32.06 ± 1.11) years. Selection requirements: All patients with recurrent abortion; Cognition meets conventional standards and consciousness is normal; Are willing to participate. Rejection requirements: low compliance and low compatibility; Concomitant with other serious diseases. The hospital ethics committee approved the research activity. The general data of patients were statistically processed and the results obtained did not have statistical significance (P>0.05).

1.2 Method

1.2.1 Control group

Implement the treatment plan of low molecular weight heparin calcium (low molecular weight heparin calcium injection, from Shenzhen Saibao Er Biological Pharmaceutical Co., Ltd., with the national drug approval number of H20060191, and the specification of 0.5ml: 5000AXa), and aspirin (from Jiangxi Pharmaceutical Co., Ltd., with the national drug approval number of H36020723). The use method of low molecular weight heparin calcium injection: subcutaneous injection, 5000 IU each time, once a day; Aspirin Usage: Take orally with warm water, 80mg each time, once a day.

1.2.2 Observation group

Based on the control group, folic acid (folic acid for injection, from Shandong Luoxin Pharmaceutical Group Co., Ltd., with the national drug approval number of H20050739 and the specification of 15mg) was used. The method of use of folic acid: intramuscular injection, 5mg each time, once a day.

1.3 Judgment criteria

Collect and organize relevant data and information, and finally use statistics for processing.

(1) The changes of hormone indexes, including serum human chorionic gonadotropin (HCG), progesterone (P), and estradiol (E1) levels, were measured and compared between the two groups before and after treatment.

(2) The pregnancy outcomes of both groups were observed and recorded, including full term delivery, premature survival, premature death, and miscarriage.

(3) Detect and observe two groups of immune function indicators, including CD3+/CD8+, CD4+/CD8+.

1.4 Statistical methods

Enter various data information into the SPSS 20.0 system, where ($\bar{x} \pm s$) is displayed as measurement data, while (n,%) is displayed as counting data. During testing, it is used, with a limit of 0.05. A P value higher than this value indicates no statistical significance, while a value lower than this value indicates statistical significance.

2. Results

2.1 Sex hormone indicators

The treatment result data were processed by the statistical system, and the results (P<0.05) showed that the observation group had better data information on hormone indicators after treatment. See Table 1.

Table 1 Comparison of hormone indicators between the two groups before and after treatment ($\bar{x} \pm s$)

Groups	HCG（IU/L）		P（ng/ml）		E1（ng/ml）	
（n=35）	Before	After treatment	Before	After	Before	After

	treatment		treatment	treatment	treatment	treatment
Observation group	983.23±92.52	7011.52±519.63	33.45±12.63	105.63±19.63	410.51±15.85	946.52±64.53
Control group	983.64±91.99	6166.16±415.36	33.50±12.69	87.52±15.33	411.01±15.54	645.17±34.11
t	0.018	6.840	0.016	4.301	0.133	24.425
P	0.985	0.001	0.986	0.001	0.894	0.001

2.2 Pregnancy outcome

The treatment result data were processed by the statistical system, and the results (P<0.05) showed that the observation group had better data information on pregnancy outcomes. See Table 2.

Table 2 Comparison of pregnancy outcomes between the two groups after treatment (n,%)

Groups（n=35）	Full term delivery	Premature survival	Premature death	Abortion
Observation group	20（57.14）	13（37.14）	1（2.85）	1（2.85）
Control group	15（42.85）	8（22.85）	6（17.14）	6（17.14）
X^2	4.084	4.862	11.349	11.349
P	0.043	0.027	0.001	0.001

3.3 Immune function indicators

The treatment result data were processed by the statistical system, and the results (P<0.05) showed that the observation group had better data information on immune function indicators. See Table 3.

Table 3 Comparison of immune function indicators between the two groups after treatment ($\bar{x} \pm s$)

Groups	Number of cases	CD3+/CD8+（%）	CD4+/CD8+（%）
Observation group	35	27.02±2.85	1.52±0.16
Control group	35	22.31±1.79	1.23±0.29
t		8.279	5.180
P		0.001	0.001

3. Discussion

3.1 Pathological characteristics of recurrent abortion

Compared with healthy pregnant women, patients with recurrent abortion have a higher risk of early miscarriage, and abnormal changes in the patient's embryonic chromosomes, luteal function, prolactin, hormones, immune function indicators, thyroid function, and cervical function can occur. As the number of abortions increases, the safety risk of pregnant women will increase. The specific cause is relatively complex, and during treatment, the patient's immune function will be improved Control of relevant hormone levels, improvement of pregnancy outcomes, and other treatment priorities [3].

3.2 Treatment of recurrent abortion

Aspirin is a commonly used drug in the treatment of recurrent abortion. In addition to its antipyretic, analgesic, anti-inflammatory, and anti rheumatic effects, aspirin also has significant advantages in inhibiting platelet aggregation. When administered to patients, it can have an impact on the pathophysiological changes in the blood of the patient's body, improve

the hypercoagulable state of the blood, reduce the risk of thrombosis, promote the restoration of normal blood supply to placental tissue, and maintain normal blood and oxygen supply to the embryo, Thereby improving pregnancy outcomes [4]. However, in actual treatment, the use of a single drug cannot effectively improve the treatment effect. With the continuous development of research, low molecular weight heparin (LMWH) has been gradually applied to clinical practice. This drug is mainly derived from antithrombotic and anticoagulant effects of ordinary heparin. The drug contains potent anticoagulant factor active substances and lower anticoagulant factor IIa (antithrombin activity) components, which can not only produce antithrombotic effects, but also reduce the risk of bleeding and, to a certain extent, have a positive impact on uterine microcirculation, Effectively regulate immune function, thereby effectively inhibiting natural killer cell function, promoting trophoblast proliferation, regulating trophoblast invasion ability, and reducing trophoblast apoptosis [5]. In addition, from the perspective of clinical practical development, an intermediate product, homocysteine, is produced during the metabolism of amino acids in the human body. In this reaction process, it mainly relies on folic acid and vitamin B12 to participate. Once the human body is deficient in folic acid and vitamin B12, it will lead to excessive secretion of homocysteine, causing damage to the human vascular endothelial function, especially in pregnant women, Vascular smooth muscle cell proliferation is extremely prone to occur, which has adverse effects on the normal blood coagulation system and fibrinolytic system, forming a hypercoagulable state of blood, causing thrombosis, blocking blood vessels, leading to restrictions on fetal growth and development, thereby increasing the risk of miscarriage [6]. Therefore, while giving aspirin and low molecular weight heparin calcium to patients with recurrent abortion, supplementing folic acid can maintain the normal progress of DNA synthesis, nucleic acid synthesis, cell growth, tissue repair, and other reaction processes during embryonic development, reduce the risk of neonatal birth defects and hyperhomocysteinemia, enhance treatment effectiveness, help patients control hormone levels in the body, and improve treatment safety [7]. Based on the research results in this article, the statistical system processed the treatment result data, and the result showed that the P value was less than 0.05. After treatment, the observation group had better data information on hormone indicators, pregnancy outcome, immune function indicators, and other aspects.

It can be seen that the application of folic acid combined with low molecular weight heparin can help the treatment of recurrent abortion to proceed smoothly, help patients control hormones within a reasonable range, improve immune function and pregnancy outcomes, and have important significance in improving treatment effectiveness.

References

[1] Zhou ZY, Chen GZ, Hu YY. Effects of Low Molecular Weight Heparin and Progesterone Combined with Folic Acid on Lymphocyte Subsets, Sex Hormones, and Pregnancy Outcome in Patients with Recurrent Abortion [J]. *Chinese Journal of Family Planning*, 2021,29 (10): 2051-2055.

[2] Cheng TT, Mao XW. The Efficacy of Folic Acid Combined with Low Molecular Weight Heparin in the Treatment of Recurrent Abortion and Its Effect on the Levels of Vascular Endothelial Growth Factor and Soluble Vascular Endothelial Growth Factor Receptor-1 in Patients with Recurrent Abortion [J]. *China Maternal and Child Health Care*, 2022, 37 (13): 2421-2424.

[3] Ke SC, Xu ZY. Effects of Low Molecular Weight Heparin Combined with Low Dose Aspirin on Coagulation Parameters and Th17/Treg Cytokines in Patients with Recurrent Abortion [J]. *Chinese Journal of Family Planning*, 2021,29 (3): 461-465.

[4] Lu XJ, Liang JM, Shen LL, et al Effects of Low Molecular Weight Heparin Combined with Low Dose Aspirin on Prethrombotic State, Liver Function, and Immune Function in Patients with Recurrent Abortion [J]. *Electronic Journal of Developmental Medicine*, 2021,9 (3): 214-219.

[5] Cai RB, He XT, Lin XH. The Effect of Low Molecular Weight Heparin Combined with Low Dose Aspirin in the

Treatment of Recurrent Abortion and Its Impact on Coagulation Indicators [J]. *Chinese Practical Medicine*, 2020,15 (23): 128-130.

[6] Li ZN, Wu SF, Wang ML. The Effect of Low Molecular Weight Heparin on the Levels of Th1, Th17, and Related Chemokines in Patients with Unexplained Recurrent Abortion During Pregnancy [J]. *Chinese Journal of Practical Medicine*, 2022,49 (23): 30-34.

[7] Li JX. Clinical Evaluation of Low Molecular Weight Heparin Combined with Low Dose Aspirin in the Treatment of Autoimmune Recurrent Abortion [J]. *Heilongjiang Medical Science*, 2019, 42 (4): 157-158.

Observation on the Curative Effect of Yiyuan Pingchuan Decoction Combined with Ultra-Low Frequency Combined with Physiological Frequency Electrical Stimulation on Chronic Obstructive Pulmonary Disease in Stable Stage

Peng Zhang[1], Qizheng Han[1], YueLi Xu[1], Jifei Geng[2*]

1. Department of Respiratory and Critical Care Medicine, Shandong Second Provincial General Hospital (Shandong ENT Hospital), Jinan 250000, China.

2. Department Emergency, Tai 'an Hospital of Traditional Chinese Medicine, Tai'an 271000, China.

Abstract: **Objective**: To observe the clinical efficacy of Yiyuan Pingchuan Decoction combined with ultra-low frequency combined with physiological frequency electrical stimulation on chronic obstructive pulmonary disease in stable phase. **Method:** 89 patients were randomly divided into control group (44 cases)and observation group (45 cases). The control group was treated with conventional western medicine, while the observation group was treated with ultra-low frequency combined with physiological frequency electrical stimulation and Yiyuan Pingchuan Decoction on the basis of the control group. The 6-minute walking score (6MWT), SGRQ score, Borg fatigue score, lung function, and clinical efficacy after 30 days were observed at day 15 and day 30, respectively. **Results:** The 6MWT, SGRQ score, Borg fatigue score and lung function were improved more significantly in observation group than those in control group ($p<0.05$). The total effective rate of observation group (91.1%) was significantly higher than that of control group (79.5%) ($p<0.05$). **Conclusion:** Yiyuan Pinghuan Decoction combined with ultra-low frequency combined physiological frequency electrical stimulation can significantly improve the 6MWT, SGRQ score, Borg fatigue score and lung function of patients with stable chronic obstructive pulmonary disease, improve clinical efficacy, and then improve the quality of life of patients, so as to improve the clinical prognosis of patients.

Keywords: Yiyuan Pingchuan Decoction; Stable Chronic Obstructive Pulmonary Disease; Upper and Lower Deficiency; Ultra-Low Frequency Combined with Physiological Frequency Electrical Stimulation; Observation of Curative Effect

Introduction

Chronic obstructive pulmonary disease (COPD) is a common preventable and treatable chronic lung disease characterized by persistent airflow restriction and progressive respiratory symptoms [1]. Stable COPD progresses slowly, patients have low immunity, decreased lung function, and the disease has repeated attacks, seriously affecting the quality of life and work [2]. The World Health Organization (WHO) projects that COPD will be one of the top three causes of death worldwide by 2030. The total number of COPD deaths is estimated to increase by 30% in the next 10 years [3]. Therefore, early prevention, discovery and scientific treatment of COPD is an important and arduous medical task in clinical practice. At present, there are many clinical applications of drugs and pulmonary function rehabilitation training for treatment, but there is still a lack of effective treatment for COPD in remission. Extracorporeal diaphragmatic pacemaker therapy is a treatment method that increases the endurance and anti-fatigue ability of the diaphragm by stimulating it with pulse current,

in order to alleviate symptoms in clinical COPD patients. It is increasingly being applied to COPD patients in remission stage [4]. Many reports have proved that traditional Chinese medicine can regulate the occurrence and development of COPD in multiple ways, multiple targets and multiple links, so as to delay the development of COPD, and has great advantages in improving patients' quality of life [5]. Therefore, on the basis of conventional western medicine treatment of COPD, combined with frequency conversion diaphragmatic pacing and Yiyuan Pingchuan Decoction can significantly improve the quality of life.

1. Materials and method

1.1 Diagnostic Criteria

1)The diagnostic criteria of Western medicine are based on the "Guidelines for Diagnosis and Treatment of Chronic Obstructive Pulmonary Disease (Revised 2021 Edition)"[6]. Patients with shortness of breath, cough, sputum and other symptoms are stable or mild, belonging to the stable period;

2)The diagnostic criteria of TCM belong to lung and kidney qi deficiency syndrome according to TCM Diagnosis and Treatment Guide for Chronic Obstructive Pulmonary Disease (2011 Edition) [7].

1.2 Exclusion Criteria

1)Serious heart and lung diseases, acute cardiovascular and cerebrovascular diseases；

2)Uncontrolled type 2 diabetes, autoimmune disease, chronic wasting disease；

3) Other patients unable to complete clinical observation.

1.3 Clinical data

A total of 89 inpatients and outpatients from Shandong Second People's Hospital and Tai 'an Hospital of Traditional Chinese Medicine from June 2019 to June 2021 were selected and divided into two groups according to random number table method. In the observation group, there were 23 males and 22 females, the average age was (62.1±5.1) years, and the average course of disease was (7.3±2.7) years. Moreover, there were 23 males and 21 females in the control group with an average age of (62.2±5.3) years and the average course of disease was (7.1±2.5) years. There was no significant difference in clinical data between the two groups (P>0.05). This study has been approved by the Medical Ethics Committee of our hospital.

1.4 Methods

Patients in control group received conventional Western medicine treatment, mainly inhaling salmeterol ticasone powder (50ug/500ug*60 capsules, produced by Glaxo Operations UK Limited), appropriate nutritional support, oxygen therapy and disease health guidance. Patients in observation group was additionally treated with ultra-low frequency combined physiological frequency electrical stimulation and Yiyuan Pingchuan decoction. The Yiyuan Pingchuan decoction was consisted by Psoralea (15g), walnut (15g), Gecko (Chong) (3g,) platycodon (15g), Houttuynia Cordata (30g), almond (10g), Fructus suzi (15)g, Trichosanthes (15g), which was made into decoction and patients took it in two doses for 20 days.

1.5 Observation indicators

The 6-minute walk test (6MWT), St George's Respiratory questionnaire (SGRQ) score, Borg fatigue score, lung function at 15 days and 30 days and clinical efficacy at 30 days of the two groups were observed. Then the degree of influence on various scores and clinical efficacy changes were observed after treatment in the two groups.

1.5.1 6MWT

6-minute walk distance after treatment.

1.5.2 SGRQ score [8]

SGRQ was used to evaluate the quality of life of patients before and after treatment, including respiratory symptoms, disease impact and activity limitation. Respiratory symptoms: The score was based on the severity of symptoms such as chest tightness (shortness of breath), cough and expectoration. Severe (3 score): Chest tightness (shortness of breath), cough and expectoration were obvious； Mild (1 score): Intermittent chest tightness (shortness of breath), cough, and sputum production were not obvious. A score of 2 was given for symptoms in between. Response score for respiratory symptoms: a decrease of ≥2 points was considered to indicate significant improvement， a decrease of ≥1 point was considered mild improvement and no change in score was considered to be futility. Disease Impact Score: significantly improve—the score decreased by ≥8 points; Slight improvement—a score decrease of ≥4 points was invalid if the score was < 8; Mobility—limitation Score. Invalid: The score decreased by <4 points.

1.5.3 Borg fatigue score

A total of 10 points were scored according to the degree of dyspnea and fatigue: 0—No difficulty breathing or fatigue at all，0.5—very mild difficulty breathing or fatigue, difficult to detect，1—very mild difficulty breathing or fatigue, difficult to detect， 2—Mild dyspnea or fatigue， 3—Moderate dyspnea or fatigue, 4—Mild severe difficulty breathing or fatigue， 5—Severe difficulty breathing or fatigue，6-8—Very severe difficulty breathing or fatigue，9—Very, very severe difficulty breathing or fatigue，10—Extreme difficulty breathing or fatigue, reaching the limit.

1.5.4 clinical efficacy

Excellent: After treatment, pulmonary function tests showed FEV1≥80% predicted value, FEV/FVC≥70%, dyspnea, expectoration, cough and other respiratory symptoms disappeared, and the results of chest X-ray showed that the pulmonary infection disappeared.

Effectivity: After treatment, the predicted value of FEV1 was significantly improved compared with that before treatment, FEV/FVC < 70%, dyspnea, expectoration, cough and other respiratory symptoms disappeared, and chest X-ray results showed that pulmonary infectious lesions partially disappeared.

Invalid: Patients who did not meet the above efficacy criteria.

Total effective rate =(Number of Excellent cases + Number of effective cases)/31×100%

1.6 Statistical analysis

SPSS 21.0 statistical software was used to analyze the data. Measurement data were expressed as mean ± standard deviation ($\overline{X}$ ±s). The differences between two groups or among three groups were compared by t test or $\chi 2$ test. $P < 0.05$meant the difference was significant.

2. Results

2.1 The 6MWT and Brog fatigue score were compared between the two groups before and after treatment

As shown in Table 1, the levels of 6MWT and Brog fatigue score 15 days and 30 days after treatment in the two groups were higher than those before treatment, and the improvement in the observation group was more significant than that in the control group(P＜0.05)

Table 1. The 6MWT and Brog fatigue score were compared between the two groups before and after treatment

Groups	n	time	6MWT (m)	Brog fatigue score
Observation group	45	Before treatment	285.63±65.73	5.43±0.51
		15 days after treatment	331.69±72.73*	4.72±0.56*
		30 days after treatment	383.64±76.16**▲	4.61±0.43**▲
Control group	44	Before treatment	287.31±70.62	5.39±0.48
		15 days after treatment	322.47±71.69	5.12±0.51
		30 days after treatment	347.73±72.37	5.07±0.43

*P<0.05、**P<0.01 VS before treatment；▲P<0.05 VS control group.

2.2 SGRQ scores were compared between the two groups during the treatment

As displayed in Table 2, the SGRQ scores of the two groups after treatment were improved compared with those before treatment, and the improvement in the observation group was more significant (P < 0.05).

Table 2 SGRQ scores were compared between the two groups

Groups	n	time	Respiratory symptom score	Disease impact score	Mobility limitation score
Observation group	45	Before treatment	25.76±4.33	23.46±4.52	14.73±2.31
		15 days after treatment	18.68±3.64*	17.98±3.01*	10.62±1.86*
		30 days after treatment	12.73±2.13**▲	12.36±1.98**▲	6.78±1.39**▲
Control group	44	Before treatment	25.69±4.41	23.54±4.62	14.69±2.28
		15 days after treatment	21.48±4.11	20.17±3.88	12.79±2.11
		30 days after treatment	18.14±3.32	17.36±2.89	9.07±1.44

*P<0.05、**P<0.01 VS before treatment；▲P<0.05 VS control group.

2.3 The improvement of lung function after treatment was compared between the two groups

As shown in Table 3, the lung function levels of the two groups after 15 days and 30 days of treatment were improved compared with those before treatment, and the improvement of the observation group was more obvious cmpared to those in control group (P<0.05).

Table 3 The improvement of lung function after treatment was compared between the two groups

Groups	n	time	FVC(L)	FEV1(L)	FEV1/FVC(%)
Observation group	45	Before treatment	1.92±0.23	1.78±0.27	66.67±8.32
		15 days after treatment	2.28±0.37*	2.21±0.31*	75.45±9.86*
		30 days after treatment	2.57±0.44**▲	2.96±0.38**▲	83.17±11.89**▲
Control group	44	Before treatment	1.94±0.25	1.81±0.28	66.69±8.29
		15 days after treatment	2.15±0.35	1.98±0.28	71.78±8.98
		30 days after treatment	2.32±0.39	2.36±0.33	74.54±9.49

*P<0.05、**P<0.01 VS before treatment；▲P<0.05 VS control group.

2.4 The clinical efficacy was compared between the two groups after treatment

The total effective rate of the observation group was 91.1%, which was significantly higher than 79.5% of the control group(P<0.05,Tbale 4).

Table 4. The clinical efficacy was compared between the two groups after treatment (%)

Groups	n	Effective	Valid	Invalid	Total effective rate
Observation group	45	25(55.6)	16(35.5)	4(8.9)	91.1▲
Control group	44	21(47.7)	14(31.8)	9(20.5)	79.5

▲P<0.05 VS control group.

3. Discussion

Chronic obstructive pulmonary disease (COPD) is a common chronic respiratory disease. The 2017 Global Initiative for COPD pointed out that the main pathological change of the disease is airflow limitation and recurrent respiratory disease. Due to the high fatality rate, this disease easily poses a serious threat to the life safety of patients [9]. Diaphragm is an important source of respiratory power in the body, and the power generated by diaphragm activity can account for more than 3/4 of the total lung ventilation power. However, the diaphragm movement amplitude of COPD patients is reduced and atrophic, and the contractility and fatigue tolerance of the diaphragm are significantly reduced, which further aggravates the patient's condition. At present, the clinical treatment for patients with stable COPD mainly includes drug control, pulmonary function rehabilitation exercise, and long-term home oxygen therapy. Although drug control can relieve the disease and improve the clinical symptoms to a certain extent, organic lesions also gradually aggravate with the recurrence of the disease. Moreover, respiratory function exercise is difficult to achieve long-term stable efficacy due to the limitation of treatment conditions, patient's willpower, compliance and other problems.

At present, physiological frequency electrical stimulation is mostly used in clinical practice, which can improve the ventilation function of patients to a certain extent. However, in recent years, many studies have shown that although physiological frequency electrical stimulation can improve the contractility and fatigue resistance of the diaphragm to a certain extent, the fiber remodeling of the respiratory muscles of patients has not reached the optimal structure. Many studies have shown that ultra-low complex physiological frequency chronic electrical stimulation can improve the diaphragm contractility and anti-fatigue ability in patients with stable COPD compared with physiological frequency electrical stimulation alone [10].

COPD belongs to the categories of "asthma syndrome", "cough", "lung distension" and other diseases in traditional Chinese medicine. Traditional Chinese medicine believes that the pathological changes in the stable stage of COPD are mainly based on the deficiency of the original qi and the deficiency of the internal organs, with kidney deficiency being the most important. Phlegm turbidity, blood stasis, and water consumption are the criteria. The interaction between the deficiency of the original qi and the deficiency of the internal organs promotes the development of the disease [11]. 《Spiritual pivot: The Meridians.》 says: The lung vein of the hand Taiyin,..... Is the movement between the lung distension, inflation and wheezing. It has been pointed out that the pathogenesis of lung distension is the syndrome of mixed deficiency and excess. In the stable stage of COPD, the deficiency of the root and the deficiency of the upper and the deficiency of the lower are the main symptoms, and the deficiency of the kidney is the main symptoms, while phlegm and drink, blood stasis and water and drink are the main symptoms. Researchers considered that the source of qi is in the kidney, and the main is in the lung. The old body function declines, or the kidney is affected by a long illness, the lower element is damaged, the main qi function of the lung is damaged, and the qi machine is reversed, the qi machine of the lung and kidney cannot be integrated and penetrates, resulting in the clear qi is difficult to enter the body, and the turdy qi is difficult to discharge, and stays in the chest. The lung regulates the waterway, the kidney is the main water, and the lung and kidney function are dysfunctional, which leads to the stagnation of water and fluid, thus forming phlegm and drink, phlegm is cloudy for a long time, which is left in the lung, the lung is not smooth, and the qi is also ascribed to the lung, resulting in the lung fullness and cannot collect and fall. Therefore, the disease is marked in the lung, and its origin is in the kidney, which is most closely related to the lung and kidney [12].

Yiyuan Pingchuan Decoction is composed of drugs such as psoraleae, walnut meat, gecko, platycodon grandiflorum, houttuynia cordata, almond, Suzi and Trichosanthis fructus. Among them, psoraleae and walnut meat are the main drugs to invigorate the kidney, absorb qi and relieve asthma, and have the right to gasification. Gecko nourishing essence blood, cough and asthma as the subject medicine, which can enhance the power of warm kidney and Yang, and can absorb qi and asthma. The combination of the monarch and the minister can make up the effect of tonifying the kidney, absorbing qi and relieving asthma. Platycodon grandiflorum, Houttuynia cordata, almond, Trichosanthis fructus and Fructus radix fructus were used as adjuvant drugs to clear heat, benefit lung and dissipate phlegm. Platycodon grandiflorum was also the leading agent of medicine, carrying medicine to the diseased places. All the prescriptions together to fill the kidney, phlegm, asthma effect. Many modern pharmacological studies have confirmed that many components of Yiyuan Pingchuan decoction can improve the respiratory muscle strength of patients, significantly relieve diaphragmatic fatigue, thereby improving lung function and improving the activity tolerance of patients. In addition, Yiyuan Pingchuan decoction can improve the body's immunity, reduce the dosage of western medicine, and reduce the toxic effects of drugs.

In conclusion, Yiyuan Pingchuan decoction combined with ultra-low frequency combined physiological frequency electrical stimulation in the treatment of stable COPD can improve the 6-minute walk test distance, BROG score, Brog fatigue score and other related clinical indicators, relieve related clinical symptoms, so as to improve the quality of life of patients and improve the clinical prognosis. Moreover, the operation of ultra-low frequency combined with physiological frequency electrical stimulation is convenient, and the price of traditional Chinese medicine is relatively low, which is worthy of further clinical application.

References

[1] Chen YK, Feng YK. Interpretation of the key points of GOLD 2017 guideline [J] Modern Medicine Hygiene,2017, 33 (4):481-486.

[2] Shen JY, Shen GZ. Research on traditional Chinese Medicine differentiation and treatment of respiratory failure in acute exacerbation of chronic obstructive pulmonary disease. Chin J Traditional Chinese Medicine, 2018, 36(2):482-484.

[3] Chronic Obstructive Pulmonary Disease Group of Chinese Respiratory Society, Chinese Medical Doctor Association, Chronic Obstructive Pulmonary Disease Working Committee of Chinese Society of Respiratory Physicians. Guidelines for diagnosis and treatment of chronic obstructive pulmonary disease (2021 revision) [J]. Chin J Tuberculosis & Respiratory,2021,44(03):170-205.

[4] Luo LL, et al. Effect of diaphragm pacing on pulmonary function and quality of life in patients with pneumoconiosis complicated with chronic obstructive pulmonary disease [J]. Occupational Health and emergency rescue. 2021,39(02):163-166.

[5] Cao X, Wang Y, Chen Y, et al. Advances in traditional Chinese medicine for the treatment of chronic obstructive pulmonary disease. J Ethnopharmacol. 2023 May 10; 307:116229.

[6] Cheng SL, Lin CH, Chu KA, et al. Update on guidelines for the treatment of COPD in Taiwan using evidence and GRADE system-based recommendations. J Formos Med Assoc. 2021 Oct;120(10):1821-1844.

[7] Zhang BL, Wu MH. Internal Medicine of Traditional Chinese Medicine [M]. 4th Edition. Beijing: China Traditional Chinese Medicine Press, 2017.

[8] Chen J, Feng DC, Tan YY, et al. The efficacy and impact on lung function of Kuanxiong Lifei Tang combined with budesonide in the treatment of stable stage lung qi deficiency syndrome patients with chronic obstructive pulmonary disease [J]. Chinese Journal of Traditional Chinese Medicine. 2021,4.

[9] Ye RH, Zou LL. Clinical observation on the treatment of 100 stable cases of chronic obstructive pulmonary disease in Lingnan region with integrated traditional Chinese and Western medicine [J]. Chinese Journal of Ethnic and Folk Medicine, 2019,28 (12): 102-105.

[10] Cao HL, Liu ZJ, Jiang HY, et al. Observation of the therapeutic effect of ultra-low frequency combined with physiological frequency chronic electrical stimulation on stable COPD [J]. Shandong Pharmaceutical, 2018,58 (40), 57-59.

[11] Li JS, Yu XQ, Traditional Chinese Medicine Staging and Grading Prevention and Treatment Strategies for Chronic Obstructive Pulmonary Disease [J]. Journal of Traditional Chinese Medicine, 2019, 60 (22): 1895-1899.

[12] Zheng J, Huang P, Wu CH. The effect of modified Liuwei Dihuang Tang combined with cardiopulmonary rehabilitation training on serum IL-6, IL-8, Cys-C levels in stable COPD patients [J] Hebei Medical Journal. 2021,27 (05): 767-772.

Fundings: The Science and Technology Development Project of Traditional Chinese Medicine in Shandong Province (No.2020M215).

Corresponding author: Jifei Geng, Department Emergency, Tai 'an Hospital of Traditional Chinese Medicine, Tai'an, 271000, China.

Clinical Effect of Yunkang Granule Combined with Low Dose Aspirin in the Treatment of Unexplained Recurrent Abortion and Its Influence on Pregnancy Outcome

Yanchun Zhang*

Department of Reproductive, Kunming Jinxin Hewanjia Obstetrics and Gynecology Hospital, Kunming 650031, China.

Abstract: Purpose: To study the clinical effect of Yunkang Granule combined with low dose aspirin in the treatment of unexplained recurrent abortion (URSA) and its impact on pregnancy outcome. Methods: Seventy-two patients with URSA were randomly divided into a control group and an experimental group. The control group was given conventional treatment, and the experimental group was given pregnancy-kang granules combined with low-dose aspirin. The clinical efficacy of the two treatments and their effects on hormone levels, coagulation function indexes and pregnancy outcome were compared. Results: After medication, the levels of β-HCG, P and E2 in 2 groups were higher than before medication, and the levels of β-HCG, P and E2 in observation group were higher than control group, the difference was statistically significant ($P < 0.05$). Compared with before medication, the levels of coagulation function indexes PT, TT and APTT were increased in both groups after medication, while the levels of FIB were decreased. The levels of coagulation function indexes PT, TT, APTT and FIB in observation group were better than those in control group after medication, and the difference was statistically significant ($P < 0.05$). After treatment, the total effective rate of the experimental group was significantly increased, and the pregnancy outcome was significantly improved. Conclusion: The combination of Yunkang granule and low-dose aspirin in the treatment of URSA has obvious curative effect, can significantly improve the pregnancy outcome, and is worthy of clinical promotion.

Keywords: Yunkang Granule; Aspirin; Recurrent Abortion of Unknown Cause; Clinical Effect; Pregnancy Outcome

Introduction

Recurrent spontaneous abortion (RSA) or recurrent pregnancy loss (RPL) is a recurrent spontaneous abortion (RSA) or recurrent pregnancy loss (RPL) that occurs with the same partner for two or more consecutive or discontinuous pregnancies before 24 weeks[1, 2]. The causes of URSA are complex and varied, including genetic factors, anatomical abnormalities, infection, endocrine abnormalities, immune dysfunction, autoantibody abnormalities (such as antiphospholipid syndrome), thrombotic diseases, etc [3]. However, the etiology of nearly 50% of patients with recurrent abortion is currently unclear, and the clinical diagnosis is URSA or unexplained recurrent pregnancy loss (URPL)[4]. As the etiology and pathogenesis of URSA are still being explored, clinical treatment methods are relatively limited. At present, most therapeutic methods are clinical small sample, observational and experimental studies under the guidance of existing theories, including immunotherapy, anticoagulant therapy, hormone therapy, etc., which still need to be verified by further clinical studies. Yunkang granules are composed of Dixie, Chinese yam, angelica and astragalus, etc., which have the effects of nourishing blood, calming fetus, strengthening spleen and strengthening kidney. Its role in habitual abortion has been verified [5]. This

study intends to discuss the clinical effect of Yunkang granules combined with low-dose aspirin on URSA, and study its influence on pregnancy outcome.

1. Materials and methods

1.1 General data

A total of 72 patients with unexplained recurrent abortion admitted to our hospital from January 2021 to January 2022 were selected as research objects and divided into control group and experimental group according to random number table method, with 36 cases in each group. Patients in the control group ranged in age from 20 to 40 years, with an average age of 30.92±5.88 years. The number of abortions ranged from 2 to 4, with an average of 2.69±0.86. Patients in the experimental group ranged in age from 21 to 39 years old, with an average age of 30.22±5.08 years old; The number of abortions ranged from 2 to 4, with an average of 2.81±0.82. There were no significant differences in age, abortion frequency and other general information between the two groups ($P>0.05$), indicating comparability. This study has been approved by the hospital ethics committee and all patients have signed informed consent.

1.2 Inclusion and exclusion criteria

Inclusion criteria: ①The number of abortion for patients ≧2 times, including biochemical pregnancy is not included, and the gestational week is about 10 weeks； ②Both husband and wife received chromosome examination, chromosome karyotype results showed no abnormal phenomenon, and neither husband and wife had family genetic history； ③Doppler ultrasonography and hysterosalpingography were performed, both of which revealed normal genital anatomy； ④No chlamydia, mycoplasma, treponema pallidum and toxoplasma were infected;⑤The test results of anti-nuclear antibody, anti-phospholipid antibody and anti-sperm antibody were negative.⑥No relevant treatment was received recently and no drugs were taken that affected the observed effect.

Exclusion criteria: ①Patients with hepatic and renal dysfunction and thyroid dysfunction； ②Patients with antiphospholipid syndrome, coagulation dysfunction and organic disease of uterus； ③Laxity of the inner cervix and hereditary disease;④History of venous or arterial embolism； ⑤Who were not willing to participate in the study or had recently taken medications that affected the observation.

1.3 Methods

Control group was given aspirin (Hulunbuir Kangyi Pharmaceutical Co., LTD., National drug approval number H15020766) orally, 75mg/ time, once a day, until 12 weeks of gestation, and then the dose was adjusted according to the patient's situation. Patients in experimental group were administered with oral YunKang granules, 1 bag/time, 3 times/day on the basis of control group. Clinical efficacy was evaluated after 10 weeks of continuous treatment in both groups.

1.4 Obvervational index

1.4.1 Hormone level test

The levels of serum chorionic gonadotropin (β-HCG), progesterone (P) and estradiol (E_2) before and after treatment were observed in two groups.

1.4.2 Detection of coagulation function index

2ml of venous blood was extracted from 2 groups of patients in the morning before and after medication, and serum

was centrifuged at 4℃. Prothrombin time (PT), thrombin time (TT), activated partial thrombin time (APTT) and fibrinogen (FIB) levels were detected by the analyzer, with matching kits and in strict accordance with instructions.

1.4.3 Evaluation of clinical curative effect

The two groups of subjects maintained a pregnancy of more than 28 weeks and successfully delivered a child as a cure, the pregnancy was not successful as invalid.

Total response rate = number of cured cases/total cases.

1.4.4 Pregnancy outcome

Follow-up for 1 year, pregnancy outcome and newborn deformity were recorded in both groups.

1.5 Statistical analysis

SPSS 26.0 software was used to process the data. The measurement data were in line with normal distribution and were expressed as ($\bar{x}$±s). Independent sample T-test was used for comparison between the two groups, and paired T-test was used for differences before and after treatment. The count data were expressed by frequency, and χ^2 test was used to compare the two groups.

2. Results

2.1 Comparison of hormone levels between the two groups

As shown in Table 1, after medication, the levels of β-HCG, P and E2 in 2 groups were higher than before medication, and the levels of β-HCG, P and E2 in observation group were higher than those in control group, with statistical significance (P < 0.05).

Table 1. Comparison of hormone levels between the two groups（ $\bar{x}$±SD）

Indexes	Experimental group（n=36）		Control group（n=36）	
	Prior-treatment	Post-treatment	Prior-treatment	Post-treatment
β-HCG（mIU/mL）	1173.00±81.74	16588.00±1299.00$^{***\#\#\#}$	1156.00±80.59	12325.00±1383.00***
P（ng/mL）	12.85±1.25	36.95±2.63$^{***\#\#\#}$	12.38±1.09	31.63±2.12***
E_2（ng/mL）	271.10±50.26	605.30±51.56$^{***\#\#\#}$	275.30±45.65	547.70±62.42***

Note: *P<0.05，**P<0.01，***P<0.001 VS Prior-treatment；#P<0.05，##P<0.01，###P<0.001 VS control group.

2.2 Comparison of coagulation function indexes between two groups

Compared with before medication, the levels of coagulation function indexes PT, TT and APTT were increased in both groups after medication, while the levels of FIB were decreased. After medication, the levels of coagulation function indexes PT, TT, APTT and FIB in the observation group were better than those in the control group, with statistical significance (P < 0.05, Table 2).

Table 2. Comparison of coagulation function indexes（ $\bar{x}$±SD）

Indexes	Experimental group（n=36）		Control group（n=36）	
	Prior-treatment	Post-treatment	Prior-treatment	Post-treatment

PT（s）	11.24±0.76	14.71±1.16***###	10.91±0.68	12.14±0.96***
TT（s）	12.03±0.60	15.58±0.58***###	12.22±0.45	13.54±0.80***
APTT（s）	24.09±1.55	32.71±1.75***###	24.73±1.30	27.82±1.79***
FIB（g/L）	4.69±0.39	2.80±0.18***###	4.62±0.45	3.64±0.33***

Note: *P<0.05，**P<0.01，***P<0.001 VS Prior-treatment；#P<0.05，##P<0.01，###P<0.001 VS control group.

2.3 Comparison of clinical efficacy between the two groups

After treatment, the total effective rate of the experimental group was significantly higher than that of the control group, and the difference between the two groups was statistically significant (P < 0.05, Table 3).

Table 3. Comparison of clinical efficacy

	Cure	Invalid	Total effective rate（%）
Experimental group（n=36）	33	3	91.67
Control group（n=36）	21	15	58.33
t			3.226
P			0.0019

2.4 Comparison of pregnancy status between two groups

According to statistics, there were statistically significant differences between the experimental group and the control group in the incidence of premature live infants, full-term delivery, abortion/fetal development arrest (P< 0.05, Table 4).

Table 4. Comparison of pregnancy status

	Premature birth living child	term birth	Incidence of miscarriage/fetal arrest
Experimental group（n=36）	2（5.56%）	26（72.22%）	2（5.56%）
Control group（n=36）	6（16.67%）	20（55.56%）	5（13.89%）
t			5.234
P			0.035

3. Discussion

URSA is a special type of spontaneous abortion, with an incidence of about 2% [6], which seriously threatens the physical and mental health, family and social harmony and stability of women of childbearing age. In recent years, URSA has become a hot and difficult topic in the field of reproductive medicine. As the etiology and pathogenesis of URSA are still being explored, the clinical treatment methods are relatively limited, and most empirical therapies, such as traditional Chinese medicine for fetal protection and progesterone therapy, etc. [7], have unsatisfactory therapeutic effects. Therefore, how to improve the therapeutic effect of patients with URSA is still the focus of clinical research.

In this study, 72 patients with URSA admitted to our hospital were randomly divided into two groups, which were respectively given conventional treatment and treatment with Yunkang granules combined with low-dose aspirin. The results showed that after treatment, the hormone level of the experimental group was significantly increased, the coagulation function index was significantly improved, and the total effective rate of clinical treatment reached, and the pregnancy outcome was significantly optimized, which indicated that the combination of pregnancy-kang granules and low-dose aspirin therapy is an effective method for the treatment of URSA, and its mechanism of action needs to be further studied.

In conclusion, the combination of Pregnkang granules and low-dose aspirin in the treatment of URSA has obvious curative effect, indicating the clinical promotion.

References

[1] Bender AR, Christiansen OB, Elson J, et al. ESHRE guideline: recurrent pregnancy loss[J]. 2018; 2018(2): hoy004.

[2] Practice Committee of the American Society for Reproductive Medicine. Definitions of infertility and recurrent pregnancy loss: a committee opinion. Fertil Steril. 2013 Jan;99(1):63.

[3] Ju JG. Clinical effect of didrogesterone combined with low-dose aspirin and low molecular weight heparin in the treatment of unexplained recurrent abortion and its effect on pregnancy outcome [J]. Journal of Clinical Rational Drug Use,2022; 014): 015.

[4] Garrido-Gimenez C, & Alijotas-Reig J. Recurrent miscarriage: causes, evaluation and management[J]. Postgraduate Medical Journal,2015; 91(1073): 151-162.

[5] Yang CR. Clinical study on the treatment of habitual abortion with Pregnancy-Kang Granules combined with choriotropin [J]. Modern Medicine and Clinic, 2019; 9): 3.

[6] Chen JY. Clinical effect of Zishen-yutong Pill combined with dydrogesterone on patients with early threatened abortion complicated with subchorionic hemorrhage [J]. Electronic Journal of Modern Medicine and Health Research,2021; 5(11): 3.

[7] Sun Q, Gao Y, Wang F, et al. Research progress of low molecular weight heparin in the treatment of unexplained recurrent abortion [J]. Hainan Medical Science,2019; 4): 5.

Corresponding author: Yanchun Zhang, Department of Reproductive, Kunming Jinxin Hewanjia Obstetrics and Gynecology Hospital, Kunming City, 650031, Yunnan Province, China.

Analysis of the Clinical Characteristics of Malignant Tumor Patients with Rheumatic Symptoms and Rheumatic Disease Combined with Malignant Tumor Patients

Yingjie Zhang, Haipeng Xie, Minghua Xu, Biao Zhang, Yanhui Jia*, Xin Zhang
Affiliated Hospital of Hebei University, Baoding 071000, China.

Abstract: **Objective:** We study the relationship between rheumatic immune disease and malignant tumor to provide the basis for clinical diagnosis and treatment. **Methods:** We selected 53 patients who were hospitalized in our department from January 2013 to February 2020, including 26 patients with rheumatic immune disease combined with malignant tumor and 27 patients with malignant tumor with rheumatic symptoms. We retrospectively analyzed the relationship between gender, age, main clinical manifestations, tumor system distribution, metastasis rate, rheumatic immune disease type and tumor type. **Results:** Among the patients with rheumatic immune disease complicated with tumor, 26.1% were male and 66.7% were female. Among the tumor patients with rheumatic symptoms, 73.9% were male and 33.3% were female. There was a significant difference in gender composition between the two groups. Among the patients with rheumatic immune disease complicated with tumor, respiratory system tumor was the highest. Among the tumor patients with rheumatic symptoms, the incidence of hematological tumors was the highest. The distribution of tumor system was different between the two groups. The proportion of metastatic tumor in patients with rheumatic symptoms is higher than that in patients with rheumatic immune disease combined with malignant tumor. The percentage of concurrent tumor in three diseases in the same period was 0.363% for rheumatoid arthritis, 2.02% for polymyositis/ dermatomyositis and 0.24% for Sjogren's syndrome. This study shows that patients with polymyositis/ dermatomyositis are more likely to develop malignant tumors. **Conclusion:** There were significant differences in gender composition, distribution of tumor system and the proportion of metastatic tumor between patients with rheumatic immune disease complicated with malignant tumor and patients with rheumatic symptoms, and malignant tumor was more common in patients with polymyositis/ dermatomyositis.

Keywords: Rheumatic Immune Disease; Malignant Tumor

Introduction

Rheumatic immune disease is a common clinical disease, its etiology is still unknown, its clinical manifestations are diverse, it often damages multiple systems, and the patient's condition is unstable and has a trend of continuous aggravation. Current research shows that the main pathogenesis of rheumatic immune disease is the abnormality of the immune system of the body, which leads to the immune response to the autoantigen, causing the damage of the own tissue. Many studies have shown that the main causes of death of patients with rheumatic immune diseases are infection, respiratory diseases, cardio-cerebrovascular diseases and malignant tumors. In recent years, the number of deaths caused by malignant tumors in patients with rheumatic immune diseases has increased significantly [1]. Autoimmune system can eliminate tumor cells or inhibit their growth through various ways. When the immune function is abnormal, it can cause tumor cells to escape immune surveillance and induce tumor [2]. Many kinds of rheumatic immune diseases, such as rheumatoid arthritis,

polymyositis/dermatomyositis, Sjogren's syndrome, systemic lupus erythematosus and so on, can be associated with malignant tumors. Malignant tumors have many extra-tumor clinical manifestations, such as bone, joint and muscle pain, polymorphic rash, repeated fever, etc. These symptoms are similar to the clinical manifestations of rheumatic immune disease. Some of them are the first symptoms of malignant tumors, and may also be signs of recurrence or metastasis of malignant tumors [3]. In our study, 53 patients with rheumatic immune disease combined with malignant tumor or malignant tumor with rheumatic immune disease symptoms as the main manifestation were collected. By analyzing the clinical characteristics of these patients, we expounded the relationship between rheumatic immune disease and malignant tumor. Our aim is to reduce the misdiagnosis rate of patients with malignant tumors associated with rheumatic immune diseases.

1. Data and methods

1.1 Research object

We collected the clinical data of 6032 patients. These patients were hospitalized in our department from January 2013 to February 2020. We selected 53 patients for this study. These patients were finally diagnosed as malignant tumors. Some patients were diagnosed with rheumatic immune disease, and the other patients had similar initial manifestations to rheumatic immune disease. The patients were divided into two groups. 1. Rheumatic immune disease group: patients with rheumatic immune disease and malignant tumor. 2. Non-rheumatic immune disease group: malignant tumor patients with initial clinical symptoms similar to rheumatic immune disease. Inclusion criteria: 1. The diagnosis of rheumatic immune disease meets the corresponding diagnosis and classification criteria; 2. Malignant tumors were diagnosed by clinical manifestations, physical signs, imaging and histopathological examination. We retrospectively analyzed the relationship between gender, age, main clinical manifestations, tumor type, incidence of tumor metastasis, type of rheumatic immune disease and tumor type.

1.2 Data analysis

The medical records were recorded with Excel software, the database was established, and analyzed with spss 21.0 statistical software. Continuous variables are expressed as mean ± standard deviation (SD). Qualitative variables are expressed as percentages. $P<0.05$ was considered statistically significant.

2. Results

2.1 Comparison of gender and age of patients in the two groups

There were 26 patients with rheumatic immune disease and malignant tumor, ranging from 33 to 79 years old. There were 27 patients with malignant tumor with rheumatic symptoms, ranging from 33 to 87 years old. The average age of patients in the two groups was 60.8 years old. There was no statistical difference in the average age of onset (Table 1 and Table 2). There was no statistical difference in the age stratification between the two groups (Table 3).

Table 1 Age of onset

	Rheumatism or not	Number of cases	Average value	Standard deviation	Mean standard error
Age	Yes	26	60.808	11.6482	2.2844

of onset	No	27	60.852	13.8083	2.6574

Table 2 Independent sample test

		Levin's variance equivalence test		Mean equivalence t-test						
		F	significance	t	Degree of freedom	Significance (two-tailed)	Mean difference	Standard error difference	Difference 95% confidence interval	
									Lower limit	Upper limit
Age of onset	Assumed equal variance	1.144	.290	-.013	51	.990	-.0442	3.5157	-7.1022	7.0139
	Equivariance is not assumed	-.013		50.146	.990	-.0442	3.5043	-7.0823	6.9940	

Sig>0.05, the total variance of the two samples is the same; p> 0.05, there was no difference in the age of onset between the two groups.

Table 3 Cross table of age stratification * rheumatism

			Rheumatism or not		Sum
			No	Yes	
Age stratification (age)	18-45	Count	5_a	3_a	8
		Percentage of age stratification	62.5%	37.5%	100.0%
	46-69	Count	26_a	34_a	60
		Percentage of age stratification	43.3%	56.7%	100.0%
	>69	Count	27_a	18_a	45
		Percentage of age stratification	60.0%	40.0%	100.0%
Sum		Count	58	55	113

	Percentage of age stratification	51.3%	48.7%	100.0%
Each subscript letter indicates whether there is a subset of rheumatic disease categories. At the. 05 level, there is no significant difference between the column proportions of these categories.				

Chi-square test

	Number	Degree of freedom	Progressive significance (bilateral)	Accuracy significance (bilateral)
Pearson chi-square	3.289[a]	2	.193	.192
Likelihood ratio	3.308	2	.191	.192
Fisher's exact test	3.270			.192
Number of valid cases	113			

a. 2 cells (33.3%) have an expected count less than 5. The minimum expected count is 3.89.

P> 0.05, there is no significant difference between the two groups in age stratification.

Of the 26 patients with rheumatic immune disease and malignant tumor, 6 were male and 20 were female, with male patients accounting for 26.1% and female patients accounting for 66.7%. Among the 27 patients with malignant tumors with rheumatic symptoms as the main manifestation, 17 were male and 10 were female, with 73.9% of male patients and 33.3% of female patients. There were significant differences in gender composition between the two groups (Tables 4 and 5).

Table 4 Sex * Presence or absence of rheumatic crosstabs

			Rheumatism or not		Sum
			No	Yes	
Gender	Male	Count	17	6	23
		Percentage of sex	73.9%	26.1%	100.0%
	Female	Count	10	20	30
		Percentage of sex	33.3%	66.7%	100.0%
Sum		Count	27	26	53
		Percentage of sex	50.9%	49.1%	100.0%

Table 5 Chi-square test

	Number	Degree of freedom	Progressive significance (bilateral)	Precision significance (bilateral)	Precision significance (unilateral)
Pearson chi-square	8.578[a]	1	.003		
Continuity correction [b]	7.031	1	.008		
Likelihood ratio	8.862	1	.003		
Fisher's Exact Test				.005	.004
McNimar test				.[c]	

Number of valid cases	53				
A. The expected count of 0 cells (0.0%) is less than 5. The minimum expected count is 11.28.					
B. Calculation only for 2x2 tables					
C. Both variables must have the same category value.					

P=0.000<0.05, the gender composition of the two groups is significantly different

2.2 Comparison of tumor types between two groups of patients

26 patients with rheumatic immune disease combined with malignant tumor, including 9 cases of respiratory system tumor (8 cases of lung cancer, 1 case of nasopharyngeal cancer), 4 cases of hematological system tumor (1 case of T-lymphocyte leukemia, 2 cases of lymphoma, 1 case of multiple myeloma), 4 cases of breast cancer cancer, 4 cases of digestive system tumor (1 case of colon cancer, 1 case of pancreatic cancer cancer, 1 case of liver cancer, 1 case of rectal cancer), 2 cases of reproductive system tumor (1 case of endometrial cancer, 1 case of cervical cancer), 1 case of endocrine system tumor (thyroid cancer) One case of urinary system tumor (renal cancer) and one case of metastatic cancer (unknown primary focus).

There were 27 cases of malignant tumor patients with rheumatic symptoms as the main manifestation, including 13 cases of hematological system tumor (6 cases of lymphoma, 7 cases of multiple myeloma), 9 cases of respiratory system tumor (8 cases of lung cancer, 1 case of nasopharyngeal cancer), 2 cases of urinary system tumor (prostate cancer), 1 case of digestive system tumor (pancreatic cancer), and 2 cases of metastatic tumor (the primary focus is unknown).

There were differences in tumor system distribution between the two groups. Among the patients with rheumatic immune disease and tumor, the incidence of respiratory system tumor is the highest, followed by hematological system tumor, digestive system tumor and breast cancer. Among the tumor patients with rheumatic symptoms as the main manifestation, the proportion of blood system tumors is the highest, followed by respiratory system tumors (Figure 1).

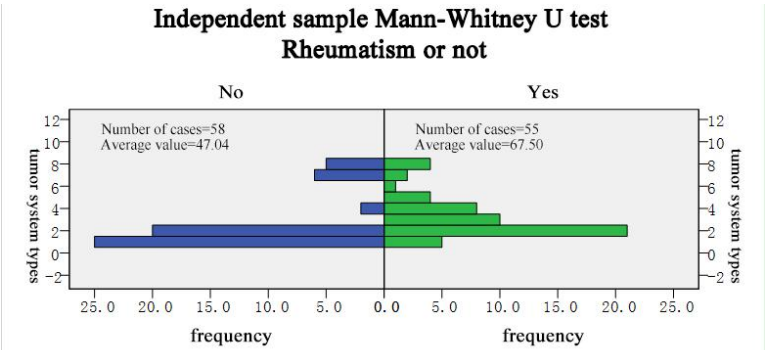

sum	113
Mann-Whitney U	2, 172. 500
Wilcockson W	3, 712. 500
Inspection statistics	2, 172. 500
Standard error	167. 997
Standardized test statistics	3. 438
Progressive significance (bilateral)	. 001

Column	Row	V3
Check	1	Independent sample Mann-Whitney U test
Decision	1	Reject the null hypothesis.
Significance	1	5.86999435471913E-4
Null hypothesis	1	The distribution of tumor system types was the same in the rheumatic-free category.

TYPES	TYPES	MEANS	sum(COUNTS)
Yes	Yes	1	5
Yes	Yes	2	21
Yes	Yes	3	10
Yes	Yes	4	8
Yes	Yes	5	4
Yes	Yes	6	1
Yes	Yes	7	2
Yes	Yes	8	4
No	No	1	25
No	No	2	20
No	No	4	2
No	No	7	6
No	No	8	5

Legend:
1Hematologic tumor
2Respiratory system tumor
3Breast cancer
4Tumor of digestive system
5Tumor of reproductive system
6Endocrine system neoplasms
7Tumor of urinary system
8The primary metastatic tumor remains to be determined

There were 4 cases of metastatic tumor in patients with rheumatism and 7 cases of metastatic tumor in patients with malignant tumor mainly manifested by rheumatism. There was a statistical difference in the proportion of metastatic tumors between the two groups. The proportion of metastatic tumors in patients with malignant tumors mainly manifested by rheumatic symptoms was higher than that in patients with malignant tumors combined with rheumatological diseases. (Table 6, 7).

Table 6 Metastases * Presence of rheumatic crosstabs

			Rheumatism or not		Sum
			no	yes	
Transfer situation	No	Count	43_a	50_b	93
		As a percentage of transfer cases	46.2%	53.8%	100.0%
	Yes	Count	15_a	5_b	20
		As a percentage of transfer cases	75.0%	25.0%	100.0%
Sum		Count	58	55	113
		As a percentage of transfer cases	51.3%	48.7%	100.0%

Each subscript letter indicates the presence or absence of a subset of the rheumatic categories whose column proportions do not differ significantly from each other at the.05 level.

Table 7 Chi-square test

	number	Degree of freedom	Progressive significance (bilateral)	Accuracy significance (bilateral)	Accuracy significance (unilateral)
Pearson chi-square	5.451[a]	1	.020	.026	.017
Continuity correction [b]	4.361	1	.037		
Likelihood ratio	5.680	1	.017	.026	.017
Fisher's exact test				.026	.017
Number of valid cases	113				

a. The expected count of 0 cells (0.0%) is less than 5. The minimum expected count is 9.73.
b. Calculate only for 2x2 tables

P<0.05, the difference was statistically significant, and the percentage of metastasis was different between the two groups.

2.3 The first clinical manifestation of patients with rheumatic immune disease and malignant tumor

We observed the following initial clinical manifestations in patients with rheumatic immune disease combined with malignant tumor: 11 cases of arthralgia, 2 cases of fever, 3 cases of rash, 1 case of low back pain, 1 case of myalgia, 1 case of fever combined with arthralgia, 1 case of fever combined with myalgia, 1 case of rash combined with fever, 1 case of both hands combined with fever, 1 case of myalgia combined with myasthenia, 1 case of myalgia combined with rash, 1 case of lymph node swelling, and 1 case of granulocytopenia. We observed the following initial clinical manifestations in malignant tumor patients with rheumatism as the main manifestation. There were 5 cases of arthralgia, 5 cases of fever, 2 cases of rash, 4 cases of low back pain, 3 cases of myalgia, 1 case of chest and back pain, 1 case of anorexia, 1 case of nodular erythema, 1 case of fatigue, 1 case of fever combined with rash, 1 case of lymph node enlargement combined with fever, 1 case of myalgia combined with arthralgia, 1 case of short breath and joint pain. There was no difference in the first clinical manifestation between the two groups in this study. Because the number of cases studied in this group is small, it is still uncertain whether there are differences in the initial clinical manifestations of patients, which will be the main direction of our further research.

2.4 Relationship between the types of rheumatic immune diseases and malignant tumors

The 26 patients with rheumatic immune disease and malignant tumor in this study are the following three kinds of rheumatic immune diseases, including 11 cases of rheumatoid arthritis, 7 cases of myositis/dermatomyositis, and 3 cases of Sjogren's syndrome. A total of 3027 patients with rheumatoid arthritis, 346 patients with myositis/dermatomyositis and 1249 patients with Sjogren's syndrome were hospitalized in the same period. The percentage of concurrent tumors in the three diseases in the same period was 0.363% for rheumatoid arthritis, 2.02% for myositis/dermatomyositis, and 0.24% for Sjogren's syndrome. This study shows that myositis/dermatomyositis patients are more likely to develop malignant tumors. Of the 26 patients with rheumatic immune disease and malignant tumor, 8 patients were diagnosed with rheumatic immune disease and tumor at the same time, and 18 patients developed tumor after the diagnosis of rheumatic immune disease (1-40 years)

3. Discussion

The pathogenesis of rheumatic immune disease with malignant tumor is not clear, which may be related to the following factors. Immune abnormalities: Under normal circumstances, the abnormal protein complex on the surface of tumor cells can be recognized by the immune system to inhibit tumor growth or target tumor cells through various ways. When the immune function of the body is abnormal, the cellular immunity is defective and low, and the T cell immune monitoring function is decreased. Cancerous cells cannot be killed in time, and tumor cells escape immune surveillance to induce tumor. Shankaran et al. found that cancer cells showed an accelerated growth trend in immune deficient mice [4].

Chronic inflammation: It is well known that rheumatic immune disease is a chronic immune inflammatory disease, and patients have low immune function. Pathogenic microorganisms, etc., release a variety of inflammatory factors and mediators by inducing autoimmune reactions, causing DNA damage to tissue cells, making normal cells more susceptible to mutagenesis and causing tumors [5]. Chronic inflammation can also affect the activity of NK cells, and reduce the killing power of tumor cells. At the same time, inflammation can be used as a tumor promoter to promote the survival, proliferation Migration and invasion accelerate the growth and metastasis of tumor cells [6,7]. To sum up, inflammation is the key factor leading to the occurrence and development of tumor. Therefore, strict control of immune inflammation and reduction of infection can reduce the risk of tumor occurrence [8]. The patient's anti-tumor immune response is inhibited after the use of anti-rheumatic drugs and immunosuppressants, and the immune microenvironment after the use of drugs is also conducive to the growth of malignant tumors [9]. Some studies have shown that organ transplant patients need long-term immunosuppressive treatment, and the incidence of cancer is increasing [10].

The cause of malignant tumor after patients suffering from rheumatic immune disease is not clear, but according to the immune status of the body, it can be divided into three situations, and the three are not immutable. Direct infiltration: Rheumatic immune diseases caused by direct infiltration of tumor are mostly seen in metastatic cancer, primary tumor of synovial membrane/joint, and tumor of blood system (such as leukemia, lymphoma, etc.). In this study, one case of T-lymphocytic leukemia and two cases of lymphoma-associated rheumatic immune disease may be related to the direct infiltration of tumor cells. Paraneoplastic syndrome: some tumors with endocrine function can cause patients to have symptoms similar to rheumatic immune disease, such as arthritis, rash and myalgia. Many studies believe that this may be related to tumor immunity or autoimmunity. Tumor cells can release humoral factors, antigens and other substances. These substances can activate lymphocytes to produce autoimmune antibodies [11]. Rheumatic immune disease coexists with tumor: Stertz proposed in 1916 that the coexistence rate of inflammatory myopathy and malignant tumor is about 5% - 25%, most of which are dermatomyositis patients.

Relevant research shows that the incidence of RA combined with malignant tumor is 0.56%, which is 10% higher than that of the general population. The main tumor types are lymphoma and lung cancer. In this study, there were 11 cases of RA combined with malignant tumors, with a tumor detection rate of 0.363%. Lung cancer was the majority (4 cases), followed by reproductive system tumors. A prospective cohort study indicated that lung cancer in RA may be related to many risk factors such as interstitial lung disease, lung infection, oxidative damage, smoking, etc. [12]. Among many autoimmune diseases, inflammatory myopathy such as myositis dermatomyositis is the most closely related to tumor. Some tumors occur earlier than myositis dermatomyositis, and some occur at the same time with myositis dermatomyositis. It is also possible to develop new malignant tumors in the years or even decades of diagnosis of myositis dermatomyositis. Relevant literature reports that the detection rate of malignant tumors in PM/DM patients is about 17.05% [13], which is 5-7 times higher than that in the natural population. In this study, the detection rate of malignant tumors in PM/DM patients is 2.02%. This result may differ greatly from the report due to the small sample size and data bias. A meta-analysis showed that the risk factor of dermal PM/DM developing into malignant tumor was 4.4/2.1. The most common tumors were reproductive system tumors in women and lung cancer in men. Both of them may have gastrointestinal tumors [14]. Some studies have shown that PM/DM is closely related to the occurrence of ovarian cancer, lung cancer, pancreatic cancer, gastric cancer, colorectal cancer and lymphoma [15]. In this study, there are 7 cases of inflammatory myopathy with tumors, and the tumor detection rate is the highest, of which 2 cases are mainly lung cancer in men and 5 cases are mainly breast cancer in women. Tumors can occur at any stage of inflammatory myopathy. 35% of patients have tumors before PM/DM, 47% of patients have tumors detected at the same time or within half a year after the onset of PM/DM, and only 17% of patients have tumors after PM/DM. This study showed that the highest detection rate of tumors was 5 cases at the same time or within half a year of the onset of PM/DM. Due to the high incidence of tumor in inflammatory myopathy, PM/DM patients who are older than 50

years old, with normal muscle enzyme and positive tumor serology must be vigilant and actively look for evidence of tumor to avoid delaying the disease. PSS is a chronic autoimmune disease with lymphocytic infiltration of exocrine glands as its main manifestation. Relevant studies show that the incidence of malignant tumors in PSS patients is 1.04 to 2.6 times that of normal people matched by gender and age [16,17]. The relative risk rate of malignant lymphoma in PSS patients is 44 times that of ordinary people, and has a high incidence rate and mortality. In particular, the patients with recurrent exocrine gland enlargement, lymph node enlargement and hyperglobulinemia have a greater risk of lymphoma [18]. At the same time, the incidence of thyroid cancer, lung cancer, breast cancer, digestive tract tumor and urinary system tumor in PSS patients is higher, which may be related to the existence of secretion function of some glands and the involvement of PSS in multiple organs. Among the 3 patients with PSS in this study, 2 were lymphoma and 1 was liver cancer, which was consistent with the data reported. The incidence of malignant tumors in SLE patients reported in different literatures is very different. A multi-center study by Bernatsky et al. shows that the incidence of malignant tumors in SLE patients is 1.5 times that of the general population, and the tumor manifestations are diverse, which can involve hematological swelling, respiratory system, digestive system, urogenital system and thyroid [19]. However, Chun's research believes that SLE patients have the same risk of cancer as normal people. SLE patients in this study were diagnosed with rheumatism and malignant tumor at the same time, but due to the small number of cases, it can not be determined that SLE patients are more prone to malignant tumor than normal people.

The relationship between the time of patients suffering from tumor and the time of patients suffering from rheumatic immune disease showed significant diversity. Routine tumor screening should be carried out for patients with rheumatic immune disease who have clinical symptoms that cannot be explained by the primary disease or who have poor efficacy in routine use of hormones and immunosuppressants. Malignant tumor patients with rheumatic symptoms as the main manifestation are often misdiagnosed. Therefore, the main clinical manifestations of middle-aged and elderly patients are joint muscle pain, atypical rash or repeated fever that can not be effectively controlled by NSAIDs and hormones. When we can not clearly diagnose a certain kind of rheumatic immune disease. Whether these symptoms are intermittent or persistent, acute or chronic. We should highly suspect that the patient has malignant tumor. These clinical manifestations may be the first symptoms of the tumor, or the symptoms after the tumor has metastasized to joints, skin and other organs. It is necessary to carry out multiple and multi-site pathological examinations for such people.

References

[1] Shinomiya F, Mima N, Nanba K,etal.Life expectancies of Japanese patients with rheumatoid arthritis[J] A review of deaths over a 20-year period.Mod Rheumatol 2008;18:165-169.

[2] Wang HL, Zhou YM, Zhu GZ, etal. Malignancy as a comorbidity in rheumatic diseases: a retrospective hospital-based study[J] . Clinical Rheumatology, 2018, 37(1):81-85.

[3] Fam AG . Paraneoplastic rheumatic syndromes[J]. Baillieres Best Pract Res Clin Rheumatol, 2000, 14(3): 515-533.

[4] Shankaran V, Ikeda H, Bruce AT, et al. IFNγ and lymphocytes prevent primary tumour development and shape tumour immunogenicity[J]. Nature, 2001, 410(6832): 1107-1111.

[5] Francescone R,Hou V,Microbiome.inflammation,and cancer[J].Cancer journal (Sudbury,Mass.), 2014,20(3):181-189.

[6] Beyaert R, Beaugerie L, Van Assche G, et al.Cancer risk in immune-mediated inflammatory diseases (IMID) [J]. Molecular cancer, 2013,12(1):98-100.

[7] Cutolo M, Paolino S. Possible contribution of chronic inflammation in the induction of cancer in rheumatic diseases[J].Clinical and experimental rheumatology, 2014, 32(6): 839-847.

[8] Francescone R, Hou V, Grivennikov SI. Microbiome, inflammation, and cancer [J]. Cancer Journal, 2014, 20(3):181-189.

[9] Wolfe F. Lymphoma in rheumatoid arthritis: the effect of methotrexate and antitumor necrosis factor therapy in 18, 572 patients[J]. Arthritis and Rheumatism, 2004, 50(6): 1740-1751.

[10] Shankaran V, Ikeda H, Bruce AT, et al. IFN gamma and lympho cytesprevent primary tumour development and shape tumour immunogenicity. Nature, 2001, 410 (6832): 1107-1111.

[11] Marmur R, Kagen L. Cancer associated neuromusculo-skeletal syndromes. Recognizing the rheumatic-neoplas-tic connection[J]. Postgrad Med, 2002, 111 (4): 95-98, 101-102.

[12] Simon TA, Thompson A, Gandhi KK, etal. Incidenceof malignancy in adult patients with rheumatoid arthritis: A meta-analysis[J] .Arthritis Res Ther, 2015, 17: 212.

[13] Fang YF, Wu YJ, Kuo CF, et al. Malignancy in dermatomyositis and polymyositis: analysis of 192 patients[J]. Clinical Rheumatology, 2016, 35(8): 1977- 1984.

[14] Abu Shakra M, Buskila D, Ehrenfeld M, et al. Cancer and autoimmunity: autoimmune and rheumatic feature in patients with malignancies[J]. Ann Rheum Dis 2001, 60: 433-440.

[15] Yang Z, Lin F, Qin B, etal.Polymyositis/dermatomyositis and malignancy risk: a metaanalysis study[J]. The Journal of Rheumatology, 2015, 42(2): 282-291.

[16] Lazarus MN, Robinson D, Mak V, et al. Incidence of cancer in a cohort of patients with primary Sjgren's syndrome[J]. Rheumatology (Oxford), 2006, 45: 1012- 1015.

[17] Weng MY, Huang YT, Liu MF, et al. Incidence of cancer in a nationwide population cohort of 7852 patients with primary Sjgren's syndrome in Taiwan [J]. Ann Rheum Dis, 2012, 71:524-527.

[18] Sela O, Shoenfeld Y. Cancer in autoimmune diseases.Semin Arthritis, 1988, 18: 77-86.

[19] Bernatsky S, Boivin JF, Joseph L, et al. An international cohort study of cancer in SLE[J]. Arthritis Rheum 2005,52:1481-1490.

About the author: Yingjie Zhang (1986.10-), female, Han nationality, born in Tangshan, Hebei, master's degree candidate, attending physician, research direction: rheumatic immunity.

Co-first author: Haipeng Xie

Corresponding author: Yanhui Jia

Clinical Treatment of Gastroenterology in Patients with Chronic Atrophic Gastritis

Fang Zheng
Sichuan Vocational College of Art, Chengdu 610000, China.

Abstract: Objective: To observe the clinical manifestations of selected patients with chronic atrophic gastritis, and to collect data to explore the clinical treatment effect of tepredone in the Department of Gastroenterology in patients with chronic atrophic gastritis. Methods: A total of 160 patients with chronic atrophic gastritis were selected among the patients admitted to the hospital for treatment from August 2019 to August 2022, and a total of 160 patients were selected as the experimental subjects of this clinical treatment study of gastroenterology in patients with chronic atrophic gastritis. 160 patients with chronic atrophic gastritis will be randomly divided into two groups, 80 cases in each group, to ensure that the difference between the study group and the control group is statistically significant to ensure the availability of experimental data. In the experiment, 80 patients with chronic atrophic gastritis in the control group received triple therapy with conventional treatment in gastroenterology, while 80 patients with chronic atrophic gastritis in the study group added tipredone therapy to the triple therapy of conventional treatment in gastroenterology. A two-week treatment cycle compares the effects of treatment between the study and control groups, collects data and draws corresponding conclusions. Results: After treatment, the total effective rate of treatment in the study group was 97.5%, which was higher than that in the control group, and the difference was statistically significant. Conclusion: In patients with chronic atrophic gastritis, on the basis of conventional treatment in gastroenterology, the addition of tepredone therapy has positive significance for the treatment effect of chronic atrophic gastritis, and can be promoted.

Keywords: Chronic Atrophic Gastritis; Gastroenterology; Tepredone

Introduction

Chronic atrophic gastritis is a common digestive system disease, which can be affected by a variety of factors, such as Helicobacter pylori infection, immune factors, constitution, genetics, etc., easy to aggravate the condition due to overeating, alcoholism and other bad living habits, more common in middle-aged and elderly people. The disease is not specific, and the clinical symptoms and lesion range are inconsistent. Diagnosis requires gastroscopy, gastric mucosal examination, or histopathology. Chronic atrophic gastritis is a common form of inflammatory disease of the stomach. Patients with such diseases have gastrointestinal side effects (nausea, abdominal discomfort, etc.) due to abnormal gastric function, and may also have complications such as gastric bleeding and gastric ulcers, and the incidence and recurrence rate are high. In clinical treatment, it is a type of disease with a long treatment period and a relatively painful course. If left untreated, it will not only affect the patient's health and quality of life, but also become cancerous and life-threatening.

At present, the treatment of chronic atrophic gastritis mainly relies on drug treatment, but the treatment effect has not been significantly improved, so it needs to be improved on the basis of traditional drug therapy, and this study has achieved certain positive results on the basis of the triple therapy of conventional treatment in gastroenterology

1. Object and method

1.1 Basic information

A total of 160 patients with chronic atrophic gastritis were selected from the Department of Gastroenterology of our hospital from August 2019 to August 2022 as the experimental subjects of this clinical treatment study of gastroenterology in patients with chronic atrophic gastritis. 160 patients with chronic atrophic gastritis will be randomly divided into two groups, 80 patients in each group, and the difference between the two groups is not statistically significant (P>0.05), which is comparable to ensure the availability of experimental data.

The study was approved by the institutional ethics committee and all patients were informed of the study. All patients in the study were diagnosed by gastroscopy, and patients with contraindications to medication, organic lesions, and language disorders were excluded.

1.2 Method

In the experiment, 80 patients with chronic atrophic gastritis in the control group were treated with triple therapy (4 g of pectin bismuth + 1000 mg of amoxicillin + 500 mg of clarithromycin orally once daily) with a two-week treatment cycle.

The 80 patients with chronic atrophic gastritis in the study group need to be distinguished from the control group, and after the usual treatment of triple therapy (4 g pectin bismuth + 1000mg amoxicillin + 500 mg clarithromycin orally once daily) is used as the control group, the doctor should make a clinical diagnosis, and on the basis of triple therapy, use oral tepredone in patients with chronic atrophic gastritis to assist the patient's treatment. The dose of tepredone is 50 mg three times daily and should be instructed to 80 patients with chronic atrophic gastritis in the study group half an hour before meals. The treatment cycle was the same as that of the control group, with a two-week treatment cycle to better compare the data.

1.3 Observe the judgment indicators

Through observation and judgment of a total of 160 patients with chronic atrophic gastritis in the two groups, the clinical manifestations (such as nausea, dyspepsia, nausea, etc.) basically disappeared, the patient's appetite was significantly improved compared with the disease, the condition was normal when the gastric mucosa examination was performed by gastroscopy, and the atrophy disappeared significantly, and the clinical treatment results were judged to be effective. The symptoms of the patient's clinical manifestations (such as nausea, indigestion, nausea, etc.) are reduced, and the area of gastric mucosal lesions is reduced by more than 50% when the gastric mucosal examination is performed by gastroscopy, and the symptoms of gastric mucosal inflammation and atrophy are reduced, then the clinical treatment results are judged to be effective; The patient's clinical manifestations (such as nausea, indigestion, nausea, etc.) have not changed, the patient's appetite has not improved significantly compared with the disease, and the condition has not changed or even worsened when using gastroscopy for gastric mucosal examination, then the clinical treatment results are judged to be invalid.

The total response rate of treatment is the sum of the number of effective cases and the number of effective cases as a percentage of the total number of treatment cases.

1.4 Statistical analysis

SPSS18.0 was used to analyze and process the relevant data in this paper, and the difference in P<0.05 was statistically significant.

2. Results

After the end of the course of treatment, the overall effective rate of treatment in the control group was 87.5%, the treatment response rate in the study group was 97.5%, and the treatment response rate of the patients in the study group had a clear advantage ($P<0.05$). In addition, the researchers also conducted follow-up visits to the two groups of patients, 7 patients in the control group relapsed, and 2 patients in the study group relapsed, and there was also a statistical difference between the two groups ($P<0.05$).

3. Discussion

The number of patients with chronic atrophic gastritis has increased in recent years, which has had many adverse effects on patients. According to relevant data, chronic atrophic gastritis has been listed as a precancerous lesion by the World Health Organization, which seriously affects the quality of life and safety of patients. Therefore, effective treatment plans and related measures should be sought in clinical treatment to promote early health and improve the quality of life of patients. Current treatment of these patients is based on eliminating Hp, which helps reduce morbidity and damage caused by inflammation.

There are certain treatment options for chronic atrophic gastritis, and most of them use triple therapy of pectin bismuth, amoxicillin, and clarithromycin to control the remission of the condition. However, at present, the combination of three classes of drugs still has certain limitations, and many treatment cases show that the combination of pectin bismuth + amoxicillin+ clarithromycin has a high probability of recurrence. Therefore, how to improve the treatment effect of chronic atrophic gastritis has become one of the key research directions of gastroenterology treatment.

Tepredone is a clinical conventional drug for the treatment of gastric ulcers and other diseases, which can promote the production of endogenous prostaglandins, and induce the expression of HSP70 to repair damaged proteins, promote the reformation of epithelial cells, repair gastric mucosal tissue, reduce the occurrence of inflammation, and better protect the gastric mucosa.

Based on this, the treatment of chronic atrophic gastritis is clinically started with tepredone for the treatment of chronic atrophic gastritis. Teprenone can effectively inhibit gastric acid secretion, protect and repair gastric mucosa, is a clinical conventional drug for the treatment of gastric ulcer and other diseases, used in the clinical treatment of chronic atrophic gastritis, has the positive therapeutic effect of improving the patient's appetite, improving the patient's adverse symptoms, reducing the recurrence rate, can effectively repair the patient's gastric mucosal tissue, and improve the patient's gastric mucosal defense ability, can significantly improve the patient's quality of life, help the patient build confidence.

In summary, the use of teprenone in the clinical treatment of gastroenterology in patients with chronic atrophic gastritis can effectively improve the treatment effect of chronic atrophic gastritis, alleviate the adverse symptoms of patients with chronic atrophic gastritis, reduce the recurrence rate, and improve the quality of life of patients. Therefore, in the treatment of patients with chronic atrophic gastritis, combination drugs can be used to improve the efficacy and promote the application of tepredone in the treatment of chronic atrophic gastritis.

References

[1] Qian E. Clinical Treatment Analysis of Gastroenterology in Patients with Chronic Atrophic Gastritis [J]. *World's Latest Medical Information Abstract*, 2017,17 (90): 156.

[2] Li XH. Clinical Treatment Analysis of Gastroenterology in Patients with Chronic Atrophic Gastritis [J]. *World's Latest Medical Information Abstract*, 2017,17 (73): 35+43.

[3] Han DH. Clinical Treatment Analysis of Gastroenterology in Patients with Chronic Atrophic Gastritis [J]. *Electronic*

Journal of Clinical Medical Literature, 2017,4 (47): 9196.

[4] Yang Z. Clinical Analysis of Internal Medicine Treatment for Patients with Chronic Atrophic Gastritis [J]. *Chinese Journal of Practical Medicine*, 2017,12 (06): 125-126.

[5] Cai N. Clinical Treatment Experience of Gastroenterology in Patients with Chronic Atrophic Gastritis [J]. *Journal of Clinical Rational Drug Use*, 2016,9 (35): 47-48.

[6] Liu XM. Clinical Treatment Experience in Gastroenterology for Patients with Chronic Atrophic Gastritis [J]. *World Latest Medical Information Digest*, 2016,16 (38): 54+57.

[7] Chen DL. Study on the Effectiveness of Standardized Treatment in Digestive Medicine for Patients with Chronic Atrophic Gastritis [J]. *Contemporary Medicine*, 2016,22 (06): 130-131.

Effectiveness of Plastic Breast-Conserving Surgery in the Treatment of Early Breast Cancer

Zhu Wu, Zhuo Wang, Qingqing Ye, Rong Fan*
Jingzhou First People's Hospital, Jingzhou 434000, China.

Abstract: Objective: To observe and compare the effects of different surgical procedures in the treatment of early breast cancer. Methods: Seventy patients admitted from 2020.7 to 2022.4 were selected as the study sample and divided into control and trial groups, 35 patients each received conventional and reconstructive breast-conserving treatment, respectively, to compare the treatment of patients between groups. Results: The excellent rate of breast repair in the trial group was 91.42% compared with 71.43% in the control group, with a significant difference ($P < 0.05$); the indicators of intraoperative blood loss and hospital stay were better in the trial group than in the control group, with significant differences between the groups ($P < 0.05$). Conclusion: Early breast cancer patients treated with plastic breast-conserving surgery not only have better results in breast repair, but also achieve early discharge from hospital, which is worth promoting.

Keywords: Early-Stage Breast Cancer; Plastic Breast-Conserving Surgery; Restorative Effect

Introduction

For patients with early stage breast cancer, clinicians usually recommend surgical removal of the tumour lesion to control the disease and optimise the prognosis. As the breast is the second female sex symbol and the pride of women, many breast cancer patients are very concerned about the aesthetics of their breasts and therefore have higher requirements for excisional surgery. Conventional breast-conserving surgery is a simple procedure and allows for the complete removal of the tumour, but usually does not meet the aesthetic needs of the patient [1]. Plastic breast-conserving surgery is a minimally invasive technique that allows for the transfer of rearranged breast tissue and the replacement of surrounding non-breast tissue, with a wider margin of incision and a more desirable aesthetic outcome while allowing for a guaranteed tumour treatment. In this paper, 70 patients were included and grouped together to compare conventional and reconstructive breast-conserving treatment, and are reported and analysed below.

1. Information and methods

1.1 General information

Seventy cases of early breast cancer patients were used as the subjects of this study, with a consultation time range of 2020.7 to 2022.4. Breast criteria: ① breast cancer met the diagnostic criteria and was confirmed by examination; ② all were female; ③ indications for surgical excision; ④ consent to review the case data. Those with concomitant other oncological diseases, contraindications to anaesthesia, and abnormal coagulation function were excluded. The above selected individuals were divided equally into 2 groups of 35 cases each, and the status of each group was as follows.

Control group: age ranged from 33 to 56 years old, mean (41.29±9.25) years old; tumour size ranged from 2.3 to 3.0 ㎝, mean (2.39±0.23)㎝; TNM stage: 8, 10 and 17 cases in T1 stage, T2 stage and T3 stage respectively.

Test group: age 31-59 years old, median age (42.07±9.33) years old; tumour size range 2.2-3.3 ㎝, average (2.44±0.28) ㎝; TNM stage: T1 stage, T2 stage and T3 stage in order of 9, 11 and 15 cases.

The above basic data of the two groups of patients were compared (P＞0.05) and were comparable.

1.2 Methods

(1) Test group: plastic breast-conserving surgery. Routine imaging and pathological examination was performed before surgery to clarify the anatomical location of the lesion. If the lesion was in the nipple plane, a curved incision of appropriate length was made at the lesion; if the lesion was below the nipple plane, a radial incision was made. The tumour and the surrounding tissue within 1.0 to 1.5 cm are removed and the lymph nodes are carefully cleared. After excision of the tumour, the nipple-areola complex is transferred to a central location by shaping and suturing the gland and etc. Some of the distant or surrounding normal tissues are transferred through flap transfer repair to replace the defective breast tissue.

(2) Control group: conventional breast-conserving surgery. Pre-operative examination and selection of suitable incision were carried out in the same way as in the experimental group. After determining the anatomical location of the lesion, the tumour and the surrounding tissues within 1.0~1.5 ㎝ were removed and the lymph nodes were cleared, and no surgical cavity suturing was performed after the operation.

1.3 Observation index

Breast repair was assessed in terms of surgical incision scar, skin colour, skin touch, surface flatness, symmetry and shape of both breasts, and transverse (longitudinal) nipple displacement. The corresponding score ranges for excellent, good, fair and poor were >30, 26~30, 21~25 and ≤20 points in that order. Excellent rate = (number of excellent + number of good) / total number of cases in the group x 100%. Intraoperative blood loss, operative time and length of stay were recorded for each group.

1.4 Statistical processing

SPSS26.0 software was used to process the data. The mean age and surgery-related indexes were expressed as t-test; the excellent rate was expressed as rate % and calculated by X^2. Difference detection criteria: P < 0.05.

2. Results

2.1 Breast repair situation

The excellent breast repair rate in the trial group vs. the control group was 91.42% vs. 7.43%, which was higher in the trial group, suggesting better repair results in this group (P < 0.05), Table 1.

Table 1 Comparison of the status of breast repair in the two groups[n，(%)]

Group（n）	Excellent	Good	Fair	difference	Excellent rate
Test group（35）	24	8	2	1	32（91.42）
Control group（35）	15	10	6	4	25（71.43）

2.2 Surgical-related indicators

The test group had less intraoperative blood loss than the control group compared to a shorter hospital stay and longer surgical operation time than the control group, all data differences reached a significance level (P < 0.05). Table 2.

Table 2 Comparison of surgery-related indicators between groups of patients $(\bar{x} \pm s)$

Group（n）	Intraoperative blood loss（ml）	Surgery time（min）	Length of stay in hospital（d）
Test group（35）	97.14±10.62	126.24±15.24	9.41±1.36
Control group（35）	120.34±10.62	104.62±14.26	15.27±2.07

3. Discussion

Breast cancer is a common clinical condition in breast surgery, and in recent years there has been a trend towards a younger age group of patients attending the clinic [2]. In the early stage, many patients do not show many specific manifestations, which may manifest as breast lumps, nipple overflow, etc., and are usually detected during physical examination. In the late stage, the disease may cause lesions in multiple organs and organs due to distant metastasis of some cancer cells, posing a serious threat to life safety.

In recent years, people's income level has generally increased, their spiritual needs have grown and their aesthetic level has improved. Therefore, it is very important to choose the appropriate surgical method for treatment. Conventional breast-conserving surgery is simple, safe and can reduce the risk of distant metastases, but many patients are prone to recurrence and imperfect recovery of the breast shape, which can cause a great deal of mental burden for women. In the context of the widespread implementation of minimally invasive concepts, reconstructive mammaplasty has emerged as a procedure that can rearrange the residual cavity and thus effectively deal with special conditions such as large breast volumes, significant local breast sagging and large tumours, resulting in a greater guarantee of disease treatment and postoperative safety, as well as maintaining the symmetry of the right and left breast and the initial external shape of the breast [3]. In this study, it was found that the excellent rate of breast repair in the trial group was 91.42%, which was significantly higher than that of the control group (67.43%), suggesting that the patients in the trial group had better repair treatment results. The intraoperative blood loss, operative time and hospital stay were (97.14±10.62) ml, (126.24±15.24) min and (9.41±1.36) d respectively in the trial group, compared to (120.34±10.62) ml, (104.62±14.26) min and (15.27±2.07) min in the control group, with significant differences. Plastic breast-conserving surgery is a minimally invasive technique, which is more delicate and therefore takes longer intraoperative time, and because it is less invasive, it reduces bleeding, promotes early recovery of all body functions after surgery and shortens hospital stay.

References

[1] Wang L. Effectiveness of plastic breast-conserving surgery in the treatment of early breast cancer [J]. Chinese Medicine Guide,2022,20(28):45-48.

[2] Yang YY, Ma YM, Lei HQ, et al. Safety and efficacy of reconstructive breast-conserving surgery in the treatment of early-stage breast cancer[J]. Journal of Practical Cancer, 2021, 36(02): 287-289.

[3] Cui TS, Yu MS, Ma TH. Effectiveness of breast-conserving surgery with simultaneous plastic repair in the treatment of early breast cancer[J]. Tissue Engineering and Reconstructive Surgery, 2020, 16(05): 381-384.

Author Bio:

First author

Name: Wu zhut (1982.5.14-), Male, Han Nationality, Place of Origin: Xiangtan, Hunan, Master, Title: Attending Physician, Unit: Jingzhou First People's Hospital, Department: Breast Surgery, Main Research Interests: Comprehensive treatment of breast cancer, diagnosis and treatment of non-lactating mastitis, postoperative reconstruction of breast tumor.

Corresponding author

Fan Rong (1980.1.10-), F, Han, Place of origin: Hubei. Jingzhou, Master, Title: Attending, Unit: Jingzhou First People's Hospital, Department: Department of Respiratory and Critical Care, Major research interests: chronic obstructive pulmonary disease, interstitial lung disease, pulmonary embolism, pulmonary hypertension, ECMO life support, etc.

Second author

Wang Zhuo (1968.10.10-), Male, Ethnicity: Han, Origin: Xiangyang City, Hubei Province, Highest Education: B.S., Title: Deputy Chief Physician, Unit: Jingzhou First People's Hospital, Department: Breast Surgery, Main Research Interests: Comprehensive diagnosis and treatment of breast diseases and breast tumors, post-operative breast reconstruction, minimally invasive treatment of breast diseases, etc.

Third author

Ye Qingqing (1979.2.23-), Female, Ethnicity: Han, Place of origin: Nanning, Guangxi, Highest education: Master, Title: Deputy Chief Physician, Unit: Jingzhou First People's Hospital, Department: Breast Surgery, Main research interests: standard treatment of breast tumours, surgical management of breast cancer.

The application value of echocardiography in the diagnosis of congenital heart disease in neonates

Qiushan Qing, Xin Wei, Hong Zheng, Peirui Chen
Department of ultrasonography, People's Hospital of Deyangcity, Deyang 618001, China.

Abstract: Objective: To investigate the clinical value of echocardiography in the diagnosis of congenital heart disease (CHD) in newborns. Methods: A total of 1000 suspected cases of CHD in newborns were selected as the research subjects, and all underwent echocardiography examination and surgical/cardiac catheterization examination. The diagnostic efficacy of echocardiography in the diagnosis of CHD in newborns was analyzed using the surgical/cardiac catheterization examination results as the gold standard. Results: Among the 1000 suspected cases of CHD in newborns, 881 cases (88.10%) were not detected with CHD, 119 cases (11.90%) were detected with CHD, 2 normal newborns were misdiagnosed as having ventricular septal defect, and 6 cases were missed. The remaining results were consistent with the results of surgical/cardiac catheterization examination. Among the 1000 suspected cases of CHD in newborns, 125 cases were detected with CHD through surgical/cardiac catheterization examination. The specificity of echocardiography in the diagnosis of CHD in newborns was 99.77%, the sensitivity was 93.60%, the accuracy was 99.00%, the positive predictive value was 98.32%, and the negative predictive value was 99.09%. Conclusion: Echocardiography has a high diagnostic efficacy in the diagnosis of CHD in newborns and can reflect the condition of CHD newborns, providing better guidance for clinical diagnosis and treatment.

Keywords: Echocardiography; Newborn; Congenital Heart Disease

Introduction

Congenital heart disease (CHD) is a common cardiac malformation caused by abnormal development of the heart and blood vessels during embryonic stage. It is the leading cause of birth defects, with an incidence rate of approximately 0.8%-1.0%, accounting for 0.5%-0.8% of cardiovascular diseases in newborns. CHD is influenced by various factors such as peripheral environmental factors and genetic factors, and its incidence is gradually increasing, which affects the growth and development of newborns and even endangers their life safety. In recent years, great progress has been made in pediatric cardiac surgery technology, and most CHD patients can achieve good prognosis through surgical or interventional treatment.

This study included 1000 suspected CHD neonatal cases from June 2020 to March 2023 in our hospital as the research object, all of which underwent echocardiography examination, aiming to explore the clinical value of echocardiography in diagnosing neonatal CHD, and the specific content is reported as follows.

1. Materials and Methods

1.1 General Information

A total of 1000 newborns suspected of congenital heart disease (CHD) from June 2020 to March 2023 were randomly selected as the study subjects. All newborns underwent echocardiography and the results were analyzed. Among the 1000

newborns, the age range was 1-22 days, with a mean age of (10.25±3.14) days; the birth weight range was 2050-4160g, with a mean birth weight of (3015.12±102.39) g; there were 519 males and 481 females. All families of the newborns were informed and agreed to participate in this study, and the study was approved by the ethics committee.

1.2 Inclusion and Exclusion Criteria

Inclusion criteria: presence of symptoms such as dyspnea and cyanosis of the lips, heart murmur upon auscultation, normal liver and kidney function.

Exclusion criteria: concurrent infectious diseases, respiratory failure, other congenital diseases, difficulty in actively participating in the study.

1.3 Methods

All hospitalized infants received cardiac auscultation and routine examinations. The examination was performed using a Mindray Resona 70B color Doppler ultrasound diagnostic instrument, assisting the neonate to maintain a left lateral or supine position, and performing the examination as much as possible in its natural sleep state. The left ventricular long-axis section was obtained between the 2nd and 3rd ribs on the left edge of the neonate's sternum. Using M-mode echocardiography, the aortic valve annulus diameter, ascending aortic diameter, right atrial diameter, aortic sinus width, left ventricular internal diameter, interventricular septal thickness, left ventricular posterior wall thickness, interventricular septal motion direction, and motion amplitude were measured. The left and right atrial and ventricular upper and lower diameters, transverse diameter, interatrial septal motion direction, and blood flow spectra of the aortic valve and atrioventricular valve were measured in the four-chamber view of the cardiac apex. The continuity of the ventricular septum, right ventricular diameter, and right ventricular pressure situation were obtained in the short-axis section of the great artery, mainly for tricuspid regurgitation, pulmonary artery blood flow spectrum morphology, and pulmonary artery valve curve. The mitral valve orifice area was measured in the left ventricular short-axis view at the level of the mitral valve. At the same time, it was checked whether there was shunt in the neonatal ductus arteriosus, the specific shunt speed, location, direction, shunt volume, and pressure difference.

1.4 Observation indicators

Using surgical/cardiac catheterization results as the gold standard, the diagnostic efficacy of echocardiography for newborns with CHD was analyzed. The main indicators include specificity, sensitivity, accuracy, positive predictive value, and negative predictive value. Specificity = true negative cases (/true negative cases + false positive cases) × 100%, sensitivity = true positive cases (/true positive cases + false negative cases) × 100%, accuracy = (true positive cases + true negative cases) / total cases × 100%, positive predictive value = true positive cases / (true positive cases + false positive cases) × 100%, and negative predictive value = true negative cases (/true negative cases + false negative cases).

1.5 Statistical methods

SPSS 21.0 statistical software was used to analyze the data. Count data was expressed as n/%, and the chi-square test was used. Measurement data was expressed as mean ± standard deviation (s), and the t-test was used. A P value < 0.05 indicated a statistically significant difference.

2. Results

2.1 Analysis of Detection of CHD in Newborns using Echocardiography

Among 1000 suspected cases of CHD in newborns undergoing echocardiography, 881 cases (88.10%) were not detected with CHD, while 119 cases (11.90%) were detected with CHD. Among them, 43 cases (36.13%) were simple patent foramen ovale, 25 cases (21.01%) were patent ductus arteriosus, including 2 cases with associated ventricular septal defect and 3 cases with associated atrial septal defect, 27 cases (22.69%) were ventricular septal defect, including 3 cases with associated patent ductus arteriosus and 4 cases with associated membranous subaortic stenosis, 16 cases (13.45%) were atrial septal defect, including 2 cases with associated patent ductus arteriosus and 2 cases with associated pulmonary vein drainage anomaly, 2 cases (1.68%) were endocardial cushion defect, including 1 complete type, 3 cases (2.52%) were Tetralogy of Fallot, 2 cases (1.68%) were pulmonary artery stenosis, and 1 case (0.84%) was complete transposition of great arteries. Two normal newborns were misdiagnosed as ventricular septal defect, and 6 cases were missed. The remaining results were consistent with the results of surgical/cardiac catheterization examination.

2.2 Analysis of Diagnostic Performance of Echocardiography in CHD Newborns

Among 1000 suspected cases of CHD in newborns undergoing surgical/cardiac catheterization examination, 125 cases had CHD. The specificity of echocardiography in diagnosing CHD in newborns was 99.77% (873/875), the sensitivity was 93.60% (117/125), the accuracy was 99.00% (990/1000), the positive predictive value was 98.32% (117/119), and the negative predictive value was 99.09% (873/881). See Table 1.

Table 1 Diagnostic Results of Echocardiography in CHD Newborns (n)

Surgery/Cardiac Catheter Diagnosis	Echocardiogram		total
	Positive	negative	
positive	117	8	125
negative	2	873	875
total	119	881	1000

3. Discussion

Congenital heart disease (CHD) in newborns is the leading cause of fatal birth defects in infants, and can significantly impair their overall health. In severe cases, symptoms such as cyanosis (blue discoloration of the skin), fainting, and breathing difficulties can occur, putting the newborn's life at risk. Data shows that over 50% of CHD patients die within the first year of life.

Clinical screening methods for newborn CHD include cardiac auscultation, electrocardiogram (ECG), and ultrasound examination. The most common clinical presentation of CHD in newborns is a heart murmur, but murmurs in neonates are often atypical and require multiple auscultations for preliminary screening, followed by further examination.

ECG mainly reflects changes in blood flow dynamics and conduction pathways. ECG changes in CHD depend on the type of malformation, and can roughly reflect changes in blood flow dynamics and the location of the defect. It can be used as a preliminary screening method.

Echocardiography is a type of ultrasound examination that can form a reflected echo on the organ in the body through the relevant physical properties of ultrasound, to explore the large blood vessels and heart in the body, and obtain relevant

parameters and images. Echocardiography is a radiation-free and safe auxiliary examination method, and its physical properties ensure that it will not have any adverse effects on mothers or newborns. A value analysis of the screening equipment for high-risk newborn CHD conducted by Liu Chunyan using cardiac ultrasound technology showed that timely application of cardiac ultrasound technology equipment is necessary for high-risk newborns, in order to quickly screen for CHD and adopt appropriate treatment measures according to the severity of the condition and symptoms, to improve the quality of life of affected infants, and establish a good foundation for subsequent treatment.

Through exploring the value of multiplane echocardiography in the early diagnosis of congenital heart disease (CHD) and analyzing the factors that lead to missed diagnosis and misdiagnosis, Wu Yi-yi et al. found that age over 35, excessive body weight, oligohydramnios, and abdominal wall scars are all factors that contribute to the missed diagnosis and misdiagnosis of CHD using multiplane echocardiography. Furthermore, multiplane echocardiography has high value in the early diagnosis of fetal CHD and is an important means of prenatal assessment of fetal cardiac abnormalities.

References

[1] Zhang J, Wei J, Lei TY. Clinical value of echocardiography in the diagnosis of congenital heart disease in neonates[J]. Clinical Medical Research and Practice, 2023, 8(03): 98-101.

[2] Hu WW, Xu YX. Analysis of the diagnostic value of echocardiography combined with percutaneous oxygen saturation monitoring for critically ill neonates with congenital heart disease[J]. Imaging Research and Medical Applications, 2022, 6(15): 110-112.

[3] Wang JW. Study on the value of echocardiography in the diagnosis of congenital heart disease in infants and young children[J]. Contemporary Medicine, 2021, 27(31): 164-166.

[4] Liu YX. Application value of color Doppler echocardiography combined with cardiac ultrasound examination in screening for congenital heart disease in neonates[J]. Modern Medical Imaging, 2021, 30(02): 269-272.

[5] Zhu YQ. Meta-analysis of risk factors for congenital heart disease and the value of prenatal ultrasound diagnosis[D]. Southern Medical University, 2020.

Analysis of the application of methylprednisolone injection combined with ambroxol injection in the treatment of asthma

Rong Fan, Wei Xiao, Weihua Hu, Wu Zhu*
Jingzhou First People's Hospital, Jingzhou 434000, China.

Abstract: Objective: To observe the effectiveness of different medication regimens in the treatment of asthma diseases. Methods: Sixty-four patients with asthma who attended the medical records department from 2020.6 to 2022.8 were analyzed. 32 patients in group A were treated with methylprednisolone alone, while group B was treated with intravenous amiloride injection in addition to the medication regimen in group A. The improvement time of symptoms in each group was observed, the total effective rate was calculated and the differences between groups were analyzed. Results: In Group B, the improvement time of wheeze, cough, croup and wet rales was earlier than that in Group A ($P < 0.05$). In terms of total effective rate, the difference was 65.63% vs. 93.75% in group A vs. group B ($P < 0.05$). Conclusion: The combination of methylprednisolone and ambroxol injection in the treatment of asthma can provide more rapid relief of symptoms and improve the efficacy, which is worth promoting.

Keywords: Asthma; Methylprednisolone; Ambroxol; Effect Observation

Introduction

Asthma has become a global chronic disease, and airway hyperresponsiveness is one of the main pathological features of the disease. Wheezing, shortness of breath and chronic cough are typical symptoms, and acute attacks occur at night or in the morning [1]. Inadequate treatment may result in irreversible narrowing and remodelling of the airway, disrupting normal life and reducing work efficiency. Methylprednisolone and ambroxol are commonly used in clinical medicine for respiratory diseases both at home and abroad, and this paper focuses on comparing single and combined drug therapy, as reported below.

1. Information and methods

1.1 General data

Sixty-four patients with asthma who came to our department from 2020.6 to 2022.8 were used as the sample for this study, all of whom had a clear diagnosis of the disease, were conscious, had good compliance and tolerated the drugs. The following groups were made according to the randomization principle.

Group A (n=32):The number of males and females was 9:7, the minimum and maximum ages were 22 and 74 years, with a mean value of (45.95±10.23) years.

Group B (n=32): male to female ratio 1:1, minimum and maximum ages 23 and 76 years respectively, mean (50.29±10.34) years.

Patients in the group showed balanced information on the above data, and the differences were not significant ($P > 0.05$) and comparable. This subject meets the ethical requirements.

1.2 Methods

Patients in all groups received oxygen therapy, anti-infection and maintenance of acid-base balance.

(1) Group A: Treatment with injectable sodium methylprednisolone succinate at a dose of 200 p.p. administered intravenously for about 5 min in the early stages, and subsequently reduced to 80 p.p. twice daily in accordance with the patient's condition.

(2) Group B: The treatment regimen of methylprednisolone is the same as that of group A, and combined with 30 p.p.m. of amiloride + 200 ml of 5% dextrose injection twice a day. All groups were given continuous medication for 1 week.

1.3 Observation index

Record the improvement time of wheezing, cough, rales and wet rales in each group. After 1 week of continuous medication, the patient's symptoms disappeared completely and no rales were detected on auscultation of the lungs, which was regarded as effective. The total effective rate was calculated as the percentage of the number of effective cases in the total number of cases in the group.

1.4 Statistical processing

SPSS33.0 software processed the data, and, rate (%) indicated the measurement and counting data respectively, X^2 test. Difference criteria: $P<0.05$.

2. Results

2.1 Clinical efficacy

The total effective rate in group A was 65.63%; in group B, it was 93.75%, and the treatment effect of patients in group B was better than that in group A ($P<0.05$). Table 1.

Table 1 Comparison of the clinical efficacy of patients in the two groups [n,(%)

Group（n）	Effective	Improved	Ineffective	Total effective
Group B（32）	24	6	2	30（93.75）
Group A（32）	13	8	11	21（65.63）

2.2 Time to improvement of symptoms

The improvement time of symptoms related to asthma disease was shorter in all patients in Group B than in Group A. The difference in the data reached the level of significance ($P < 0.05$).

Table 2 Comparison of the improvement time of symptoms between the two groups of patients$(\bar{x} \pm s, d)$

Group（n）	Gasping for breath	Cough	rumbling sound	wet rosin
Group B（32）	3.51±1.24	4.37±1.07	4.23±1.09	4.42±1.23
Group A（32）	4.25±1.39	5.62±1.25	5.22±1.14	5.57±1.39

3. Discussion

Although scholars at home and abroad have conducted a large number of studies on the pathogenesis of asthma, no unified conclusion has been reached so far. Disease research and treatment mostly focus on the control of the inflammatory response, and it is generally believed that the inflammatory response is involved in the process of airway hyperresponsiveness [2].

The timely reduction of asthma symptoms, prevention and control of exacerbations or recurrences, and the normalisation of lung function and the restoration of normal daily activity are the goals that are being pursued in the clinical treatment of asthma. The mechanism of action of methylprednisol is mainly to enhance lysosomal membrane stability, reduce prostaglandin synthesis and release, weaken vasodilatation and inhibit phagocytosis, which in turn exerts immunomodulatory and anti-allergic effects, and is the drug of choice in the treatment of patients with acute asthma attacks. Ambroxol is an expectorant drug whose mechanism of action is to induce the synthesis of more respiratory surface active substances, which can reduce the viscosity of sputum, thereby increasing neutral mucin, reducing acidic urinary proteins and facilitating the coughing up process. Moreover, the drug also intensifies the oscillatory effect of the cilia and enhances their transport capacity in order to further increase the efficiency of sputum excretion [3]. In the current study, the improvement times of wheeze, cough, rales and wet rales in group B were (3.51 ± 1.24) d, (4.37 ± 1.07) d, (4.23 ± 1.09) d and (4.42 ± 1.23) d respectively, which were shorter than those in group A (4.25 ± 1.39) d, (5.62 ± 1.25) d, (5.22 ± 1.14) d and (5.57 (5.57 ± 1.39) d, a significant difference, suggesting that the treatment effect achieved in group B was better. The reason may be that methylprednisolone has a good inhibitory effect on the inflammatory response of the airways and better regulates the immune function, while amiloride significantly improves the ventilation status of the airways. The combination of drugs can superimpose the effect of drugs, better control the disease, improve the efficacy and improve the prognosis of the disease.

References

[1] Sun MC. Treatment of 60 cases of bronchial asthma in the elderly with the combination of warm lung descending method and ambroxol hydrochloride glucose injection [J]. Chinese medicine research,2018,31(03):39-41.

[2] Li J. Effect of aminophenazone combined with aminophylline in the treatment of children with bronchial asthma[J]. Henan Medical Research,2019,28(17):3187-3188.

[3] Xu JW. Exploring the effect of aminophenazone hydrochloride in the treatment of pediatric asthma[J]. Contemporary Medicine Series,2017,15(23):114-115.

Author Bio

First author

Fan Rong (1980.1.10-), F, Han, Place of origin: Hubei. Jingzhou, MA, Title: Attending, Unit: Jingzhou First People's Hospital, Department: Department of Respiratory and Critical Care, Major research interests: Chronic obstructive pulmonary disease, interstitial lung disease, pulmonary embolism, pulmonary hypertension, ECMO life support, etc.

Corresponding author

Wu zhu (1982.5.14-), Male, Han Nationality, Place of Origin: Xiangtan, Hunan Province, Master's Degree, Title: Attending Physician, Unit: Jingzhou First People's Hospital, Department: Breast Surgery, Main Research Interests: Comprehensive treatment of breast cancer, diagnosis and treatment of non-lactating mastitis, postoperative reconstruction of breast tumors, etc.

Second author

Xiao Wei (1969.9.8-), Male, Ethnicity: Han, Origin: Jingzhou, Hubei Province, Highest Education: Master, Title: Chief Physician, Unit: Jingzhou First People's Hospital, Department: Department of Respiratory and Critical Care, Main research

interests: chronic obstructive pulmonary disease; bronchial asthma; lung cancer; pulmonary embolism; interstitial lung disease, etc.

Third author

Hu Weihua (1977.10.12-) Female, Ethnicity: Han, Place of origin: Jingzhou, Hubei, Highest education: Master, Title: Chief Physician

Unit: Jingzhou First People's Hospital, Department: Department of Respiratory and Critical Care Main research interests: chronic obstructive pulmonary disease; bronchial asthma; lung cancer; interstitial lung diseases, etc.

Research Progress in the Treatment of Pituitary Tumors

Wengan Ji[1], Ruixue Xie[1], Shaoze Qin[1], Long Wang[2*], Wenlong Tang[2*]

1. Department of Changzhi Medical College, Changzhi 046000, China.

2. Department of Neurosurgery, Heping Hospital Affiliated to Changzhi Medical College, Changzhi 046000, China.

Abstract: Pituitary tumor is a common intracranial neuroendocrine tumor, generally belonging to benign tumors. It mainly originates from pituitary cells in the sella region. There is no significant difference in the ratio of men to women. The tumor grows to the lower part of the parasellar thalamus, and may even reach the third ventricle to involve the cavernous sinus, extend into the middle cranial fossa, grow into the interpeduncular cistern, and enter the nasopharynx in the sphenoid sinus. A few tumors are rich in blood supply and easy to bleed, leading to pituitary tumor stroke. The incidence of pituitary tumor ranks the third among intracranial tumors. In recent years, with the development of endocrine examination and imaging technology, the detection rate is increasing year by year. The hormone disorder and the pressure on the surrounding important tissues will have a great impact on the quality of life of patients, and have a great impact on the growth and development of patients, labor ability, growth and development and social psychology. In this paper, the research progress of three methods for the treatment of pituitary tumor (surgical therapy, drug therapy, radiation therapy) is reviewed, aiming to provide reference for the clinical treatment of this disease.

Keywords: Pituitary Tumor; Treatment; Research Progress

Introduction

Adenohypophysial, neurohypophysial and residual squamous epithelial cells of embryonic craniopharyngeal tube sac are the main sources of pituitary tumors, among which the pituitary adenoma originating from adenohypophysial gland is the most common, with the incidence of pituitary tumors up to 16.7%. Most pituitary tumors in intracranial tumors are benign, accounting for about 15% [1], after glioma and meningioma, and malignant pituitary tumors are less than 1%. Among pituitary tumors, prolactinomas accounted for 32% ~ 66%, growth hormone tumors accounted for 8% ~ 16%, adrenocorticotropin tumors accounted for 2% ~ 6%, thyrotropin stimulating tumors accounted for 1%, and nonfunctional tumors accounted for 15% ~ 54% [2]. The common clinical symptoms of pituitary tumor include the expression of hormone enhancement and decrease, mass effect, pituitary tumor stroke. Pituitary tumor generally grows slowly. If it is not interfered for a long time, it may cause headache, blindness, heart failure and other symptoms, and is easy to be complicated by cerebrovascular accident, diabetes, infection, and even loss of labor force or death in severe cases. This article reviews the research progress of three methods for the treatment of pituitary tumor (surgical therapy, drug therapy and radiotherapy), aiming to provide reference for the clinical treatment of this disease.

1. Surgical treatment of pituitary tumor

Surgical treatment is the preferred initial treatment for patients with pituitary tumor [3]. In 1889, the first pituitary tumor resection through frontal approach was successfully performed in the world. In 1907, Jing Dijie Road was established; In

1912, it improved and created a new surgical method of resection of vertical tumor through the sublip, nasal septum and sphenoid sinus. In 1960, the Hopkins cylindrical endoscope and instrument system appeared, and the hardware technology of neuroendoscopy made a leap forward. In 1967, with the aid of Hardy microscope and X-ray, the transsphenoidal approach was revived, and then craniotomy gradually decreased. In 1992, the first endoscopic transnasal sphenoidal resection of pituitary adenoma was performed. With the development of imaging and medical instruments, surgical strategies for pituitary tumors have been changing. The development of modern surgical microscopes has allowed for better illumination and resolution of the deep structures through the nasal tunnel, thus providing a closer view, better illumination, and thus a more complete understanding of the environment at the base of the skull. Endoscopy can not only be used for simple intraoperative observation, but also as an auxiliary tool for transsphenoidal surgery under the microscope. A large number of data show that endoscopy can improve the resection rate of tumors with fewer complications. Single-nostril resection of tumors through neuroendoscope or microscopy-assisted sphenoidal approach is currently a clinically recognized classic surgical approach around the world. The extended transsphenoidal approach can be designed as a wide opening at the base of the skull, so endoscopy can provide almost unrestricted observation of intracranial anatomy. However, some technical problems still limit the wide application of these approaches, such as the difficulty of skull base reconstruction, the high incidence of cerebrospinal fluid leakage, and the unskilled endoscopic technique.

2. Radiotherapy of pituitary tumor

Due to the pituitary internal and external irradiation due to more side effects, has been less used. Radiotherapy is a second-line treatment in the treatment of pituitary tumor, mainly applicable to tumor patients with postoperative residual tumor, tumor recurrence, no surgical indications, intolerance to surgical treatment or refusal to surgical treatment. Conventional 2-D radiotherapy has a high complication rate and takes a long time to effectively control abnormal hormone levels. Therefore, conventional radiotherapy is gradually replaced by stereotactic radiotherapy (SRT)/stereotactic radiosurgery (SRS) in recent years [4]. SRS is as effective as craniotomy, but it does not have the morbidity and mortality associated with craniotomy. SRS is less invasive, bloodless, and infection-free, and has no damage to important tissue structures around the lesion target area. Traditional radiotherapy is mainly used in cases where the tumor is difficult to achieve volume reduction and the hormone level is not up to standard after surgery, but the pituitary dysfunction and nervous system damage that may be caused by radiotherapy greatly limit its use [5]. The development of CT and MRI, as well as its integration with the gamma knife radiation platform, has been critical to the advancement of radiation therapy for pituitary tumors. Similarly, advances in the computerised SRS programme have led to safer and more precise doses per unit of time. In patients with residual, recurrent and recalcitrant pituitary tumors, endocrine or surgical decompression is usually used. However, clinical data over the past 10 years support the use of SRT because of its good local tumor control, endocrine remission, and low toxicity. The basic principle of radiotherapy for all pituitary tumors is to deliver a high dose of radiation to the tumor tissue while minimizing the dose to key structures such as the optic structure,hypothalamus, internal temporal lobe, and brain stem.

3. Drug therapy of pituitary tumor

There are mainly two kinds of pituitary tumor treatment drugs: the first kind acts directly on tumor cells to inhibit proliferation and hormone secretion, which is the most ideal treatment method; Studies have shown that the specific expression of genes or proteins in pituitary tumors provide a good target for diagnosis and treatment of pituitary tumors. The most widely used drugs of this kind are bromohentine and carbergoline. In addition, potential targets under investigation are estrogen receptors, retinoic acid receptors and peroxisome proliferator-activated receptor-γ, folate receptor-alpha. The

second is to indirectly control the symptoms and complications caused by excessive hormones, which are widely used in acromegaly and Cushing's disease, mostly hormone release inhibitors and hormone receptor antagonists.

3.1 Bromocriptine

Bromocriptine is an ergot derivative that binds D_1 and D_2 dopamine receptors. Most prolactinomas atrophy within 6 weeks of taking bromocriptine. Side effects such as indigestion, nausea and vomiting, dizziness and headache, movement disorders, hypotension, and syncope can limit tolerance. However, it is still an effective drug for those who can tolerate it. After treatment, 80% ~ 90% of microprolactinomas and 70% of large prolactinomas return to normal prolactin, tumor regression, and gonadal function recovery [6]. The results of bromocriptine administration were similar to those of surgical intervention, with a meta-analysis showing that 74% of microadenomas and 32% of macroadenomas returned to normal prolactin within 12 weeks after surgery [7].

3.2 Carbergoline

Carbergoline is a D_2 receptor agonist. Compared with bromocriptine, carbergoline is better tolerated and has fewer side effects. It can normalize prolactin levels and is currently the preferred initial treatment for prolactinoma. According to the results of Webster et al. [8], 7% of the patients taking cabegoline had abnormal menstruation, while 16% of the patients taking bromoannetin had abnormal menstruation. Only 3% of patients stopped carbergoline because of side effects, compared with 12% of those taking bromocriptine. Another multicentre randomized study of 120 female patients with prolactinoma showed that 93% of the patients taking cabergoline returned to normal prolactin, while only 48% of the patients taking bromohentine returned to normal prolactin, further confirming the superiority of cabergoline monotherapy in the treatment of prolactinoma [9].

3.3 Other drugs

Octreotide has a good effect on acromegaly of auxin adenoma, but a poor effect on the tumor itself. Mifepristone has a long half-life and shows dose-dependent anti-glucocorticoid effect. It is the only glucocorticoid receptor antagonist currently available for clinical use, which can antagonize the effects of cortisol and progesterone [10]. Cyproheptadine has a certain effect on patients with increased cortisol, but the effect is not satisfactory, and can only be used as short-term adjuvant therapy. Temozolomide is used as a first-line chemotherapy agent for refractory pituitary adenoma and pituitary cancer in the clinical guidelines for refractory pituitary adenoma and pituitary cancer released by the European Endocrine Society [11].

4. Summary and Outlook

As a complex neuroendocrine tumor, the treatment of pituitary tumor requires close collaboration and cooperation among various departments, such as neurosurgery, radiology and endocrinology. However, with the development of science and technology, its treatment concepts and methods are constantly updated, and the boundaries of the treatment of pituitary tumors in various departments gradually expand and even overlap with each other. Endoscopic therapy for prolactinoma may bring some risk of trauma and surgical failure to patients, while drug therapy should consider the long-term medication costs and side effects, and it is necessary to weigh the benefits of the two treatments. In addition, more large-scale clinical studies are needed to determine the exact dose of pituitary radiation and the duration of dopamine therapy. At present, frontier researches at home and abroad are trying to understand the pathogenesis of pituitary tumor from the microscopic aspects of genes, proteins, transcription factors, etc. With the deepening of the research, it will bring more good news to patients with pituitary tumor.

References

[1] Karimian-Jazi K. [Pituitary gland tumors]. Radiologe. 2019 ;59(11):982-991.

[2] Zhang Q, Wang Y, Zhou Y, et al. Potential biomarkers of miRNA in non-functional pituitary adenomas. World J Surg Oncol. 2021;19(1):270.

[3] Molitch M E. Diagnosis and treatment of pituitary adenomas: a review. JAMA. 2017; 317(5):516-524.

[4] Kalogeridi MA, Kougioumtzopoulou A, Zygogianni A, et al. Stereotactic radiosurgery and radiotherapy for acoustic neuromas. Neurosurg Rev. 2020; 43(3): 941-949.

[5] Gupta T, Chatterjee A. Modern Radiation Therapy for Pituitary Adenoma: Review of Techniques and Outcomes. Neurol India. 2020;68(Supplement):113-122.

[6] Zou Y, Li D, Gu J, et al. The recurrence of prolactinoma after withdrawal of dopamine agonist: a systematic review and meta-analysis. BMC Endocr Disord. 2021; 21(1):225.

[7] Petersenn S, Giustina A. Diagnosis and management of prolactinomas: current challenges. Pituitary. 2020;23(1):1-2.

[8] Webster J, Piscitelli G, Polli A, et al. A comparison of cabergoline and bromocriptine in the treatment of hyperprolactinemic amenorrhea. Cabergoline Comparative Study Group. N Engl J Med. 1994;331(14):904-909.

[9] Mancini T, Casanueva FF, Giustina A. Hyperprolactinemia and prolactinomas. Endocrinol Metab Clin North Am. 2008;37(1):67-99.

[10] Fleseriu M, Biller BM, Findling JW, et al. Seismic Study Investigators. Mifepristone, a glucocorticoid receptor antagonist, produces clinical and metabolic benefits in patients with Cushing's syndrome. J Clin Endocrinol Metab. 2012; 97(6): 2039-2049.

[11] Raverot G, Burman P, McCormack A, et al. European Society of Endocrinology. Eur J Endocrinol. 2018;178(1):1-24.